

ATTACHMENT 1 TO AEP:NRC:8054-02

REFERENCES

- 1) NRC Generic Letter 2004-02, "Potential Impact of Debris Blockage on Emergency Recirculation During Design Basis Accidents at Pressurized-Water Reactors," dated September 13, 2004 (ML042360586).
- 2) Letter from D. P. Fadel, I&M, to NRC Document Control Desk, "90 Day Response to Nuclear Regulatory Commission Generic Letter 2004-02: Potential Impact of Debris Blockage on Emergency Recirculation During Design Basis Accidents at Pressurized-Water Reactors," AEP:NRC:5054-04, dated March 4, 2005 (ML050750069).
- 3) Letter from J. N. Jensen, I&M, to NRC Document Control Desk, "Nuclear Regulatory Commission Generic Letter 2004-02 – Information Requested by September 1, 2005," AEP:NRC:5054-11, dated August 31, 2005 (ML052510512).
- 4) Letter from J. N. Jensen, I&M, to NRC Document Control Desk, "Nuclear Regulatory Commission Generic Letter 2004-02 – Revision of Commitments," AEP:NRC:5054-14, dated December 19, 2005 (ML060030459).
- 5) Letter from P. S. Tam, NRC, to M. K. Nazar, I&M, "Donald C. Cook Nuclear Plant, Units 1 and 2 - Request for Additional Information Re: Response to Generic Letter 2004-02, 'Potential Impact of Debris Blockage on Emergency Recirculation During Design-Basis Accidents at Pressurized-Water Reactors' (TAC Nos. MC4679 and MC4680)," dated February 9, 2006 (ML060370547).
- 6) Letter from C. Haney, NRC, to Holders of Licenses for Pressurized Water Reactors, "Alternative Approach for Responding to the Nuclear Regulatory Commission Request for Additional Information Letter Re: Generic Letter 2004-02," dated March 28, 2006. (ML060870274).
- 7) Letter from J. N. Jensen, I&M, to NRC Document Control Desk, "Update to Response to Nuclear Regulatory Commission Generic Letter 2004-02: Potential Impact of Debris Blockage on Emergency Recirculation During Design Basis Accidents at Pressurized-Water Reactors," AEP:NRC:6054-05, dated June 27, 2006 (ML061860257).
- 8) Letter from J. N. Jensen, I&M, to NRC Document Control Desk, "Revision of Commitment for Update of Response to Request for Additional Information Regarding Nuclear Regulatory Commission Generic Letter 2004-02," AEP:NRC:6054-07, dated December 19, 2006 (ML063610088).
- 9) Letter from W. H. Ruland, NRC, to A. Pietrangelo, NEI, "Revised Content Guide for Generic Letter 2004-02 Supplemental Responses," dated November 21, 2007 (ML073110269 and ML073110278).

- 10) Letter from J. N. Jensen, I&M, to NRC Document Control Desk, "Request for Extension of Completion Date for Unit 1 Actions in Response to Generic Letter 2004-02, 'Potential Impact of Debris Blockage on Emergency Recirculation During Design Basis Accidents at Pressurized-Water Reactors,'" AEP:NRC:6054-06, dated June 27, 2006 (ML061860251).
- 11) Letter from J. N. Jensen, I&M, to NRC Document Control Desk, "License Amendment Request to Revise Technical Specifications Associated with Generic Letter (GL) 2004-02," AEP:NRC:7036, dated June 27, 2007 (ML071910354).
- 12) Letter from J. N. Jensen, I&M, to NRC Document Control Desk, "Response to Requests for Additional Information re. License Amendment Request to Revise Technical Specifications Associated with Generic Letter (GL) 2004-02," AEP:NRC:7036-01, dated September 21, 2007 (ML072750687).
- 13) Letter from P. S. Tam, NRC, to M. K. Nazar, I&M, "Donald C. Cook Nuclear Plant, Unit 1 (DCCNP-1) - Extension of Completion Date for Actions in Response to Generic Letter 2004-02 (TAC No. MC4679)," dated July 28, 2006 (ML062020768).
- 14) Letter from P. S. Tam, NRC, to M. K. Nazar, I&M, "Donald C. Cook Nuclear Plant, Units 1 and 2 (DCCNP-1 and DCCNP-2) - Issuance of Amendments Re: Containment Sump Modifications per Generic Letter 2004-02 (TAC Nos. MD5901 and MD5902)", dated October 18, 2007 (ML072780605).
- 15) Letter from J. N. Jensen, I&M, to NRC Document Control Desk, "Request for Extension of Completion Date for Unit 1 and Unit 2 Actions in Response to Generic Letter 2004-02, 'Potential Impact of Debris Blockage on Emergency Recirculation During Design Basis Accidents at Pressurized-Water Reactors,'" AEP:NRC:7054-07, dated December 6, 2007 (ML073470140).
- 16) Letter from P. S. Tam, NRC, to M. W. Rencheck, I&M, "Donald C. Cook Nuclear Plant, Units 1 and 2 - Generic Letter 2004-02, "Potential Impact of Debris Blockage on Emergency Recirculation During Design Basis Accidents at Pressurized-Water Reactors," Extension Request Approval" (TAC NOS. MC4679 and MD4680), dated December 26, 2007 (ML073540189).
- 17) NEI Report, NEI 04-07, "Pressurized Water Reactor Sump Performance Methodology," dated December 2004 (ML041550332).
- 18) NRC RG 1.97, "Instrumentation for Light-Water-Cooled Nuclear Power Plants to Assess Plant and Environs Conditions During and Following an Accident," Revision 3, dated May 1983 (ML003740282).
- 19) NRC NUREG/CR-6224, "Parametric Study of the Potential for BWR ECCS Strainer Blockage Due to LOCA Generated Debris," Final Report Dated October 1, 1995.

- 20) NRC NUREG/CR-6272, Vol. 1, "GSI-191 Technical Assessment: Parametric Evaluations for Pressurized Water Reactor Recirculation Sump Performance," dated August, 2002.
- 21) Letter from S. A. Varga, NRC, to J. Dolan, I&M, issuing License Amendment No. 76 to Facility Operating License No. DPR-74 and Safety Evaluation for the I&M responses to Generic Letter 84-04, dated November 22, 1985 (ML021010521).
- 22) Letter from J. F. Stang, NRC, to R. P. Powers, I&M, "Issuance of Amendments – Donald C. Cook Nuclear Plant, Units 1 and 2 (TAC Nos. MA6766 and MA6767)," dated December 13, 1999 (ML993570158).
- 23) Westinghouse, WCAP-16406-P, "Evaluation of Downstream Sump Debris Effects in Support of GSI-191," Rev. 0, dated June 2005.
- 24) Westinghouse, WCAP-16530-NP, Evaluation of Post-Accident Chemical Effects in Containment Sump Fluids to Support GSI-191," dated February 2006 (ML060890509).
- 25) ALION Report, ALION-REP-AEP-3085-11, Revision 0, "D.C. Cook Units 1 & 2: Characterization and Sequence of Events associated with ECCS Sump Recirculation."
- 26) ALION Calculation, ALION-CAL-AEP-3085-12, Revision 0, "D.C. Cook Recirculation Sump Debris Generation Calculation."
- 27) ALION Calculation, ALION-CAL-AEP-3085-14, Revision 1, "D.C. Cook Recirculation Containment Sump Hydraulic Analysis – Task 3 Results."
- 28) ALION Calculation, ALION-CAL-AEP-3085-15, Revision 0, "D.C. Cook Units 1 and 2 Reactor Building GSI-191 Debris Transport Calculation."
- 29) Enercon Services Project Report, WES005-PR-01, Revision 0, "Evaluation of Containment Recirculation Sump Downstream Effects for the DC Cook Nuclear Plant."
- 30) Wyle Laboratories Test Report, 54497R07, Revision B, "Jet Impingement Test of Electromark Labels and Thermal and Fire Barrier Insulation."

- 31) Alden Research Laboratory Reports
 - a) "Hydraulic Model Investigation of Vortexing and Swirl within a Reactor Containment Recirculation Sump – Donald C. Cook Nuclear Power Station," dated September 1978.
 - b) "Experimental Investigation of Air Entrainment at a Reactor Containment Sump due to Break and Drain Flows – Donald C. Cook Nuclear Power Station", dated December 1979.
- 32) CNP Containment Water Level License Amendment Correspondence:
 - a) Letter from R. P. Powers, I&M, to NRC document Control Desk, "Technical Specification Change Request Containment Recirculation Sump Water Inventory," C1099-08, dated October 1, 1999, including Fauske & Associates Calculation, FAI/99-77, Revision 2; "Containment Sump Level Evaluations for the D. C. Cook Plant".
 - b) Letter from M. W. Rencheck, I&M, to NRC Document Control Desk, "Donald C. Cook Nuclear Plant Units 1 and 2 - Response to Request for Additional Information, Technical Specification Change Request, Containment Recirculation Sump Water Inventory, (TAC Nos. MA6766 and MA6767)," dated November 19, 1999, C1195-25 (ML993350042).
 - c) Letter from J. F. Stang, NRC, to R. P. Powers, I&M, "Issuance of Amendments – Donald C. Cook Nuclear Plant, Units 1 and 2 (TAC Nos. MA6766 and MA6767)," dated December 13, 1999 (ML993570158), including Enclosures 1 and 2: "Amendment No. 234 to DPR-58" and "Amendment No. 217 to DPR-74" (ML993570166), and Enclosure 3: Safety Evaluation (ML993570171).
- 33) I&M Calculation, MD-12-CONT-005-N, Revision 1, "Determine Latent Debris in Containment in Accordance with GSI 191."
- 34) I&M Calculation, MD-1-CONT-006-N, Revision 0, "Determine Latent Debris in Unit 1 Containment in Accordance with GSI 191."
- 35) I&M Calculation, MD-2-CONT-007-N, Revision 0, "Determine Latent Debris in Unit 2 Containment in Accordance with GSI 191."
- 36) I&M Calculation, MD-02-DR-001-N, Revision 1, "Verify Capacity of Rerouted CEQ Room Floor Drains."
- 37) I&M Calculation, MD-01-ECCS-004-N, Revision 3, "Unit 1 ECCS Pumps NPSH Analysis."
- 38) I&M Calculation, MD-02-ECCS-005-N, Revision 4, "Unit 2 ECCS Pumps NPSH Analysis."
- 39) I&M Calculation, SD-990825-003, Revision 0, "HELB: Identification of Unit 2 High Energy Lines and Postulation of High Energy Line Breaks."

- 40) I&M Calculation, SD-991008-001, Revision 0, "Seismic Response Spectra for Containment Building."
- 41) I&M Calculation, SD-991021-002, Revision 3, "Calculation for Shields to Cover Penetration Holes in the Flood Up Wall and Grating in the Crane Wall Opening."
- 42) I&M Calculation, SD-991021-003, Revision 3, "Evaluation of the Containment Flood Up Overflow Wall".
- 43) I&M Calculation, SD-000410-001, Revision 0, "Seismic Evaluation of Mounting Details for Lambda Power Supply, Potter & Brumfield Relay, and Master Specialties Pushbutton Switch, and Seismic Qualification of Bussman Fuseblock."
- 44) I&M Calculation, SD-000429-023, Revision 2, "Evaluation of the Reinforced Concrete Containment Flood Up Overflow Wall Inside the Unit 1 Containment Building."
- 45) I&M Calculation, SD-000620-002, Revision 1, "Seismic Qualification of Containment Water Level Switch 1-NLI-330, -331, -340, -341, GEMS sensor Model LS-57761."
- 46) I&M Calculation, SD-000620-003, Revision 1, "Seismic Qualification of Electrical Components Associated with Containment Water Level Indication System."
- 47) I&M Calculation, SD-010307-003, Revision 3, "Design Basis Analysis of Unit 1 and 2 Primary Shield Wall, Operating Deck and Crane Wall."
- 48) I&M Calculation, SD-050209-001, Revision 2, "Containment Insulation Database."
- 49) I&M Calculation, SD-060213-001, Revision 1, "Piping and Support Structural Evaluation for Unit 1 Containment Recirculation Sump Vent Line In Support of Modification 1-MOD-65754."
- 50) I&M Calculation, SD-060307-001, Revision 1, "Qualification of Mounting Details for Containment Recirculation Sump Level Switches for 1-MOD-65754."
- 51) I&M Calculation, SD-060307-002, Revision 1, "Qualification of Debris Interceptors and Anchorage."
- 52) I&M Calculation, SD-060307-006, Revision 1, "Qualification of Anchorage for Main and Remote Strainers."
- 53) I&M Calculation, SD-070104-001, Revision 0, "Qualification of Mounting Details for Containment Recirculation Sump Level Switches."
- 54) I&M Calculation, SD-070104-002, Revision 0, "Qualification of Debris Interceptors and Anchorage."

- 55) I&M Calculation, SD-070104-004, Revision 0, "Qualification of Conduit Supports for EC-MOD-EMOD-0000047476 (2-MOD-65755)."
- 56) I&M Calculation, SD-070104-005, Revision 1, "Qualification of Anchorage for Main Strainer."
- 57) I&M Calculation, SD-070207-001, Revision 0, "Piping and Support Structural Evaluation for Unit 2 Containment Recirculation Sump Vent Line in Support of Engineering Change EC-47476."
- 58) I&M Calculation, SD-070308-001, Revision 0, "Seismic Qualification of Containment Water Level Switches 2-NLI-300 and 2-NLI-301 GEMS Sensors Model LS-57761."
- 59) I&M Calculation, SD-070315-001, Revision 0, "Qualification of Waterway and Waterway Supports for Remote Strainer 2-STN-321 for EC-0000047800."
- 60) I&M Calculation, SD-070315-003, Revision 0, "Qualification of Conduit and Terminal Box Support Design for the Containment Sump."
- 61) I&M Calculation, SD-070315-004, Revision 0, "Qualification of the Anchorage for the Remote Strainer."
- 62) I&M Calculation, SD-070315-005, Revision 0, "Qualification of New Annular Barrier Gate at Azimuth 190 Degrees in Unit 2 Containment Building for EC-047800."
- 63) I&M Calculation, SD-070315-007, Revision 0, "Qualification of Debris Interceptors and Anchorage."
- 64) I&M Calculation, SD-070315-008, Revision 0, "Qualification of Containment Pipe Tunnel Sump Cover."
- 65) I&M Calculation, SD-07315-009, Revision 0, "Qualification of Radiation Gate Near Azimuth 103 Degrees in Unit 2 Containment Building for EC-0000047800."
- 66) I&M Calculation, SD-070516-001, Revision 0, "Piping and Support Structural Evaluation for Unit 2 Reactor Coolant Drain Tank Relief Line in Support of EC-0000047800."
- 67) I&M Calculation, SD-070517-001, Revision 0, "D.C. Cook, Units 1 and 2 GSI-191 Containment Building Materials Inventory Calculation."
- 68) I&M Calculation, SD-070904-001, Revision 0, "Short Term Pressure Values for Containment Recirculation Sump Component Design."
- 69) I&M Calculation, TH-97-16, Revision 2, "D.C. Cook Containment Flood-Up."

- 70) CCI Calculation, 3 SA-096-026, Revision 2, "Structural Analysis of a Wall Strainer Cartridge."
- 71) CCI Calculation, 3 SA-096.035, Revision 4, "Calculation of the Main Strainer."
- 72) CCI Calculation, 3 SA-096.056, Revision 3, "Structural Analysis of the Remote Strainer."
- 73) CCI Calculation, 3 SA-096.062, Revision 0, "Unit A Support Stiffness."
- 74) CCI Test Specification, Q.003.84.795, Revision 3, "Bypass and Head Loss Test."
- 75) CCI Test Report, 680/41404, Revision 0, "Bypass Tests."
- 76) CCI Test Specification, Q.003.84.796, Revision 0, "Chemical Effect Head Loss Test Specification."
- 77) CCI Test Report, 680/41408, Revision 0, "Chemical Effect Head Loss Test."
- 78) CCI Test Specification, Q.003.84.797, Revision 0, "Chemical Laboratory Bench Top Test."
- 79) CCI Test Report, 680/41407, Revision 0, "Laboratory Bench Test for Chemical Effect Testing."
- 80) CCI Test Specification, Q.003.84.798, Revision 1, "Containment Sump Strainer Replacement: Large Size Filter Performance Test."
- 81) CCI Test Report, 680/41400, Revision 1, "Containment Sump Strainer Replacement: Large Size Head Loss Test Report."
- 82) I&M Modification, 1-MOD-65754 (EC-46946), Revision 0, "Containment Sump Debris Accumulation Modifications."
- 83) I&M Engineering Change, EC-47476, Revision 0, "2-MOD-65755 Unit 2 Containment Sump Modification."
- 84) I&M Engineering Change, EC-47800, Revision 1, "Unit 2 Recirculation Sump Remote Strainer."
- 85) I&M Engineering Change, EC-47994, Revision 0, "Unit 1 Recirculation Sump Remote Strainer."
- 86) Letter from J. F. Stang, NRC, to R. P. Powers, I&M, "Donald C. Cook Nuclear Plant, Units 1 and 2 – Review of Leak-Before-Break for the Pressurizer Surge Line Piping as Provided by 10 CFR Part 50, Appendix A, GDC 4" (TAC NOS. MA7834 and MA7835), dated November 8, 2000 (ML003767675).

- 87) Westinghouse, WCAP-16568-P, Revision 0, "Jet Impingement Testing to Determine the Zone of Influence (ZOI) for DBA-Qualified/Acceptable Coatings," dated June 2006.
- 88) Westinghouse, WCAP-16793-NP, Revision 0, "Evaluation of Long-Term Cooling Considering Particulate, Fibrous and Chemical Debris in the Recirculating Fluid," dated May 2007.
- 89) NRC NUREG/CR-6808, "Knowledge Base for the Effect of Debris on Pressurized Water Reactor Emergency Core Cooling Sump Performance," dated February 2003.
- 90) S&L Report, SL-009195, Revision 0, "Wyle Jet Impingement Testing Data Evaluation."
- 91) ALION Report, ALION-REP-AEP-4462-03, Revision 0, "Marinite 36 Material Property Comparison."
- 92) EPRI Technical Report, 1011753, "Design Basis Accident Testing of Pressurized Water Reactor Unqualified Original Equipment Manufacturer Coatings," dated September, 2005.
- 93) Nuclear Energy Institute Report, NEI 02-01, Revision 1, "Condition Assessment Guidelines: Debris Sources Inside PWR Containments," dated September, 2002.
- 94) I&M/Westinghouse Report, NED-2001-004-REP, Revision 1, "Loop Subcompartment Analysis," dated June 2001.
- 95) NRC NUREG/CR-6916, "Hydraulic Transport of Coating Debris, A Subtask of GSI-191", dated December 2006.
- 96) Bostelman, Jan, and Zigler, Gil, "Failed Coatings Debris Characterization," Prepared for BWROG Containment Group Committee, ITS Corporation, Duke Engineering & Services, July 21, 1998.
- 97) Keeler & Long, Report No. 06-0413, "Design Basis Accident Testing of Coatings Samples for Unit 1 Containment, TXU Comanche Peak SES," dated April 13, 2006.
- 98) I&M Procedure, EHI-5065, Revision 2, "Safety-Related Coatings Program."
- 99) I&M Design Specification, ES-CIVIL-0408-QCN, Revision 3, "Requirements for Material Selection, Surface Preparation, Application and Inspection,"
- 100) I&M Design Specification, ES-CIVIL-0400-QCN, Revision 0, "Procurement, Receipt, Storage and Documentation of Protective Coatings,"

- 101) I&M Procedure, 12-CHP-5021-CCD-011, Revision 4, Change Sheet 3, "Application of Protective Coating to Steel Surfaces in Areas Classified as Coating Service Level I and for Coating Service Level III Lining Applications."
- 102) I&M Procedure, 12-CHP-5021-CCD-012, Revision 4, "Application of Protective Coating to Concrete Floor, Wall, Ceiling and Block Wall Surfaces in Areas Classified as Coating Service Level I."
- 103) I&M Procedure, 12-EHP-5065-SRC-001, Revision 4, "Condition Assessment of Safety-Related Coatings."
- 104) I&M Procedure, 12-EHP-5065-SRC-002, Revision 2, "Management and Evaluation of Nonconforming Coatings."
- 105) I&M Design Specification, DCC-CEST-145-QCN, Revision 6, "Painter Training, Qualification and Certification."
- 106) I&M Procedure, PDP-7040-001, Revision 5, "Qualification and Certification of Inspection, Test, Examination and NDE Personnel."
- 107) EPRI Report No. 1014883, "Plant Support Engineering: Adhesion Testing of Nuclear Coating Service Level I Coatings," dated August 2007.
- 108) Letter from M. W. Rencheck, I&M, to NRC Document Control Desk, "Generic Letter 98-04: Potential for Degradation of the Emergency Core Cooling System and the Containment Spray System After a Loss-of-Coolant Accident because of Construction and Protective Coating Deficiencies and Foreign Material in Containment," AEP:NRC:C0599-01, dated May 21, 1999.
- 109) Letter from J. F. Stang, NRC, to R. P. Powers, I&M, "Donald C. Cook Nuclear Plant, Unit 1 and 2 – Completion of Licensing Action for Generic Letter 98-04, "Potential for Degradation of the Emergency Core Cooling System and the Containment Spray System After a Loss-of-Coolant accident Because of Construction and Protective Coating Deficiencies and Foreign Material in Containment (TAC Nos. MA4038 and MA4039)," dated February 2, 2000 (ML003678845).
- 110) Final NRC SER, Topical Report WCAP-16530-NP, "Evaluation of Post-Accident Chemical Effects in Containment Sump Fluids to Support GSI-191," Pressurized Water Reactor Owners Group, Project No. 694 (ML073520891).
- 111) NRC SER, Topical Report (TR) WCAP-16406-P, Revision 1, "Evaluation of Downstream Sump Debris Effects in Support of GSI-191," Pressurized Water Reactor Owners Group, Project No. 694 (ML073520295).
- 112) I&M Calculation, SD-000727-001, Revision 2, "HELB: Identification of Unit 1 High Energy Lines and Postulation of High Energy Line Breaks."

- 113) S&L Calculation, 2008-00062, Revision 0, "HELB: Jet Impingement and Pipe Whip Evaluation of Generic Safety Issue (GSI)-191 Related Components."
- 114) Westinghouse, WCAP-16406-P, Revision 1, "Evaluation of Downstream Sump Debris Effects in Support of GSI-191," dated August 2007.
- 115) I&M Procedure, 12-MHP-4030-031-001, Revision 10, "Inspection of Recirculation Sumps."
- 116) I&M Procedure, 1-EHP-4030-108-208, Revision 4, "ECCS Flow Balance – Safety Injection System."
- 117) I&M Procedure, 1-EHP-4030-103-208, Revision 13, "Unit 1 ECCS Flow Balance – Boron Injection System."
- 118) I&M Procedure, 2-EHP-4030-208-001, Revision 7, "ECCS Flow Balance – Safety Injection System."
- 119) I&M Procedure, 2-EHP-4030-203-208, Revision 10, "Unit 2 ECCS Flow Balance – Boron Injection System."
- 120) Letter, W. H. Ruland to A. R. Pietrangelo, "Draft Conditions and Limitations for Use of Westinghouse Topical Report WCAP-16793-NP, Revision 0, "Evaluation of Long-Term Cooling Considering Particulate, Fibrous and Chemical Debris in the Recirculating Fluid"," dated February 4, 2008.
- 121) I&M Procedure, PMP-2220-HSK-001, Revision 4, "Housekeeping and Material Condition."
- 122) I&M Procedure, 1-OHP-4030-001-002, Revision 25, "Containment Inspection Tours."
- 123) I&M Procedure, 2-OHP-4030-001-002, Revision 21, "Containment Inspection Tours."
- 124) I&M Procedure, 12-EHP-5201-SPP-001, Revision 0, "Assessment of Containment Debris Sources."
- 125) I&M Procedure, PMP-2220-SPP-002, Revision 0, "Evaluation and Control of Materials Affecting the Containment Recirculation Sump Protection Program."
- 126) I&M Procedure, PMP-2220-001-001, Revision 12, "Foreign Material Exclusion (FME)."
- 127) I&M Procedure, PMP-4010-CAC-001, Revision 9, "Containment Access Control."
- 128) I&M Procedure, PMP-2291-PLN-001, Revision 29, "Work Control Activity Planning Process."

- 129) I&M Procedure, PMP-3010-PDC-001, Revision 18, "Preparing Purchase Requisition(s) from a Material Request(s)."
- 130) I&M Procedure, 12-EHP-5043-ERP-001, Revision 6, "Engineering Review of Procurement Documents."
- 131) I&M Design Specification, ES-CIVIL-0430-QCN, Revision 2, "Requirements for Materials Inside Containment."
- 132) I&M Procedure, OHI-2115, Revision 1, "Labeling Standard."
- 133) I&M Procedure, EHI-5201, Revision 4, "Containment Recirculation Sump Protection Program."
- 134) I&M Procedure, 12-EHP-5040-MOD-009, Revision 16, "Engineering Change Reference Guide."
- 135) I&M Procedure, PMP-2291-OLR-001, Revision 12, "On-Line Risk Management."
- 136) I&M Procedure, PMP-4100-SDR-001, Revision 16, "Plant Shutdown Safety and Risk Management."
- 137) I&M Design Standard, MDS-618, Revision 0, "Containment Insulation Inside the Crane Wall, Below the 650 Ft EI."
- 138) I&M Design Specification, ES-PIPE-1007-QCS, Revision 3, "Thermal Insulation."
- 139) I&M Procedure, 12-CHP-5021-CCD-023, Revision 2, "Thermal Insulation in Containment."
- 140) I&M Containment Structure/System Maintenance Rule Scoping Document, dated June 27, 2002.
- 141) I&M Calculation, MD-12-RCS-027-N, Revision 0, "Refueling Canal Drain Flow."
- 142) I&M Calculation, MD-12-CNTMT-003, Revision 1, "Reconciliation of Head Loss Measured for the Strainer System Test Configuration to the Head Loss for the Recirculation Sump Strainer System Actual Configuration."
- 143) CCI Calculation, 3 SA-096.067, Revision 0, "System Head Loss Calculation."
- 144) Letter from W. H. Ruland, NRC, to A. R. Pietrangelo, NEI, "DRAFT NRC Staff Review Guidance Regarding Generic Letter 2004-02 Closure in the Area of Strainer Head Loss and Vortexing," dated September 2007 (ML0726007425).

- 145) NRC NUREG/CR-6874, "GSI-191: Experimental Studies of Loss-of-Coolant-Accident-Generated Debris Accumulation and Head Loss with Emphasis on the Effects of Calcium Silicate Insulation," dated May 2005.
- 146) Westinghouse, WCAP-16785-NP, Revision 0 "Evaluation of Additional Inputs to the WCAP-16530-NP Chemical Model," dated May 2007.
- 147) S&L Analysis, 2007-11602, Revision 0, "Post-LOCA Chemical Effects Analysis in Support of GSI-191."
- 148) I&M Calculation, SD-070517-001, Revision 1, "D.C. Cook, Units 1 and 2 GSI-191 Containment Building Materials Inventory Calculation."
- 149) Idelchik, I.E., "Handbook of Hydraulic Resistance," 3rd Edition, Begell House, Inc., 1996.
- 150) Letter from J. A. Grobe, NRC, to A. R. Pietrangelo, NEI, "Nuclear Regulatory Commission Request for Additional Information to Pressurized Water Reactor Licensees Regarding Responses to Generic Letter 2004-02," dated November 14, 2006 (ML063110263).
- 151) Letter from W. H. Ruland, NRC, to A. R. Pietrangelo, NEI, "Supplemental Licensee Responses to Generic Letter 2004-02, 'Potential Impact Of Debris Blockage on Emergency Recirculation During Design Basis Accidents at Pressurized-Water Reactors,'" dated November 30, 2007 (ML073320176).
- 152) ALION Calculation, ALION-CAL-AEP-3085-16, Revision 1, "D. C. Cook Units 1 & 2 Summary of Debris Generation and Debris Transport Results."
- 153) I&M Calculation, MD-12-CTS-118-N, Revision 0, "Containment Spray System and Recirculation Sump Minimum and Maximum pH."
- 154) ALION Calculation, ALION-ECR-AEP-3085-001, Revision 0, "Engineering Change Request for ALION-CAL-AEP-3085-12 - D.C. Cook Recirculation Sump Debris Generation Calculation."
- 155) ALION Calculation, ALION-ECR-AEP-3085-002, Revision 0, "Engineering Change Request for ALION-CAL-AEP-3085-15 - D.C. Cook Units 1 and 2 Reactor Building GSI-191 Debris Transport Calculation."
- 156) I&M Calculation MD-01-DR-001-N, Revision 2, "Verify Capacity of CEQ Fan Room Floor Drains."
- 157) I&M Calculation MD-02-DR-001-N, Revision 2, "Verify Capacity of Rerouted CEQ Room Floor Drains."
- 158) NRC RG 1.82, Revision 0, "Water Sources for Long-Term Recirculation Cooling Following a Loss-Of-Coolant-Accident."

- 159) Letter from Westinghouse to PWR Owners Group Systems and Equipment Engineering Subcommittee and PWR Owners Group GSI-191 Point of Contact, OG-06-255, August 7, 2006, "PWR Owners Group Letter Releasing Revised Chemical Model Spreadsheet from WCAP-16530-NP (PA-SEE-0275)."
- 160) Letter from Westinghouse to PWR Owners Group Systems and Equipment Engineering Subcommittee and PWR Owners Group GSI-191 Point of Contact, OG-06-273, August 28, 2006, "PWR Owners Group Method Description of Error Discovered August 16, 2006 in Revised Chemical Model Spreadsheet (PA-SEE-0275)."

ATTACHMENT 2 TO AEP:NRC:8054-02

ABBREVIATIONS AND ACRONYMS

A/E	architect/engineer	FMEA	failure modes and effects analysis
AECL	Atomic Energy of Canada Limited	ft	feet
AEP	American Electric Power	ft abs	feet of water absolute
AISC	American Institute of Steel Construction	ft/s	feet per second
ALION	ALION Science and Technology	ft H ₂ O	feet of water
ANSI	American National Standards Institute	ft WC	feet – water column
ASME	American Society of Mechanical Engineers	g	grams
AWS	American Welding Society	gal	gallon
BWROG	Boiling Water Reactor Owner's Group	GDC	General Design Criteria
°C	degrees centigrade	GL	Generic Letter
CAD	computer aided design	gpm	gallons per minute
Cal-Sil	calcium silicate insulation	GR	NEI 04-07 Guidance Report
CCI	Control Components Incorporated	GSI	Generic Safety Issue
CC	centrifugal charging	HELB	high energy line break
CCW	Component Cooling Water	HSSSS	high safety significance SSCs
CCP	centrifugal charging pump	I&M	Indiana Michigan Power Company
CEQ	hydrogen skimmer/containment pressure equalization	ID	inside diameter
CFD	computational fluid dynamics	in	inches
CFR	Code of Federal Regulations	IOZ	inorganic zinc
CNP	Donald C. Cook Nuclear Plant	IPE	Individual Plant Examination
CRDM	control rod drive mechanism	kg	kilogram
CTS	Containment Spray System	K&L	Keeler and Long, PPG Industries
CVCS	Chemical and Volume Control System	ksi	thousand pounds per square inch
DBA	design basis accident	LBB	leak-before-break
DECL	double ended cold leg	LBLOCA	large break loss of coolant accident
DBE	design basis earthquake	lbm	pounds-mass
DEGB	double ended guillotine break	lbs	pounds
DFT	dry film thickness	LDFG	low-density fiberglass
DGBS	debris generation break size	LOCA	loss of coolant accident
DI	debris interceptor	m	meter
dm ³	cubic decimeters	m ³ /h	cubic meters per hour
DP	Diamond Power	m ³ /s	cubic meters per second
ECCS	Emergency Core Cooling System	MAAP	Modular Accident Analysis Program
EOP	Emergency Operating Procedure	mbar	millibar
EPRI	Electric Power Research Institute	M&E	mass and energy
EQ	environmentally qualified	MFTL	Multi-Functional Test Loop
ESF	engineered safety features	mil	0.001 in
ESW	Essential Service Water	Min-K	micro-porous insulation
°F	degrees Fahrenheit	mm	millimeter
FAI	Fauske and Associates	MPa	mega-Pascals
FME	foreign material exclusion	MSLB	main steam line break
		NEI	Nuclear Energy Institute

NESW	Non-Essential Service Water	TMD	transient mass distribution
NPSH	net positive suction head	TS	Technical Specification
NRC	Nuclear Regulatory Commission	UFSAR	Updated Final Safety Analysis Report
OBE	operating basis earthquake	VCT	Volume Control Tank
OEM	original equipment manufacturer	Wyle	Wyle Laboratories, Incorporated
OPG	Ontario Power Generation	ZOI	zone of influence
ORAM	Outage Risk Assessment and Management		
PORV	power operated relief valve		
ppm	parts per million		
PRA	probabilistic risk assessment		
PRT	pressurizer relief tank		
psia	pounds per square inch - absolute		
psig	pounds per square inch - gauge		
PVC	polyvinyl chloride		
PWR	pressurized water reactor		
PZR	pressurizer		
RAI	request for additional information		
RAT	Risk Assessment Team		
RCP	reactor coolant pump		
RCS	Reactor Coolant System		
RFO	refueling outage		
RG	Regulatory Guide		
RHR	Residual Heat Removal		
RMI	reflective metal insulation		
RNG	renormalized group theory		
ROG	reactor operators group		
rpm	revolutions per minute		
RWST	refueling water storage tank		
s	second or seconds		
SAT	spray additive tank		
SBLOCA	small break loss of coolant accident		
SEM	scanning electron microscope		
SER	NEI 04-07 Safety Evaluation Report		
SG	steam generator		
SI	safety injection		
SIS	Safety Injection System		
S&L	Sargent & Lundy LLC		
SS	stainless steel		
SSC	system, structure, and component		
SSE	safe shutdown earthquake		
S _v	specific surface area		
TBE	thin bed effect		
TKE	turbulent kinetic energy		
TMD	transient mass distribution		

ATTACHMENT 3 TO AEP:NRC:8054-02

SUPPLEMENTAL RESPONSE TO GL 2004-02 AND REQUEST FOR ADDITIONAL
INFORMATION

Table Of Contents

<u>Section</u>	<u>Topic</u>	<u>Page</u>
	Summary-Level Description	2
1.	Overall Compliance	13
2.	General Description of and Schedule for Corrective Actions	14
3.	Specific Information Regarding Methodology for Demonstrating Compliance	
	Background	16
a.	Break Selection	19
b.	Debris Generation/Zone of Influence (ZOI) (excluding coatings)	51
c.	Debris Characteristics	96
d.	Latent Debris	101
e.	Debris Transport	108
f.	Head Loss and Vortexing	176
g.	Net Positive Suction Head (NPSH)	230
h.	Coatings Evaluation	239
i.	Debris Source Term	249
j.	Screen Modification Package	255
k.	Sump Structural Analysis	263
l.	Upstream Effects	272
m.	Downstream Effects - Components and Systems	276
n.	Downstream Effects - Fuel and Vessel	279
o.	Chemical Effects	280
p.	Licensing Basis	308
	Conclusions	311

SUPPLEMENTAL RESPONSE TO GL 2004-02 AND REQUEST FOR ADDITIONAL INFORMATION

This attachment provides I&M's supplemental response to GL 2004-02 (Reference 1) for CNP. This attachment also provides I&M's response to the NRC RAIs transmitted by Reference 5. The supplemental response follows the format and guidance provided by the NRC in Reference 9. All text from Reference 9 is presented in italic script.

NRC Request, Summary-Level Description

The GL supplemental response should begin with a summary-level description of the approach chosen. This summary should identify key aspects of design modifications, process changes, and supporting analyses that the licensee believes are relevant or important to the NRC staff's verification that corrective actions to address the GL are adequate. The summary should address significant conservatisms and margins that are used to provide high confidence the issue has been addressed even with uncertainties remaining. Licensees should address commitments and/or descriptions of plant programs that support conclusions.

Summary-Level Description for CNP

The key aspects of the approach chosen by I&M to resolve the concerns identified in GL 2004-02 are as follows:

- Extensive design modifications to significantly reduce the potential effects of post-accident debris and latent material on the functions of the ECCS and CTS during the recirculation phase of accident mitigation.
- Extensive testing and analysis to determine break locations, identify and quantify debris sources, quantify debris transport, determine upstream and downstream effects, and confirm the recirculation function.
- Use of the Alternate Evaluation methodology as described in Chapter 6 of the GR and SER.
- Changes to the CNP licensing basis, including TS changes, to reflect the plant modifications, and the change to a mechanistic sump strainer blockage evaluation.
- Extensive changes to plant programs, processes, and procedures to limit the introduction of materials into containment that could adversely impact the recirculation function, and establish monitoring programs to ensure containment conditions will continue to support the recirculation function.
- Application of conservative measures to assure adequate margins throughout the actions taken to address the GL 2004-02 concerns.

Additional detail regarding these key aspects is provided below.

Design Modifications

I&M is performing design modifications as described below to address the concerns identified in GL 2004-02. The noted completion dates for modifications that have not yet been installed are in accordance with the extensions documented in Reference 16.

- The recirculation sump trash racks and screens have been replaced in Unit 1 and Unit 2 with pocket style strainers fabricated by CCI. These strainers integrate the trash rack and screen functions while significantly increasing the overall surface area. I&M also provided additional strainer area by installing a strainer in a remote location outside the RCS loop compartment. This remote strainer is connected to the recirculation sump via a sealed waterway. The total recirculation sump strainer area was increased from 85 ft² to 1972 ft². The screen/strainer openings were reduced from nominal 1/4 in square openings to circular openings with nominal diameters of approximately 1/12 in to approximately 3/32 in. The remote strainer has been installed in Unit 2 and will be installed in Unit 1 during the Spring 2008 RFO.
- The recirculation sump vent configuration has been modified in Unit 1 and Unit 2 to ensure the design vent functions would not be inhibited by accident generated debris and that debris larger than the recirculation sump strainer openings would not bypass the strainers. This involved reconfiguring some vent paths and installing covers with openings consistent with the sump strainer openings.
- New level instruments were installed inside the recirculation sump enclosures in Unit 1 and Unit 2. These instruments would alert the operators to a condition in which the head loss across the strainers is such that pump vortex limits may be approached.
- In Unit 1 and Unit 2, debris interceptors have been installed over the drains from the CEQ fan rooms to assure CTS water from these rooms would be available for recirculation. In Unit 2, debris interceptors have been installed on the loop compartment side of the flood-up overflow wall to prevent debris from blocking the flood-up overflow wall openings. This assures sufficient water inventory would be available to the remote strainers. In Unit 1, debris interceptors will be installed on the loop compartment side of the flood-up overflow wall during the Spring 2008 RFO.
- In Unit 2, the five existing 10 inch diameter openings in the flood-up overflow wall have been modified to reduce head loss. Additionally, the radiation shields on the annulus side of the openings were modified to assure water flowing through the openings would not be restricted by small debris. The same modifications will be completed in Unit 1 in the Spring 2008 RFO.
- A blank plate has been installed in the crossover pipe that connects the recirculation sump with the adjacent lower containment sump to prevent debris from bypassing the recirculation sump strainers.

- In Unit 2, an opening was installed on the lower containment sump, and the internals from the check valves in the West CEQ fan room drain lines were removed to ensure any CTS water entering the CEQ fan rooms would flow to the containment sump. The check valve internals had previously been removed from the Unit 2 East CEQ fan room drain line. These modifications were not necessary in Unit 1 due to the existing configuration.
- The Cal-Sil insulation was removed from the PRT and PZR safety and relief valve discharge line in both Units 1 and 2. In Unit 1, LDFG on a non-RCS systems relief valve discharge line to the PRT was removed. The condition did not exist in Unit 2. In Unit 2, the Cal-Sil insulation on the PRT drain line was removed. The condition did not exist in Unit 1. Several hundred tags, labels, and other materials that presented a potentially significant debris source term were removed from Unit 1 and Unit 2. Additional labels will be removed during the Unit 1 Spring 2008 RFO.

Testing

I&M has completed extensive plant-specific testing of the new recirculation sump strainer design, the effects of chemical reactions on post-accident strainer head loss, the debris generation behavior of several potential debris sources when subjected to a high pressure, high temperature two-phase jet, and the erosion behavior of selected insulation materials when subjected to spray and pool transport. I&M will be completing testing for determination of the potential failure modes and quantities of cold galvanizing compound under DBA conditions.

I&M participated in the performance of an initial series of strainer head loss tests at CCI in late Fall 2005. This testing was based on preliminary debris generation and transport quantities. The testing confirmed the adequacy of the approach that had been selected by I&M for resolution of GL 2004-02 concerns.

I&M participated in strainer head loss, strainer bypass, and chemical effects tests at CCI in 2007. These tests involved the debris quantities from both the DEGB and DGBS. These tests conservatively used scaled, equivalent strainer areas for the main strainer and the remote strainer, including the use of sacrificial strainer surface area. For the DEGB test with debris quantities and flow rates established at 100%, the measured head loss was approximately 0.77 ft H₂O. For the DGBS test using the same test approach as the DEGB test, the measured head loss was approximately 0.43 ft H₂O.

Sensitivity tests were also performed to determine the effects of debris arrival sequence and the anticipated event sequence for CNP. For the debris arrival sequence tests, the flow rate was established at the 100% value and debris was added in the following order: fibrous debris, Cal-Sil and Marinite, particulates, and RMI. Following each debris addition, the system was allowed to recirculate until at least five pool turnovers (approximately 15 minutes) had occurred prior to the next debris addition. For the DEGB test, the measured head loss was approximately 0.39 ft H₂O. For the DGBS test, the measured head loss was approximately 0.13 ft H₂O. For the event sequence tests, the test sequence was established to model as closely as possible the extent of debris loading of the main strainer during pool fill, followed by the addition of debris to both the main and remote strainers to establish the expected 100% debris quantities with sequential increases in flow rate to 100% equivalent flow. For the DEGB test, the measured

head loss was approximately 0.72 ft H₂O at the end of the test. For the DGBS test, the measured head loss was approximately 0.67 ft H₂O, at the end of the test.

Based on the testing performed, and after normalizing the values to 20°C, the baseline DEGB head loss was established at 0.94 ft H₂O, and 0.47 ft H₂O for DGBS. The values conservatively bound the results of the 100% debris quantity and flow rate test and the results of the sensitivity tests. These test results were then used as input to a calculation (Reference 142) to establish strainer system head loss values since the tested configuration did not match the installed plant configuration. The results of this calculation determined the system head loss, normalized to 20°C, for the DEGB case was 1.046 ft H₂O, and 0.819 ft H₂O for the DGBS case. To address uncertainty and provide margin, the calculated system head loss values for the DEGB and DGBS cases will be increased by a factor of 1.5. This results in a debris-only strainer system head loss of 1.57 ft H₂O for the DEGB case, and 1.23 ft H₂O for the DGBS case.

I&M participated in CCI chemical effects testing, performed in accordance with the intent of the methodology provided in WCAP-16530-NP, prior to NRC approval. This testing determined that the head loss across the most heavily debris loaded strainer (the main strainer) increased by approximately 43% during the DEGB test and approximately 53% during the DGBS test. Due to the CNP main and remote strainer configuration, only the main strainer and its expected debris loads were tested in the chemical effects test performed in the MFTL. I&M intends to conservatively apply the head loss associated with chemical effects test to the debris only head loss results, by use of a factor of 1.7, in lieu of the percentage increase determined during the testing. The final determination will be made following receipt of the 30 Day Integrated Chemical Effects test results described below and completion of supplementary analysis being performed by CCI to resolve NRC questions.

I&M had ALION conduct a CNP-specific 30 Day Integrated Chemical Effects test at the Vuez test facility in the large loop. I&M will provide the results of this testing following receipt of the associated ALION report. I&M will provide these results per the schedule provided in the response to Information Item 2, in accordance with the extension granted, per Reference 16.

I&M participated in testing at Wyle to determine the effects of high pressure, high temperature, two-phase jets on potential debris sources that exist in the CNP containments. The following materials were tested with 2200 psig, 520°F blowdown jets lasting approximately 30 seconds: Marinite fire barrier boards attached to cable tray sections, single and double stainless steel jacketed Armaflex insulation installed on a carbon steel pipe section, Scotch 77 fire barrier tape applied to a section of rigid conduit, and Electromark Series 1000 labels attached to stainless steel backing material. This testing established conservative debris generation quantities with appropriate ZOIs for the Marinite, fire barrier tape, and Electromark labels. The testing of the Armaflex established a configuration which resulted in no debris being generated.

Under contract to I&M, ALION performed dissolution and erosion testing of the Cal-Sil insulation and one type of the Marinite fire boards installed at CNP. The results of this testing conservatively established that 17% of the associated large and small pieces would be reduced to fines following debris generation.

I&M has contracted with K&L to perform DBA testing of cold galvanizing compound applied to prototypical configurations of galvanized steel. This testing is being conducted to determine if

the quantity of cold galvanizing compound that has been calculated to fail within the CNP containment is overly conservative. A reduction in the assumed quantity of the associated debris would provide available margin for sump strainer head loss, and would also be used to reduce the quantity of particulate assumed to pass through the strainer. The quantity of particulate passing through the strainer is an input to the downstream effects analyses that are currently in progress.

Through the USA utilities group, I&M supported testing performed by Westinghouse to determine an appropriate, but conservative ZOI for qualified coatings in containment.

Analyses

I&M has had comprehensive and conservative mechanistic analyses performed to address the concerns identified in GL 2004-02. These analyses are summarized below.

I&M has had the following analyses performed by ALION to identify the potential sources, transport mechanisms, and hydraulic concerns regarding the effect of debris on the ECCS and CTS recirculation functions following a LOCA:

- Characterization and sequence of events associated with sump recirculation.
- Debris generation.
- Debris transport.
- Summary of debris generation and debris transport results (determination of limiting break location).
- Containment recirculation sump hydraulic analysis.
- Marinite 36 fire barrier material property comparison.

The debris transport analysis was conservatively performed such that the sum of the debris transport fractions for many of the debris sources was greater than 1.0, and in some cases as high as 1.3. This was necessary because the head loss associated with a particular debris loading on the main strainer could not be precisely defined.

In support of these analyses, I&M performed multiple walkdowns of containment during several previous outages to document the location of actual and potential debris sources. The calculations to quantify the debris sources in containment were performed such that the results are conservatively bounding.

I&M has had analyses performed to structurally qualify the new main and remote strainers accounting for appropriate combinations of the following loads:

- Dead weight loads.
- Thermal loads.
- Seismic loads.
- Nozzle loads from the waterway.
- Hydraulic loads.
- Hydrodynamic loads.
- Hydrostatic loads.

- Recirculation hydraulic loads.
- Debris loads.
- Short term pressure pulse loads.

These analyses were performed by CCI.

I&M has had the other plant modifications conservatively qualified to meet the current CNP design and licensing basis and the new design and licensing basis that will include the mechanistic evaluation of the effect of post-accident debris on the ECCS and CTS recirculation function as described in this letter. The qualification calculations were performed by the A/E for the plant modifications, S&L.

I&M has had evaluations performed to ensure required components that support the recirculation function will not be subject to pipe whip or jet impingement loads from high energy piping breaks. The evaluations did not consider a HELB from the RCS loop piping since I&M has been granted a LBB exemption for this piping, per Reference 21. These evaluations were performed by S&L.

I&M has had an evaluation performed of ex-vessel recirculation path blockage from debris laden fluid in accordance with WCAP-16406-P, Revision 0 (Reference 23). This evaluation considered potential blockage in valves, orifices, heat exchangers, etc., in the recirculation flow path downstream of the strainers. This evaluation conservatively assumed a strainer opening size of 1/8 in which is larger than the installed strainer openings of nominal 1/12 in, maximum 3/32 in. The evaluation was performed by Enercon, under contract to Westinghouse.

I&M is having evaluations performed of ex-vessel wear, abrasion, erosion, and pump blockage using the guidance of WCAP-16406-P, Revision 1, as clarified and accepted by the associated NRC Safety Evaluation Report. I&M will provide the results of these evaluations per the schedule provided in Information Item 2, in accordance with the extension granted per Reference 16. These evaluations are being performed by S&L.

I&M is having analyses performed of the in-vessel blockage, localized debris buildup, and plate-out. This evaluation is being performed in accordance with WCAP-16793 using the LOCADM analysis methodology. I&M will provide the results of these analyses per the schedule provided in Information Item 2, in accordance with the extension granted per Reference 16. These analyses are being performed by Westinghouse.

Alternate Evaluation Methodology

The Alternate Evaluation Methodology identified in the GR and SER (Reference 17) requires that mitigative capability be demonstrated for the DEGB. One of the methods that can be used to demonstrate mitigative capability is performing flow reductions to reduce the head loss across the strainer. I&M has installed fully qualified, RG 1.97 level switches inside the recirculation sump to alert the operators to a condition in which the head loss across the strainers is such that vortex limits may be approached. As previously discussed in Reference 12, and acknowledged by the NRC in Reference 14, EOPs would direct operators to remove up to one train of CTS and ECCS from service to restore level inside the recirculation sump upon receipt of an alarm in the Control Room from these level switches.

The effectiveness of such flow reductions was demonstrated by debris-only head loss testing performed at CCI. As part of the testing, a flow reduction sequence was performed following a 24-hour period of 100% equivalent flow and debris operation. The flow reduction sequence determined that by reducing flow equivalent to stopping one CTS pump (23.6% flow reduction), the head loss across the strainer decreased by approximately 38%. When flow was further reduced by the equivalent flow of a second CTS pump, head loss across the strainer decreased such that the change in head loss from the 100% flow condition was approximately 66%.

The strategy of securing CTS and ECCS pumps to reduce flow and, thereby reduce strainer head loss has been addressed with respect to single failure concerns. The CNP licensing basis for single failure criteria requires assumption of an active failure during the injection phase, or an active or passive failure during the recirculation phase. In the unlikely event that the operating pump in the system containing the pump that was secured to reduce head loss failed, the pump that had been secured could be restarted to restore the function.

Additionally, the assumed limiting single failure for the sump inventory analysis is the failure of one of the two CEQ fans. If this failure is not assumed, the resulting minimum containment water level would be higher than is currently assumed. This would result in a greater allowable head loss across the strainer. Since the CNP licensing basis does not require assumption of multiple failures, a failure of an operating pump following a failure of a CEQ fan would be considered to be a beyond design basis condition.

Changes to the Licensing Basis

I&M has initiated changes to the CNP UFSAR to recognize the plant modifications performed to address the concerns identified in GL 2004-02. These changes have been, and will be, made effective as the associated modifications are completed.

I&M has obtained NRC approval of TS changes that reflect the GL 2004-02 related plant modifications and provide new Surveillance Requirements as necessary to assure that important components are operable to support the recirculation function. In accordance with the requirements of the associated amendment request, these new TS requirements have been implemented for Unit 2 and will be implemented for Unit 1 prior to entry into Mode 4 at the end of the Spring 2008 Unit 1 RFO.

I&M intends to change the licensing basis to reflect the mechanistic evaluation of the effect of post-accident debris on the ECCS and CTS recirculation function as described in this letter. I&M intends to implement this licensing basis change by May 31, 2008, which is in accordance with the extension approved by Reference 16.

Improvements in Processes and Programs

I&M has significantly improved or created process and program requirements to ensure the analysis inputs and assumptions can be maintained. The changes include:

- Development of a station procedure outlining the attributes of the Containment Recirculation Sump Protection Program and responsibilities for ensuring compliance with the specified requirements.
- Development of an engineering program for the containment recirculation sump function including requirements for monitoring and assessment of containment debris sources during RFOs.
- Changes to the Engineering Change process to ensure that design changes to any SSC inside containment or associated with the recirculation flow path are evaluated to ensure they support the resolution of GL 2004-02 concerns.
- Changes to the procedures that control entry into containment during periods when the recirculation function is required to be operable.
- Changes to the Safety Related Coatings Program procedures to require extent of condition evaluations and determination of the probable failure mode of any identified failure of the qualified coatings.
- Changes to the labeling procedure to prevent the introduction of unqualified labels.
- Improvements to the containment closeout procedure to identify potential debris sources and appropriate actions.
- Changes to the engineering design specification that specifies the requirements for materials in containment to support resolution of GL 2004-02 concerns.
- Changes to the procedure for purchase requisitions to ensure material ordered for containment is identified and conforms to requirements for materials in containment.
- Changes to the procedure for engineering review of procurement documents to ensure that the requirements for materials in containment are identified to suppliers when necessary.
- Changes to engineering design specifications and standards for the labeling of cables, conduits, and cable trays in containment, installation of fire barrier materials in containment, and installation of insulation materials in containment.

I&M will maintain the necessary programmatic and process controls, such as those described above, to ensure the ECCS and CTS recirculation functions are maintained in accordance with the applicable regulatory requirements identified in GL 2004-02.

I&M is continuing to evaluate programs and processes to ensure that requirements necessary to support resolution of GL 2004-02 concerns will be in place when the licensing basis is changed to reflect the mechanistic evaluation of the effect of post-accident debris on the ECCS and CTS recirculation function as described in this letter.

Conservatisms and Margins

I&M applied conservative measures to assure adequate margins throughout the actions taken to address the GL 2004-02 concerns. The key areas in which these conservative measures were applied are summarized below.

Debris Generation

- I&M conservatively assumed that 100% of all unqualified coatings have failed by the time recirculation is initiated following a LOCA.
- I&M conservatively calculated the total quantity of unqualified coatings by assuming greater coating thicknesses and surface areas than likely exist in containment.
- I&M assumed a conservative value for the quantity of debris generated and the associated ZOI with respect to the destructive test results documented in Reference 30 for the associated materials.
- I&M conservatively applied a ZOI of 5D for qualified coatings within a ZOI in lieu of 4D, recommended by Reference 87.

Latent Debris

- I&M conservatively assumed a bounding quantity of latent debris in containment of 200 lbs with respect to the quantity determined by sampling during walkdowns.
- I&M conservatively assumed 15% of the latent debris to be fiber, per the SER, even though there is very little fiber insulation in the CNP containments, and none in an area that would be subjected to jet impingement from an event that would lead to recirculation.
- I&M conservatively assumed the available sacrificial strainer areas to be 76 ft² for the main strainer and 83 ft² for the remote strainer. This provides a margin of approximately 50 ft² for the main strainer and 54 ft² for the remote strainer based on the bounding quantity of material that was determined to be at the strainers, i.e., approximately 26 ft² and 29 ft², respectively.

Debris Transport

I&M conservatively assumed that:

- Unqualified labels and PVC jacketing would be transported the same as readily transportable fines.
- Debris in the sump pool would not be transported to the reactor cavity while it was filling through the nuclear instrumentation positioning device penetrations.
- All debris in, or blown into, the ice condenser would wash back into the containment pool.
- There would be no debris hold-up on containment equipment or structural elements as a result of transport from the initial blowdown, or during washdown.
- Water falling from the break would enter the pool without impacting any interferences, maximizing the pool turbulence and providing for greater debris transport potential.
- 100% of the debris sources in upper containment would fail and be transported to the area of the refueling canal drains.
- Debris that had not been transported to the annulus or into the main strainer during pool fill would be available for transport to the main strainer during recirculation.

Additionally, a significant number of the debris sources were conservatively assigned transport fractions for the main and remote strainer, that when added together, resulted in a

greater quantity of debris available for transport than would exist in the active containment pool.

Head Loss and Vortexing

- The head loss results from strainer testing were conservatively normalized to 20°C (68°F), which is below the expected minimum sump temperature of 80° to 100°F.
- A multiplier of 1.5 was conservatively applied to the calculated system head loss for the DEGB and DGBS that was based on the large scale strainer test results. This multiplier provided a margin of 0.524 ft H₂O for system head loss for the DEGB, and a margin of 0.41 ft H₂O for the DGBS.
- The head loss analysis conservatively assumed the water level in containment was at its minimum water level at the time of maximum head loss.
- The vortex analysis conservatively evaluated the potential for formation of a vortex assuming the water surface being evaluated was in the same chamber of the sump as the suction piping for the recirculation sump, even though the water surface would actually be in the front chamber of the recirculation sump (flowing area) and the vent pipe (non-flowing area).
- Conservatively high flow rates were assumed for the ECCS and CTS while on recirculation. A reasonably assumed 10% reduction in flow would result in an approximate 15% reduction in head loss.

The containment water level analysis that established the minimum water level for containment included several conservatisms.

- The assumed mass and energy release from the RCS summed the contribution of water and steam flows leaving the RCS and assumed a thermodynamic equilibrium for this mixture. This maximized the water enthalpy and minimized the steam released to the containment atmosphere, thereby minimizing the contribution of ice melt to the sump water inventory.
- The assumed actuation setpoint for CTS was biased low such that CTS would provide a greater contribution to cooling the containment atmosphere.
- The assumed CEQ fan flow was biased low to minimize flow through the ice condenser and thereby minimize the contribution of ice melt to the sump water inventory.
- CTS was assumed to remain in service until a low biased reset point was reached.
- The volumes of the annulus and loop compartment were modeled without displacement from internal structures. Including a conservatively low volume for this displacement would provide an additional 2.2 in to the minimum water level.
- Input parameters were conservatively assumed to be at a value that would minimize ice melt.
- Assumed hold-up volumes were conservatively biased high to minimize water available for the containment sump pool.

NPSH

A water temperature of 190°F was used in the determination of NPSH margin for the pumps that take suction on the recirculation sump even though this temperature would exist for only a short duration at the beginning of recirculation.

Downstream Effects – Components and Systems

In the completed portion of this evaluation, it was conservatively assumed that the size of the openings in the strainer was 33% larger than the size of the actual maximum strainer opening.

Chemical Effects

- A bump-up factor of 1.7 was applied to the results of the chemical effects testing rather than the determined maximum increase of 1.53.
- The test specification for the DGBS test conservatively used the values for chemical addition that were determined for the DEGB test. This resulted in the addition of non-aluminum chemicals of nearly three times the 100% value.
- The pH values used for determination of the chemical precipitates were conservatively biased higher than the values expected in the post accident containment pool.
- In the analysis to determine the amount of precipitate formed by the reaction between aluminum in containment and CTS spray, it was assumed that 100% of the RCP motor air cooler aluminum fins were subjected to the spray. However, due to the configuration of the fins and the primarily vertical direction of the spray flow, it is unlikely that the spray would reach all fins in the coolers. It is likely that 30% or more of the fins would not be subjected to the spray.

NRC Request - 2006 RAI

Licensees should ensure that GL supplemental response information fully address issues identified in the RAIs provided to each licensee in early 2006. A separate response to the RAIs is not necessary if they are appropriately addressed in the GL supplemental response.

I&M Response to 2006 RAI

The 2006 RAIs (Reference 5) are addressed in this attachment to the extent that supporting activities have been completed. Attachment 6 to this letter lists each RAI question in Reference 5 and provides a reference to the section of Attachment 3 in which the requested information is provided, and/or provides other information to address the question.

NRC Information Item 1 Overall Compliance:

Provide information requested in GL 2004-02 Requested Information Item 2(a) regarding compliance with regulations.

GL 2004-02 Requested Information Item 2(a)

Confirmation that the ECCS and CSS [CTS at CNP] recirculation functions under debris loading conditions are or will be in compliance with the regulatory requirements listed in the Applicable Regulatory Requirements section of this GL. This submittal should address the configuration of the plant that will exist once all modifications required for regulatory compliance have been made and this licensing basis has been updated to reflect the results of the analysis described above.

I&M Response to Information Item 1**Confirmation**

By May 31, 2008, I&M will complete all necessary analyses and update the CNP licensing basis to reflect that the ECCS and CTS recirculation functions under debris loading conditions are in compliance with the regulatory requirements listed in the Applicable Regulatory Requirements section of GL 2004-02. I&M has completed all associated plant modifications in Unit 2, and will complete the associated modifications in Unit 1 by the end of the Spring 2008 RFO.

Applicable Regulatory Requirements

The applicable regulatory requirements identified in GL 2004-02 are:

- 10 CFR 50.46 "Acceptance Criteria for Emergency Core Cooling Systems for Light-Water Nuclear Power Reactors"
- 10 CFR 50.67 "Accident Source Term"
- 10 CFR 100 "Reactor Site Criteria"

For plants not licensed to the GDC in 10 CFR 50, Appendix A, such as CNP, the applicable regulatory requirements include plant specific design criteria in their licensing basis similar to the following: Criterion 35, "Emergency Core Cooling," Criterion 38, "Containment Heat Removal," Criterion 41, "Containment Atmosphere Cleanup."

Plant Configuration

The plant modifications that have been completed in Unit 2 and will be completed in Unit 1 include: replacement of recirculation sump trash racks and screens with pocket-style strainers, installation of a remote pocket-style strainer assembly, creation of a waterway between the remote strainer and the recirculation sump, installation of level instruments in the recirculation sump, reconfiguration of sump vents, installation of debris interceptors at key locations, modification of various flowpaths, and removal of significant debris sources.

NRC Information Item 2. General Description of and Schedule for Corrective Actions:

Provide a general description of actions taken or planned, and dates for each. For actions planned beyond December 31, 2007, reference approved extension requests or explain how regulatory requirements will be met as per Requested Information Item 2(b). (Note: All requests for extension should be submitted to the NRC as soon as the need becomes clear, preferably not later than October 1, 2007.)

GL 2004-02 Requested Information Item 2(b)

A general description of and implementation schedule for all corrective actions, including any plant modifications, that you identified while responding to this GL. Efforts to implement the identified actions should be initiated no later than the first refueling outage starting after April 1, 2006. All actions should be completed by December 31, 2007. Provide justification for not implementing the identified actions during the first refueling outage starting after April 1, 2006. If all corrective actions will not be completed by December 31, 2007, describe how the regulatory requirements discussed in the Applicable Regulatory Requirements section will be met until the corrective actions are completed.

I&M Response to Information Item 2

The corrective actions to address the concerns identified in GL 2004-02 at CNP consist of plant modifications, testing and analysis, changes to plant programs and processes, and changes to the licensing basis. These actions are described in the summary-level description starting on page 2 of this attachment. The schedule for completion of these actions is provided below. Although not part of the corrective actions, the schedule for submittal of a final response to GL 2004-02 is also provided.

Plant Modifications

The plant modifications needed to address the GL 2004-02 concerns were completed in Unit 2 during the Fall 2007 RFO, which ended November 6, 2007. Except as approved by References 13 and 16, these modifications were completed in Unit 1 during the Fall 2006 RFO, which ended November 13, 2006. As approved by References 13 and 16, certain Unit 1 modifications will be completed prior to entry into Mode 4 at the end of the Spring 2008 RFO. These modifications are installation of a remote strainer and waterway, and associated modifications involving overflow wall flow openings, overflow wall radiation shields, overflow wall debris interceptors, and removal of labels and other debris sources.

Testing and Analyses

Except as approved by Reference 16, the testing and analyses needed to address GL 2004-02 concerns were completed by December 31, 2007. As approved by Reference 16, certain analyses will be completed prior to May 31, 2008. These analyses are the downstream effects analysis and the 30-day integrated chemical effects analysis.

Plant Programs and Processes

The program and process changes identified to date as necessary to address the GL 2004-02 concerns were completed by December 31, 2007.

Licensing Basis

The licensing basis changes needed to address the GL 2004-02 concerns consist of UFSAR changes related to the plant modifications described in the summary-level description starting on page 2 of this attachment, TS changes related to those plant modifications, and a licensing basis change to reflect the mechanistic evaluation of the effect of post-accident debris on the ECCS and CTS recirculation functions.

The UFSAR changes related to the Unit 2 GL 2004-02 plant modifications were made effective during the Fall 2007 RFO, which ended November 6, 2007. Except as approved by Reference 16, the UFSAR changes related to the Unit 1 GL 2004-02 plant modifications were made effective during the Fall 2006 RFO, which ended November 13, 2006. As approved by Reference 16, the UFSAR changes related to certain Unit 1 GL 2004-02 modifications will be made effective prior to entry into Mode 4 at the end of the Spring 2008 RFO. These GL 2004-02 modifications are identified above under "Plant Modifications."

The TS changes related to the GL 2004-02 plant modifications were implemented for Unit 2 prior to entry into Mode 4 during the Fall 2007 RFO, which ended November 6, 2007. In accordance with Reference 14 and Reference 16 the TS changes related to the GL 2004-02 plant modifications will be implemented for Unit 1 prior to entry into Mode 4 at the end of the Spring 2008 Unit 1 RFO.

In accordance with Reference 16, the CNP licensing basis will be changed to reflect the mechanistic evaluation of the effect of post-accident debris on the ECCS and CTS recirculation function by May 31, 2008.

Final Response

In accordance with Reference 9, a final response to GL 2004-02 will be submitted within 90 days of completion of all actions. As indicated above, all actions will be completed by May 31, 2008.

3. Specific Information Regarding Methodology for Demonstrating Compliance:

Background Information

To facilitate understanding of the methodology for demonstrating compliance with the applicable regulations, I&M has provided background information regarding the design of the CNP containment, and the manner in which the modified containment will function to address GL 2004-02 concerns.

CNP Containment Design

The CNP ice condenser containment consists of four uniquely defined and separated volumes: 1) upper containment, 2) ice condenser, 3) lower containment, and 4) reactor cavity. Refer to Attachment 4, Figures A4-2 through A4-10 for illustrations of various views of lower containment and a plan view of upper containment.

The upper containment area (Figure A4-2), which does not contain any high energy piping, is physically separated from the lower compartment by the divider barrier and the ice condenser.

The ice condenser forms an approximate 300° arc around containment between the containment wall and the crane wall. The ice condenser has 24 paired doors in the lower containment area that will open following a pipe break allowing for suppression of the initial pressure surge in containment. There are also doors just above the ice bed and at the top of the ice condenser section to allow steam and non-condensable gases to vent to the upper containment volume.

The lower containment volume contains both the loop compartment inside the crane wall and the annulus area between the crane wall and the containment wall. The crane wall that separates these two regions is three feet thick. There are ventilation openings in the crane wall which are above the maximum flood elevation of containment. These ventilation openings provide for the supply of cooled air to the loop compartment from the containment lower ventilation units, and also provide a relief path for the mass and energy release (TMD) from a HELB for short term containment subcompartment pressurization considerations. Within the loop compartment above nominal elevation 648 ft are the SG and PZR enclosures. These enclosures utilize the crane wall as one part of the enclosure with cylindrical concrete walls forming the rest of the enclosures. Each of these enclosures has a concrete roof, the top of which is at nominal elevation 695 ft. The cylindrical wall sections and the roof comprise a portion of the divider barrier separating the lower containment from the upper containment. The loop compartment is surrounded on its outside perimeter by the crane wall. The primary shield wall and refueling cavity walls are on the inside perimeter of the loop compartment. The nominal distance from the primary shield wall to the crane wall varies from 22 to 23 ft. The nominal distance from the crane wall to the containment wall is 13 ft.

The final volume, the reactor cavity, is the volume that is below (the lower reactor cavity), above (the upper reactor cavity), and around the reactor vessel (annular area). The upper reactor cavity is bounded by the primary shield wall, the vertical bulkheads, and the CRDM

missile shields. The primary communication path between the lower reactor cavity and lower containment via the overflow wall exists only after water level in either of the volumes exceeds the 610 ft elevation. This level is approximately 11.2 ft above the lower containment floor (where the recirculation sump strainers are located) and approximately 42.3 ft above the lower reactor cavity floor. A secondary communication path exists between the loop compartment and the lower reactor cavity. This path is through the sleeves in the primary shield wall that contain the hardware to position the ex-core nuclear instrumentation in the operating or maintenance positions. The containment liner is attached to the exterior containment wall concrete.

Event Sequence

All postulated pipe break LOCAs for which sump recirculation would be required would take place within the loop compartment, which is the area inside the crane wall, or in the reactor cavity. For an LBLOCA, once water level in the loop compartment exceeds approximately 4 in during the injection phase, debris laden water would begin to flow through the main strainer into the recirculation sump. When the level in the recirculation sump reaches slightly above floor level (598 ft 9 3/8 in elevation), strained water from the recirculation sump would begin to flow through the waterway toward the remote strainer. Initially, this would only fill the waterway until the water level reaches approximately 8 1/2 in above the floor, the height of the lowest set of strainer elements in the remote strainer. When the loop compartment water level exceeds this height, strained water would begin back-flowing out of the remote strainer. A significant quantity of debris laden fluid would be transported to the main strainer, partially loading it with debris. During this pool fill (injection) phase, the calculated maximum reverse flow rate is approximately 6400 gpm (Reference 27).

Debris laden water would also flow from inside the loop compartment to the debris interceptor installed to protect the 10 in diameter flow holes through the overflow wall. This flow into the area between the overflow wall and the curb at the annulus side of the crane wall opening would continue until the level reached approximately 12 in above the floor. This is the height of the curb on the annulus side of the overflow wall area. By the time this level is reached, water flow out of the remote strainer would have been established.

Actuation of CTS in containment would have occurred when lower containment pressure reached a nominal 2.9 psig. CNP's design has CTS spray in the upper containment volume, loop compartment, and annulus region. The CTS spray in the containment upper compartment would primarily return to the loop compartment via the three drains in the lower refueling cavity. Some of the spray would also flow to the two CEQ fan rooms. The water would drain through the new debris interceptors covering the drain line openings and down the CEQ fan room drain lines. In Unit 1, the CEQ fan room drain lines lead to the annulus drain system which flows to the annulus pipe tunnel sump. The pipe tunnel sump contains a flow opening to allow water to flow into the lower containment annulus region. In Unit 2, the CEQ fan room drain lines lead to the lower containment sump. The lower containment sump contains a flow opening to allow water to flow into the loop compartment.

When the RWST reaches 20% level (approximately 18 to 20 minutes after the LBLOCA), the operators will manually initiate recirculation core and containment cooling flow. This sequence, as described in CNP's UFSAR (Section 6.2.2), results in the securing of the low

head RHR, and CTS pumps. The intermediate head SI pumps and high head CCPs continue to draw from the RWST and inject into the RCS. The RHR and CTS pumps are realigned to take suction from the recirculation sump. At the time of initiation of recirculation flow, the water level in lower containment is approximately 7.7 ft above the floor (606 ft 6 in). Once water level in the RWST decreases below 11%, the SI and CCPs are realigned to receive their suction from the RHR pumps (piggyback mode).

With recirculation flow established, the reverse flow through the remote strainer will cease. Water will then flow into the sump through both the main strainer and through the remote strainer and waterway. Since a pipe break requiring recirculation would not occur in the annulus, the debris that would be available to the remote strainer would be the debris that was transported from the loop compartment to the annulus region from the initial blowdown, the debris that was transported to the annulus region through the overflow wall flow holes during pool fill, and latent debris resident in the annulus prior to the event. As a result, the remote strainer(s) would be essentially debris free at the beginning of recirculation. Due to the waterway head loss, the preferential flow path would be through the main strainer until the main strainer became substantially blocked by debris. The division of flow between the main and remote strainers would therefore be a function of the head loss through the associated strainer and the waterway.

Water level in lower containment would decrease from the level that existed at the beginning of recirculation flow (7.7 ft) until the minimum water level of 5.9 ft above the floor (604 ft 7 in) is reached approximately 9.1 hours into the event. This decrease in water level is the result of a conservatively assumed minimum ice melt and the flow into the lower reactor cavity via the ex-core nuclear instrumentation position device sleeves in the primary shield wall.

A cross-section view of CNP's recirculation sump is provided in Attachment 4, Figure A4-1. CNP's sump is a fully vented sump in that the vent extends above the maximum predicted containment flood elevation for both units. The absolute limit for continued operation of the recirculation sump to satisfy core and containment cooling requirements is the prevention of significant air entrainment in the suction piping supplying the ECCS and CTS pumps. This means that the rear chamber of the recirculation sump must remain essentially water solid to prevent slugging air into the suction pipes exiting the sump, and significant air entraining vortices must not develop within the recirculation sump that would allow the transport of gas bubbles to these same suction pipes. With the rear chamber and a portion of the vent pipe remaining full of water, the potential for a gas intrusion event originating in the sump and challenging the operation of the pumps is negligible. The minimum level in the recirculation sump to ensure NPSH required for the most limiting pump is at approximately 2 ft below the centerline of the suction piping at its connection to the recirculation sump. As stated above, a water level this low would result in significant air entrainment into the operating pumps.

NRC Information Item 3.a - Break Selection

The objective of the break selection process is to identify the break size and location that present the greatest challenge to post-accident sump performance.

- 1. Describe and provide the basis for the break selection criteria used in the evaluation.*
- 2. State whether secondary line breaks were considered in the evaluation (e.g., main steam and feedwater lines) and briefly explain why or why not.*
- 3. Discuss the basis for reaching the conclusion that the break size(s) and locations chosen present the greatest challenge to post-accident sump performance.*

I&M Response to Information Item 3.a.1

The break selection process consisted of determining the size and location of the HELBs that would produce debris and potentially challenge the performance of the recirculation sump strainer. The break selection process required evaluating a number of potential break locations in order to identify the location that would be likely to present the greatest challenge to post-accident sump performance. The debris inventory and the transport path were both considered when making this determination.

Section 3.3.4.1 in the GR recommends that a sufficient number of breaks in each high-pressure system that rely on recirculation be considered to ensure that the breaks that bound variations in debris generation by the size, quantity, and type of debris are identified. The following break locations were considered:

- Break No. 1: Breaks in the RCS with the largest potential for debris.
- Break No. 2: Large breaks (with two or more different types of debris). Large breaks are defined in CNP UFSAR Section 14.3 as breaks with greater than a 1.0 ft² cross sectional area. This equates to a guillotine break of a 14 in or greater ID pipe.
- Break No. 3: Breaks in the most direct path to the sump.
- Break No. 4: Large breaks with the largest potential particulate debris to insulation ratio by weight.
- Break No. 5: Breaks that generate a "thin bed" – i.e., high particulate with 1/8 in fiber bed.

Only those line breaks that require the recirculation sump function were evaluated. A review of accident analyses and operational procedures was performed to determine the scenarios that require the recirculation sump function. This review determined that LBLOCAs and certain SBLOCAs require the sump function.

A review of the flow diagrams associated with the RCS was performed to identify those large bore lines directly attached to the RCS (up to the first normally closed manual isolation valve, second automatic isolation valve, and first check valve). The LBLOCA lines to be evaluated for debris generation were determined to be (See Attachment 4, Figure A4-11):

- 31 in RCS crossover line from the bottom of the RCPs down to the 603 ft 8 1/4 in elevation and up to the SG cold leg nozzles.
- 29 in RCS hot leg at the 614 ft elevation.
- 27 1/2 in RCS cold leg at the 614 ft elevation.

- 14 in PZR surge line from RCS loop 3 hot leg piping at the 614 ft elevation to the bottom of the PZR at the 625 ft 9 in elevation.
- 14 in RHR suction line from RCS loop No. 2 hot leg piping connection up to the first isolation valve which is closed with motive power removed except when on shutdown cooling.

The CNP UFSAR classifies SBLOCAs as the break of any RCS piping in excess of the capacity of a CCP (approximately 0.375 in diameter hole) but less than 1.0 ft² total cross sectional area. An SBLOCA must be considered for debris generation because it may not be isolable and may lead to recirculation. In accordance with Section 3.3.4.1, Item 7, of the GR and the SER, only SBLOCA lines 2 in diameter and larger (but less than 14 in diameter) up to the first isolation point were included in the evaluation. The isolation point was defined as a single passive component (such as a normally closed manual isolation valve or a check valve) or two active automatic isolation valves. Consistent with the CNP single failure criteria, check valves were considered as passive components. A review showed that all SBLOCA locations that required evaluation were inside the crane wall. The SBLOCA lines to be evaluated for debris generation were determined to be (see Attachment 4, Figures A4-11 through A4-13):

- 10 in diameter RHR lines from the RCS cold legs to the accumulator check valves SI-170-L1, SI-170-L2, SI-170-L3, and SI-170-L4. This piping runs from the cold leg injection location inside the crane wall to the first check valve at each of the four RCS loops. A break at these lines would be enveloped by the LBLOCA break.
- 10 in diameter SI lines from the accumulator injection lines to the check valves. This is a short run of piping just off of the accumulator injection line near the cold leg. A break at these lines would be enveloped by the LBLOCA break.
- 6 in diameter SI lines from the RCS hot legs to check valves SI-158-L1, SI-158-L2, SI-158-L3, and SI-158-L4. These lines run from the hot legs inside the crane wall to the check valves near the loop piping. A break at these lines would be enveloped by the LBLOCA break.
- 6 in diameter PZR safety relief line to safety valves SV-45A, SV-45B, and SV-45C. These valves are located at the top of the PZR inside the PZR enclosure area. A break at this point high in the RCS piping would be terminated by the operators by lowering RCS water level below the elevation where the piping connects to the PZR. Thus, this break was not required to be analyzed.
- 6 in diameter PZR PORV line to valves NRV-151, NRV-152 and NRV-153. These valves are located at the top of the PZR inside the PZR enclosure area. A break at this point high in the RCS piping would be terminated by the operators by lowering RCS water level below the elevation where the piping connects to the PZR. In addition, the PORVs have motor operated isolation valves between them and the PZR. Thus, this break was not required to be analyzed.
- 4 in diameter PZR spray line from cold leg loops No. 3 and No. 4. These lines run from the top of the pressurizer to the cold leg piping inside the crane wall. A break at these lines would be enveloped by the LBLOCA break.
- 3 in diameter CVCS letdown and charging lines from cold leg loops 1 and 4 to valves CS-329-L1, CS-329-L4, and QRV-112. This piping runs from the RCS loops 1 and 4 cold legs inside the crane wall to the isolation valves inside the crane wall. A break at these lines would be enveloped by the LBLOCA break.

Break locations were evaluated to identify the breaks that produce the maximum amount of debris and also the worst combination of debris with the possibility of being transported to the recirculation sump strainers. In addition to the customary DEGB locations, DGBS break locations were also evaluated. These break locations, as identified above, utilized the equivalent area of a double-ended guillotine break of the largest pipe connected to the RCS loop piping. In this case, this is the PZR surge line. These breaks are further discussed in the response to NRC Information Item 3.b.

Section 3.3.5.2 of the SER states that break selection at 5 ft intervals along a pipe in question is acceptable, with the clarification that "...the concept of equal increments is only a reminder to be systematic and thorough." The SER provides further clarification by stating that "For the purpose of identifying limiting break conditions, a more discrete approach driven by the comparison of debris source term and transport potential can be effective at placing postulated breaks. The key difference between many breaks (especially large breaks) will not be the exact location along the pipe, but rather the envelope of containment material targets that is affected."

Due to the size of the RMI ZOI assumed in the debris generation analysis, and the consequential volume of debris generated, it was not necessary to evaluate pipe breaks at 5 ft increments. The ZOI for RMI encompassed several areas in the loop compartment for a LBLOCA. Similar to RMI, it was not necessary to evaluate 5 ft increments due to the size of the Min-K insulation ZOI. For other insulation types (Cal-Sil and Marinite), break locations were selected by plotting the ZOI along the RCS piping (hot leg, cold leg, and crossover leg) to maximize the major targets that fell within the perimeter of the ZOI sphere. The ZOI was assumed to be located in the area of the largest concentration of debris source material. Specific break locations were selected by plotting the ZOI along the crossover leg to maximize the major targets that fell within the ZOI sphere. This methodology is consistent with the GR, which states that a sufficient number of breaks in each high-pressure system that rely on recirculation should be evaluated to ensure the most limiting quantity of debris is generated and transported to the sump.

I&M Response to Information Item 3.a.2

While LOCAs are considered the most likely type of debris generating HELBs that could lead to recirculation, other break scenarios were evaluated to determine if they would result in debris generation followed by the need for recirculation for long-term core cooling.

As long as the RCS remains intact, the intent in PWR design is to provide decay heat removal via the SGs until the plant can be cooled down, depressurized, and cooled via the RHR system. Therefore, UFSAR analyses of secondary system breaks do not address ECCS recirculation. The analyses show that decay heat removal via at least one SG is established and maintained throughout the event. If secondary system HELBs are to be excluded from debris generation and transport analyses, it must be shown that containment spray is not needed after transfer of the CTS pumps to the recirculation mode of operation.

Chapter 14.3.4.1.3.2 and Chapter 14.3.4.4 of the UFSAR document an analysis of the containment response to the mass and energy release for postulated secondary pipe ruptures inside containment. The analysis includes the assumption that only a single train of

containment spray flow is operating. The analysis credits the containment spray (supplied from the RWST) and the ice condenser for the initial mitigation of the overall mass and energy release. The RWST inventory is more than enough to accommodate the containment pressure transient, since RCS pressure never drops below RHR pump shutoff head. Therefore, the RWST would be available for at least 30 minutes if both safeguards trains were in operation. With only one train in operation, the RWST would be available for over one hour. Even if the RWST was depleted, containment heat removal would continue with the ice condenser and operating CEQ fan(s).

In all of the cases of various size and initial power level events, the analysis was terminated at approximately 10 minutes after the event with containment temperature and pressures significantly reduced and trending downward. The analysis was terminated based on the end of the mass and energy release. With the feed flow terminated to the faulted SG, no further energy release occurs to containment once the SG has emptied. The termination of the analysis implies that no further challenge to containment integrity exists past 10 minutes. I&M has concluded from this analysis that further mitigation of the containment pressure transient does not require sump recirculation. This conclusion is further supported by a statement in UFSAR Section 14.3.4.1.3.2.1 that "ESW is not assumed for the MSLB transient." ESW is necessary for sump recirculation cooling. Therefore, secondary system breaks were not considered in the break selection.

I&M also noted that UFSAR Section 14.3.9 documents an evaluation of MSLBs and containment sump inventory. The objective of this analysis was to determine if there would be sufficient water in the containment following a steam line break to initiate CTS recirculation. Because a secondary system line break does not breach the RCS, only a small amount of RWST water is transferred to the RCS. The remainder of the RWST enters the recirculation pool via the CTS. This evaluation determined that there would be sufficient water in the sump pool to initiate CTS recirculation without draining the RWST to the recirculation condition. This analysis was performed to identify accident scenarios in which there would be the capability to initiate recirculation. The analysis did not demonstrate that recirculation would be needed.

I&M Response to Information Item 3.a.3

The results from the debris generation calculation (Reference 26) and the debris transport calculation (Reference 28) were used to determine the amount of debris located at the main strainer and remote strainer for breaks in the RCS loop piping, the surge line break, and the Alternate Breaks in the RCS loop piping. With this information, the worst case debris load for strainer qualification was then determined.

Debris Generation

The debris generation calculation (Reference 26) determined the amount of debris destroyed for the break locations listed below. The Alternate Break size was determined using the methodology provided in Chapter 6 of the GR.

- Loop 1 RCS Crossover Leg Break
- Loop 2 RCS Crossover Leg Break
- Loop 3 RCS Crossover Leg Break

- Loop 4 RCS Crossover Leg Break
- PZR Surge Line Break
- Loop 1 Alternate Break in RCS Loop Piping
- Loop 2 Alternate Break in RCS Loop Piping
- Loop 3 Alternate Break in RCS Loop Piping
- Loop 4 Alternate Break in RCS Loop Piping

The debris generation calculation (Reference 26) also considered a break in the reactor cavity. The only insulation debris generated by the reactor cavity break is RMI. Since the majority of the RMI would not be likely to transport out of the reactor cavity and RMI is generally not a problematic insulation type with respect to strainers that are mounted on the containment floor, this case was not analyzed.

Debris Types

Debris types commonly found at CNP and addressed in the evaluation included:

- RMI
- Fibrous debris
 - Fibrous insulation products
 - Fibrous latent debris
- Particulate debris
 - Cal-Sil
 - Microporous insulation (i.e., Min-K)
 - Fire barrier material (i.e., Marinite I and Marinite 36)
 - Failed coatings (qualified, OEM and non-OEM)
 - Particulate latent debris
- Miscellaneous latent debris
 - Fire proof tape
 - Ice storage bag fibers
 - Ice storage bag liner shards
 - Pieces of work platform rubber
 - Electromark labels
 - Unqualified labels
 - Flexible conduit PVC jacketing

Debris Transport

The debris transport calculation (Reference 28) predicted the blowdown, washdown, pool fill transport, and recirculation transport of the debris that would be generated from a HELB that requires recirculation.

A hydraulic CFD analysis was performed for the different cases that can occur with the CNP main strainer and remote strainer configuration. During pool fill, the main strainer starts to load with debris. Due to the hydraulics, initial flow through the remote strainer is backward. Therefore, at the start of recirculation, the main strainer is partially loaded with debris and the remote strainer is completely clean. The CFD analysis demonstrated that, with 90% of the main

strainer blocked, the flow split is 67.5% to the main strainer and 32.5% to the remote strainer. To determine the debris transport fraction to the main strainer, it was conservatively assumed that there was no flow impedance due to any debris deposition (i.e., full pool fill flow).

For some debris types, this approach resulted in a highly conservative overall transport fraction such that the sum of the transport fractions to the main and remote strainers exceeded 100%. The hydraulic analysis showed that, if less than the predicted debris load is transported to the main strainer, the flow to the main strainer would increase and flow to the remote strainer would decrease, since there would be less area blocked by debris on the main strainer. This would result in debris transport to the remote strainer that is equal to or less than originally predicted (for the 90% blocked main strainer case). Therefore, the assumption regarding debris transport to the remote strainer with 90% of the main strainer blocked is conservative.

The steps taken to calculate the debris loads at the main strainer and remote strainer were as follows:

Main Strainer

The debris located at the main strainer was calculated by multiplying the debris generated value from the debris generation calculation by the transport fraction for the main strainer from the transport calculation.

Remote Strainer

- The debris generated value was multiplied by the remote transport fraction to determine the predicted amount of debris at the remote strainer.
- The amount of debris that is available for transport to the remote strainer was calculated, since the portion of debris that is located at the main strainer would not be available for transport to the remote strainer. The amount of debris available for transport to the remote strainer was determined by subtracting the amount of debris at the main strainer from the debris generated value.

After the debris quantities at each of the strainers (main and remote) were determined for each of the breaks, the HLOSS computer code was used to determine the worst case break scenario. The HLOSS code was developed for flat plate analysis of head loss and is not directly applicable to strainers with complex geometries. The HLOSS code used for this evaluation is the same that is used to implement the NUREG/CR-6224 (Reference 19) head loss algorithm. Therefore, the results of a HLOSS analysis for strainers with complex geometries can be used to establish the relative significance of debris impact on that strainer if the strainer geometry does not include consideration of filling of interstitial volumes, but the results can not be directly used for establishing the head loss for the strainer. The use of the HLOSS code is appropriate for use at CNP for this application. Once the breaks that resulted in the highest calculated head loss using this approach were identified, strainer testing was performed to establish a more realistic, yet conservative head loss.

Worst Case Debris Load Determination

Nine separate break locations were considered in determining the worst case break locations. HLOSS was then utilized to determine the bounding break locations. Since CNP is using GR Chapter 6 methodology for Alternate Break (i.e., DGBS) evaluation, these break locations were also included. For each of the break locations, the quantity of each of the debris types that could be transported to the strainers was tabulated. These breaks, and the debris quantities at the main and remote strainers for both the DEGB and DGBS conditions are provided in Tables 3a3-3 through 3a3-24 at the end of this section. The breaks in loops 2 and 4 were modeled for pool fill. The separate tables for these loops include the quantity of debris at the main strainer following pool fill and the total debris at the main strainer after transfer to recirculation which includes the pool fill debris values.

The two worst case break locations were then determined; one for the RCS loop break and one for the Alternate Break in the RCS loop piping. In determining the worst case break locations, I&M considered the break locations that would transport the largest amount of debris as well as the break locations that may involve a larger amount of problematic debris (i.e., Min-K or Cal-Sil) as compared to other breaks. For example, the loop 4 Alternate Break generated the largest amount of debris (when compared to all loop Alternate Breaks) but did not generate Min-K debris. However, the Alternate Break in either loop 2 or 3 would generate and transport Min-K to the main and remote strainers but would not transport the largest amount of Cal-Sil debris. The surge line break was not considered bounding because the amount of debris generated (Cal-Sil, Marinite, and RMI) was less than the amount generated for the loop 4 Alternate Break. Therefore, the loop 4 Alternate Break bounds the surge line break.

The following RCS loop break cases were analyzed using HLOSS and the results were compared to determine the bounding scenario. The HLOSS runs were only performed for the main strainer since it has the smallest surface area with the largest debris loads.

- Loop 3 RCS Crossover Leg Break
- Loop 4 RCS Crossover Leg Break

Table 3a3-1 below was used as input into the HLOSS code. This table was generated from Table 3a3-8 and Table 3a3-11. An equivalent coatings density was calculated for the qualified epoxy, unqualified alkyd, and unqualified epoxy. The multiple debris terms were combined by weighted averaging of the material properties and summing the quantity of the individual debris source terms into a single source term. The debris material properties were weight averaged in accordance with the following equation for density.

Equation 1:

$$\rho_a = \frac{\sum_{i=1}^{N_c} m_i}{\sum_{i=1}^{N_c} m_i / \rho_i}$$

Where,

 ρ_a = Averaged density m_i = Mass of debris source i ρ_i = Density of debris source i**Table 3a3-1 HLOSS Inputs for Determination of Worst Case RCS loop Break**

Debris Type	Loop 3 RCS Crossover Leg Debris Quantity	Loop 4 RCS Crossover Leg Debris Quantity	Density, lb/ft ³	Characteristic Size, ft
Insulation				
Cal-Sil, Marinite I, Marinite 36, lbs	32.051	170.677	144	1.64E-05
Min-K, lbs	2.34	0.704	162	8.20E-06
Coatings				
Qualified Epoxy, lbs	95.625 ⁽¹⁾	93.5 ⁽¹⁾	111.6	3.28E-05
Unqualified Alkyd, lbs	13.243	13.224	98	3.28E-05 ⁽²⁾
Unqualified Epoxy, lbs	24.455 ⁽¹⁾	24.42 ⁽¹⁾	94	3.28E-05 ⁽²⁾
<i>Equivalent Coatings</i>	133.32	131.14	160.5 (Loop 3) 160.4 (Loop 4)	3.28E-05
Cold Galvanizing Compound lbs	723.075	723.075	250	3.28E-05
Latent Debris				
Dirt/Dust, lbs	88.4	88.4	168	5.68E-05
Latent Fiber/Bag Fiber, ft ³	6.517	6.516	175	2.30E-05
Blockage, ft ²	52.35 ⁽³⁾	34.06 ⁽³⁾	NA	NA
Strainer Area, ft ²	900	900	NA	NA
Flow Rate, gpm	9,720 ⁽⁴⁾	9,720 ⁽⁴⁾	NA	NA

- (1) A portion of the epoxy coatings within the ZOI are unqualified coatings with a density of 94 lb/ft³. This portion of coatings was included in the unqualified epoxy quantity in this table. For the loop 3 break this equates to 1.575 lb (3.5 lbs x 0.45) and for the loop 4 break this equates to 1.54 lb (3.5 lbs x 0.44).
- (2) The debris generation calculation shows these coatings as larger than 10 micron. For HLOSS, it is conservatively assumed that the unqualified coatings are 10 micron particles.
- (3) Includes Electromark labels (inside and outside the ZOI), unqualified labels (paper and other types), fire-proof tape small and large pieces, and flex conduit PVC jacketing.
- (4) The maximum sump recirculation flow rate is 14,400 gpm. With this debris load, 90% of the main strainer is blocked resulting in a 67.5% flow split to the main strainer. Therefore, the flow through the main strainer is 9,720 gpm.

The break in loop 4 was selected because it would generate the largest debris load and have the largest amount of Cal-Sil at the strainer. The loop 3 break was selected because it would generate the largest Min-K and Marinite debris load when compared to debris loads for loops 1 and 2. For all cases, the Min-K and Marinite debris loads would be a small fraction of the Cal-Sil debris load. Based on the HLOSS results, the loop 4 break would generate the highest head

loss, suggesting that Min-K and Marinite would not have as large an impact on head loss as Cal-Sil for these cases. The head loss results using HLOSS for the loop 4 break was 147.74 ft H₂O and the head loss results using HLOSS for the loop 3 break was 92.63 ft H₂O.

The following Alternate Break cases were analyzed using HLOSS and the results were compared to determine the bounding scenario.

- Loop 2 Alternate Break in RCS Loop Piping
- Loop 4 Alternate Break in RCS Loop Piping

Table 3a3-2 below was used as input into the HLOSS code. This table was generated from Table 3a3-18 and Table 3a3-23. An equivalent coatings density was calculated for the qualified epoxy, unqualified alkyd, and unqualified epoxy using Equation 1.

Table 3a3-2 HLOSS Inputs for Determination of Worst Case Alternate Break

Debris Type	Loop 2 Alternate Main Coolant Debris Quantity	Loop 4 Alternate Main Coolant Debris Quantity	Density, lb/ft ³	Characteristic Size, ft
Insulation				
Cal-Sil, Marinite I, Marinite 36, lbs	13.418	41.928	144	1.64E-05
Min-K, lbs	2.34	0	162	8.20E-06
Coatings				
Qualified Epoxy, lbs	0.99 ⁽¹⁾	0.968 ⁽¹⁾	111.6	3.28E-05
Unqualified Alkyd, lbs	13.243	13.224	98	3.28E-05 ⁽²⁾
Unqualified Epoxy, lbs	20.425 ⁽¹⁾	24.42 ⁽¹⁾	94	3.28E-05 ⁽²⁾
<i>Equivalent Coatings</i>	34.658	38.612	95.9 (Loop 2) 95.7 (Loop 4)	3.28E-05
Cold Galvanizing Compound lbs	723.075	723.075	250	3.28E-05
Latent Debris				
Dirt/Dust, lbs	88.4	88.4	168	5.68E-05
Latent Fiber/Bag Fiber, ft ³	6.517	6.516	175	2.30E-05
Blockage, ft ²	31.81 ⁽³⁾	34.06 ⁽³⁾	NA	NA
Strainer Area, ft ²	900	900	NA	NA
Flow Rate, gpm	9,720 ⁽⁴⁾	9,720 ⁽⁴⁾	NA	NA

- (1) A portion of the epoxy coatings within the ZOI are unqualified coatings with a density of 94 lb/ft³. This portion of coatings was included in the unqualified epoxy quantity in this table. For the loop 3 break this equates to 1.575 lb (3.5 lbs x 0.45) and for the loop 4 break this equates to 1.54 lb (3.5 lbs x 0.44).
- (2) The debris generation calculation shows these coatings as larger than 10 micron. For HLOSS, it is conservatively assumed that the unqualified coatings are 10 micron particles.
- (3) Includes Electromark labels (inside and outside the ZOI), unqualified labels (paper and other types), fire-proof tape small and large pieces, and flex conduit PVC jacketing.
- (4) The maximum sump recirculation flow rate is 14,400 gpm. With this debris load, 90% of the main strainer is blocked resulting in a 67.5% flow split to the main strainer. Therefore, the flow through the main strainer is 9,720 gpm.

The Alternate Break in loop 4 RCS piping was selected because it would generate the largest debris load and have the largest amount of Cal-Sil at the strainer. The loop 2 Alternate Break

was selected because it would generate the largest Min-K debris load coupled with the largest Cal-Sil debris load when compared to debris loads for loops 1 and 3 Alternate Breaks. For all Alternate Break cases, the Min-K and Marinite debris loads would be a small fraction of the Cal-Sil debris load. Similar to the RCS loop breaks, the HLOSS results showed that the loop 4 Alternate Break generated the highest head loss, suggesting that Min-K and Marinite do not have as large an impact on head loss as Cal-Sil. The head loss using HLOSS for loop 4 Alternate Break was determined to be 24.59 ft H₂O and the head loss using HLOSS for the loop 2 Alternate Break was determined to be 21.31 ft H₂O.

Table 3a3-3 Loop 1 RCS Crossover Leg Break Debris at Main Strainer

Debris Type	Debris Generated	Transport Fraction	Debris at Strainer
RMI Small Pieces, ft ²	48996	0.63	30867.48
RMI Large Pieces, ft ²	16332	0.43	7022.76
Cal-Sil Fines, lbs	62.4	0.45	28.08
Erosion of Cal-Sil Small Pieces to fines, lbs	49.3	0.1	4.93
Cal-Sil Small Pieces, lbs	49.3	0.38	18.734
Marinite I fines, lbs	0.6	0.45	0.27
Erosion of Marinite I Small Pieces to fines, lbs	0.2	0.1	0.02
Marinite I Small Pieces, lbs	0.2	0.38	0.076
Erosion of Marinite I Large Pieces to fines, lbs	1.4	0.11	0.154
Marinite I Large Pieces, lbs	1.4	0.35	0.49
Marinite 36 fines, lbs	0	0	0
Erosion of Marinite 36 Small Pieces to fines, lbs	0	0	0
Marinite 36 Small Pieces, lbs	0	0	0
Erosion of Marinite 36 Large Pieces to fines, lbs	0	0	0
Marinite 36 Large Pieces, lbs	0	0	0
Min-K, lbs	3.6	0.45	1.62
Epoxy Paint (inside ZOI), lbs	216	0.45	97.2
Alkyd Paint (inside ZOI), lbs	1.9	0.45	0.855
Unqualified OEM Epoxy (outside ZOI), lbs	16.9	0.4	6.76
Unqualified OEM Alkyd (outside ZOI), lbs	74.4	0.14	10.416
Unqualified Non-OEM Epoxy (outside ZOI), lbs	31	0.52	16.12
Unqualified Non-OEM Alkyd (outside ZOI), lbs	3.4	0.58	1.972
Unqualified Cold Galvanizing Compound, lbs	777.5	0.93	723.075
Dirt/Dust, lbs	170	0.52	88.4
Latent Fiber, ft ³	12.5	0.52	6.5
Fire Proof Tape Fines, ft ²	11.4	0.45	5.13
Fire Proof Tape Small Pieces, ft ²	6.5	0.63	4.095
Fire Proof Tape Large Pieces, ft ²	24.5	0.63	15.435
Ice Storage Bag Fibers, ft ³	0.026	0.64	0.01664
Ice Storage Bag Liner Shards, ft ³	0.00022	0.64	0.0001408
Pieces of Work Platform Rubber, ft ³	0.002	0.64	0.00128
Electromark Label (inside ZOI), ft ²	0.7	0.63	0.441
Electromark Label (outside ZOI), ft ²	39.6	0.17	6.732
Unqualified Labels – Paper, ft ²	0.28	0.86	0.2408
Unqualified Labels – Other, ft ²	25.66	0.86	22.0676
Flex Conduit PVC Jacketing, ft ²	1.57	1	1.57

**Table 3a3-4 Loop 1 RCS Crossover Leg Break Debris at Remote Strainer
(90% Blocked Main)**

Debris Type	Debris Generated	Transport Fraction	Debris at Strainer
RMI Small Pieces, ft ²	48996	0	0
RMI Large Pieces, ft ²	16332	0	0
Cal-Sil Fines, lbs	62.4	0.52	29.852 ⁽¹⁾
Erosion of Cal-Sil Small Pieces to fines, lbs	49.3	0.08	3.944
Cal-Sil Small Pieces, lbs	49.3	0	0
Marinite I fines, lbs	0.6	0.52	0.312
Erosion of Marinite I Small Pieces to fines, lbs	0.2	0.08	0.016
Marinite I Small Pieces, lbs	0.2	0	0
Erosion of Marinite I Large Pieces to fines, lbs	1.4	0.06	0.084
Marinite I Large Pieces, lbs	1.4	0	0
Marinite 36 fines, lbs	0	0	0
Erosion of Marinite 36 Small Pieces to fines, lbs	0	0	0
Marinite 36 Small Pieces, lbs	0	0	0
Erosion of Marinite 36 Large Pieces to fines, lbs	0	0	0
Marinite 36 Large Pieces, lbs	0	0	0
Min-K, lbs	3.6	0.52	1.872
Epoxy Paint (inside ZOI), lbs	216	0.52	112.32
Alkyd Paint (inside ZOI), lbs	1.9	0.52	0.988
Unqualified OEM Epoxy (outside ZOI), lbs	16.9	0.72	12.168
Unqualified OEM Alkyd (outside ZOI), lbs	74.4	0.9	66.96
Unqualified Non-OEM Epoxy (outside ZOI), lbs	31	0	0
Unqualified Non-OEM Alkyd (outside ZOI), lbs	3.4	0.59	2.006
Unqualified Cold Galvanizing Compound, lbs	777.5	0.35	272.125
Dirt/Dust, lbs	170	0.56	95.2
Latent Fiber, ft ³	12.5	0.56	7.00
Fire Proof Tape Fines, ft ²	11.4	0.52	5.928
Fire Proof Tape Small Pieces, ft ²	6.5	0	0
Fire Proof Tape Large Pieces, ft ²	24.5	0	0
Ice Storage Bag Fibers, ft ³	0.026	0.42	0.01092
Ice Storage Bag Liner Shards, ft ³	0.00022	0.42	0.0000924
Pieces of Work Platform Rubber, ft ³	0.002	0.42	0.00084
Electromark Label (inside ZOI), ft ²	0.7	0.47	0.329
Electromark Label (outside ZOI), ft ²	39.6	0.69	27.324
Unqualified Labels – Paper, ft ²	0.28	0.4	0.112
Unqualified Labels – Other, ft ²	25.66	0.4	10.264
Flex Conduit PVC Jacketing, ft ²	1.57	0.3	0.471

- (1) 8% of Cal-Sil fines transport to the reactor cavity (References 28 and 94) and are subtracted from the debris generated value prior to determining the debris at the strainer and the amount available to transport.

Table 3a3-5 Loop 2 RCS Crossover Leg Break Debris Transported to the Main Strainer during Pool Fill

Debris Type	Debris Generated	Transport Fraction	Debris at Strainer
RMI Small Pieces, ft ²	55718	0.4	22287.2
RMI Large Pieces, ft ²	18573	0.38	7057.74
Cal-Sil Fines, lbs	33.4	0.33	11.022
Erosion of Cal-Sil Small Pieces to fines, lbs	26.1	0	0
Cal-Sil Small Pieces, lbs	26.1	0.31	8.091
Marinite I fines, lbs	0.4	0.33	0.132
Erosion of Marinite I Small Pieces to fines, lbs	0.1	0	0
Marinite I Small Pieces, lbs	0.1	0.31	0.031
Erosion of Marinite I Large Pieces to fines, lbs	0.7	0	0
Marinite I Large Pieces, lbs	0.7	0.3	0.21
Marinite 36 fines, lbs	0	0	0
Erosion of Marinite 36 Small Pieces to fines, lbs	0	0	0
Marinite 36 Small Pieces, lbs	0	0	0
Erosion of Marinite 36 Large Pieces to fines, lbs	0	0	0
Marinite 36 Large Pieces, lbs	0	0	0
Min-K, lbs	5.2	0.33	1.716
Epoxy Paint (inside ZOI), lbs	216	0.33	71.28
Alkyd Paint (inside ZOI), lbs	1.9	0.33	0.627
Unqualified OEM Epoxy (outside ZOI), lbs	16.9	0	0
Unqualified OEM Alkyd (outside ZOI), lbs	74.4	0	0
Unqualified Non-OEM Epoxy (outside ZOI), lbs	31	0	0
Unqualified Non-OEM Alkyd (outside ZOI), lbs	3.4	0	0
Unqualified Cold Galvanizing Compound, lbs	777.5	0	0
Dirt/Dust, lbs	170	0.25	42.5
Latent Fiber, ft ³	12.5	0.25	3.125
Fire Proof Tape Fines, ft ²	0.5	0.33	0.165
Fire Proof Tape Small Pieces, ft ²	0.3	0.4	0.12
Fire Proof Tape Large Pieces, ft ²	1	0.4	0.4
Ice Storage Bag Fibers, ft ³	0.026	0.47	0.01222
Ice Storage Bag Liner Shards, ft ³	0.00022	0.47	0.0001034
Pieces of Work Platform Rubber, ft ³	0.002	0.47	0.000954
Electromark Label (inside ZOI), ft ²	0.6	0.4	0.24
Electromark Label (outside ZOI), ft ²	39.6	0	0
Unqualified Labels – Paper, ft ²	0.28	0	0
Unqualified Labels – Other, ft ²	25.66	0	0
Flex Conduit PVC Jacketing, ft ²	1.57	0	0

Table 3a3-6 Loop 2 RCS Crossover Leg Break Debris at Main Strainer

Debris Type	Debris Generated	Transport Fraction	Debris at Strainer
RMI Small Pieces, ft ²	55718	0.63	35102.34
RMI Large Pieces, ft ²	18573	0.43	7986.39
Cal-Sil Fines, lbs	33.4	0.45	15.03
Erosion of Cal-Sil Small Pieces to fines, lbs	26.1	0.1	2.61
Cal-Sil Small Pieces, lbs	26.1	0.38	9.918
Marinite I fines, lbs	0.4	0.45	0.18
Erosion of Marinite I Small Pieces to fines, lbs	0.1	0.1	0.01
Marinite I Small Pieces, lbs	0.1	0.38	0.038
Erosion of Marinite I Large Pieces to fines, lbs	0.7	0.11	0.077
Marinite I Large Pieces, lbs	0.7	0.35	0.245
Marinite 36 fines, lbs	0	0	0
Erosion of Marinite 36 Small Pieces to fines, lbs	0	0	0
Marinite 36 Small Pieces, lbs	0	0	0
Erosion of Marinite 36 Large Pieces to fines, lbs	0	0	0
Marinite 36 Large Pieces, lbs	0	0	0
Min-K, lbs	5.2	0.45	2.34
Epoxy Paint (inside ZOI), lbs	216	0.45	97.2
Alkyd Paint (inside ZOI), lbs	1.9	0.45	0.855
Unqualified OEM Epoxy (outside ZOI), lbs	16.9	0.4	6.76
Unqualified OEM Alkyd (outside ZOI), lbs	74.4	0.14	10.416
Unqualified Non-OEM Epoxy (outside ZOI), lbs	31	0.39	12.09
Unqualified Non-OEM Alkyd (outside ZOI), lbs	3.4	0.58	1.972
Unqualified Cold Galvanizing Compound, lbs	777.5	0.93	723.075
Dirt/Dust, lbs	170	0.52	88.4
Latent Fiber, ft ³	12.5	0.52	6.5
Fire Proof Tape Fines, ft ²	0.5	0.45	0.225
Fire Proof Tape Small Pieces, ft ²	0.3	0.63	0.189
Fire Proof Tape Large Pieces, ft ²	1	0.63	0.63
Ice Storage Bag Fibers, ft ³	0.026	0.64	0.01664
Ice Storage Bag Liner Shards, ft ³	0.00022	0.64	0.0001408
Pieces of Work Platform Rubber, ft ³	0.002	0.64	0.00128
Electromark Label (inside ZOI), ft ²	0.6	0.63	0.378
Electromark Label (outside ZOI), ft ²	39.6	0.17	6.732
Unqualified Labels – Paper, ft ²	0.28	0.86	0.2408
Unqualified Labels – Other, ft ²	25.66	0.86	22.0676
Flex Conduit PVC Jacketing, ft ²	1.57	1	1.57

**Table 3a3-7 Loop 2 RCS Crossover Leg Break Debris at Remote Strainer
(90% Blocked Main)**

Debris Type	Debris Generated	Transport Fraction	Debris at Strainer
RMI Small Pieces, ft ²	55718	0	0
RMI Large Pieces, ft ²	18573	0	0
Cal-Sil Fines, lbs	33.4	0.51	15.671 ⁽¹⁾
Erosion of Cal-Sil Small Pieces to fines, lbs	26.1	0.04	1.044
Cal-Sil Small Pieces, lbs	26.1	0	0
Marinite I fines, lbs	0.4	0.51	0.204
Erosion of Marinite I Small Pieces to fines, lbs	0.1	0.04	0.004
Marinite I Small Pieces, lbs	0.1	0	0
Erosion of Marinite I Large Pieces to fines, lbs	0.7	0.04	0.028
Marinite I Large Pieces, lbs	0.7	0	0
Marinite 36 fines, lbs	0	0	0
Erosion of Marinite 36 Small Pieces to fines, lbs	0	0	0
Marinite 36 Small Pieces, lbs	0	0	0
Erosion of Marinite 36 Large Pieces to fines, lbs	0	0	0
Marinite 36 Large Pieces, lbs	0	0	0
Min-K, lbs	5.2	0.51	2.652
Epoxy Paint (inside ZOI), lbs	216	0.51	110.16
Alkyd Paint (inside ZOI), lbs	1.9	0.51	0.969
Unqualified OEM Epoxy (outside ZOI), lbs	16.9	0.72	12.168
Unqualified OEM Alkyd (outside ZOI), lbs	74.4	0.9	66.96
Unqualified Non-OEM Epoxy (outside ZOI), lbs	31	0	0
Unqualified Non-OEM Alkyd (outside ZOI), lbs	3.4	0.59	2.006
Unqualified Cold Galvanizing Compound, lbs	777.5	0.35	272.125
Dirt/Dust, lbs	170	0.56	95.2
Latent Fiber, ft ³	12.5	0.56	7
Fire Proof Tape Fines, ft ²	0.5	0.51	0.255
Fire Proof Tape Small Pieces, ft ²	0.3	0	0
Fire Proof Tape Large Pieces, ft ²	1	0	0
Ice Storage Bag Fibers, ft ³	0.026	0.41	0.01066
Ice Storage Bag Liner Shards, ft ³	0.00022	0.41	0.0000902
Pieces of Work Platform Rubber, ft ³	0.002	0.41	0.00082
Electromark Label (inside ZOI), ft ²	0.6	0.05	0.03
Electromark Label (outside ZOI), ft ²	39.6	0.6	23.76
Unqualified Labels – Paper, ft ²	0.28	0.4	0.112
Unqualified Labels – Other, ft ²	25.66	0.4	10.264
Flex Conduit PVC Jacketing, ft ²	1.57	0.3	0.471

- (1) 8% of Cal-Sil fines transport to the reactor cavity (References 28 and 94) and are subtracted from the debris generated value prior to determining the debris at the strainer and the amount available to transport.

Table 3a3-8 Loop 3 RCS Crossover Leg Break Debris at Main Strainer

Debris Type	Debris Generated	Transport Fraction	Debris at Strainer
RMI Small Pieces, ft ²	70342	0.63	44315.46
RMI Large Pieces, ft ²	23448	0.43	10082.64
Cal-Sil Fines, lbs	34.8	0.45	15.66
Erosion of Cal-Sil Small Pieces to fines, lbs	30.5	0.1	3.05
Cal-Sil Small Pieces, lbs	30.5	0.38	11.59
Marinite I fines, lbs	0.2	0.45	0.09
Erosion of Marinite I Small Pieces to fines, lbs	0.09	0.1	0.009
Marinite I Small Pieces, lbs	0.09	0.38	0.0342
Erosion of Marinite I Large Pieces to fines, lbs	0.5	0.11	0.055
Marinite I Large Pieces, lbs	0.5	0.35	0.175
Marinite 36 fines, lbs	0.86	0.45	0.387
Erosion of Marinite 36 Small Pieces to fines, lbs	0.36	0.1	0.036
Marinite 36 Small Pieces, lbs	0.36	0.38	0.1368
Erosion of Marinite 36 Large Pieces to fines, lbs	1.8	0.11	0.198
Marinite 36 Large Pieces, lbs	1.8	0.35	0.63
Min-K, lbs	5.2	0.45	2.34
Epoxy Paint (inside ZOI), lbs	216	0.45	97.2
Alkyd Paint (inside ZOI), lbs	1.9	0.45	0.855
Unqualified OEM Epoxy (outside ZOI), lbs	16.9	0.4	6.76
Unqualified OEM Alkyd (outside ZOI), lbs	74.4	0.14	10.416
Unqualified Non-OEM Epoxy (outside ZOI), lbs	31	0.52	16.12
Unqualified Non-OEM Alkyd (outside ZOI), lbs	3.4	0.58	1.972
Unqualified Cold Galvanizing Compound, lbs	777.5	0.93	723.075
Dirt/Dust, lbs	170	0.52	88.4
Latent Fiber, ft ³	12.5	0.52	6.5
Fire Proof Tape Fines, ft ²	12.50	0.45	5.625
Fire Proof Tape Small Pieces, ft ²	7.1	0.63	4.473
Fire Proof Tape Large Pieces, ft ²	26.8	0.63	16.884
Ice Storage Bag Fibers, ft ³	0.026	0.64	0.01664
Ice Storage Bag Liner Shards, ft ³	0.00022	0.64	0.0001408
Pieces of Work Platform Rubber, ft ³	0.002	0.64	0.00128
Electromark Label (inside ZOI), ft ²	0.6	0.63	0.378
Electromark Label (outside ZOI), ft ²	39.6	0.17	6.732
Unqualified Labels – Paper, ft ²	0.28	0.86	0.2408
Unqualified Labels – Other, ft ²	25.66	0.86	22.0676
Flex Conduit PVC Jacketing, ft ²	1.57	1	1.57

**Table 3a3-9 Loop 3 RCS Crossover Leg Break Debris at Remote Strainer
(90% Blocked Main)**

Debris Type	Debris Generated	Transport Fraction	Debris at Strainer
RMI Small Pieces, ft ²	70342	0	0
RMI Large Pieces, ft ²	23448	0	0
Cal-Sil Fines, lbs	34.8	0.52	16.648 ⁽¹⁾
Erosion of Cal-Sil Small Pieces to fines, lbs	30.5	0.08	2.44
Cal-Sil Small Pieces, lbs	30.5	0	0
Marinite I fines, lbs	0.2	0.52	0.104
Erosion of Marinite I Small Pieces to fines, lbs	0.09	0.08	0.0072
Marinite I Small Pieces, lbs	0.09	0	0
Erosion of Marinite I Large Pieces to fines, lbs	0.5	0.06	0.03
Marinite I Large Pieces, lbs	0.5	0	0
Marinite 36 fines, lbs	0.86	0.52	0.4472
Erosion of Marinite 36 Small Pieces to fines, lbs	0.36	0.08	0.0288
Marinite 36 Small Pieces, lbs	0.36	0	0
Erosion of Marinite 36 Large Pieces to fines, lbs	1.8	0.06	0.108
Marinite 36 Large Pieces, lbs	1.8	0	0
Min-K, lbs	5.2	0.52	2.704
Epoxy Paint (inside ZOI), lbs	216	0.52	112.32
Alkyd Paint (inside ZOI), lbs	1.9	0.52	0.988
Unqualified OEM Epoxy (outside ZOI), lbs	16.9	0.72	12.168
Unqualified OEM Alkyd (outside ZOI), lbs	74.4	0.9	66.96
Unqualified Non-OEM Epoxy (outside ZOI), lbs	31	0	0
Unqualified Non-OEM Alkyd (outside ZOI), lbs	3.4	0.59	2.006
Unqualified Cold Galvanizing Compound, lbs	777.5	0.35	272.125
Dirt/Dust, lbs	170	0.56	95.2
Latent Fiber, ft ³	12.5	0.56	7
Fire Proof Tape Fines, ft ²	12.50	0.52	6.5
Fire Proof Tape Small Pieces, ft ²	7.1	0	0
Fire Proof Tape Large Pieces, ft ²	26.8	0	0
Ice Storage Bag Fibers, ft ³	0.026	0.42	0.01092
Ice Storage Bag Liner Shards, ft ³	0.00022	0.42	0.0000924
Pieces of Work Platform Rubber, ft ³	0.002	0.42	0.00084
Electromark Label (inside ZOI), ft ²	0.6	0.47	0.282
Electromark Label (outside ZOI), ft ²	39.6	0.69	27.324
Unqualified Labels – Paper, ft ²	0.28	0.4	0.112
Unqualified Labels – Other, ft ²	25.66	0.4	10.264
Flex Conduit PVC Jacketing, ft ²	1.57	0.3	0.471

- (1) 8% of Cal-Sil fines transport to the reactor cavity (References 28 and 94) and are subtracted from the debris generated value prior to determining the debris at the strainer and the amount available to transport.

Table 3a3-10 Loop 4 RCS Crossover Leg Break Debris Transported to the Main Strainer during Pool Fill

Debris Type	Debris Generated	Transport Fraction	Debris at Strainer
RMI Small Pieces, ft ²	58528	0.09	5267.52
RMI Large Pieces, ft ²	19510	0.05	975.5
Cal-Sil Fines, lbs	279.9	0.32	89.568
Erosion of Cal-Sil Small Pieces to fines, lbs	232	0	0
Cal-Sil Small Pieces, lbs	232	0.05	11.6
Marinite I fines, lbs	0.14	0.32	0.0448
Erosion of Marinite I Small Pieces to fines, lbs	0.05	0	0
Marinite I Small Pieces, lbs	0.05	0.05	0.0025
Erosion of Marinite I Large Pieces to fines, lbs	0.23	0	0
Marinite I Large Pieces, lbs	0.23	0.04	0.0092
Marinite 36 fines, lbs	1.08	0.32	0.3456
Erosion of Marinite 36 Small Pieces to fines, lbs	0.36	0	0
Marinite 36 Small Pieces, lbs	0.36	0.05	0.018
Erosion of Marinite 36 Large Pieces to fines, lbs	2.16	0	0
Marinite 36 Large Pieces, lbs	2.16	0.04	0.0864
Min-K, lbs	1.6	0.32	0.512
Epoxy Paint (inside ZOI), lbs	216	0.32	69.12
Alkyd Paint (inside ZOI), lbs	1.9	0.32	0.608
Unqualified OEM Epoxy (outside ZOI), lbs	16.9	0	0
Unqualified OEM Alkyd (outside ZOI), lbs	74.4	0	0
Unqualified Non-OEM Epoxy (outside ZOI), lbs	31	0	0
Unqualified Non-OEM Alkyd (outside ZOI), lbs	3.4	0	0
Unqualified Cold Galvanizing Compound, lbs	777.5	0	0
Dirt/Dust, lbs	170	0.24	40.8
Latent Fiber, ft ³	12.5	0.24	3.00
Fire Proof Tape Fines, ft ²	25.1	0.32	8.032
Fire Proof Tape Small Pieces, ft ²	14.4	0.09	1.296
Fire Proof Tape Large Pieces, ft ²	54.1	0.09	4.869
Ice Storage Bag Fibers, ft ³	0.026	0.45	0.0117
Ice Storage Bag Liner Shards, ft ³	0.00022	0.45	0.000099
Pieces of Work Platform Rubber, ft ³	0.002	0.45	0.0009
Electromark Label (inside ZOI), ft ²	0.7	0.09	0.063
Electromark Label (outside ZOI), ft ²	39.6	0	0
Unqualified Labels – Paper, ft ²	0.28	0	0
Unqualified Labels – Other, ft ²	25.66	0	0
Flex Conduit PVC Jacketing, ft ²	1.57	0	0

Table 3a3-11 Loop 4 RCS Crossover Leg Break Debris at Main Strainer

Debris Type	Debris Generated	Transport Fraction	Debris at Strainer
RMI Small Pieces, ft ²	58528	0.13	7608.64
RMI Large Pieces, ft ²	19510	0.08	1560.8
Cal-Sil Fines, lbs	279.9	0.44	123.156
Erosion of Cal-Sil Small Pieces to fines, lbs	232	0.1	23.2
Cal-Sil Small Pieces, lbs	232	0.1	23.2
Marinite I fines, lbs	0.14	0.44	0.0616
Erosion of Marinite I Small Pieces to fines, lbs	0.05	0.1	0.005
Marinite I Small Pieces, lbs	0.05	0.1	0.005
Erosion of Marinite I Large Pieces to fines, lbs	0.23	0.14	0.0322
Marinite I Large Pieces, lbs	0.23	0.07	0.0161
Marinite 36 fines, lbs	1.08	0.44	0.4752
Erosion of Marinite 36 Small Pieces to fines, lbs	0.36	0.1	0.036
Marinite 36 Small Pieces, lbs	0.36	0.1	0.036
Erosion of Marinite 36 Large Pieces to fines, lbs	2.16	0.14	0.3024
Marinite 36 Large Pieces, lbs	2.16	0.07	0.1512
Min-K, lbs	1.6	0.44	0.704
Epoxy Paint (inside ZOI), lbs	216	0.44	95.04
Alkyd Paint (inside ZOI), lbs	1.9	0.44	0.836
Unqualified OEM Epoxy (outside ZOI), lbs	16.9	0.4	6.76
Unqualified OEM Alkyd (outside ZOI), lbs	74.4	0.14	10.416
Unqualified Non-OEM Epoxy (outside ZOI), lbs	31	0.52	16.12
Unqualified Non-OEM Alkyd (outside ZOI), lbs	3.4	0.58	1.972
Unqualified Cold Galvanizing Compound, lbs	777.5	0.93	723.075
Dirt/Dust, lbs	170	0.52	88.4
Latent Fiber, ft ³	12.5	0.52	6.5
Fire Proof Tape Fines, ft ²	25.1	0.44	11.044
Fire Proof Tape Small Pieces, ft ²	14.4	0.13	1.872
Fire Proof Tape Large Pieces, ft ²	54.1	0.13	7.033
Ice Storage Bag Fibers, ft ³	0.026	0.63	0.01638
Ice Storage Bag Liner Shards, ft ³	0.00022	0.63	0.0001386
Pieces of Work Platform Rubber, ft ³	0.002	0.63	0.00126
Electromark Label (inside ZOI), ft ²	0.7	0.13	0.091
Electromark Label (outside ZOI), ft ²	39.6	0.03	1.188
Unqualified Labels – Paper, ft ²	0.28	0.86	0.2408
Unqualified Labels – Other, ft ²	25.66	0.86	22.0676
Flex Conduit PVC Jacketing, ft ²	1.57	1	1.57

**Table 3a3-12 Loop 4 RCS Crossover Leg Break Debris at Remote Strainer
(90% Blocked Main)**

Debris Type	Debris Generated	Transport Fraction	Debris at Strainer
RMI Small Pieces, ft ²	58528	0	0
RMI Large Pieces, ft ²	19510	0	0
Cal-Sil Fines, lbs	279.9	0.52	133.904 ⁽¹⁾
Erosion of Cal-Sil Small Pieces to fines, lbs	232	0.08	18.56
Cal-Sil Small Pieces, lbs	232	0	0
Marinite I fines, lbs	0.14	0.52	0.0728
Erosion of Marinite I Small Pieces to fines, lbs	0.05	0.08	0.004
Marinite I Small Pieces, lbs	0.05	0	0
Erosion of Marinite I Large Pieces to fines, lbs	0.23	0.06	0.0138
Marinite I Large Pieces, lbs	0.23	0	0
Marinite 36 fines, lbs	1.08	0.52	0.5616
Erosion of Marinite 36 Small Pieces to fines, lbs	0.36	0.08	0.0288
Marinite 36 Small Pieces, lbs	0.36	0	0
Erosion of Marinite 36 Large Pieces to fines, lbs	2.16	0.06	0.1296
Marinite 36 Large Pieces, lbs	2.16	0	0
Min-K, lbs	1.6	0.52	0.832
Epoxy Paint (inside ZOI), lbs	216	0.52	112.32
Alkyd Paint (inside ZOI), lbs	1.9	0.52	0.988
Unqualified OEM Epoxy (outside ZOI), lbs	16.9	0.72	12.168
Unqualified OEM Alkyd (outside ZOI), lbs	74.4	0.9	66.96
Unqualified Non-OEM Epoxy (outside ZOI), lbs	31	0	0
Unqualified Non-OEM Alkyd (outside ZOI), lbs	3.4	0.59	2.006
Unqualified Cold Galvanizing Compound, lbs	777.5	0.35	272.125
Dirt/Dust, lbs	170	0.56	95.2
Latent Fiber, ft ³	12.5	0.56	7
Fire Proof Tape Fines, ft ²	25.1	0.52	13.052
Fire Proof Tape Small Pieces, ft ²	14.4	0	0
Fire Proof Tape Large Pieces, ft ²	54.1	0	0
Ice Storage Bag Fibers, ft ³	0.026	0.42	0.01092
Ice Storage Bag Liner Shards, ft ³	0.00022	0.42	0.0000924
Pieces of Work Platform Rubber, ft ³	0.002	0.42	0.00084
Electromark Label (inside ZOI), ft ²	0.7	0.47	0.329
Electromark Label (outside ZOI), ft ²	39.6	0.69	27.324
Unqualified Labels – Paper, ft ²	0.28	0.4	0.112
Unqualified Labels – Other, ft ²	25.66	0.4	10.264
Flex Conduit PVC Jacketing, ft ²	1.57	0.3	0.471

- (1) 8% of Cal-Sil fines transport to the reactor cavity (References 28 and 94) and are subtracted from the debris generated value prior to determining the debris at the strainer and the amount available to transport.

Table 3a3-13 Pressurizer Surge Line Break Debris at Main Strainer

Debris Type	Debris Generated	Transport Fraction	Debris at Strainer
RMI Small Pieces, ft ²	38436	0.13	4996.68
RMI Large Pieces, ft ²	12812	0.08	1024.96
Cal-Sil Fines, lbs	46.4	0.44	20.416
Erosion of Cal-Sil Small Pieces to fines, lbs	37.7	0.1	3.77
Cal-Sil Small Pieces, lbs	37.7	0.1	3.77
Marinite I fines, lbs	0.09	0.44	0.0396
Erosion of Marinite I Small Pieces to fines, lbs	0.05	0.1	0.005
Marinite I Small Pieces, lbs	0.05	0.1	0.005
Erosion of Marinite I Large Pieces to fines, lbs	0.23	0.14	0.0322
Marinite I Large Pieces, lbs	0.23	0.07	0.0161
Marinite 36 fines, lbs	0.7	0.44	0.308
Erosion of Marinite 36 Small Pieces to fines, lbs	0.3	0.1	0.03
Marinite 36 Small Pieces, lbs	0.3	0.1	0.03
Erosion of Marinite 36 Large Pieces to fines, lbs	1.4	0.14	0.196
Marinite 36 Large Pieces, lbs	1.4	0.07	0.098
Min-K, lbs	1.6	0.44	0.704
Epoxy Paint (inside ZOI), lbs	26.3	0.44	11.572
Alkyd Paint (inside ZOI), lbs	1.9	0.44	0.836
Unqualified OEM Epoxy (outside ZOI), lbs	16.9	0.4	6.76
Unqualified OEM Alkyd (outside ZOI), lbs	74.4	0.14	10.416
Unqualified Non-OEM Epoxy (outside ZOI), lbs	31	0.52	16.12
Unqualified Non-OEM Alkyd (outside ZOI), lbs	3.4	0.58	1.972
Unqualified Cold Galvanizing Compound, lbs	777.5	0.93	723.075
Dirt/Dust, lbs	170	0.52	88.4
Latent Fiber, ft ³	12.5	0.52	6.5
Fire Proof Tape Fines, ft ²	25.1	0.44	11.044
Fire Proof Tape Small Pieces, ft ²	14.4	0.13	1.872
Fire Proof Tape Large Pieces, ft ²	54.1	0.13	7.033
Ice Storage Bag Fibers, ft ³	0.026	0.63	0.01638
Ice Storage Bag Liner Shards, ft ³	0.00022	0.63	0.0001386
Pieces of Work Platform Rubber, ft ³	0.002	0.63	0.00126
Electromark Label (inside ZOI), ft ²	0.7	0.13	0.091
Electromark Label (outside ZOI), ft ²	39.6	0.03	1.188
Unqualified Labels – Paper, ft ²	0.28	0.86	0.2408
Unqualified Labels – Other, ft ²	25.66	0.86	22.0676
Flex Conduit PVC Jacketing, ft ²	1.57	1	1.57

**Table 3a3-14 Pressurizer Surge Line Break Debris at Remote Strainer
(90% Blocked Main)**

Debris Type	Debris Generated	Transport Fraction	Debris at Strainer
RMI Small Pieces, ft ²	38436	0	0
RMI Large Pieces, ft ²	12812	0	0
Cal-Sil Fines, lbs	46.4	0.52	22.198 ⁽¹⁾
Erosion of Cal-Sil Small Pieces to fines, lbs	37.7	0.08	3.016
Cal-Sil Small Pieces, lbs	37.7	0	0
Marinite I fines, lbs	0.09	0.52	0.0468
Erosion of Marinite I Small Pieces to fines, lbs	0.05	0.08	0.004
Marinite I Small Pieces, lbs	0.05	0	0
Erosion of Marinite I Large Pieces to fines, lbs	0.23	0.06	0.0138
Marinite I Large Pieces, lbs	0.23	0	0
Marinite 36 fines, lbs	0.7	0.52	0.364
Erosion of Marinite 36 Small Pieces to fines, lbs	0.3	0.08	0.024
Marinite 36 Small Pieces, lbs	0.3	0	0
Erosion of Marinite 36 Large Pieces to fines, lbs	1.4	0.06	0.084
Marinite 36 Large Pieces, lbs	1.4	0	0
Min-K, lbs	1.6	0.52	0.832
Epoxy Paint (inside ZOI), lbs	26.3	0.52	13.676
Alkyd Paint (inside ZOI), lbs	1.9	0.52	0.988
Unqualified OEM Epoxy (outside ZOI), lbs	16.9	0.72	12.168
Unqualified OEM Alkyd (outside ZOI), lbs	74.4	0.9	66.96
Unqualified Non-OEM Epoxy (outside ZOI), lbs	31	0	0
Unqualified Non-OEM Alkyd (outside ZOI), lbs	3.4	0.59	2.006
Unqualified Cold Galvanizing Compound, lbs	777.5	0.35	272.125
Dirt/Dust, lbs	170	0.56	95.2
Latent Fiber, ft ³	12.5	0.56	7
Fire Proof Tape Fines, ft ²	25.1	0.52	13.052
Fire Proof Tape Small Pieces, ft ²	14.4	0	0
Fire Proof Tape Large Pieces, ft ²	54.1	0	0
Ice Storage Bag Fibers, ft ³	0.026	0.42	0.01092
Ice Storage Bag Liner Shards, ft ³	0.00022	0.42	0.0000924
Pieces of Work Platform Rubber, ft ³	0.002	0.42	0.00084
Electromark Label (inside ZOI), ft ²	0.7	0.47	0.329
Electromark Label (outside ZOI), ft ²	39.6	0.69	27.324
Unqualified Labels – Paper, ft ²	0.28	0.4	0.112
Unqualified Labels – Other, ft ²	25.66	0.4	10.264
Flex Conduit PVC Jacketing, ft ²	1.57	0.3	0.471

- (1) 8% of Cal-Sil fines transport to the reactor cavity (References 28 and 94) and are subtracted from the debris generated value prior to determining the debris at the strainer and the amount available to transport.

Table 3a3-15 Loop 1 Alternate RCS loop Break Debris at Main Strainer

Debris Type	Debris Generated	Transport Fraction	Debris at Strainer
RMI Small Pieces, ft ²	35850	0.63	22585.5
RMI Large Pieces, ft ²	11950	0.43	5138.5
Cal-Sil Fines, lbs	11.6	0.45	5.22
Erosion of Cal-Sil Small Pieces to fines, lbs	7.5	0.1	0.75
Cal-Sil Small Pieces, lbs	7.5	0.38	2.85
Marinite I fines, lbs	0.21	0.45	0.0945
Erosion of Marinite I Small Pieces to fines, lbs	0.08	0.1	0.008
Marinite I Small Pieces, lbs	0.08	0.38	0.0304
Erosion of Marinite I Large Pieces to fines, lbs	0.41	0.11	0.0451
Marinite I Large Pieces, lbs	0.41	0.35	0.1435
Marinite 36 fines, lbs	0	0.45	0
Erosion of Marinite 36 Small Pieces to fines, lbs	0	0.1	0
Marinite 36 Small Pieces, lbs	0	0.38	0
Erosion of Marinite 36 Large Pieces to fines, lbs	0	0.11	0
Marinite 36 Large Pieces, lbs	0	0.35	0
Min-K, lbs	0	0.45	0
Epoxy Paint (inside ZOI), lbs	5.7	0.45	2.565
Alkyd Paint (inside ZOI), lbs	1.9	0.45	0.855
Unqualified OEM Epoxy (outside ZOI), lbs	16.9	0.4	6.76
Unqualified OEM Alkyd (outside ZOI), lbs	74.4	0.14	10.416
Unqualified Non-OEM Epoxy (outside ZOI), lbs	31	0.52	16.12
Unqualified Non-OEM Alkyd (outside ZOI), lbs	3.4	0.58	1.972
Unqualified Cold Galvanizing Compound, lbs	777.5	0.93	723.075
Dirt/Dust, lbs	170	0.52	88.4
Latent Fiber, ft ³	12.5	0.52	6.5
Fire Proof Tape Fines, ft ²	11.4	0.45	5.13
Fire Proof Tape Small Pieces, ft ²	6.5	0.63	4.095
Fire Proof Tape Large Pieces, ft ²	24.5	0.63	15.435
Ice Storage Bag Fibers, ft ³	0.026	0.64	0.01664
Ice Storage Bag Liner Shards, ft ³	0.00022	0.64	0.0001408
Pieces of Work Platform Rubber, ft ³	0.002	0.64	0.00128
Electromark Label (inside ZOI), ft ²	0.7	0.63	0.441
Electromark Label (outside ZOI), ft ²	39.6	0.17	6.732
Unqualified Labels – Paper, ft ²	0.28	0.86	0.2408
Unqualified Labels – Other, ft ²	25.66	0.86	22.0676
Flex Conduit PVC Jacketing, ft ²	1.57	1	1.57

**Table 3a3-16 Loop 1 Alternate RCS loop Break Debris at Remote Strainer
(90% Blocked Main)**

Debris Type	Debris Generated	Transport Fraction	Debris at Strainer
RMI Small Pieces, ft ²	35850	0	0
RMI Large Pieces, ft ²	11950	0	0
Cal-Sil Fines, lbs	11.6	0.52	5.549 ⁽¹⁾
Erosion of Cal-Sil Small Pieces to fines, lbs	7.5	0.08	0.6
Cal-Sil Small Pieces, lbs	7.5	0	0
Marinite I fines, lbs	0.21	0.52	0.1092
Erosion of Marinite I Small Pieces to fines, lbs	0.08	0.08	0.0064
Marinite I Small Pieces, lbs	0.08	0	0
Erosion of Marinite I Large Pieces to fines, lbs	0.41	0.06	0.0246
Marinite I Large Pieces, lbs	0.41	0	0
Marinite 36 fines, lbs	0	0.52	0
Erosion of Marinite 36 Small Pieces to fines, lbs	0	0.08	0
Marinite 36 Small Pieces, lbs	0	0	0
Erosion of Marinite 36 Large Pieces to fines, lbs	0	0.06	0
Marinite 36 Large Pieces, lbs	0	0	0
Min-K, lbs	0	0.52	0
Epoxy Paint (inside ZOI), lbs	5.7	0.52	2.964
Alkyd Paint (inside ZOI), lbs	1.9	0.52	0.988
Unqualified OEM Epoxy (outside ZOI), lbs	16.9	0.72	12.168
Unqualified OEM Alkyd (outside ZOI), lbs	74.4	0.9	66.96
Unqualified Non-OEM Epoxy (outside ZOI), lbs	31	0	0
Unqualified Non-OEM Alkyd (outside ZOI), lbs	3.4	0.59	2.006
Unqualified Cold Galvanizing Compound, lbs	777.5	0.35	272.125
Dirt/Dust, lbs	170	0.56	95.2
Latent Fiber, ft ³	12.5	0.56	7
Fire Proof Tape Fines, ft ²	11.4	0.52	5.928
Fire Proof Tape Small Pieces, ft ²	6.5	0	0
Fire Proof Tape Large Pieces, ft ²	24.5	0	0
Ice Storage Bag Fibers, ft ³	0.026	0.42	0.01092
Ice Storage Bag Liner Shards, ft ³	0.00022	0.42	0.0000924
Pieces of Work Platform Rubber, ft ³	0.002	0.42	0.00084
Electromark Label (inside ZOI), ft ²	0.7	0.47	0.329
Electromark Label (outside ZOI), ft ²	39.6	0.69	27.324
Unqualified Labels – Paper, ft ²	0.28	0.4	0.112
Unqualified Labels – Other, ft ²	25.66	0.4	10.264
Flex Conduit PVC Jacketing, ft ²	1.57	0.3	0.471

- (1) 8% of Cal-Sil fines transport to the reactor cavity (References 28 and 94) and are subtracted from the debris generated value prior to determining the debris at the strainer and the amount available to transport.

Table 3a3-17 Loop 2 Alternate RCS loop Piping Break Debris Transported to the Main Strainer during Pool Fill

Debris Type	Debris Generated	Transport Fraction	Debris at Strainer
RMI Small Pieces, ft ²	40343	0.4	16137.2
RMI Large Pieces, ft ²	13448	0.38	5110.24
Cal-Sil Fines, lbs	17.4	0.33	5.742
Erosion of Cal-Sil Small Pieces to fines, lbs	11.3	0	0
Cal-Sil Small Pieces, lbs	11.3	0.31	3.503
Marinite I fines, lbs	0.1	0.33	0.033
Erosion of Marinite I Small Pieces to fines, lbs	0.046	0	0
Marinite I Small Pieces, lbs	0.046	0.31	0.01426
Erosion of Marinite I Large Pieces to fines, lbs	0.21	0	0
Marinite I Large Pieces, lbs	0.21	0.3	0.063
Marinite 36 fines, lbs	0	0.33	0
Erosion of Marinite 36 Small Pieces to fines, lbs	0	0	0
Marinite 36 Small Pieces, lbs	0	0.31	0
Erosion of Marinite 36 Large Pieces to fines, lbs	0	0	0
Marinite 36 Large Pieces, lbs	0	0.3	0
Min-K, lbs	5.2	0.33	1.716
Epoxy Paint (inside ZOI), lbs	5.7	0.33	1.881
Alkyd Paint (inside ZOI), lbs	1.9	0.33	0.627
Unqualified OEM Epoxy (outside ZOI), lbs	16.9	0	0
Unqualified OEM Alkyd (outside ZOI), lbs	74.4	0	0
Unqualified Non-OEM Epoxy (outside ZOI), lbs	31	0	0
Unqualified Non-OEM Alkyd (outside ZOI), lbs	3.4	0	0
Unqualified Cold Galvanizing Compound, lbs	777.5	0	0
Dirt/Dust, lbs	170	0.25	42.5
Latent Fiber, ft ³	12.5	0.25	3.125
Fire Proof Tape Fines, ft ²	0.5	0.33	0.165
Fire Proof Tape Small Pieces, ft ²	0.3	0.4	0.12
Fire Proof Tape Large Pieces, ft ²	1	0.4	0.4
Ice Storage Bag Fibers, ft ³	0.026	0.47	0.01222
Ice Storage Bag Liner Shards, ft ³	0.00022	0.47	0.0001034
Pieces of Work Platform Rubber, ft ³	0.002	0.47	0.00094
Electromark Label (inside ZOI), ft ²	0.6	0.4	0.24
Electromark Label (outside ZOI), ft ²	39.6	0	0
Unqualified Labels – Paper, ft ²	0.28	0	0
Unqualified Labels – Other, ft ²	25.66	0	0
Flex Conduit PVC Jacketing, ft ²	1.57	0	0

Table 3a3-18 Loop 2 Alternate RCS loop Break Debris at Main Strainer

Debris Type	Debris Generated	Transport Fraction	Debris at Strainer
RMI Small Pieces, ft ²	40343	0.63	25416.09
RMI Large Pieces, ft ²	13448	0.43	5782.64
Cal-Sil Fines, lbs	17.4	0.45	7.83
Erosion of Cal-Sil Small Pieces to fines, lbs	11.3	0.1	1.13
Cal-Sil Small Pieces, lbs	11.3	0.38	4.294
Marinite I fines, lbs	0.1	0.45	0.045
Erosion of Marinite I Small Pieces to fines, lbs	0.046	0.1	0.0046
Marinite I Small Pieces, lbs	0.046	0.38	0.01748
Erosion of Marinite I Large Pieces to fines, lbs	0.21	0.11	0.0231
Marinite I Large Pieces, lbs	0.21	0.35	0.0735
Marinite 36 fines, lbs	0	0.45	0
Erosion of Marinite 36 Small Pieces to fines, lbs	0	0.1	0
Marinite 36 Small Pieces, lbs	0	0.38	0
Erosion of Marinite 36 Large Pieces to fines, lbs	0	0.11	0
Marinite 36 Large Pieces, lbs	0	0.35	0
Min-K, lbs	5.2	0.45	2.34
Epoxy Paint (inside ZOI), lbs	5.7	0.45	2.565
Alkyd Paint (inside ZOI), lbs	1.9	0.45	0.855
Unqualified OEM Epoxy (outside ZOI), lbs	16.9	0.4	6.76
Unqualified OEM Alkyd (outside ZOI), lbs	74.4	0.14	10.416
Unqualified Non-OEM Epoxy (outside ZOI), lbs	31	0.39	12.09
Unqualified Non-OEM Alkyd (outside ZOI), lbs	3.4	0.58	1.972
Unqualified Cold Galvanizing Compound, lbs	777.5	0.93	723.075
Dirt/Dust, lbs	170	0.52	88.4
Latent Fiber, ft ³	12.5	0.52	6.5
Fire Proof Tape Fines, ft ²	0.5	0.45	0.225
Fire Proof Tape Small Pieces, ft ²	0.3	0.63	0.189
Fire Proof Tape Large Pieces, ft ²	1	0.63	0.63
Ice Storage Bag Fibers, ft ³	0.026	0.64	0.01664
Ice Storage Bag Liner Shards, ft ³	0.00022	0.64	0.0001408
Pieces of Work Platform Rubber, ft ³	0.002	0.64	0.00128
Electromark Label (inside ZOI), ft ²	0.6	0.63	0.378
Electromark Label (outside ZOI), ft ²	39.6	0.17	6.732
Unqualified Labels – Paper, ft ²	0.28	0.86	0.2408
Unqualified Labels – Other, ft ²	25.66	0.86	22.0676
Flex Conduit PVC Jacketing, ft ²	1.57	1	1.57

**Table 3a3-19 Loop 2 Alternate RCS loop Break Debris at Remote Strainer
(90% Blocked Main)**

Debris Type	Debris Generated	Transport Fraction	Debris at Strainer
RMI Small Pieces, ft ²	40343	0	0
RMI Large Pieces, ft ²	13448	0	0
Cal-Sil Fines, lbs	17.4	0.51	8.164 ⁽¹⁾
Erosion of Cal-Sil Small Pieces to fines, lbs	11.3	0.04	0.452
Cal-Sil Small Pieces, lbs	11.3	0	0
Marinite I fines, lbs	0.1	0.51	0.051
Erosion of Marinite I Small Pieces to fines, lbs	0.046	0.04	0.00184
Marinite I Small Pieces, lbs	0.046	0	0
Erosion of Marinite I Large Pieces to fines, lbs	0.21	0.04	0.0084
Marinite I Large Pieces, lbs	0.21	0	0
Marinite 36 fines, lbs	0	0.51	0
Erosion of Marinite 36 Small Pieces to fines, lbs	0	0.04	0
Marinite 36 Small Pieces, lbs	0	0	0
Erosion of Marinite 36 Large Pieces to fines, lbs	0	0.04	0
Marinite 36 Large Pieces, lbs	0	0	0
Min-K, lbs	5.2	0.51	2.652
Epoxy Paint (inside ZOI), lbs	5.7	0.51	2.907
Alkyd Paint (inside ZOI), lbs	1.9	0.51	0.969
Unqualified OEM Epoxy (outside ZOI), lbs	16.9	0.72	12.168
Unqualified OEM Alkyd (outside ZOI), lbs	74.4	0.9	66.96
Unqualified Non-OEM Epoxy (outside ZOI), lbs	31	0	0
Unqualified Non-OEM Alkyd (outside ZOI), lbs	3.4	0.59	2.006
Unqualified Cold Galvanizing Compound, lbs	777.5	0.35	272.125
Dirt/Dust, lbs	170	0.56	95.2
Latent Fiber, ft ³	12.5	0.56	7
Fire Proof Tape Fines, ft ²	0.5	0.51	0.255
Fire Proof Tape Small Pieces, ft ²	0.3	0	0
Fire Proof Tape Large Pieces, ft ²	1	0	0
Ice Storage Bag Fibers, ft ³	0.026	0.41	0.01066
Ice Storage Bag Liner Shards, ft ³	0.00022	0.41	0.0000902
Pieces of Work Platform Rubber, ft ³	0.002	0.41	0.00082
Electromark Label (inside ZOI), ft ²	0.6	0.05	0.03
Electromark Label (outside ZOI), ft ²	39.6	0.6	23.76
Unqualified Labels – Paper, ft ²	0.28	0.4	0.112
Unqualified Labels – Other, ft ²	25.66	0.4	10.264
Flex Conduit PVC Jacketing, ft ²	1.57	0.3	0.471

- (1) 8% of Cal-Sil fines transport to the reactor cavity (References 28 and 94) and are subtracted from the debris generated value prior to determining the debris at the strainer and the amount available to transport.

Table 3a3-20 Loop 3 Alternate RCS loop Break Debris at Main Strainer

Debris Type	Debris Generated	Transport Fraction	Debris at Strainer
RMI Small Pieces, ft ²	40343	0.63	25416.09
RMI Large Pieces, ft ²	13448	0.43	5782.64
Cal-Sil Fines, lbs	14.5	0.45	6.525
Erosion of Cal-Sil Small Pieces to fines, lbs	10	0.1	1
Cal-Sil Small Pieces, lbs	10	0.38	3.8
Marinite I fines, lbs	0.14	0.45	0.063
Erosion of Marinite I Small Pieces to fines, lbs	0.05	0.1	0.005
Marinite I Small Pieces, lbs	0.05	0.38	0.019
Erosion of Marinite I Large Pieces to fines, lbs	0.23	0.11	0.0253
Marinite I Large Pieces, lbs	0.23	0.35	0.0805
Marinite 36 fines, lbs	0.58	0.45	0.261
Erosion of Marinite 36 Small Pieces to fines, lbs	0.22	0.1	0.022
Marinite 36 Small Pieces, lbs	0.22	0.38	0.0836
Erosion of Marinite 36 Large Pieces to fines, lbs	1.1	0.11	0.121
Marinite 36 Large Pieces, lbs	1.1	0.35	0.385
Min-K, lbs	5.2	0.45	2.34
Epoxy Paint (inside ZOI), lbs	5.7	0.45	2.565
Alkyd Paint (inside ZOI), lbs	1.9	0.45	0.855
Unqualified OEM Epoxy (outside ZOI), lbs	16.9	0.4	6.76
Unqualified OEM Alkyd (outside ZOI), lbs	74.4	0.14	10.416
Unqualified Non-OEM Epoxy (outside ZOI), lbs	31	0.52	16.12
Unqualified Non-OEM Alkyd (outside ZOI), lbs	3.4	0.58	1.972
Unqualified Cold Galvanizing Compound, lbs	777.5	0.93	723.075
Dirt/Dust, lbs	170	0.52	88.4
Latent Fiber, ft ³	12.5	0.52	6.5
Fire Proof Tape Fines, ft ²	12.50	0.45	5.625
Fire Proof Tape Small Pieces, ft ²	7.1	0.63	4.473
Fire Proof Tape Large Pieces, ft ²	26.8	0.63	16.884
Ice Storage Bag Fibers, ft ³	0.026	0.64	0.01664
Ice Storage Bag Liner Shards, ft ³	0.00022	0.64	0.0001408
Pieces of Work Platform Rubber, ft ³	0.002	0.64	0.00128
Electromark Label (inside ZOI), ft ²	0.6	0.63	0.378
Electromark Label (outside ZOI), ft ²	39.6	0.17	6.732
Unqualified Labels – Paper, ft ²	0.28	0.86	0.2408
Unqualified Labels – Other, ft ²	25.66	0.86	22.0676
Flex Conduit PVC Jacketing, ft ²	1.57	1	1.57

**Table 3a3-21 Loop 3 Alternate RCS loop Break Debris at Remote Strainer
(90% Blocked Main)**

Debris Type	Debris Generated	Transport Fraction	Debris at Strainer
RMI Small Pieces, ft ²	40343	0	0
RMI Large Pieces, ft ²	13448	0	0
Cal-Sil Fines, lbs	14.5	0.52	6.9368 ⁽¹⁾
Erosion of Cal-Sil Small Pieces to fines, lbs	10	0.08	0.8
Cal-Sil Small Pieces, lbs	10	0	0
Marinite I fines, lbs	0.14	0.52	0.0728
Erosion of Marinite I Small Pieces to fines, lbs	0.05	0.08	0.004
Marinite I Small Pieces, lbs	0.05	0	0
Erosion of Marinite I Large Pieces to fines, lbs	0.23	0.06	0.0138
Marinite I Large Pieces, lbs	0.23	0	0
Marinite 36 fines, lbs	0.58	0.52	0.3016
Erosion of Marinite 36 Small Pieces to fines, lbs	0.22	0.08	0.0176
Marinite 36 Small Pieces, lbs	0.22	0	0
Erosion of Marinite 36 Large Pieces to fines, lbs	1.1	0.06	0.066
Marinite 36 Large Pieces, lbs	1.1	0	0
Min-K, lbs	5.2	0.52	2.704
Epoxy Paint (inside ZOI), lbs	5.7	0.52	2.964
Alkyd Paint (inside ZOI), lbs	1.9	0.52	0.988
Unqualified OEM Epoxy (outside ZOI), lbs	16.9	0.72	12.168
Unqualified OEM Alkyd (outside ZOI), lbs	74.4	0.9	66.96
Unqualified Non-OEM Epoxy (outside ZOI), lbs	31	0	0
Unqualified Non-OEM Alkyd (outside ZOI), lbs	3.4	0.59	2.006
Unqualified Cold Galvanizing Compound, lbs	777.5	0.35	272.125
Dirt/Dust, lbs	170	0.56	95.2
Latent Fiber, ft ³	12.5	0.56	7
Fire Proof Tape Fines, ft ²	12.50	0.52	6.5
Fire Proof Tape Small Pieces, ft ²	7.1	0	0
Fire Proof Tape Large Pieces, ft ²	26.8	0	0
Ice Storage Bag Fibers, ft ³	0.026	0.42	0.01092
Ice Storage Bag Liner Shards, ft ³	0.00022	0.42	0.0000924
Pieces of Work Platform Rubber, ft ³	0.002	0.42	0.00084
Electromark Label (inside ZOI), ft ²	0.6	0.47	0.282
Electromark Label (outside ZOI), ft ²	39.6	0.69	27.324
Unqualified Labels – Paper, ft ²	0.28	0.4	0.112
Unqualified Labels – Other, ft ²	25.66	0.4	10.264
Flex Conduit PVC Jacketing, ft ²	1.57	0.3	0.471

- (1) 8% of Cal-Sil fines transport to the reactor cavity (References 28 and 94) and are subtracted from the debris generated value prior to determining the debris at the strainer and the amount available to transport.

Table 3a3-22 Loop 4 Alternate RCS loop Piping Break Debris Transported to the Main Strainer during Pool Fill

Debris Type	Debris Generated	Transport Fraction	Debris at Strainer
RMI Small Pieces, ft ²	31021	0.09	2791.89
RMI Large Pieces, ft ²	10341	0.05	517.05
Cal-Sil Fines, lbs	72.5	0.32	23.2
Erosion of Cal-Sil Small Pieces to fines, lbs	46.4	0	0
Cal-Sil Small Pieces, lbs	46.4	0.05	2.32
Marinite I fines, lbs	0	0.32	0
Erosion of Marinite I Small Pieces to fines, lbs	0	0	0
Marinite I Small Pieces, lbs	0	0.05	0
Erosion of Marinite I Large Pieces to fines, lbs	0	0	0
Marinite I Large Pieces, lbs	0	0.04	0
Marinite 36 fines, lbs	0.79	0.32	0.2528
Erosion of Marinite 36 Small Pieces to fines, lbs	0.3	0	0
Marinite 36 Small Pieces, lbs	0.3	0.05	0.015
Erosion of Marinite 36 Large Pieces to fines, lbs	1.62	0	0
Marinite 36 Large Pieces, lbs	1.62	0.04	0.0648
Min-K, lbs	0	0.32	0
Epoxy Paint (inside ZOI), lbs	5.7	0.32	1.824
Alkyd Paint (inside ZOI), lbs	1.9	0.32	0.608
Unqualified OEM Epoxy (outside ZOI), lbs	16.9	0	0
Unqualified OEM Alkyd (outside ZOI), lbs	74.4	0	0
Unqualified Non-OEM Epoxy (outside ZOI), lbs	31	0	0
Unqualified Non-OEM Alkyd (outside ZOI), lbs	3.4	0	0
Unqualified Cold Galvanizing Compound, lbs	777.5	0	0
Dirt/Dust, lbs	170	0.24	40.8
Latent Fiber, ft ³	12.5	0.24	3
Fire Proof Tape Fines, ft ²	25.1	0.32	8.032
Fire Proof Tape Small Pieces, ft ²	14.4	0.09	1.296
Fire Proof Tape Large Pieces, ft ²	54.1	0.09	4.869
Ice Storage Bag Fibers, ft ³	0.026	0.45	0.0117
Ice Storage Bag Liner Shards, ft ³	0.00022	0.45	0.000099
Pieces of Work Platform Rubber, ft ³	0.002	0.45	0.0009
Electromark Label (inside ZOI), ft ²	0.7	0.09	0.063
Electromark Label (outside ZOI), ft ²	39.6	0	0
Unqualified Labels – Paper, ft ²	0.28	0	0
Unqualified Labels – Other, ft ²	25.66	0	0
Flex Conduit PVC Jacketing, ft ²	1.57	0	0

Table 3a3-23 Loop 4 Alternate RCS loop Break Debris at Main Strainer

Debris Type	Debris Generated	Transport Fraction	Debris at Strainer
RMI Small Pieces, ft ²	31021	0.13	4032.73
RMI Large Pieces, ft ²	10341	0.08	827.28
Cal-Sil Fines, lbs	72.5	0.44	31.9
Erosion of Cal-Sil Small Pieces to fines, lbs	46.4	0.1	4.64
Cal-Sil Small Pieces, lbs	46.4	0.1	4.64
Marinite I fines, lbs	0	0.44	0
Erosion of Marinite I Small Pieces to fines, lbs	0	0.1	0
Marinite I Small Pieces, lbs	0	0.1	0
Erosion of Marinite I Large Pieces to fines, lbs	0	0.14	0
Marinite I Large Pieces, lbs	0	0.07	0
Marinite 36 fines, lbs	0.79	0.44	0.3476
Erosion of Marinite 36 Small Pieces to fines, lbs	0.3	0.1	0.03
Marinite 36 Small Pieces, lbs	0.3	0.1	0.03
Erosion of Marinite 36 Large Pieces to fines, lbs	1.62	0.14	0.2268
Marinite 36 Large Pieces, lbs	1.62	0.07	0.1134
Min-K, lbs	0	0.44	0
Epoxy Paint (inside ZOI), lbs	5.7	0.44	2.508
Alkyd Paint (inside ZOI), lbs	1.9	0.44	0.836
Unqualified OEM Epoxy (outside ZOI), lbs	16.9	0.4	6.76
Unqualified OEM Alkyd (outside ZOI), lbs	74.4	0.14	10.416
Unqualified Non-OEM Epoxy (outside ZOI), lbs	31	0.52	16.12
Unqualified Non-OEM Alkyd (outside ZOI), lbs	3.4	0.58	1.972
Unqualified Cold Galvanizing Compound, lbs	777.5	0.93	723.075
Dirt/Dust, lbs	170	0.52	88.4
Latent Fiber, ft ³	12.5	0.52	6.5
Fire Proof Tape Fines, ft ²	25.1	0.44	11.044
Fire Proof Tape Small Pieces, ft ²	14.4	0.13	1.872
Fire Proof Tape Large Pieces, ft ²	54.1	0.13	7.033
Ice Storage Bag Fibers, ft ³	0.026	0.63	0.01638
Ice Storage Bag Liner Shards, ft ³	0.00022	0.63	0.0001386
Pieces of Work Platform Rubber, ft ³	0.002	0.63	0.00126
Electromark Label (inside ZOI), ft ²	0.7	0.13	0.091
Electromark Label (outside ZOI), ft ²	39.6	0.03	1.188
Unqualified Labels – Paper, ft ²	0.28	0.86	0.2408
Unqualified Labels – Other, ft ²	25.66	0.86	22.0676
Flex Conduit PVC Jacketing, ft ²	1.57	1	1.57

**Table 3a3-24 Loop 4 Alternate RCS loop Break Debris at Remote Strainer
(90% Blocked Main)**

Debris Type	Debris Generated	Transport Fraction	Debris at Strainer
RMI Small Pieces, ft ²	31021	0	0
RMI Large Pieces, ft ²	10341	0	0
Cal-Sil Fines, lbs	72.5	0.52	34.684 ⁽¹⁾
Erosion of Cal-Sil Small Pieces to fines, lbs	46.4	0.08	3.712
Cal-Sil Small Pieces, lbs	46.4	0	0
Marinite I fines, lbs	0	0.52	0
Erosion of Marinite I Small Pieces to fines, lbs	0	0.08	0
Marinite I Small Pieces, lbs	0	0	0
Erosion of Marinite I Large Pieces to fines, lbs	0	0.06	0
Marinite I Large Pieces, lbs	0	0	0
Marinite 36 fines, lbs	0.79	0.52	0.4108
Erosion of Marinite 36 Small Pieces to fines, lbs	0.3	0.08	0.024
Marinite 36 Small Pieces, lbs	0.3	0	0
Erosion of Marinite 36 Large Pieces to fines, lbs	1.62	0.06	0.0972
Marinite 36 Large Pieces, lbs	1.62	0	0
Min-K, lbs	0	0.52	0
Epoxy Paint (inside ZOI), lbs	5.7	0.52	2.964
Alkyd Paint (inside ZOI), lbs	1.9	0.52	0.988
Unqualified OEM Epoxy (outside ZOI), lbs	16.9	0.72	12.168
Unqualified OEM Alkyd (outside ZOI), lbs	74.4	0.9	66.96
Unqualified Non-OEM Epoxy (outside ZOI), lbs	31	0	0
Unqualified Non-OEM Alkyd (outside ZOI), lbs	3.4	0.59	2.006
Unqualified Cold Galvanizing Compound, lbs	777.5	0.35	272.125
Dirt/Dust, lbs	170	0.56	95.2
Latent Fiber, ft ³	12.5	0.56	7
Fire Proof Tape Fines, ft ²	25.1	0.52	13.052
Fire Proof Tape Small Pieces, ft ²	14.4	0	0
Fire Proof Tape Large Pieces, ft ²	54.1	0	0
Ice Storage Bag Fibers, ft ³	0.026	0.42	0.01092
Ice Storage Bag Liner Shards, ft ³	0.00022	0.42	0.0000924
Pieces of Work Platform Rubber, ft ³	0.002	0.42	0.00084
Electromark Label (inside ZOI), ft ²	0.7	0.47	0.329
Electromark Label (outside ZOI), ft ²	39.6	0.69	27.324
Unqualified Labels – Paper, ft ²	0.28	0.4	0.112
Unqualified Labels – Other, ft ²	25.66	0.4	10.264
Flex Conduit PVC Jacketing, ft ²	1.57	0.3	0.471

- (1) 8% of Cal-Sil fines transport to the reactor cavity (References 28 and 94) and are subtracted from the debris generated value prior to determining the debris at the strainer and the amount available to transport.

NRC Information Item 3.b - Debris Generation/Zone of Influence (ZOI) (excluding coatings)

The objective of the debris generation/ZOI process is to determine, for each postulated break location: (1) the zone within which the break jet forces would be sufficient to damage materials and create debris; and (2) the amount of debris generated by the break jet forces.

- 1. Describe the methodology used to determine the ZOIs for generating debris. Identify which debris analyses used approved methodology default values. For debris with ZOIs not defined in the guidance report/SE, or if using other than default values, discuss method(s) used to determine ZOI and the basis for each.*
- 2. Provide destruction ZOIs and the basis for the ZOIs for each applicable debris constituent.*
- 3. Identify if destruction testing was conducted to determine ZOIs. If such testing has not been previously submitted to the NRC for review or information, describe the test procedure and results with reference to the test report(s).*
- 4. Provide the quantity of each debris type generated for each break location evaluated. If more than four break locations were evaluated, provide data only for the four most limiting locations.*
- 5. Provide total surface area of all signs, placards, tags, tape, and similar miscellaneous materials in containment.*

I&M Response to Information Items 3.b.1 and 3.b.2

The CNP debris generation evaluation consisted of two principle steps:

- Determine the ZOI in which debris is generated.
- Identify the characteristics (size distribution) of the destroyed debris.

The ZOI is defined as the volume about the break in which the jet pressure is greater than or equal to the destruction damage pressure of the insulation, coatings, and other materials impacted by the break jet. Both the GR and SER define the ZOI as spherical and centered at the break site or location. The radius of the sphere is determined by the pipe diameter and the destruction pressures of the potential target insulation or debris material. All potentially important debris sources (insulation, coatings, fixed debris, etc.) within the ZOI were evaluated for CNP.

Section 4 of the GR allows for the development of target-based ZOIs, recognizing that different materials have different destruction pressures. The CNP evaluation used multiple ZOIs at the specific break location, dependent upon the target debris. The destruction pressures and associated ZOI radii for common PWR materials were taken from Table 3-2 of the SER. In addition, destruction testing was performed on several other materials (stainless steel jacketed foam insulation, Marinite fire barrier material, fire barrier tape, and Electromark valve labels) installed at CNP. The results of that testing were incorporated into the CNP analysis.

Existing robust barriers, consisting of structures and equipment that are impervious to jet impingement, were considered in the CNP evaluation. These barriers included the primary shield wall, the refueling cavity walls, the crane wall, the SG lower lateral restraints, and the

PZR deck. These barriers may prevent further expansion of the break jet but they can also cause deflection and reflection. Section 3.4.2.3 of the SER states that when a spherical ZOI extends beyond robust barriers such as walls or encompasses large components such as tanks and SGs, the extended volume may be conservatively truncated. The SER also stipulates that "shadowed" surfaces of components should be included in the analysis. These approaches were used in the CNP debris generation evaluation.

The first step in understanding the debris that is generated during a LOCA is to identify the potential debris sources in containment. For CNP, the debris sources that are in potential break locations that could lead to recirculation are listed in the following tables. There are other insulation materials in containment (encapsulated fiberglass, etc.) that are in locations where they would not be subjected to jet impingement forces, are in a location where the break would not lead to recirculation, or would not fail as a result of a break that leads to recirculation (refer to the Response to Information Item 3.b.3 for the last category).

Table 3b1-1 Insulation Quantities by Potential Break Location – Unit 1

	Transco RMI, ft ²	DP RMI, ft ²	Cal-Sil, ft ³	Fiberglass, ft ³	Marinite, ft ³	Min-K, ft ³
Lower Containment – Inside Crane Wall – Loop 1	37,726	9,995	213	--	--	--
Lower Containment – Inside Crane Wall – Loop 2	37,840	12,417	198	--	2.12	0.18
Lower Containment – Inside Crane Wall – Loop 3	37,674	13,683	213	--	0.68	0.08
Lower Containment – Inside Crane Wall – Loop 4	37,726	11,487	260	--	2.55	--
Lower Containment – Inside Crane Wall – PZR Vault area	150	20,184	118	--	--	--
Reactor Cavity	19,792	--	--	5	--	--
Total	170,908	67,766	1,002	5	5.35	0.26

Table 3b1-2 Insulation Quantities by Potential Break Location – Unit 2

	Transco RMI, ft²	DP RMI, ft²	Cal-Sil, ft³	Fiberglass, ft³	Marinite, ft³	Min-K, ft³
Lower Containment – Inside Crane Wall – Loop 1	--	39,530	348	--	2.09	--
Lower Containment – Inside Crane Wall – Loop 2	--	42,542	326	--	0.61	0.18
Lower Containment – Inside Crane Wall – Loop 3	--	43,828	352	--	7.05	0.08
Lower Containment – Inside Crane Wall – Loop 4	--	39,443	401	--	2.56	--
Lower Containment – Inside Crane Wall – PZR Vault area	--	19,942	121	--	--	--
Reactor Cavity	19,802	--	--	5	--	--
Total	19,802	185,285	1,548	5	12.31	0.26

Table 3b1-3 Latent Debris Location Unit 1 and Unit 2 Bounding Values

Debris Type	Upper Containment	Loop Compartment	Pipe Annulus	Ice Condenser	Total
Latent Fiber, lbs	5.4	15.6	8.4	0.6	30
Latent Dirt/Dust, lbs	30.6	88.4	47.6	3.4	170
Electromark Labels - break in Loop 1 or Loop 4, ft ²	--	21.8	30.48	--	52.28
Electromark Labels - break in Loop 2 or Loop 3, ft ²	--	20.14	30.48	--	50.62
Unqualified Labels, ft ²	8.77	13.62	3.55	--	25.94
Flexible Conduit PVC Jacketing, ft ²	--	1.57	--	--	1.57
Ice Storage Bag Fibers, ft ²	--	--	--	5.0	5.0
Ice Storage Bag Liner Shards, ft ²	--	--	--	0.87	0.87
Pieces of Rubber from platform where ice bags were opened, ft ²	--	--	--	0.22	0.22

The materials listed in last three rows of Table 3b1-3 were assumed to reside in the ice condenser ice bed following the reloading of ice in 1999 to 2000. In 1998, I&M completely melted the ice in both Unit 1 and Unit 2 ice condensers, performed significant refurbishment, and then reloaded both ice condensers with ice that was being made with the installed ice machines and with ice that had been made and stored in bags. During the process of loading the ice condenser baskets, a certain amount of the ice will pass through the ice basket openings and fall to the lower ice condenser area. This non-retained ice was then vacuumed and melted. Any debris in the melted ice was captured in the ice melt filter. This collected debris was saved, sorted, and conservatively quantified to establish a bounding value that could be resident in the ice bed. This debris, as indicated in the table, was determined to be from the bagged ice.

Subsequent to the complete reload effort, several hundred baskets in each unit have been emptied and reloaded. The reloaded ice is considered to be debris free because it is produced from the installed ice machines which are controlled as high risk FME areas. Therefore, each outage, the ice from baskets that potentially contain debris is replaced with ice that is debris free. However, no credit was taken for this replacement because the potential exists that during ice condenser maintenance activities small quantities of debris from other sources could be dropped into the ice bed.

Table 3b1-3 includes flexible conduit PVC jacketing as a debris source. Since there was no information available as to the response of this material to jet impingement from a HELB, I&M elected to remove this material within areas that could be impacted by a jet. However, some of the flexible conduits in these areas could not be reached without the expenditure of significant

resources and radiation dose. The flexible conduit PVC jacketing listed in Table 3b1-3 accounts for the jacketing that was not removed.

Table 3b1-3 also includes unqualified labels. Walkdown data for Unit 1 and 2 conservatively established a bounding quantity of 25.94 ft² of unqualified labels in containment. The as-left quantity of unqualified labels in Unit 2, based on the final walkdowns performed during the Fall 2007 RFO was 9.58 ft². I&M intends to perform similar walkdowns and quantification during the upcoming Spring 2008 Unit 1 RFO.

Table 3b1-4, below, provides the quantity of fire barrier tape located in Unit 1 and Unit 2 containments. These quantities were obtained from extensive walkdowns that were performed to quantify fire barrier materials in containment.

Table 3b1-4 Fire Barrier Tape Quantity

Location	Unit 1 Area, ft ²	Unit 2 Area, ft ²
Loop 1	102.71	163.10
Loop 2	29.58	6.68
Loop 3	99.61	178.68
Loop 4	6.28	360.37
Total	238.18	708.83

The ZOIs applied to specific materials and their basis are identified in Table 3b1-5.

Table 3b1-5 ZOI Radii for Debris Sources

Debris Source Types	Destruction Pressure (psi)	ZOI Radius (Radius/Break Diameter) (ft)	Basis for Assumed ZOI
Transco RMI	114	2.0D	SER Table 3-2
Marinite I and Marinite 36	~14.5	9.8D ⁽¹⁾	Testing
Cal-Sil	20	6.4D ⁽²⁾	ALION
Low Density Transco Fiberglass (Owens Corning Type AU 300)	114	2.0D ⁽³⁾	SER Table 3-2
DP RMI	2.4	28.6D	SER Table 3-2
Min-K	2.4	28.6D	SER Table 3-2
Fire-Proof Tape	~16	8.2D ⁽¹⁾	Testing
Electromark Labels	~ 21	6.0D ⁽¹⁾	Testing

(1) ZOI is based on destruction testing data and observations. This testing is discussed in the response to NRC Information Item 3.b.3.

(2) ZOI is based on ALION Analysis.

(3) See discussion following Table 3b1-6.

I&M is taking an exception to the size distribution for Cal-Sil as given in SER Section 3.4.3.3 as described below.

A more refined size distribution was developed for Cal-Sil by ALION. In developing the more refined size distribution, OPG test data for destruction of Cal-Sil insulation material (Reference 89, Table 3-6) was analyzed to develop a three category size distribution. The three sizes for Cal-Sil were fines (particulate), small pieces that are dislodged from the target (under 1 in but greater than fines to over 3 in), and intact pieces that remain on the target. It was determined that, within the overall ZOI, the size distribution would vary based on the distance of the insulation from the break (i.e. insulation debris generated near the break location would consist of more small pieces than insulation debris generated near the edge of the ZOI). Therefore, based on the OPG test data, two separate sub-zones were defined for Cal-Sil and the corresponding size distribution within each sub-zone was determined. These size distributions and sub-zone ZOIs are as follows:

Table 3b1-6 ALION ZOI & Size Distribution for Cal-Sil

Size	Zone 1 70.0 psi ZOI (2.7D)	Zone 2 20.0-70.0 psi ZOI (6.4D – 2.7D)
Fines	50%	23%
Small Pieces	50%	15%
Remains on Target	0%	62%

The fibrous insulation at the bottom of the reactor vessel is Transco supplied Owens Corning Type AU 300. This insulation type is not discussed in the GR. However, the Transco fiberglass on the bottom of the reactor vessel is fully encapsulated and is surrounded by the same stainless steel cassettes of Transco RMI existing on the remainder of the reactor. Per the SER, the destruction pressure of Transco RMI is set at 114 psig, correlating to a ZOI (L/D) of 2 (SER Table 3-2). Due to the robust nature of Transco RMI, and because the fiberglass is surrounded by Transco RMI, the Transco fiberglass was assigned the same destruction pressure and ZOI as Transco RMI (114 psi or 2.0D ZOI).

The flex conduit with PVC jacketing inside the loop compartment, but not in the SG or PZR enclosures, was conservatively assumed to fail, independent of a ZOI.

I&M Response to Information Item 3.b.3

I&M performed destruction testing for four different materials at Wyle in Huntsville, Alabama. The four materials tested were Marinite I, jacketed Armaflex insulation, Scotch 77 Fire Retardant Electric Arc Proofing Tape, and Electromark valve labels on a stainless steel backing material. As indicated in the response to Information Items 3.b.1 and 3.b.2, Marinite 36 was also listed as one of the potential debris sources. Marinite 36 is an asbestos-based fire board material that is no longer available. Testing of Marinite 36 is impractical because of the asbestos. I&M had ALION perform an evaluation of Marinite 36 to identify a suitable surrogate for destruction testing. This evaluation determined that the Marinite I, which is also used at

CNP, was a suitable and conservative surrogate for destruction testing. The principal basis for this suitability was that the asbestos fibers in Marinite 36 are significantly stronger than the cellulose fibers in Marinite I, and that the balance of the material in both boards is calcium silicate (Reference 91). The purpose of this testing was to establish conservative values for the quantity of debris generated from various distances and orientations, with the exception of the jacketed Armaflex insulation. Testing of the jacketed Armaflex insulation was performed to determine the capability of a double-jacketing system to prevent debris generation.

The Wyle testing was performed during May and June 2007 and is documented in Wyle Laboratories Test Report, Jet Impingement Test of Electromark Labels and Thermal and Fire Barrier Insulation (Reference 30). I&M contracted with S&L to provide a documented basis for the determination of ZOIs for the testing that was performed at Wyle. The evaluation of the testing is contained in Reference 90.

The test was conducted by applying nitrogen pressure to a heated fluid in a reservoir. The pressurized fluid was released by inducing the failure of a pair of rupture discs in the piping attached to the reservoir. The released fluid was directed at a target via a nozzle in the piping. The distance between the nozzle and the target was varied. The test configuration included a backstop and screen netting to help capture any debris that may be generated during a test.

The general test parameters were as follows:

- Initial Fluid Temperature – 520°F
- Initial Fluid Pressure – 2200 psig
- Volume of Fluid Reservoir – Sufficient to allow minimum blowdown duration of 30 seconds
- Nozzle Diameter – Nominal 2.45 in
- Test Initiation Time – Instantaneous through use of double rupture disk assembly

A general characterization of the system response during the testing is as follows:

- Flow Measurements – The flow measurements indicated a rapid rise to a flow of approximately 2700 gpm. The flow remained relatively steady at this level for approximately 20 to 24 seconds, and then decreased to approximately 2000 gpm at the time the test was terminated.
- Pressure Measurements – The pressure measurements indicated a slight decrease in reservoir pressure at the beginning of the test. The pressure recovered to near initial value rapidly and was controlled at that level for approximately 20 to 24 seconds. The pressure then decreased to approximately 1800 psi at the time the test was terminated.
- System Temperature Measurement – The temperature measurements indicated a rise upon initiation of the test. The total temperature rise was approximately 20°F at the time the test was terminated.
- Target Temperature Measurement – The target temperature measurements varied greatly depending on the distance from the nozzle to the target. In general, the target temperature rose to a maximum that remained constant until the termination of the test.

A total of 31 blowdown tests were conducted over several weeks. With the exception of the final test, all tests were single material tests. Thirteen (13) tests were conducted on Marinite I,

ten (10) tests were conducted on jacketed Armaflex, five (5) tests were conducted on Scotch 77 tape, and four (4) tests were conducted on Electromark valve labels. The testing was performed at distances ranging from 14 3/8 in to 140 1/8 in from the plane of the nozzle discharge to the target.

The determination of the ZOI based on the testing configuration was performed utilizing information contained within the GR and SER as described below.

The spatial relationship between the destructive pressure following a postulated PWR cold-leg pipe break and the theoretical sphere within which that pressure exists is discussed in detail in Appendix I of the SER. The NEI/NRC investigation has application to PWR plants with operating pressure and temperature not exceeding 2250 psia and 530°F, respectively, which is applicable to CNP. The results of the NEI and NRC analysis of the destructive pressure regions about the location of a postulated double-ended cold-leg pipe break are shown in Table I-3 of the SER. For convenience this table is repeated here.

Table 3b3-1 Summary of Jet Properties for the Reference Cold-Leg Break

P_{jet} (psig)	T_{jet} (°F)	Q_{jet}	R_{sphere}
2	218.7	0.35	31.5
3	221.8	0.34	25.4
4	224.6	0.34	21.6
6	230.0	0.34	17.0
10	239.6	0.33	11.9
17	253.7	0.32	7.5
24	265.5	0.31	5.4
40	287.0	0.29	4.0
80	324.2	0.26	2.6
150	366.1	0.21	1.5
190	384.0	0.20	1.1
2250	530	0.00	0.9

In this table, P_{jet} , T_{jet} , and Q_{jet} are the pressure, temperature and quality of the jet having the theoretical spherical radius, R_{sphere} , around the location of the postulated cold-leg pipe break. In this context, R_{sphere} is non-dimensional, i.e., it is the spherical radius divided by the diameter of the broken pipe. The important information in this table is the relationship between the destructive pressure, P_{jet} , and the spherical distance about the pipe break location, R_{sphere} .

The actual pressure distribution in a jet emanating from a double-ended guillotine break more appropriately resembles a conic cylinder. The destructive pressure isobars within the jet have been analyzed as indicated in the GR and SER. The analyses of these pressure isobars are summarized in the data contained in Appendix D of the GR. This data describes the jet diameter as a function of pressure and distance from the jet source, and the minimum distance downstream for which a given jet destructive pressure will exist. Thus, for plant-specific evaluations, the desired distance from the jet for a particular impact pressure can be determined. These data are summarized in the following table.

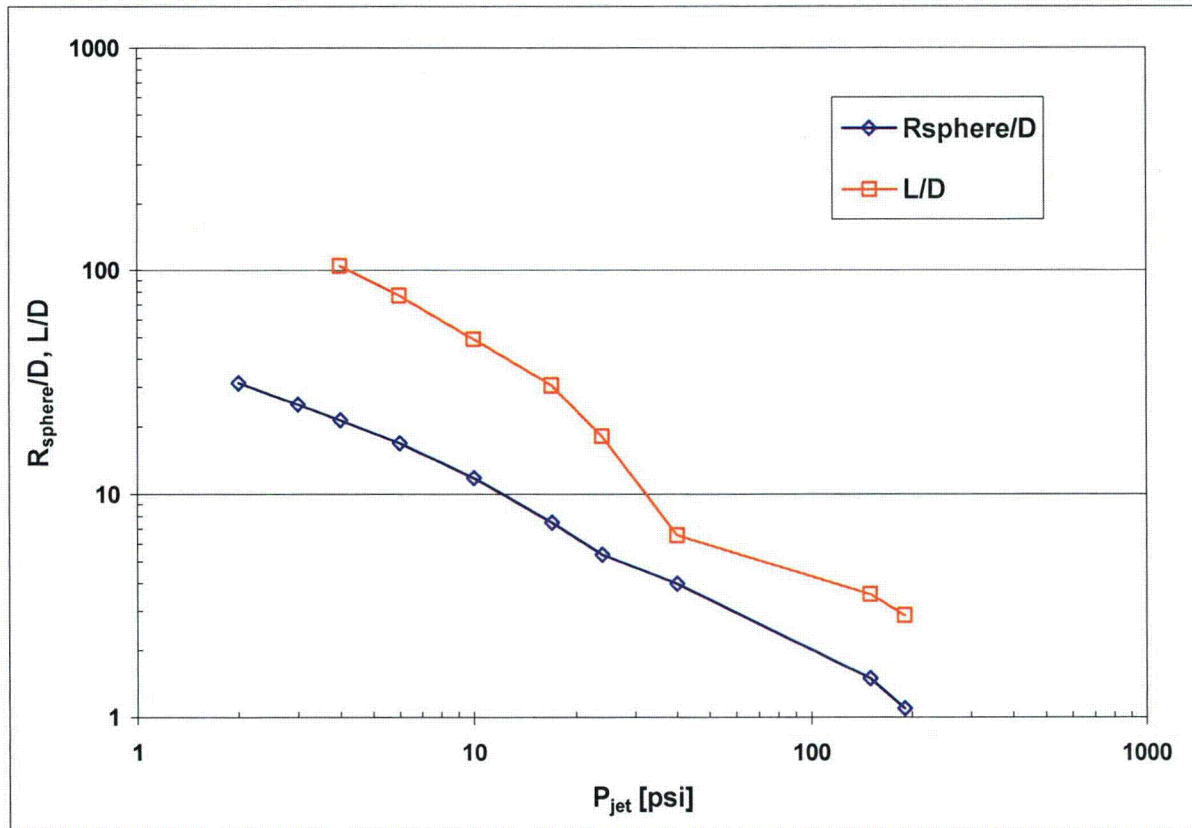
Table 3b3-2 Summary of Jet Properties for the Reference Cold-Leg Break

P_{jet}	L/D_{jet}
4	105.5
6	77.5
10	49.5
17	30.8
24	18.3
40	6.6
50	5.6
64	5.1
150	3.6
190	2.9

In this table, P_{jet} is the destructive pressure and L/D_{jet} is the distance downstream of the jet exit for which the diameter of the isobar for P_{jet} has diminished to zero, i.e., the maximum distance from the jet exit that P_{jet} can exist. The spherical radius, R_{sphere} , referenced above is defined as the radius of a sphere with a volume equal to two times the volume enveloped by a destructive pressure isobar. (The isobar volume is doubled to account for a mass of a jet emanating from both sides of the double guillotine break.)

These data are plotted in Figure 3b3-1. By use of Figure 3b3-1, the three parameters (P_{jet} , L/D_{break} , and R_{sphere}/D_{break}) can be determined. If one of the three parameters is known, the remaining pair can be determined graphically from Figure 3b3-1 or by interpolating the corresponding data in the tables above. Further, because the parameters are non-dimensional, the relationship holds for applications to determine the ZOI for a pipe break in a plant or a simulated pipe break in a test facility. The difference in the two is the diameter used to represent the discharge jet, the diameter of the cold leg or the diameter of the test nozzle.

Figure 3b3-1: Comparison of $R_{\text{sphere}}/D_{\text{break}}$ and L/D_{break} for PWR Cold Leg Breaks



The following sections describe the testing with the observed results that was performed for the four different target materials. The specific size distribution associated with the tested materials is described in the response to NRC Information Item 3.c.1.

Marinite I Testing

As stated previously, 13 tests were performed on Marinite I fire board material. These tests were performed at distances ranging from 14 3/8 in to 140 1/8 in. The Marinite I fire board was attached to 2 ft and 3 ft lengths of cable tray sections that were obtained from CNP plant stock. The cable tray sections were nominal 6 in by 12 in sections with either a solid flat bottom panel or solid corrugated bottom panel. The Marinite was attached to the cable tray sections per the CNP engineering standards for installation of Marinite. Four tests were performed with 3 ft long sections of cable tray and nine tests were performed with 2 ft long sections. The test specimens were weighed on a calibrated scale prior to testing. Following testing, the test specimens were dried in an oven at 200°F for a minimum of eight hours.

After the first test of the Marinite where there was no observable loss of material, the specimen was dried at a temperature of 150°F. The post-drying weight was greater than the pre-test weight which indicated that the drying time and temperature were insufficient to fully remove the moisture added during the test. The material was then dried at 200°F for eight hours and the post-drying weight was 0.55% less than the pre-test weight, with no loss of material during the test. Comparison of post-drying weights to pre-test weights (post less than pre) for those test specimens that did not have indicated loss of material confirmed that the drying time and temperature was adequate to remove the moisture added during the test.

The tests conducted on the Marinite were performed in three distinct orientations. In the first orientation (M-1), the longitudinal axis of the specimen was at a right angle to the jet centerline, with the centerline of the jet directed at the vertical center of the test specimen. In the second orientation (M-2), the support was axis rotated 45° toward the discharge nozzle (front face of specimen angled to the ground), the longitudinal axis was perpendicular to the jet centerline, and the jet centerline was aligned with the seam area between the front face and the side face materials. In the third orientation (M-3), the support axis was rotated 90° (front face of specimen pointed downwards), the longitudinal axis was perpendicular to the jet centerline, and the jet centerline was aligned with the seam area between the front face and side face materials. Figures 3b3-2 through 3b3-4 provide pictures of these configurations.

Figure 3b3-2 Marinite Test Orientation M-1

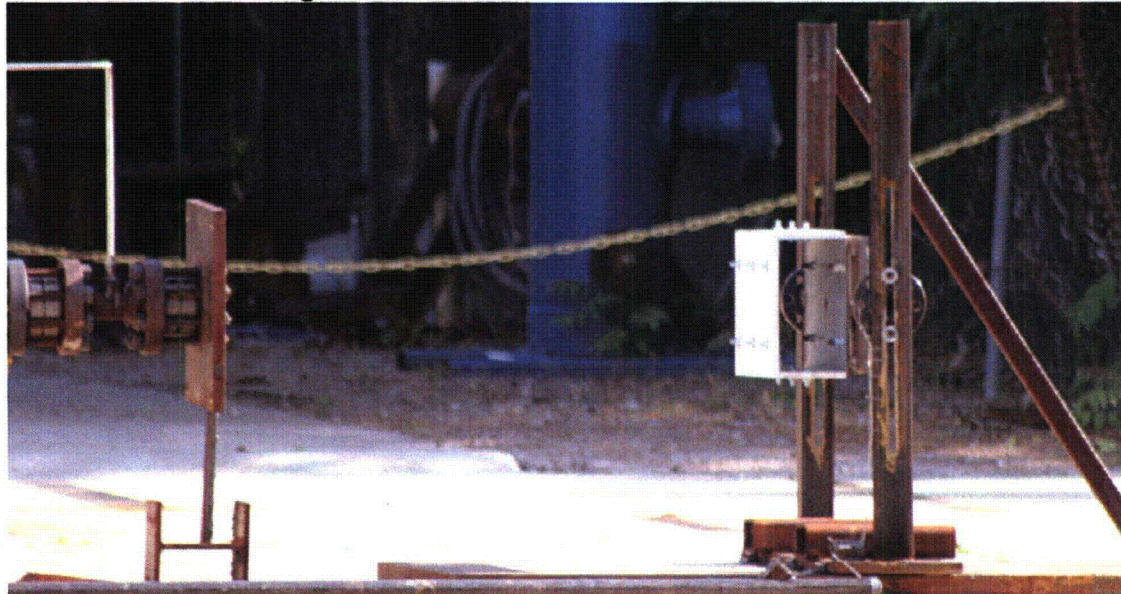


Figure 3b3-3 Marinite Test Orientation M-2

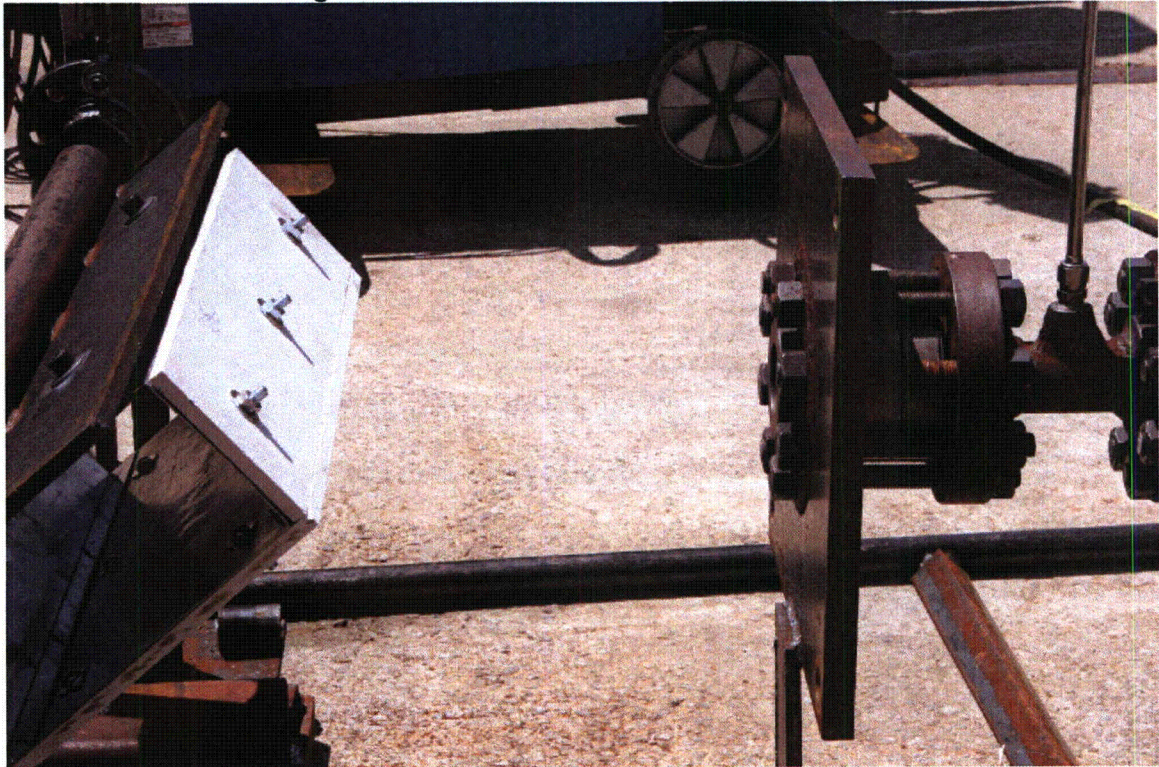


Figure 3b3-4 Marinite Test Orientation M-3



Table 3b3-3 provides the information for each of the tests for the Marinite I / Cable tray specimens.

Table 3b3-3 Marinite Jet Impingement Test Information

Test Number	Date	Test Specimen Description	Pre-Test Weight, lb _m	Post-Test Weight, lb _m	Change in Weight, %	Distance From Nozzle, in	ZOI, D	Orientation
1	5-May-07	Marinite Banded to a 3-ft section of cable tray	36.18	35.98	-0.55	140-1/8	13.3	M-1
2	6-May-07	Marinite Bolted to a 3-ft section of cable tray	35.06	34.84	-0.63	140-1/8	13.3	M-1
3	7-May-07	Marinite Bolted to a 3-ft section of cable tray	34.78	34.61	-0.49	120	11.8	M-1
4	8-May-07	Marinite Bolted to a 3-ft section of cable tray	34.28	34.13	-0.44	102	10.0	M-1
5	9-May-07	Marinite Bolted to a 2-ft section of cable tray	25.80	25.78	-0.08	84	8.3	M-1
6	10-May-07	Marinite Bolted to a 2-ft section of cable tray	25.67	25.57	-0.39	72	7.3	M-1
7	11-May-07	Marinite Bolted to a 2-ft section of cable tray	25.72	25.53	-0.74	54	6.0	M-1
8	12-May-07	Marinite Bolted to a 2-ft section of cable tray	25.55	25.34	-0.82	48	5.6	M-1
9 ⁽¹⁾	14-May-07	Marinite Bolted to a 2-ft section of cable tray	25.51	25.21	-1.18	46-1/8	5.5	M-2
10	15-May-07	Marinite Bolted to a 2-ft section of cable tray	25.44	25.30	-0.55	26-1/2	4.5	M-1
11 ⁽¹⁾	16-May-07	Marinite Bolted to a 2-ft section of cable tray	23.14	22.84	-1.30	26-1/2	4.5	M-3
12	17-May-07	Marinite Bolted to a 2-ft section of cable tray	25.26	25.04	-0.87	16	3.9	M-1
13 ⁽¹⁾	18-May-07	Marinite Bolted to a 2-ft section of cable tray	25.82	25.49	-1.28	14-3/8	3.4	M-2

(1) These tests were the only tests to generate visible debris. Refer to the discussion in NRC Information Item 3.c.1 for additional information.

Refer to Attachment 5 for before and after pictures of the Marinite testing.

Observations from Marinite I Testing

Marinite Test 1

The target remained intact and in place during the test. The cable tray face impinged upon by the jet buckled in the center and was depressed approximately 1/2 in. The Marinite on the cable tray surface facing the jet cracked horizontally, which traversed the width of the face. The crack wandered around the vertical mid-point of the face. In general, the crack penetrated approximately half the thickness of the Marinite and was open at the side away from the jet. At the center of the face, where the jet impinged on the specimen, the crack appeared to be through the Marinite. The crack did not completely sever the face.

There was no other evidence of damage or erosion. No erosion was observed in the crack described above. No observable debris was generated during this test.

Marinite Test 2

The specimen remained intact and in place during the test. The cable tray face impinged upon by the jet buckled in the center and was depressed approximately 1/8 in. The Marinite on the cable tray surface facing the jet was partially cracked. A crack that did not penetrate the Marinite ran from the upper center bolt to the right edge of the material traversing just above the upper right bolt. A second crack, approximately 4 in long, was observed just below the upper right bolt.

There was no other evidence of damage or erosion. No erosion was observed in the crack described above. No observable debris was generated during this test.

Marinite Test 3

The specimen remained intact and in place during the test. The cable tray face impinged upon by the jet buckled in the center and was depressed approximately 1/4 to 3/8 in. The Marinite on the cable tray surface facing the jet was partially cracked. A crack, that did not penetrate the Marinite, traversed horizontally across the face of the material near the vertical mid-point. No material appeared to be removed or lost.

There was no other evidence of damage or erosion. No erosion was observed in the crack described above. No observable debris was generated during this test.

Marinite Test 4

The specimen remained intact and in place during the test. The cable tray face impinged upon by the jet buckled in the center and was depressed approximately 1/2 in. The Marinite on the cable tray surface facing the jet cracked horizontally across the specimen at approximately the mid-point of the face. The crack penetrated the Marinite on the left edge, but was not distinguishable on the right edge. The crack did not appear to penetrate the face.

The face of the specimen exhibited a gouge that began above and to the left of the lower center bolt. The gouge was approximately 1/16 to 1/8 in deep, 3/16 in wide, and 5 to 6 in

long. This appeared to have been caused by debris entrained in the jet that impacted the specimen.

The Marinite board on top and bottom of the cable tray showed minor evidence of spalling that occurred in two places. The diameter and depth of the spalls was approximately the size of a dime (11/16 in diameter by 1/16 in deep).

There was no other evidence of damage or erosion. No erosion was observed in the crack described above. No observable debris was generated during this test.

Marinite Test 5

The specimen remained intact and in place during the test. The cable tray face impinged upon by the jet buckled in the center and was depressed approximately 1/2 to 3/4 in. The Marinite on the cable tray surface facing the jet cracked horizontally across the specimen at approximately the mid-point of the face. The crack penetrated the Marinite which separated into two pieces. The width of the crack varied from 1/16 to 3/16 in.

The Marinite board on top and bottom of the cable tray showed minor evidence of spalling that occurred in three places. The diameter and depth of the spalls was slightly smaller than the size of a dime (11/16 in diameter by 1/16 in deep).

There was no other evidence of damage or erosion. Evidence of minor erosion within the crack was observed. The Marinite board appeared to fracture irregularly leaving thin projections at the surface of the crack. These thin projections appeared to be eroded away by the jet. The erosion was more noticeable at the jet center than at the edge of the crack in the specimen. No observable debris was generated during this test.

Marinite Test 6

The specimen remained intact and in place during the test. The cable tray face impinged upon by the jet buckled in the center and was depressed approximately 3/4 in. The Marinite on the cable tray surface facing the jet cracked horizontally across the specimen at approximately the mid-point of the face. The crack penetrated the Marinite which separated into two pieces. The width of the crack varied from 1/8 to 3/16 in.

At the center of the crack and Marinite face, there was an eroded area approximately 3 to 3 1/2 in in diameter. This is where the jet first impacted the specimen.

The Marinite board on top and bottom of the cable tray showed no evidence of spalling.

There was no other evidence of damage or erosion. Evidence of minor erosion within the crack was observed. The Marinite board appeared to fracture irregularly leaving thin projections at the surface of the crack. These thin projections appeared to be eroded by the jet. The erosion was more noticeable at the jet center than at the edge of the crack in the specimen. No observable debris was generated during this test.

Marinite Test 7

The specimen remained intact and in place during the test. The cable tray face impinged upon by the jet buckled in the center and was depressed approximately 1/2 in. The Marinite on the cable tray surface facing the jet cracked horizontally across the specimen at

approximately the mid-point of the face. The crack penetrated the Marinite which separated into two pieces. The width of the crack varied from 1/8 to 1/4 in.

A small 3/4 in diameter chip was missing from the upper left corner of the specimen. This was later determined to be a pre-test condition.

At the center of the crack and Marinite face, there was an eroded area approximately 4 1/2 to 5 in in diameter. This is where the jet first impacted the specimen.

A secondary crack developed in the center of the face and ran approximately half the width of the face. The crack was crescent shaped and centered just below the point of jet impact. This crack did not penetrate the Marinite.

The Marinite board on top and bottom of the cable tray showed no evidence of spalling.

There was no other evidence of damage or erosion. Evidence of minor erosion within the crack was observed. The Marinite board appeared to fracture irregularly leaving thin projections at the surface of the crack. These thin projections appeared to be eroded away by the jet. The erosion was more noticeable at the jet center than at the edge of the crack in the specimen. No observable debris was generated during this test.

Marinite Test 8

The specimen remained intact and in place during the test. The cable tray face impinged upon by the jet buckled near the center and was depressed approximately 5/8 in. The Marinite on the cable tray surface facing the jet cracked horizontally across the specimen at approximately the mid-point of the face. The crack penetrated the Marinite which separated into two pieces. The width of the crack varied from 1/8 to 1/4 in.

At the center of the crack in the Marinite face, there was an eroded area approximately 4 1/2 to 5 in in diameter. This is where the jet first impacted the specimen.

A secondary crack developed in the center of the face and ran approximately three quarters of the width of the face. The crack was slightly crescent-shaped and centered just below the point of jet impact. This crack did not penetrate the Marinite.

The Marinite board on top and bottom of the cable tray showed no evidence of spalling.

The cable tray deformed by skewing approximately 5 degrees in the downward direction.

There was no other evidence of damage or erosion. Evidence of erosion within the crack was observed. The Marinite board appeared to fracture irregularly leaving thin projections at the surface of the crack. These thin projections appeared to be eroded away by the jet. The erosion was more noticeable at the jet center than at the edge of the crack in the specimen. No observable debris was generated during this test.

Marinite Test 9

The cable tray skewed downward from its pre-test 90 degree angle to an approximate angle of 30 degrees. Since the force hit at the upper edge of the front face, skewing the cable tray section, the Marinite between the top row of bolt holes and the edge (3 in from center of bolt holes to the edge of the Marinite) failed (fractured) in bending across the length of the

specimen. The side panels were not damaged during the test. The top side panel displayed indications of erosion from the steam jet.

Debris was generated as a result of the failure of the Marinite from the distortion of the cable tray. A search was performed to obtain the pieces of debris from the backstop, the test pad, and the field behind the test area. Several of the larger pieces were propelled at an angle to the test fixture into the field. The pieces of Marinite were sorted according to size, bagged, and tagged.

Marinite Test 10

The cable tray deflected inward approximately 1/4 in at the approximate center axis of the front face. A crack, approximately 1/8 in wide, developed across the front face. The most significant erosion occurred at the center of the jet. The depth of erosion at the center of the jet was approximately 1/8 in and tapered to no noticeable erosion at approximately 3 in radius. There was a secondary crack that developed near one of the bolt holes but did not result in any separation. This crack was about 4 in long. There was no destruction of the Marinite on any of the faces. The only material assumed lost was due to the erosion of the jet.

Marinite Test 11

The cable tray deflected (skewed) such that the 90 degree corner angle became 64.5 degrees. As a result of the deflection of the cable tray, a portion of the large face was dislodged from the metal tray. This section was approximately 17 in long (from the left end, facing the specimen with the nozzle behind), on an arc, with the maximum chord being approximately 3 1/2 in. An additional crack developed in the large face section that was about 5 in from the end (on the left) at the section furthest from the impingement area to about 7 in from the end at the section nearest the impingement area. This crack did not have a measurable width. The most significant erosion occurred at the center of the jet on the side piece. Some thin layers of Marinite were removed as a result of the impingement on this side piece. The depth of erosion at the center of the jet was less than 1/16 in and tapered to no noticeable erosion at an approximate 3 in radius on the side piece.

Debris was generated as a result of the failure of the Marinite from the distortion of the cable tray and jet deflection underneath the Marinite. A search was performed to obtain the pieces of debris from the backstop, the test pad, and the field behind the test area. Several of the larger pieces were propelled at an angle to the test fixture. The pieces of Marinite were sorted according to size, bagged, and tagged.

Marinite Test 12

The cable tray deflected inward approximately 1/2 in at the approximate center of the front face. An approximately 1/8 in wide crack developed across the front face. The most significant erosion occurred at the center of the jet. The depth of erosion at the center of the jet was approximately 1/8 in and tapered to no noticeable erosion at a radius of approximately 3 1/2 in. The entire length of the crack had evidence of erosion with the greatest occurring near the center of the jet. There was a secondary crack that developed

across the short face of the Marinite on the right side that ran from the top right bolt to the lower edge. This crack was about 9 1/2 in long. This crack had no separation. There were also a few isolated pits in the face of the Marinite. There was no destruction of the Marinite on any of the faces. The only material assumed lost was due to the erosion of the jet.

Marinite Test 13

The cable tray skewed downward from its pre-test 90 degree angle to an angle of approximately 23 degrees. Since the force hit at the upper edge of the front face, resulting in the skewing of the cable tray section, the Marinite between the top row of bolt holes and the edge (3 in from center of bolt holes to the edge of the Marinite) failed (fractured) in bending across the length of the specimen. The maximum width of Marinite loss was 3 3/4 in. The nominal width of Marinite loss was 3 1/4 in. The top side panel had some delamination along the edge that previously interfaced with the top (face) panel. The width of the loss was about 3/4 in. The material lost was in the form of thin pieces about 1/32 in thick. The other side panel was not damaged during the test. The top side panel also displayed indications of erosion from the steam jet.

Debris was generated as a result of the failure of the Marinite from the distortion of the cable tray. A search was performed to obtain the pieces of debris from the backstop, the test pad, and the field behind the test area. Several of the larger pieces were propelled at an angle to the test fixture into the field. The pieces of Marinite were sorted according to size, bagged, and tagged.

As discussed in the test results above, the failure mode of the Marinite was due to structural failure of the cable trays to which it was attached. The resulting debris generation is considered to be conservative since the cable trays installed in the plant would have a greater resistance to deformation as a result of the cables within the trays as well as the cable tray supports acting with longer sections of cable tray. The cable tray deformation is considered to be a dynamic effect resulting from a LBLOCA, for which I&M has received approval for use of leak-before-break for the main RCS loop piping (Reference 21) and the Unit 1 PZR surge line (Reference 86).

Scotch 77 Fire Retardant Electric Arc Proofing Tape Testing

Five tests were performed on the Scotch 77 tape material, at distances ranging from 16 1/4 in to 83 1/8 in. The Scotch 77 tape material was wrapped around a 4 in diameter conduit with the tape ends secured with a hose clamp. The conduit sections were nominally 44 in long, with tape applied to 20 in, 21 in, 27 in, 27 1/2 in, and 30 in sections of the conduit. The conduit was obtained from CNP stock. The 4 in diameter conduit is typical of the larger conduits in the CNP containments. The larger diameter conduit was chosen to provide a larger target surface area for the testing. Except for the first test, the tape was installed on the conduit with 50% overlap of lays of tape per the CNP engineering specifications for installation of fire barrier tape. The tape for the first test was wrapped with a 75% overlap. The tape used for the testing was 1 1/2 in wide and was supplied in 20 ft rolls. This tape was also obtained from CNP stock. Rolls of tape were weighed on a calibrated scale to establish a bounding weight per roll since there was some variation in the weights of each roll. Based on the weights that were obtained, a weight of 0.610 lbs per roll was used for determination of post-test weight reduction. Following testing,

the tape was removed from the conduit, and along with any recovered pieces of tape that were dislodged, were weighed to establish the before and after weights.

The tests conducted on the tape were performed in three distinct orientations. One orientation (T-1) had the longitudinal axis of the specimen at a right angle to the jet centerline, with the centerline of the jet directed at the vertical center of the test specimen. The second orientation (T-2) had the longitudinal axis of the test specimen at a 45° angle to the jet centerline. The third orientation (T-3) had the longitudinal axis rotated at a 70° angle to the jet centerline. For orientation T-2 and T-3, the jet centerline was aligned such that the jet would impact the tape between the layers, tending to lift the overlap area. Refer to Figures 3b3-5 through 3b3-7 for pictures of these configurations.

The first test conducted was of the 75% overlap configuration, with a T-1 orientation. This test was not representative of CNPs current installation but was conducted as a sensitivity test for determining the impact of an installation in this configuration.

Figure 3b3-5 Scotch 77 Test Orientation T-1

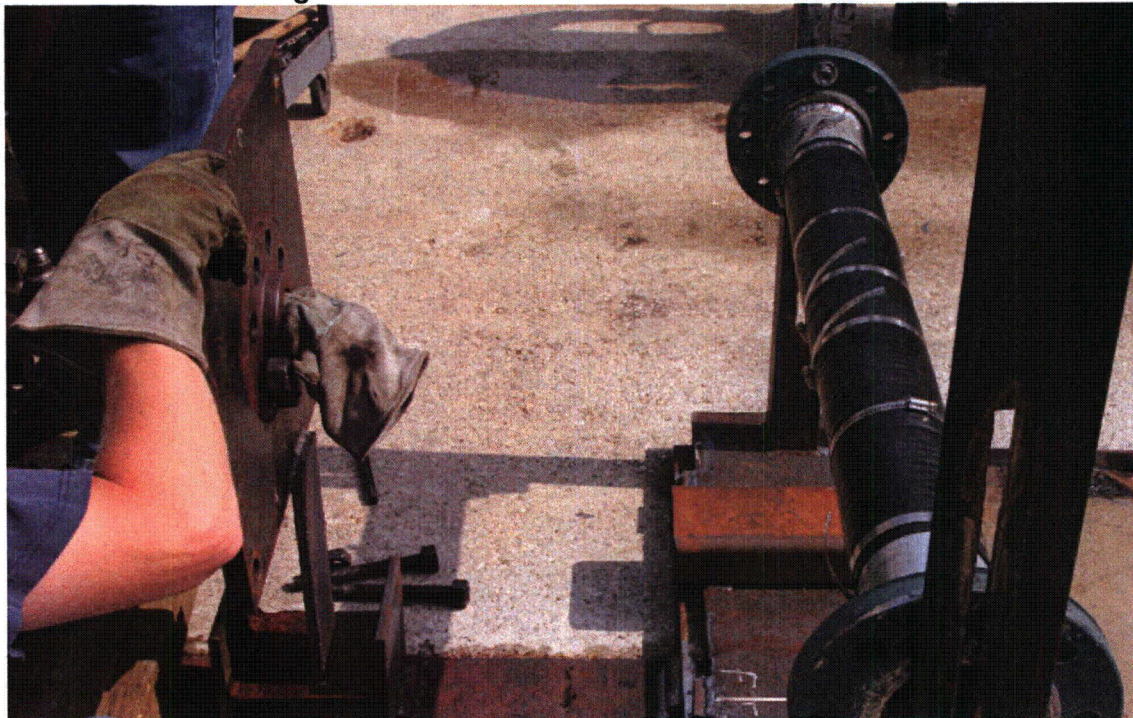


Figure 3b3-6 Scotch 77 Test Orientation T-2

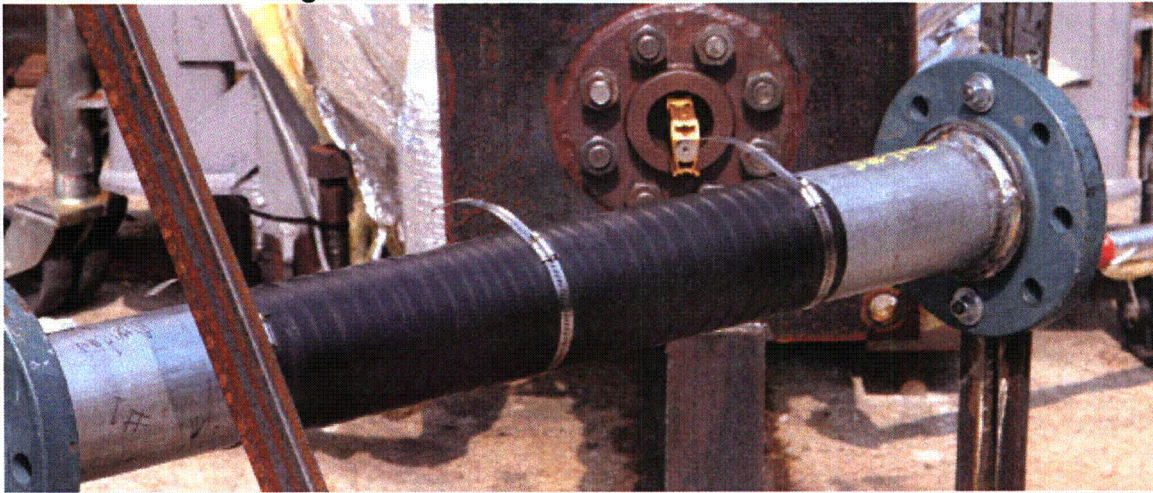


Figure 3b3-7 Scotch 77 Test Orientation T-3

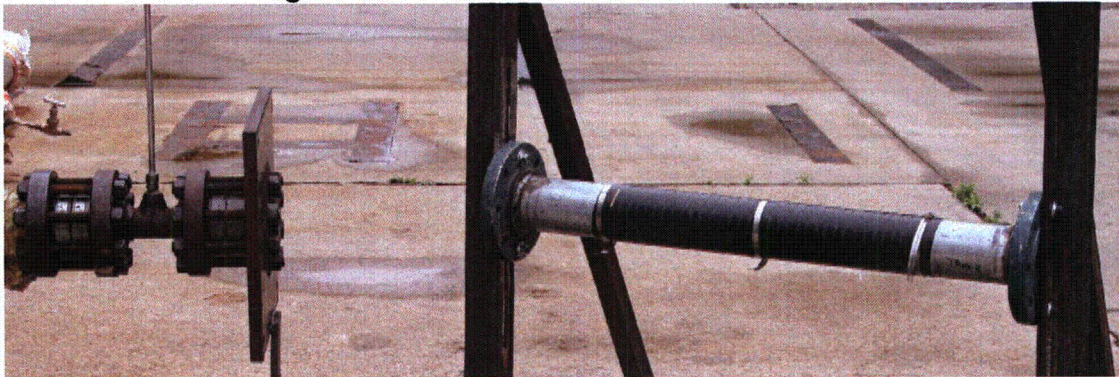


Table 3b3-4 provides the information for each of the tests for the Scotch 77 tape specimens.

Table 3b3-4 Scotch 77 Tape Jet Impingement Test Information

Test Number	Date	Test Specimen Description	Pre-Test Weight, lb _m	Post-Test Weight, lb _m	Change in Weight, %	Distance From Nozzle, in	ZOI, D	Orientation
1	30-May-07	Scotch 77 tape 1.5 in wide with 75% overlap, 100 ft wrapped	3.05	2.78	-8.85	22-1/8	4.3	T-1
2	1-Jun-07	Scotch 77 tape 1.5 in wide with 50% overlap, 30 ft wrapped	0.92	0.88	-4.35	40-1/4	5.2	T-2
3	2-Jun-07	Scotch 77 tape 1.5 in wide with 50% overlap, 40 ft wrapped	1.22	1.21	-1.02	83-1/8	8.2	T-3
4	3-Jun-07	Scotch 77 tape 1.5 in wide with 50% overlap, 40 ft wrapped	1.22	1.21	-0.98	26-1/2	4.5	T-3
5	4-Jun-07	Scotch 77 tape 1.5 in wide with 50% overlap, 40 ft wrapped	1.22	1.14	-6.56	16-1/4	4.0	T-2

Refer to Attachment 5 for before and after pictures of the Scotch 77 Tape testing.

Observations from Scotch 77 Fire Retardant Electric Arc Proofing Tape Testing

Tape Test 1

There was significant damage to the specimen. The axial center of the specimen was the impact point for the jet. Those wraps of tape that appeared to the jet to be an opposing overlap were significantly displaced resulting in the generation of loose debris ranging in size from over 4 in to very small fines. The tape appeared to stretch under the influence of the jet until the cross section was thin enough to tear the pieces away from the rest of the tape. Some long pieces remained attached to the specimen at the conclusion of the test. For those sections of the specimen that appeared to the jet to be protected by the lay of the overlap, there was only minor displacement of the tape.

As noted previously, this test configuration was not representative of the installation of fire barrier tape at CNP.

Tape Test 2

Upon observation immediately after the test, there appeared to be significant damage to the specimen. Very few small pieces of the tape were recovered. The larger pieces recovered were all greater than 4 in in major dimension and were at or near full thickness. When the

tape remaining on the specimen was removed, it was determined that the tape had separated and slid down the conduit. There was very little thinning of the cross section of the tape. The jet had essentially forced the tape to exceed ultimate tensile strength in some places and had cut it in other places, likely due to interaction with a hose clamp.

Tape Test 3

The tape was significantly displaced from its original location. The tape was cut at the location of the first hose clamp (closest to the nozzle), with a piece of tape approximately 6 in long retained by the hose clamp. A search was conducted for pieces of tape downstream of the specimen. None could be found. The tape had layered itself on the conduit. There was some tearing indicated along the edges of some of the tape which appeared to have been caused by interaction of the tape with the center hose clamp.

Tape Test 4

The tape was significantly displaced from its original location. The tape was bunched up (layered) at about the location of the hose clamp farthest from the nozzle. The center hose clamp had been forced about 9 in from its original location. The tape was cut at the location of the first hose clamp (closest to the nozzle), with a piece of tape approximately 9 in long retained by the hose clamp. A search was conducted for pieces of tape downstream of the specimen. One piece about 6 in long, some pieces about 2 in long, and a few very small pieces with an extremely thin cross section were found. There was some tearing indicated along the edges of some of the tape which appeared to have been caused by interaction of the tape with the hose clamps.

Tape Test 5

The tape was significantly displaced from its original location. The tape was bunched up (layered) at about the location of the hose clamp farthest from the nozzle. The center hose clamp had been forced about 9 in from its original location. There was no tape remaining under the nearest hose clamp. A search was conducted for pieces of tape downstream of the specimen. One piece about 12 in long, one piece about 10 in long, one piece about 6 in long, one piece about 3 in long, and one small piece with a full cross section were found. There was tearing indicated along the edges of some of the tape which appeared to have been caused by interaction of the tape with the hose clamps.

Electromark Series 1000 Valve Label Testing

Four tests were performed on the Electromark valve labels, at distances ranging from 26 1/2 in to 100 in. Three labels were tested in each test. The labels were oriented such that the center label was aligned with the centerline of the jet. The outer labels were offset approximately 3 3/4 in on each side of the center label (center to center). The labels were attached with stainless steel tie wire to a 3 1/2 in diameter pipe. The labels were 2 in by 4 in with a nominal 1/8 in diameter hole through the label, with the hole approximately 3/8 in from the end of the label. Pipe stubs were installed on the pipe to prevent the labels from being displaced toward the end of the 44 in long pipe during the test. The first test was performed with the center label having a backing plate welded to the pipe to prevent rotation of the label during the test. The last three

tests were performed with the center label having the same backing plate, with the addition of backing plates for the two outer labels. As viewed from the nozzle, the right side label backing plate was approximately 45° from vertical and the left side label backing plate was approximately 90° from the vertical, with all of the plates behind the label. The outer label backing plates would limit the rotation of the label on the pipe. Each of the backing plates also had a hole through which the tie wire for the labels were threaded to assist in maintaining position of the label during the test. The valve labels used during the test were obtained from Electromark and are the same labels and material as the valve labels in the plant. Following testing, the area on the labels where material was removed was measured to determine the quantity of material dislodged during the test.

The tests were performed with two label orientations. One orientation (L-1) was performed with the longitudinal axis of the pipe holding the labels at a right angle to the jet centerline, with the centerline of the jet directed at the center label, approximately 1 in below the top of the label. The second orientation (L-2) was performed with the longitudinal axis of the pipe holding the labels at a 45° angle to the jet centerline, with the centerline of the jet approximately 10 1/2 in above the center label. In this test, there were two test fixtures mounted on the test stand, with the labels fixture mounted below. The distance from the centerline of the nozzle to the point 1 in below the top of the center label was approximately 41 1/2 in. Refer to Figures 3b3-8 and 3b3-9 for pictures of these configurations.

Figure 3b3-8 Electromark Labels Test Orientation L-1

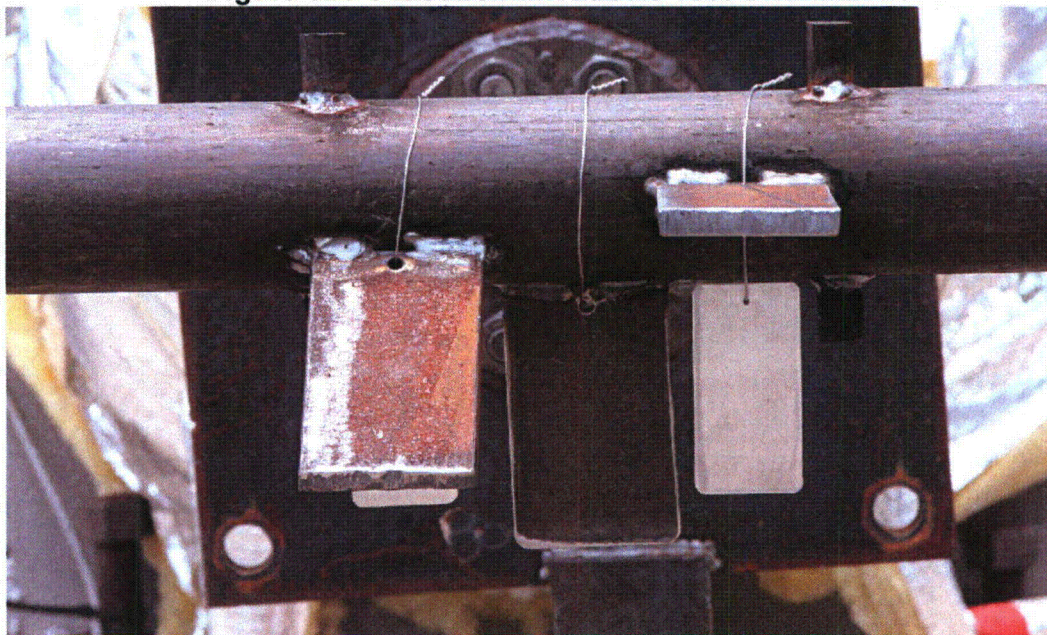


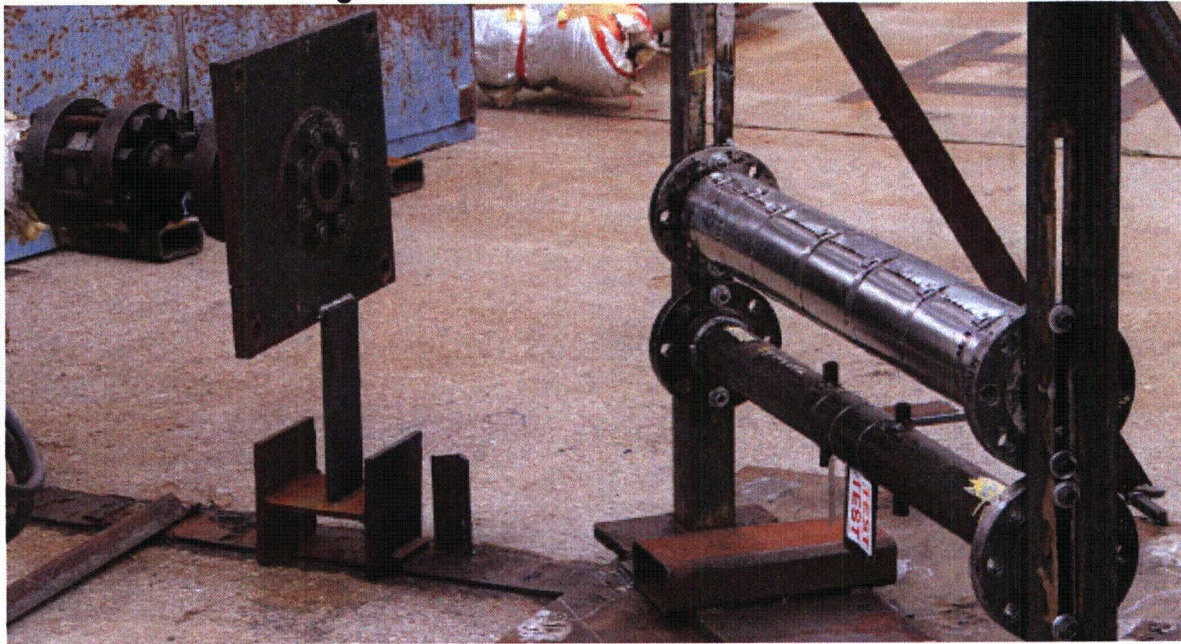
Figure 3b3-9 Electromark Labels Test Orientation L-2

Table 3b3-5 provides the information for each of the tests for the Electromark Labels specimens.

Table 3b3-5 Electromark Labels Jet Impingement Test Information

Test Number	Date	Test Specimen Description	Label Quantity Removed, in ²			Distance From Nozzle, in	ZOI, D	Orientation
			Left ⁽²⁾	Center	Right ⁽²⁾			
1	5-Jun-07	Three test labels mounted on a 3 1/2 in pipe section	0	0	0	100	9.9	L-1
2	6-Jun-07	Three test labels mounted on a 3 1/2 in pipe section	0	2-3/4	0	54	6.0	L-1
3	7-Jun-07	Three test labels mounted on a 3 1/2 in pipe section	0	0	2-2/3	26-1/2	4.5	L-1
4	8-Jun-07	Three test labels mounted on a 3 1/2 in pipe section	0	0	0	41-1/2 ⁽¹⁾	4.4 ⁽¹⁾	L-2

(1) The distance from the nozzle to the plane of the upper target specimen which established the ZOI for the test was 25 in. The Electromark labels for this test were the secondary target.

(2) Left and right are as viewed from the nozzle for the test setup.

Refer to Attachment 5 for before and after pictures of the Electromark Label testing.

Observations from Electromark Series 1000 Valve Labels Testing

Electromark Label Test 1

The labels were still intact following the test. The left and right labels (as viewed from the nozzle) were displaced behind the pipe with the right label bent at an approximate 45 degree angle, about 1/3 of the distance from the top edge. The only location where any delamination of the label from the stainless steel backing plate occurred was on the center label. The label peeled from the top edge between 1/8 and 1/4 in. This occurred to both layers of the label.

Electromark Label Test 2

The left and right labels were completely intact following the test. The left and right labels exhibited some rolling of the plate along the long axis. The center label had approximately 2 1/2 in² of the outer clear laminate removed. This clear material could not be located following the test. Three small pieces of the sub-layer of the label were recovered with the largest piece being about 1/2 in by 1/2 in. Delamination of the sub-layer occurred at the top 1/4 in of the label, except for the dislodged piece previously described. The total loss of the sub-layer was approximately 1/4 in².

Electromark Label Test 3

The left label was completely intact following the test. The right label lost approximately one-third of the outer clear layer. This clear material could not be located following the test. There was no damage to the inner layer. The center label did not lose material, but did have both the inner and outer layer peeled back approximately 1 in at each of the outer edges and tapered to the hole where the wire attaching the label to the test stand secured the material. The material rolled back to the hole, which is approximately 3/8 of an inch from the edge of the label.

Electromark Label Test 4

The right label had slight deformation. The center label had the outer layer peeled back between 1/4 in and 1/2 in from the corners closest to the attachment point. The inner layer peeled back about 1/4 in at the same location. The label experienced some deformation (roll bending). The left label experienced some minor deformation and the outer layer peeled back about 3/8 in from one corner. No material was lost from any of the labels.

Jacketed Armaflex Insulation Testing

Background

I&M previously replaced jacketed fiberglass insulation on service water piping that could potentially be impacted by a HELB inside the crane wall with Rubatex closed cell foam insulation that was glued to the piping and to itself, and was then jacketed with stainless steel and banded. Rubatex is no longer manufactured and, consequently, was not available

for testing. Armacel Armaflex insulation has been identified as the acceptable replacement for Rubatex insulation because the two are virtually identical. The Armaflex testing results may therefore be applied to Rubatex.

Following the initial CNP baseline analysis to address GL 2004-02 concerns, it was determined that, if jacketed foam insulation were to fail, it could be transported to the main strainer during the pool fill phase, potentially blocking a portion of the strainer. Absent any testing, as discussed in the SER, the assumed ZOI was 28.6D, the maximum ZOI for destruction of a potential debris source. Armaflex insulation was included in the scope of the testing performed at Wyle to determine its response to a two-phase jet.

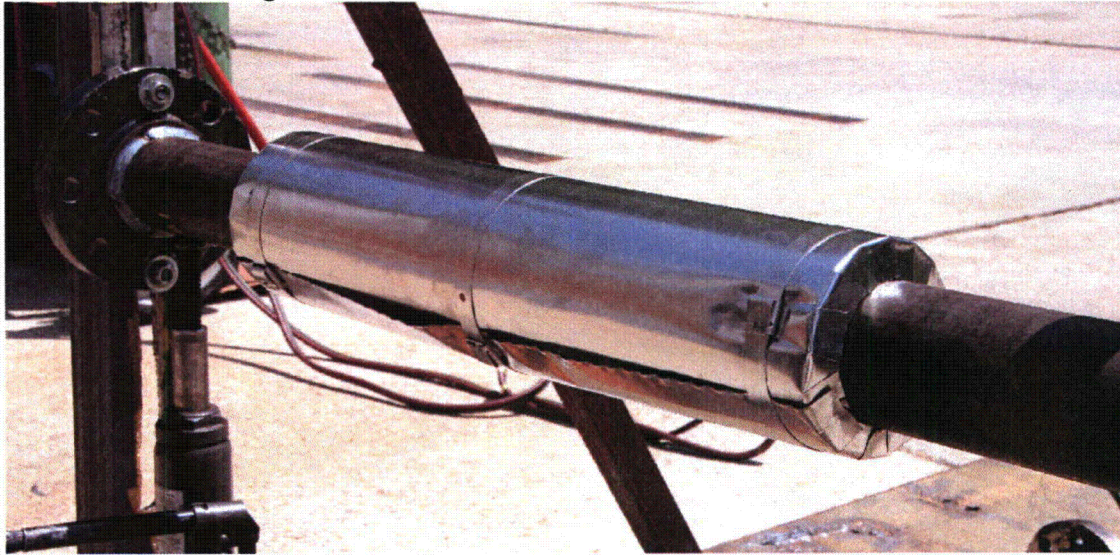
Ten tests were performed on stainless steel jacketed Armaflex insulation installed on a 3 1/2 in pipe, at distances ranging from 21 5/8 in to 49 in. The jacketing used was 10 mil polyethylene backed stainless steel with 3/4 in stainless steel bands and clamps applied at various intervals. Eight of the test specimens were nominal 2 ft long sections of insulation on a 44 in pipe. One test was performed with a 40 in insulated section and the remaining test was performed with a 40 3/4 in insulated section. In seven of the tests, the specimen was prepared with a single layer of jacketing. The test results for single jacketed foam insulation are included to demonstrate the robustness of the single jacket. The remaining three tests were performed with a double jacketed configuration, either a second layer of jacketing applied over a jacketed and banded inner layer, or a second layer of jacketing applied over an inner layer that was not banded. I&M is replacing all single jacketed foam insulation in the vicinity of postulated break locations with double jacketed foam insulation.

The determination of material lost during the tests was accomplished by preparing a 24 in section of the Armaflex insulation with two layers of glue to represent the material added to the test pipe, and then obtaining the weight of that specimen. After the completion of most of the tests, the Armaflex and glue remaining on the test pipe was scraped off and weighed. In three of the tests, the specimen was not disassembled since there was no apparent damage or release of the insulation material. The details of the tested configurations for each of the tests are provided below.

Jacketed Armaflex Test 1

A 2 ft single jacketed Armaflex insulation specimen was mounted in a horizontal configuration with the centerline of the jet perpendicular to, and at the vertical mid-plane of the specimen. The jacketing was installed with an approximate 2 in overlap, with the overlap seam approximately 1 in below the centerline of the jet. Two bands were applied approximately 1 in from each end of the specimen and one band was applied near the center of the specimen. The distance from the nozzle to the specimen was 22 1/4 in. Refer to Figure 3b3-10 for a picture of this configuration.

Figure 3b3-10 Jacketed Armaflex Insulation Test 1



Jacketed Armaflex Test 2

A 2 ft single jacketed Armaflex insulation specimen was mounted in a horizontal configuration with the centerline of the jet perpendicular to, and at the vertical mid-plane of the specimen. The jacketing was installed with an approximate 2 in overlap, with the overlap seam approximately 45° above the centerline facing the nozzle. Two bands were applied approximately 1 in from each end of the specimen, and one band was applied near the center of the specimen. The distance from the nozzle to the specimen was 49 in. Refer to Figure 3b3-11 for a picture of this configuration.

Figure 3b3-11 Jacketed Armaflex Insulation Test 2



Jacketed Armaflex Test 3

A 2 ft single jacketed Armaflex insulation specimen was mounted in a horizontal configuration with the centerline of the jet perpendicular to and at the vertical mid-plane of

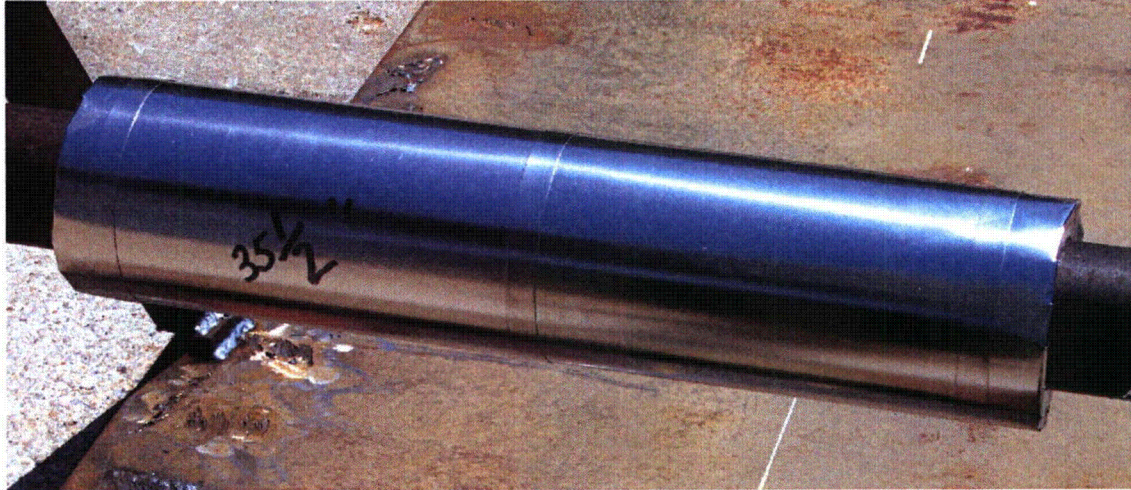
the specimen. The jacketing was installed with an approximate 2 in overlap, with the overlap seam approximately 1 1/2 in above the centerline facing the nozzle. The center of the nozzle was aligned with the center band, approximately 1/2 in below the clamp. Two bands were applied approximately 1 in from each end of the specimen and one band was applied near the center of the specimen. The distance from the nozzle to the specimen was 49 in. Refer to Figure 3b3-12 for a picture of this configuration.

Figure 3b3-12 Jacketed Armaflex Insulation Test 3



Jacketed Armaflex Test 4

A 2 ft single jacketed Armaflex insulation specimen was mounted in a horizontal configuration with the centerline of the jet perpendicular to and at the vertical mid-plane of the specimen. The jacketing was installed with an approximate 2 in overlap, with the overlap seam on the bottom side of the specimen, oriented away from the jet. The center of the nozzle was aligned with the center band, with all clamps facing away from the jet. Two bands were applied approximately 1 in from each end of the specimen and one band was applied near the center of the specimen. The distance from the nozzle to the specimen was 35 1/2 in. Refer to Figure 3b3-13 for a picture of this configuration

Figure 3b3-13 Jacketed Armaflex Insulation Test 4**Jacketed Armaflex Test 5**

A 2 ft single jacketed Armaflex insulation specimen was mounted in a horizontal configuration with the centerline of the jet perpendicular to and at the vertical mid-plane of the specimen. The jacketing was installed with an approximate 2 in overlap, with the overlap seam approximately 1 1/2 in above the centerline facing the nozzle. The center of the nozzle was aligned with the center band, approximately 1 1/2 in below the clamp. Two bands were applied approximately 1 in from each end of the specimen and one band was applied near the center of the specimen. The distance from the nozzle to the specimen was 35 1/2 in. Refer to Figure 3b3-14 for a picture of this configuration.

Figure 3b3-14 Jacketed Armaflex Insulation Test 5

Jacketed Armaflex Test 6

A 2 ft single jacketed Armaflex insulation specimen was mounted in a horizontal configuration with the centerline of the jet at a 45° angle to and at the vertical mid-plane of the specimen. The jacketing was installed with an approximate 2 in overlap, with the overlap seam approximately 1 1/2 in above the centerline facing the nozzle. The center of the nozzle was aligned with the center band, approximately 1 1/2 in below the clamp. Two bands were applied approximately 1 in from each end of the specimen and one band was applied near the center of the specimen. The distance from the nozzle to the specimen was 27 in. The center of the jet was aligned with the point approximately 6 in from the end that was nearest the nozzle. Refer to Figure 3b3-15 for a picture of this configuration.

Figure 3b3-15 Jacketed Armaflex Insulation Test 6

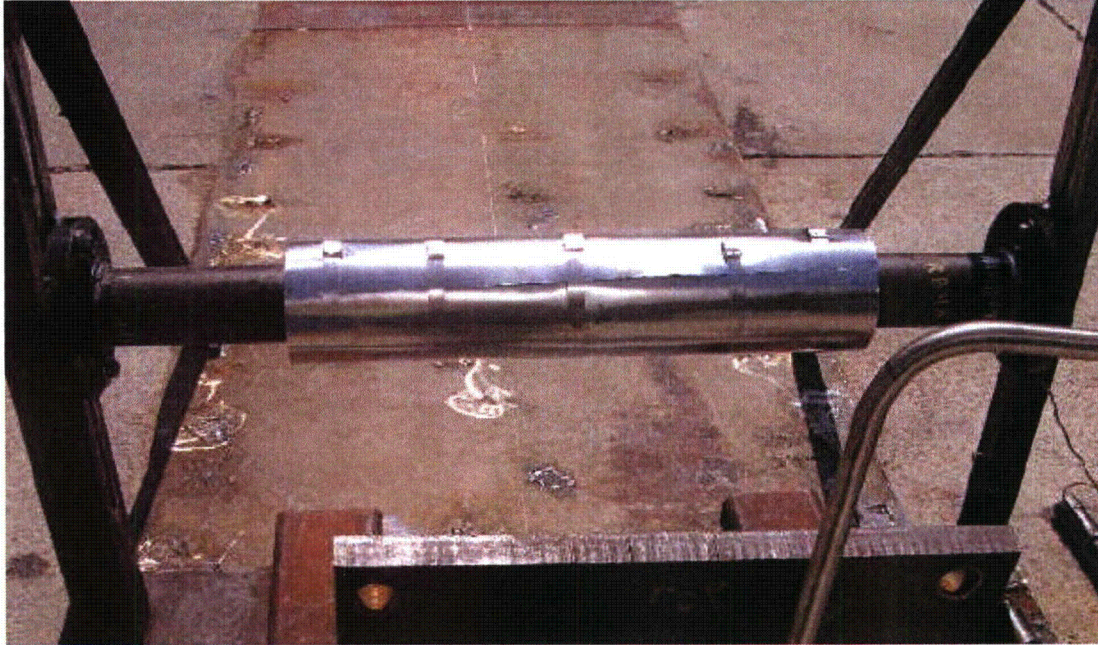


Jacketed Armaflex Test 7

A 2 ft double jacketed Armaflex insulation specimen was mounted in a horizontal configuration with the centerline of the jet perpendicular to and at the vertical mid-plane of the specimen. The distance from the nozzle to the specimen was approximately 21 7/8 in. The open edge (seam) of the jacketing was located approximately 1 1/2 in above the jet centerline facing the jet. The test specimen was prepared such that there were 2 layers of jacketing, each having a minimum overlap of 2 in. The inner layer was not banded. The layers were arranged such that they were approximately diametrically opposed, with the exposed seam aligned such that it was approximately 45 degrees above the center of the jet. The banding was applied starting at approximately 1 in from each end of the insulation to the edge of the band, with four additional bands placed approximately every 4 in. The clamps for the bands were placed such that they were approximately centered over the exposed seam. Refer to Figure 3b3-16 for a picture of this configuration.

Figure 3b3-16 Jacketed Armaflex Insulation Test 7**Jacketed Armaflex Test 8**

A 2 ft double jacketed Armaflex insulation specimen was mounted in a horizontal configuration with the centerline of the jet perpendicular to and at the vertical mid-plane of the specimen. The distance from the nozzle to the specimen was approximately 21 5/8 in. The test specimen was prepared such that there were 2 layers of jacketing with the inner layer having a minimum overlap of 2 in and the outer layer having a minimum overlap of 6 in. The inner layer had the end bands placed approximately 4 in from each end of the insulation with one additional band placed near the center of the specimen. The bands were clamped with random orientation of the clamps. The outer layer of jacketing had the end bands between 1 1/2 to 2 in from each end of the insulation with additional bands spaced approximately 3 1/2 to 4 in apart for the second bands in from each end and the remaining band approximately 5 1/2 in from the second bands. The objective was to avoid having bands on the outer layer on top of bands on the inner layer. The layers were arranged such that they were approximately diametrically opposed, with the exposed seam aligned such that it was approximately 45 degrees above the center of the jet. The clamps for the bands were placed such that they were approximately centered over the exposed seam. Refer to Figure 3b3-17 for a picture of this configuration.

Figure 3b3-17 Jacketed Armaflex Insulation Test 8**Jacketed Armaflex Test 9**

A 40 in single jacketed Armaflex insulation specimen was mounted in a horizontal configuration with the centerline of the jet at a 45° angle to and at the vertical mid-plane of the specimen. The specimen was prepared with two single layers of jacketing with an axial overlap of approximately 2 in. Two bands were applied approximately 1 1/2 in from each end of the specimen and one band was applied near the center of the specimen. The distance from the nozzle to the specimen was approximately 40 1/4 in. The center of the nozzle was aligned with the point approximately 18 1/2 in from the end that was nearest the nozzle. This point was approximately 2 in from the axial overlap seam (nearest the nozzle), and approximately 2 in from the axial seam. Refer to Figure 3b3-18 for a picture of this configuration.

Figure 3b3-18 Jacketed Armaflex Insulation Test 9**Jacketed Armaflex Test 10**

A 40 3/4 in double jacketed Armaflex insulation specimen was mounted in a horizontal configuration with the centerline of the jet at a 45° angle to and at the vertical mid-plane of the specimen. The specimen was prepared with a banded axially overlapping inner jacket (2 in overlap) with a circumferential overlap of 2 in. The outer jacket had a 6 in overlap for both the axial and circumferential seams. The axial seam for the inner jacket was approximately 180° from the outer jacket seam. The axial overlap of both the inner and outer jackets were such that the outer layer of the overlap was facing the direction of the nozzle. The distance from the nozzle to the specimen was approximately 25 in. The center of the nozzle was aligned with a point approximately 5 in from the end of the specimen nearest the nozzle. This was approximately 6 to 7 in from the axial seam for the outer jacket. The outer jacket was banded with seven bands and clamps at distances ranging from 4 1/2 in to 7 3/8 in, with the tighter spacing upstream of the jet centerline. The specimen was rotated such that the outer jacket axial overlap seam was at an approximate 45 degree angle up from the centerline of the jet. Refer to Figure 3b3-19 for a picture of this configuration.

Figure 3b3-19 Jacketed Armaflex Insulation Test 10

Table 3b3-6 provides the information for each of the tests for the jacketed Armaflex insulation specimens.

Table 3b3-6 Jacketed Armaflex Jet Impingement Test Information

Test Number	Date	Test Specimen Description	Pre-Test Weight, lb _m ⁽¹⁾	Post-Test Weight, lb _m ⁽²⁾	Change in Weight, % ⁽³⁾	Distance From Nozzle, in	ZOI, D
1	19-May-07	2 ft length of single jacketed Armaflex glued to 3-1/2 in test pipe	0.86	0.86	-0.35	22-1/4	4.3
2	20-May-07	2 ft length of single jacketed Armaflex glued to 3-1/2 in test pipe	0.86	0.85	-0.70	49	5.7
3	21-May-07	2 ft length of single jacketed Armaflex glued to 3-1/2 in test pipe	0.86	0.84	-2.33	49	5.7
4	22-May-07	2 ft length of single jacketed Armaflex glued to 3-1/2 in test pipe	0.86	0.86	-0.35	35-1/2	4.9
5	23-May-07	2 ft length of single jacketed Armaflex glued to 3-1/2 in test pipe	0.86	0.85	-1.16	35-1/2	4.9
6	24-May-07	2 ft length of single jacketed Armaflex glued to 3-1/2 in test pipe	0.86	0.79	-8.14	27	4.5
7	26-May-07	2 ft length of double jacketed Armaflex glued to 3-1/2 in test pipe	0.86	N/A ⁽⁴⁾	N/A	21-7/8	4.3

8	29-May-07	2 ft length of double jacketed Armaflex glued to 3-1/2 in test pipe	0.86	N/A ⁽⁴⁾	N/A	21-5/8	4.3
9	31-May-07	40 in length of single jacketed Armaflex glued to 3-1/2 in test pipe	1.43	0.72	-49.58	40-1/4	5.2
10	8-Jun-07	40-3/4 in length of double jacketed Armaflex glued to 3-1/2 in test pipe	1.46	N/A ⁽⁴⁾	N/A	25	4.4

- (1) The weight was determined from weighing a 24 in section of glued Armaflex.
- (2) The post test weight was the weight (after drying) of the Armaflex and glue scraped from the test pipe section.
- (3) The weighing scale was accurate to three decimal places and the readings obtained were used to calculate the percentage weight change.
- (4) These test specimens were not disassembled since there was no visible damage to the insulation material.

Refer to Attachment 5 for before and after pictures of the jacketed Armaflex insulation testing.

Observations from Jacketed Armaflex Insulation Testing

Jacketed Armaflex Test 1

The center band on the jacketing separated at the clamp and was transported downstream of the specimen. The outer bands were dislodged from the jacketing but remained intact around the pipe. The jacketing, was compressed against the foam. There were several small tears or perforations of the jacketing at the center of jet area. The longest of these was approximately 1/4 in. Other than significant deformation, there was no damage to the jacketing, except for the polyethylene film on the backside of the jacketing. The polyethylene film had partially separated resulting in free edges and blisters. The free edges were ragged with a very small amount of the material missing. There was minimal loss of the foam material itself. The jacket had protected it from direct impact. The foam appeared (by feel and observation) to retain its as-made resiliency, i.e., there didn't appear to be any temperature damage to the foam itself. There was no indication of separation of the foam from the core pipe.

Jacketed Armaflex Test 2

Two of the three bands remained intact and in place on the test specimen. One band slid off the end of the jacketing. The jacketing remained intact around the insulation. The jacketing rotated on the insulation as a result of the jet forces. The jacketing was compressed against the foam. There were several small tears or perforations of the jacketing at the center of jet area. The longest of these was approximately 3/8 in. Other than significant deformation, there was no damage to the jacketing, except for very minor lifting of the polyethylene film that is on the backside of the jacketing. The polyethylene film had partially separated at some locations (1/2 in maximum) without indication that any of the film had been removed. There was a depression in the insulation at the jet impact area. There was very minimal loss of the foam material itself. The foam appeared (by feel and observation) to retain its as-made resiliency, i.e., there didn't appear to be any temperature

damage to the foam itself. There was no indication of separation of the foam from the core pipe.

Jacketed Armaflex Test 3

All three bands remained intact and in place on the test specimen. The sheathing migrated to the left (as viewed from the nozzle) approximately 1 in. The jacketing remained intact around the insulation. The jacketing, at the conclusion of the test showed some compression against the foam at the point of jet impact. There were several small tears or perforations of the jacketing at the center of jet area. The longest of these was approximately 3/8 in. Other than significant deformation and the tears noted above, there was no damage to the jacketing. No lifting of the polyethylene film was observed. There was very minimal loss of the foam material. The foam appeared (by feel and observation) to retain its as-made resiliency, i.e., there didn't appear to be any temperature damage to the foam. There was no indication of separation of the foam from the core pipe.

A search of the area between the target and backstop identified no debris.

After the jacket was removed, two places where the Armaflex adhered to the inside of the jacketing were observed. These appeared to be places where the drips of glue used to secure the Armaflex had gotten on the jacketing and caused the Armaflex to adhere to the jacketing. These did not appear to be the results of thermal effects.

Jacketed Armaflex Test 4

All three bands remained intact and in place on the test specimen. The jacketing remained intact around the insulation. The jacketing seam opened approximately 1 in at the widest point on the right side (facing the specimen) and 1/2 in at the widest point on the left side. No evidence of erosion or damage to the Armaflex was observed in these openings. The jacketing showed some compression against the foam at the point of jet impact. The end flaps that were folded against the pipe flexed outward, but showed no evidence of damage. The cause of the flexure was judged to be the compression and deformation of the face of the jacketing. There were several small tears/perforations of the jacketing at the center of the jet area. The longest of these was approximately 1/4 in. Other than deformation and the tears noted above, there was no damage to the jacketing. No lifting of the polyethylene film was observed. There was no observable loss of the foam material. The foam appeared (by feel and observation) to retain its as-made resiliency, i.e., there did not appear to be any temperature damage to the foam. There was no indication of separation of the foam from the core pipe.

A search of the area between the target and backstop identified no debris.

After the jacket was removed, adhesion of the Armaflex to the inside of the jacketing was observed. This adhesion was due to glue leakage at the seam in the Armaflex. The adhesion was approximately 12 in long and approximately 1 in wide at the widest point. At the point of jet impact the Armaflex was compressed and deformed inward. The Armaflex in this area did not adhere to the jacketing.

Jacketed Armaflex Test 5

Two of the three bands remained intact and in place on the test specimen. The third band remained intact, migrated off the specimen, and was retained by the pipe. The jacketing experienced significant deformation, opening under the effect of the jet and rotating more than 45° away from the jet impact point. On the end where the band dislodged, the opening was more pronounced, exposing the Armaflex below the jacketing to the jet. On the opposite end of the specimen, the jacketing opened significantly, but was held in place by the center and end bands. The polyethylene film on the back of the jacketing was dislodged at both openings in the overlap. On the left side (as viewed from the nozzle) the polyethylene film peeled from the jacketing and was forced into the opening by the jet. On the right side, the polyethylene film was partially peeled from the jacketing and was hanging loosely at the end of the test. The jacketing seam opened approximately 1 in at the widest point on the right side (facing the specimen) and 1 1/2 in at the widest point on the left side. No evidence of erosion or damage to the Armaflex was observed in these openings. The jacketing, at the conclusion of the test, showed compression against the foam at the point of jet impact. The end flaps that were folded against the pipe flexed outward, but showed no evidence of damage. The cause of the flexure is judged to be the compression and deformation of the face of the jacketing. There were several small tears/perforations of the jacketing at the center of the jet area. The longest of these was approximately 3/8 in. Other than deformation and the tears noted above, there was no damage to the jacketing. There was no observable loss of the foam material. The foam appeared (by feel and observation) to retain its as-made resiliency, i.e., there didn't appear to be any temperature damage to the foam. There was no indication of separation of the foam from the core pipe.

A search of the area between the target and backstop identified no debris.

After the jacket was removed, adhesion of the Armaflex to the inside of the jacketing was observed. This adhesion was due to glue leakage at the seam in the Armaflex. These adhesion areas were approximately 1/2, 3/4, 1 1/2, and 1 3/4 in long, and approximately 1/4 in to 1/2 in wide at the widest point. At the point of jet impact the Armaflex was compressed and deformed inward. The Armaflex in this area did not adhere to the jacketing. Approximately 35 to 40% of the polyethylene film had been peeled away from the jacketing during the test.

Jacketed Armaflex Test 6

The jacketing moved laterally along the supporting pipe until it encountered the support structure. This movement was approximately 1 1/2 ft. The three bands remained intact, but moved laterally with the jacketing. Approximately 1 1/2 ft of the Armaflex material was exposed to the jet after the jacketing relocated. The bulk of the Armaflex material remained in place on the pipe, but the majority of the material exposed to the jet was removed from the pipe. In this area, the material removed was from the front face of the specimen with the removal extending more than 3/4 of the circumference of the pipe. The Armaflex material remained in place on the back side of the specimen.

The jacketing experienced significant deformation, opening under the effect of the jet. On the impact side of the jacketing, the Armaflex material was extruded through a triangular

opening that was approximately 7 in long with a 4 in wide base. The protruding Armaflex did not appear to erode under the influence of the jet. Delamination of the polyethylene film on the jacketing was evident due to the protrusion in the openings of the loose ends. The jacketing seam on the impact end opened as described above. The jacketing seam on the end away from the impact exhibited only minimal separation, mostly due to the buckling of the seam as the jacketing was compressed against the support structure (test stand). The jacketing showed no compression against the foam at the point of jet impact. The end flaps that were folded against the pipe flexed outward, but showed no evidence of damage. There were no small tears or perforations of the jacketing at the center of jet area as had been observed in earlier tests. The foam appeared (by feel and observation) to retain its as-made resiliency, i.e., there didn't appear to be any temperature damage to the foam.

A search of the area between the target and backstop identified several pieces of Armaflex. The material was strewn fairly uniformly over the horizontal surface behind the specimen and the vertical backstop and netting. Two or three larger pieces of material were recovered in the field behind the backstop.

After the jacket was removed, adhesion of the Armaflex to the inside of the jacketing was observed. This adhesion was due to glue leakage at the seam in the Armaflex. This adhesion ran almost the entire length of the jacketing at a width varying from 3/8 to 1 in. At the point of impact, there was no observable deformation or marking of the jacketing. Approximately 35 to 40% of the polyethylene film dislodged from the inside of the jacketing. Some of the polyethylene film peeled away from the jacketing. Several small pieces of Armaflex material were located under the polyethylene film material.

Jacketed Armaflex Test 7

There was no significant damage to the specimen noted following the test. The jacketing, bands, and clamps all remained in place. The jacketing did not rotate on the insulation and its un-banded inner jacket. However, a small arc was created in the seam line at the impact centerline of the specimen. The jacket seam was displaced in the direction of the jet flow by about 3/8 in. This section of the outer jacketing was raised slightly which provided a path for the jet to act on the space between the 2 layers of jacketing. This resulted in some of the polyethylene film being displaced from the outer jacketing at both ends of the specimen. At the jet impact point, deformation of the jacketing occurred but not nearly as pronounced as in previous single jacket layer tests.

Jacketed Armaflex Test 8

There was no significant damage to the specimen noted following the test. The jacketing, bands, and clamps all remained in place. Neither the inner or outer jacketing appeared to rotate on the specimen. The jacketing near the center of the jet buckled upwards approximately 2 in allowing the jet to enter the space between the inner and outer jacketing. There was significant extrusion of the polyethylene backing on the jacketing on each end of the specimen. Two small pieces of the polyethylene (1/4 in x 2 in, and a triangular section with a base of 3 in with a height of 1 1/2 in) were found downstream of the test fixture. At the jet impact point, deformation of the jacketing occurred, but was not as pronounced as in previous single jacket layer tests.

Jacketed Armaflex Test 9

Significant destruction of the specimen occurred during the test. The bands remained intact but the jacketing was completely displaced from the specimen. One piece of the jacketing landed about 75 ft from the specimen and the other piece of jacketing was about 25 ft from the specimen. Approximately two-thirds of the insulation material was dislodged during the test. The insulation was dislodged the greatest in the section of the specimen beyond the centerline of the jet. There was also some Armaflex removed upstream of the jet centerline, but not to the same extent as the downstream section. The material was removed around the entire circumference of pipe in the area closest to the jet. The dislodged pieces of insulation ranged in size from very small particles up to approximately 7 in by 12 in. This insulation was distributed in an arc coinciding with the expanding jet, with the largest pieces approximately 40 ft from test specimen location.

Jacketed Armaflex Test 10

There was damage to the specimen jacketing. One of the bands was dislodged and some of the bands were displaced from their original location. The outer jacketing had opened up exposing the inner jacket. There was no damage done to the Armaflex insulation material. With the exception of the one band that was dislodged, there was no evidence of any other material removal during the test.

Based on the Armaflex testing results, the foam insulation (Rubatex) on the NESW lines inside the loop compartment below the SG enclosures were double jacketed in Unit 2 during the Fall 2007 RFO. I&M prepared a new design standard for the installation of the double jacketing configuration to match the tested configuration and revised the engineering thermal insulation specification to require use of the design standard when performing any insulation maintenance activities on these lines. Additionally, the new design standard and revised insulation specification prohibit the use of jacketing material with a moisture barrier backing in containment to prevent generation of backing debris following an accident. The use of jacketing with backing material was previously specified for those locations where insulation was being installed for condensation control. I&M will be performing the same changes to the NESW lines inside the crane wall below the SG enclosures in Unit 1 during the Spring 2008 RFO. Based on the Armaflex testing results and the changes being made to the plant configuration, the double jacketed foam insulation (Rubatex, Armaflex, or equivalent) is not being considered as a potential debris source in containment because it is not located immediately adjacent to postulated break locations.

Cold Galvanizing Compound Testing

I&M is performing testing of cold galvanizing compound at K&L to determine the quantity of material that would fail during DBA conditions. The primary purpose of this testing is to determine if the debris load that is assumed to pass through the strainers and impact components downstream of the strainer may be reduced. The testing to be performed is similar to the testing that was performed for Reference 92, Design Basis Accident Testing of Pressurized Water Reactor Unqualified Original Equipment Manufacturer Coatings, EPRI Technical Report 1011753, September 2005. I&M intends to provide the results of this testing

in the final response to GL 2004-02 which will be submitted in accordance with the schedule provided in the response to Information Item 2.

I&M Response to Information Item 3.b.4

I&M evaluated nine different break locations to encompass both the DEGB and DGBS. The limiting break locations provided in Tables 3b4-1 through 3b4-9 below are the Loop 4 RCS Crossover Leg break for the DEGB and the Loop 4 Alternate Break in RCS Loop Piping for the DGBS.

Table 3b4-1 Loop 1 RCS Crossover Leg Break Debris Generated

Debris Type	Debris Generated
RMI Small Pieces, ft ²	48996
RMI Large Pieces, ft ²	16332
Cal-Sil Fines, lbs	62.4
Cal-Sil Small Pieces, lbs	49.3
Marinite I Fines, lbs	0.6
Marinite I Small Pieces, lbs	0.2
Marinite I Large Pieces, lbs	1.4
Marinite 36 Fines, lbs	0
Marinite 36 Small Pieces, lbs	0
Marinite 36 Large Pieces, lbs	0
Min-K, lbs	3.6
Epoxy Paint (inside ZOI), lbs	216
Alkyd Paint (inside ZOI), lbs	1.9
Fire Barrier Tape Fines, ft ²	11.4
Fire Barrier Tape Small Pieces (<4 in), ft ²	6.5
Fire Barrier Tape Large Pieces (≥4 in), ft ²	24.5
Electromark Label (inside ZOI), ft ²	0.7
Flex Conduit PVC Jacketing, ft ²	1.57

Table 3b4-2 Loop 2 RCS Crossover Leg Break Debris Generated

Debris Type	Debris Generated
RMI Small Pieces, ft ²	55718
RMI Large Pieces, ft ²	18573
Cal-Sil Fines, lbs	33.4
Cal-Sil Small Pieces, lbs	26.1
Marinite I Fines, lbs	0.4
Marinite I Small Pieces, lbs	0.1
Marinite I Large Pieces, lbs	0.7
Marinite 36 Fines, lbs	0
Marinite 36 Small Pieces, lbs	0
Marinite 36 Large Pieces, lbs	0
Min-K, lbs	5.2
Epoxy Paint (inside ZOI), lbs	216
Alkyd Paint (inside ZOI), lbs	1.9
Fire Barrier Tape Fines, ft ²	0.5
Fire Barrier Tape Small Pieces (<4 in), ft ²	0.3
Fire Barrier Tape Large Pieces (≥4 in), ft ²	1.0
Electromark Label (inside ZOI), ft ²	0.6
Flex Conduit PVC Jacketing, ft ²	1.57

Table 3b4-3 Loop 3 RCS Crossover Leg Break Debris Generated

Debris Type	Debris Generated
RMI Small Pieces, ft ²	70342
RMI Large Pieces, ft ²	23448
Cal-Sil Fines, lbs	34.8
Cal-Sil Small Pieces, lbs	30.5
Marinite I Fines, lbs	0.2
Marinite I Small Pieces, lbs	0.09
Marinite I Large Pieces, lbs	0.5
Marinite 36 Fines, lbs	0.86
Marinite 36 Small Pieces, lbs	0.36
Marinite 36 Large Pieces, lbs	1.8
Min-K, lbs	5.2
Epoxy Paint (inside ZOI), lbs	216
Alkyd Paint (inside ZOI), lbs	1.9
Fire Barrier Tape Fines, ft ²	12.5
Fire Barrier Tape Small Pieces (<4 in), ft ²	7.1
Fire Barrier Tape Large Pieces (≥4 in), ft ²	26.8
Electromark Label (inside ZOI), ft ²	0.6
Flex Conduit PVC Jacketing, ft ²	1.57

Table 3b4-4 Loop 4 RCS Crossover Leg Break Debris Generated

Debris Type	Debris Generated
RMI Small Pieces, ft ²	58528
RMI Large Pieces, ft ²	19510
Cal-Sil Fines, lbs	279.9
Cal-Sil Small Pieces, lbs	232
Marinite I Fines, lbs	0.14
Marinite I Small Pieces, lbs	0.05
Marinite I Large Pieces, lbs	0.23
Marinite 36 Fines, lbs	1.08
Marinite 36 Small Pieces, lbs	0.36
Marinite 36 Large Pieces, lbs	2.16
Min-K, lbs	1.6
Epoxy Paint (inside ZOI), lbs	216
Alkyd Paint (inside ZOI), lbs	1.9
Fire Barrier Tape Fines, ft ²	25.1
Fire Barrier Tape Small Pieces (<4 in), ft ²	14.4
Fire Barrier Tape Large Pieces (≥4 in), ft ²	54.1
Electromark Label (inside ZOI), ft ²	0.7
Flex Conduit PVC Jacketing, ft ²	1.57

Table 3b4-5 PZR Surge Line Break Debris Generated

Debris Type	Debris Generated
RMI Small Pieces, ft ²	38436
RMI Large Pieces, ft ²	12812
Cal-Sil Fines, lbs	46.4
Cal-Sil Small Pieces, lbs	37.7
Marinite I Fines, lbs	0.09
Marinite I Small Pieces, lbs	0.05
Marinite I Large Pieces, lbs	0.23
Marinite 36 Fines, lbs	0.7
Marinite 36 Small Pieces, lbs	0.3
Marinite 36 Large Pieces, lbs	1.4
Min-K, lbs	1.6
Epoxy Paint (inside ZOI), lbs	26.3
Alkyd Paint (inside ZOI), lbs	1.9
Fire Barrier Tape Fines, ft ²	25.1
Fire Barrier Tape Small Pieces (<4 in), ft ²	14.4
Fire Barrier Tape Large Pieces (≥4 in), ft ²	54.1
Electromark Label (inside ZOI), ft ²	0.7
Flex Conduit PVC Jacketing, ft ²	1.57

Table 3b4-6 Loop 1 Alternate RCS Loop Break Debris Generated

Debris Type	Debris Generated
RMI Small Pieces, ft ²	35850
RMI Large Pieces, ft ²	11950
Cal-Sil Fines, lbs	11.6
Cal-Sil Small Pieces, lbs	7.5
Marinite I Fines, lbs	0.21
Marinite I Small Pieces, lbs	0.08
Marinite I Large Pieces, lbs	0.41
Marinite 36 Fines, lbs	0
Marinite 36 Small Pieces, lbs	0
Marinite 36 Large Pieces, lbs	0
Min-K, lbs	0
Epoxy Paint (inside ZOI), lbs	5.7
Alkyd Paint (inside ZOI), lbs	1.9
Fire Barrier Tape Fines, ft ²	11.4
Fire Barrier Tape Small Pieces (<4 in), ft ²	6.5
Fire Barrier Tape Large Pieces (≥4 in), ft ²	24.5
Electromark Label (inside ZOI), ft ²	0.7
Flex Conduit PVC Jacketing, ft ²	1.57

Table 3b4-7 Loop 2 Alternate RCS Loop Break Debris Generated

Debris Type	Debris Generated
RMI Small Pieces, ft ²	40343
RMI Large Pieces, ft ²	13448
Cal-Sil Fines, lbs	17.4
Cal-Sil Small Pieces, lbs	11.3
Marinite I Fines, lbs	0.1
Marinite I Small Pieces, lbs	0.046
Marinite I Large Pieces, lbs	0.21
Marinite 36 Fines, lbs	0
Marinite 36 Small Pieces, lbs	0
Marinite 36 Large Pieces, lbs	0
Min-K, lbs	5.2
Epoxy Paint (inside ZOI), lbs	5.7
Alkyd Paint (inside ZOI), lbs	1.9
Fire Barrier Tape Fines, ft ²	0.5
Fire Barrier Tape Small Pieces (<4 in), ft ²	0.3
Fire Barrier Tape Large Pieces (≥4 in), ft ²	1.0
Electromark Label (inside ZOI), ft ²	0.6
Flex Conduit PVC Jacketing, ft ²	1.57

Table 3b4-8 Loop 3 Alternate RCS Loop Break Debris Generated

Debris Type	Debris Generated
RMI Small Pieces, ft ²	40343
RMI Large Pieces, ft ²	13448
Cal-Sil Fines, lbs	14.5
Cal-Sil Small Pieces, lbs	10
Marinite I Fines, lbs	0.14
Marinite I Small Pieces, lbs	0.05
Marinite I Large Pieces, lbs	0.23
Marinite 36 Fines, lbs	0.58
Marinite 36 Small Pieces, lbs	0.22
Marinite 36 Large Pieces, lbs	1.1
Min-K, lbs	5.2
Epoxy Paint (inside ZOI), lbs	5.7
Alkyd Paint (inside ZOI), lbs	1.9
Fire Barrier Tape Fines, ft ²	12.5
Fire Barrier Tape Small Pieces (<4 in), ft ²	7.1
Fire Barrier Tape Large Pieces (≥4 in), ft ²	26.8
Electromark Label (inside ZOI), ft ²	0.6
Flex Conduit PVC Jacketing, ft ²	1.57

Table 3b4-9 Loop 4 Alternate RCS Loop Break Debris Generated

Debris Type	Debris Generated
RMI Small Pieces, ft ²	31021
RMI Large Pieces, ft ²	10341
Cal-Sil Fines, lbs	72.5
Cal-Sil Small Pieces, lbs	46.4
Marinite I Fines, lbs	0
Marinite I Small Pieces, lbs	0
Marinite I Large Pieces, lbs	0
Marinite 36 Fines, lbs	0.79
Marinite 36 Small Pieces, lbs	0.3
Marinite 36 Large Pieces, lbs	1.62
Min-K, lbs	0
Epoxy Paint (inside ZOI), lbs	5.7
Alkyd Paint (inside ZOI), lbs	1.9
Fire Barrier Tape Fines, ft ²	25.1
Fire Barrier Tape Small Pieces (<4 in), ft ²	14.4
Fire Barrier Tape Large Pieces (≥4 in), ft ²	54.1
Electromark Label (inside ZOI), ft ²	0.7
Flex Conduit PVC Jacketing, ft ²	1.57

I&M Response to Information Item 3.b.5

I&M has completed removal of a significant quantity of labels, tags, signs, tape, and similar materials from CNP Unit 2 containment. I&M has partially completed removal of a significant quantity of these materials from CNP Unit 1 containment. I&M will complete removal, to the extent practical, of these materials from Unit 1 during the Spring 2008 RFO. The currently established bounding values for the surface area of these materials are provided in Table 3b5-1 below.

Table 3b5-1 Bounding Quantity of Debris Available to Transport That Can Reduce Effective Strainer Area

Debris Type	Upper Containment	Loop Compartment	Pipe Annulus	Ice Condenser
Submerged Electromark Labels below Elevation 614 ft, ft ²	-	9.86	30.48	-
Unqualified Labels, ft ²	8.77	13.62	3.55	-
Fire Barrier Tape Small Pieces (< 4 in), ft ²	-	14.4	-	-
Fire Barrier Tape Large Pieces (≥ 4 in), ft ²	-	54.1	-	-
Flexible Conduit PVC Jacketing, ft ²	-	1.57	-	-
Ice Storage Bag Liner Shards, ft ²	-	-	-	0.87
Pieces of Work Platform Rubber, ft ²	-	-	-	0.22
Total, ft²	8.77	93.55	34.03	1.09

Electromark labels that are used at CNP have been qualified for DBA conditions if installed on stainless steel or galvanized backing material. These labels are not qualified for submergence regardless of the material they are attached to unless mechanically restrained. I&M is deviating from the guidance contained in Section 3.5.2.2.2 of the SER which considers all adhesive backed labels to fail in the post accident containment.

I&M will provide an update to this table with updated unit-specific values in the final response to GL 2004-02 which will be submitted in accordance with the schedule provided in the response to Information Item 2.

NRC Information Item 3.c - Debris Characteristics

The objective of the debris characteristics determination process is to establish a conservative debris characteristics profile for use in determining the transportability of debris and its contribution to head loss.

1. Provide the assumed size distribution for each type of debris.
2. Provide bulk densities (i.e., including voids between the fibers/particles) and material densities (i.e., the density of the microscopic fibers/particles themselves) for fibrous and particulate debris.
3. Provide assumed specific surface areas for fibrous and particulate debris.
4. Provide the technical basis for any debris characterization assumptions that deviate from NRC-approved guidance.

I&M Response to NRC Information Item 3.c.1

Table 3c1-1, provided below, lists all debris sources and their assumed debris size.

Table 3c1-1 Debris Size Distribution

Debris Type	Debris Size	
Stainless Steel RMI	Small Pieces (<4 in)	
	Large Pieces (>4 in)	
Cal-Sil	Fines (5 micron particulate)	
	Small Pieces (<1 in to >3 in)	
Marinite	Fines (5 micron particulate)	
	Small Pieces (<2 in)	
	Large Pieces (2 in to > 4 in)	
Min-K	Fines (2.5 micron particulate)	
Qualified Epoxy	Fines (10 micron particulate)	
Unqualified Epoxy (Inside ZOI)	Fines (10 micron particulate)	
Unqualified Alkyd (Inside ZOI)	Fines (10 micron particulate)	
Unqualified OEM Epoxy (Outside ZOI)	Fines (83 micron particulate)	
Unqualified OEM Alkyd (Outside ZOI)	Fines (83 micron particulate)	
Unqualified Non-OEM Epoxy (Outside ZOI)	Chips	10% (250 – 500 micron)
		80% (500 - 1000 micron)
		10% (1000 – 4000 micron)
Unqualified Non-OEM Alkyd (Outside ZOI)	Chips	10% (250 – 500 micron)
		80% (500 - 1000 micron)
		10% (1000 – 4000 micron)
Unqualified Cold Galvanizing Compound (Outside ZOI)	Fines (10 micron particulate)	
Latent Fiber (Outside ZOI)	Fines (7 micron fibers)	
Latent Dirt/Dust (Outside ZOI)	Fines (17.3 micron particulate)	
Electromark Labels (Inside ZOI)	Small Pieces (1/2 in × 1/2 in)	

Debris Type	Debris Size
Electromark Labels (Outside ZOI)	Small Pieces (2 in × 4 in to 3 in × 5 in)
Unqualified Labels (Outside ZOI)	N/A ⁽¹⁾
Flexible Conduit PVC Jacketing (Outside ZOI)	N/A ⁽¹⁾
Fire Barrier Tape (Inside ZOI)	Fines (10 micron particulate)
	Small Pieces (< 4 in)
	Large Pieces (≥ 4 in)
Ice Storage Bag Fibers (Outside ZOI)	Fines (7 micron fibers)
Ice Storage Bag Liner Shards (Outside ZOI)	Fines (3 mils thick)
Pieces of Work Platform Rubber (Outside ZOI)	Fines (3/32 in thick)

(1) These materials are of various sizes. The total surface area is used as an input in establishing an effective unavailable strainer surface area.

The size distributions recommended in the GR and SER were used except as described below.

Insulation

Section 3.4.3.3 of the GR classifies the destroyed insulation debris in two categories, small fines and large pieces. Small fines include individual fibers and small pieces less than 4 in x 4 in, and large pieces include material 4 in and larger. Exceptions were taken to this guidance for Marinite and Cal-Sil insulation.

Marinite

As described in the response to Information Item 3.b.3, jet impingement testing was performed on Marinite fire board material. A size distribution was developed for recovered debris and for the conservatively determined unaccounted for material. The size distribution for Marinite is given in Table 3c1-2 below.

Table 3c1-2 Marinite Size Distribution

Size	14.5 psi ZOI (9.8D)
Fines (Particulate)	1.3%
Small Pieces (<1/2 in to <2 in)	0.5%
Large Pieces (2 in to >4 in)	2.7%
Remains on Target	95.5%

Cal-Sil

A more refined size distribution was developed for Cal-Sil by ALION. OPG test data for destruction of Cal-Sil insulation material (Reference 89, Table 3-6) was analyzed to develop a three category size distribution. The sizes for Cal-Sil are fines (particulate), small pieces that are dislodged from the target (under 1 in but greater than fines, to over 3 in), and intact pieces that remain on the target. It was determined that within the overall ZOI, the size

distribution would vary based on the distance of the insulation from the break (i.e. insulation debris generated near the break location would consist of more small pieces than insulation debris generated near the edge of the ZOI). Therefore, based on the data, two separate sub-zones were defined for Cal-Sil and the corresponding size distribution within each sub-zone was determined. These size distributions and sub-zone ZOIs are provided in Table 3c1-3 below.

Table 3c1-3 Cal-Sil Size Distribution

Size	Zone 1 70.0 psi ZOI (2.7D)	Zone 2 20.0-70.0 psi ZOI (6.4D – 2.7D)
Fines (Particulate)	50%	23%
Dislodged Small Pieces (Under 1 in to Over 3 in)	50%	15%
Remained on Target	0%	62%

Coatings

As described in Sections 3.4.3.3.3 and 3.4.3.3.4 of the GR, qualified and unqualified coatings within the coating ZOI, and all unqualified coatings outside the coating ZOI were assumed to fail.

Within ZOI

The size distribution provided in the GR and SER were used for coatings inside the ZOI. Based on recommendations in the SER, all coatings inside the ZOI were assumed to fail as 10-micron spherical particles.

Outside ZOI

There are several types of unqualified coatings at CNP – unqualified OEM epoxy and alkyd, unqualified non-OEM alkyd and epoxy, and cold galvanizing compound. EPRI has tested OEM and other unqualified coating systems to determine debris characteristics. The EPRI report (Reference 92) documented testing on various types of unqualified coatings, alkyds, epoxies, and IOZ. A 100% failure of all OEM unqualified coatings (including Limatorque and handwheel paint) was used for input to the debris generation analysis. This assumption is conservative because Reference 92 has indicated that only about 20% of unqualified OEM coatings actually detached as a result of autoclave DBA testing.

The GR and SER do not provide size distributions for coatings outside the ZOI. In the CNP debris generation analysis, it was assumed the OEM unqualified coatings outside the ZOI failed with an average particle size of 83 microns. Use of this particle size (i.e., 83 microns) is consistent with findings documented in Reference 92. The non-OEM unqualified coatings outside the ZOI have the same failure rate as the OEM coatings outside the ZOI (100% failure). Since these coatings were not applied to a correctly prepared substrate, engineering judgment indicates that these coatings would fail as chips of various sizes.

Therefore, the non-OEM unqualified coatings outside the ZOI were assumed to fail with the following distribution of chip sizes: 10% (250 – 500 μm), 80% (500 - 1000 μm), and 10% (1000 – 4000 μm). Based on experience regarding autoclave testing (Reference 97), results indicate that paint chips are generated in sizes larger than 4000 μm . This shows that the distribution used in the debris generation evaluation is conservative.

Scotch 77 Fire Retardant Electric Arc Proofing Tape

The GR and SER do not provide size distributions for Scotch 77 fire retardant electric arc proofing (fire barrier) tape. Based on the jet impingement testing described in the response to Information Item 3.b.3, it was conservatively assumed that 6.97% of the fire barrier tape is destroyed as fines with a diameter of 10 microns, 4% is destroyed as pieces < 4 in, and 15% is destroyed as pieces \geq 4 in.

Electromark Labels

The GR and SER do not provide size distributions for Electromark labels. Based on the jet impingement testing described in the response to Information Item 3.b.3, it was assumed that 10% of the outer layer and 1% of the sub-layer of the Electromark labels are destroyed as small pieces (1/2 in x 1/2 in).

Ice Condenser Debris

The GR and SER do not provide size distributions for ice condenser debris. As described in the response to Information Item 3.b.1, the ice condenser debris was material that was collected from the ice melt filter. This material was sorted by material type, and the range of sizes were established for each of the materials by measurement and visual observation.

I&M Response to NRC Information Items 3.c.2 and 3.c.3

Table 3c2-1, below, provides the assumed microscopic and macroscopic densities, and the assumed characteristic sizes for the debris.

Table 3c2-1 Debris Characteristics

Debris Type	Microscopic Density, lbm/ft^3	Macroscopic Density, lbm/ft^3	Characteristic Size	
			microns	S_v , ft
Cal- Sil	144	14.5	5.0	1.64E-05
Min-K	162	16	2.5 ⁽¹⁾	8.2E-06 ⁽¹⁾
Marinite I	144	46	5.0	1.64E-05
Marinite 36	144	36	5.0	1.64E-05
Qualified Coatings	N/A	111.6	10.0	3.28E-05

Debris Type	Microscopic Density, lbm/ft ³	Macroscopic Density, lbm/ft ³	Characteristic Size	
			microns	S _v , ft
Unqualified Coating Inside ZOI - Alkyds	N/A	98	10.0	3.28E-05
Unqualified Coating Inside ZOI - Epoxy	N/A	94	10.0	3.28E-05
Unqualified OEM Coatings Outside ZOI - Alkyds	N/A	98	83.0	8.2E-05
Unqualified OEM Coatings Coating Outside ZOI - Epoxy	N/A	94	83.0	8.2E-05
Unqualified non-OEM Coatings Outside ZOI - Alkyds	N/A	98	10% (250–500 micron) 80% (500–1000 micron) 10% (1000–4000 micron)	
Unqualified non-OEM Coatings Coating Outside ZOI - Epoxy	N/A	94	10% (250–500 micron) 80% (500–1000 micron) 10% (1000–4000 micron)	
Cold Galvanizing Compound	N/A	250	10.0	3.28E-05
Dirt and Dust	168	N/A	17.3	5.68E-05
Latent Fiber and Bag Fiber	175	2.4	7.0	2.3E-05
Tape (Fines)	N/A	97.6	10.0	3.28E-05
Tape (Pieces < 4 in and Pieces ≥ 4 in)	N/A	97.6	N/A	N/A

(1) SEM data suggests that the characteristic size of the Min-K is 29.8 micron. However, 2.5 micron is conservatively used for head loss predictions.

The S_v values were used during the preliminary analytical determination of head loss for establishing a strainer size for resolution of GL 2004-02 concerns. Most recently, these values (as provided in Table 3c2-1) were used as inputs to the ALION HLOSS code for determination of the worst break locations, as described in the response to Information Item 3.a.3.

I&M Response to NRC Information Item 3.c.4

Except as noted in the response to Information Item 3.c.1, the material characteristics of the GR and SER were followed for the debris generation and transport evaluations.

NRC Information Item 3.d - Latent Debris

The objective of the latent debris evaluation process is to provide a reasonable approximation of the amount and types of latent debris existing within the containment and its potential impact on sump screen head loss.

- 1. Provide the methodology used to estimate quantity and composition of latent debris.*
- 2. Provide the basis for assumptions used in the evaluation.*
- 3. Provide results of the latent debris evaluation, including amount of latent debris types and physical data for latent debris as requested for other debris under c. above.*
- 4. Provide amount of sacrificial strainer surface area allotted to miscellaneous latent debris.*

I&M Response to Information Item 3.d.1

I&M performed walkdowns of both Unit 1 and Unit 2 containments to collect latent debris samples for determination of the latent debris source term. These sample collections were performed during the Spring 2005 and Fall 2006 Unit 1 RFOs (U1C20 and U1C21), and the Spring 2006 and Fall 2007 Unit 2 RFOs (U2C16 and U2C17). These walkdowns followed the debris source identification walkdowns that were performed in previous RFOs in support of NEI 02-01 (Reference 93).

Section 3.5 of the GR and SER provided guidance on the determination of Latent Debris in containment. With the exception of the Unit 1 Spring 2005 RFO, the guidance in the GR and SER was followed for the determination of the latent debris source term.

Representative surface samples were obtained based on the following four categories for each sample location selected.

- Major Equipment (cable trays, junction boxes, ductwork, valves, motors, pumps, and light fixtures)
- Piping or Conduit
- Floors
- Walls

The methodology for obtaining the samples consisted of several distinct steps:

- Pre-weigh Masslin sample cloths in zip-lock plastic bags on a calibrated scale. Weights were measured and recorded to a tenth of a gram.
- Identify the specific area in containment to be sampled.
- Determine the sample area through measurement and document on a tape recorder.
- Take a pre-sample photograph of the area to be sampled.
- Using the Masslin cloth, collect the debris in the designated sample area.
- Take a photograph of the Masslin with the debris collected.

- Visually characterize the debris collected in the sample.
- Take a post-sample photograph of the area that was sampled.
- Obtain the post-sample collection weight of the Masslin and bag on the same scale that was used for the pre-sample weights.
- Where the pre- and post-sample weights were the same as indicated on the scale, a tenth of a gram was conservatively added to the post-sample weight that was recorded.

The calculation for determination of latent debris loads was conservatively developed to overestimate the surface areas of floors, major equipment, and piping and conduit. An additional conservatism applied to the results was that the sampling occurred prior to the concentrated effort to clean containment near the end of the Fall 2006 Unit 1 RFO and the Fall 2007 Unit 2 RFO.

For the Spring 2005 Unit 1 RFO, latent debris sampling was a biased sampling method rather than a random sampling method because the sampling occurred after activities had started in containment. Instead of performing random selection of areas to obtain samples, a walkdown was performed with the objective of obtaining samples from locations having the highest visible debris loading. Latent debris sample locations were selected in the upper containment, CEQ fan rooms, the loop compartment, and the annulus, focusing on areas that contained heavy debris loads. This included areas of oil and grease deposits and the top of light fixtures. The other sample locations were selected by using engineering judgment to identify areas that would not be routinely cleaned following RFOs. A total of 36 samples were obtained during the outage.

During the Spring 2006 Unit 2 RFO, areas of containment were randomly selected from the following locations:

- Inside Crane Wall – Floor Elevation 598 ft 9 3/8 in
- Outside Crane Wall – Floor Elevation 598 ft 9 3/8 in
- Inside Crane Wall – Floor Elevations 617 ft 9 in to 638 ft
- Outside Crane Wall – Floor Elevation 612 ft
- Lower Containment Enclosures
- Upper Containment – Floor Elevation 652 ft 7 1/2 in
- Upper Containment – Floor Elevation 695 ft and above

Two sample sets (each set consisting of one sample from each of the four sample categories identified above) was obtained from each of the above identified locations. Additionally, two samples were taken in the RCP area and at the polar crane rails. These samples represented areas of potentially higher accumulation of debris due to oil and grease residue. A total of 60 samples were obtained during this outage.

During the Fall 2006 Unit 1 RFO, latent debris samples were taken at random locations in selected areas, with certain areas targeted due to major maintenance activities which had the potential to generate significant quantities of debris. This approach was consistent with SER Section 3.5.2.2, which states: "For the purposes of latent debris characterization, surveys taken after every second outage should be sufficient.

Exceptions to this schedule warrant surveys after any invasive or extended maintenance such as steam generator replacement."

The results of the sampling from this outage were combined with the results of the previous Unit 1 outage, unless the same location was previously sampled. A total of 44 samples were obtained during this outage from the following locations:

- Specific Equipment Locations

RCP number 2 – two samples

Ice condenser top deck – Elevation 715 ft 7 1/2 in, two samples

PRT – two samples

- General Area Locations

Inside the crane wall - Basement floor elevation 598 ft 9 3/8 in, all quadrants

PZR deck – Floor elevation 625 ft

Reactor vessel head stand – Floor elevation 652 ft 7 1/2 in

Recirculation Sump – Floor elevation 591 ft 1 in, wall and floor samples only

CRDM fan deck platform - Elevation 638 ft 6 in

Annulus region – Floor elevation 598 ft 9 3/8 in, two sample sets

With the exception of the recirculation sump, samples were taken from each of the four sample categories identified above.

During the Fall 2007 Unit 2 RFO, samples were randomly taken in selected areas with specific areas targeted due to major maintenance activities consistent with SER Section 3.5.2.2. The sample results from this outage were combined with the results of the previous Unit 2 outage. A total of 44 samples were obtained during this outage from the following locations:

- Specific Equipment Location: PRT – two samples

- General Area Locations

Inside the crane wall - Basement floor elevation 598 ft 9 3/8 in, all quadrants

PZR deck – Floor elevation 625 ft

Reactor vessel head stand – Floor elevation 652 ft 7 1/2 in

CRDM fan deck platform - Elevation 638 ft 6 in

Annulus region – Floor elevation 598 ft 9 3/8 in, two sample sets

Samples were taken from each of the four sample categories identified above.

I&M Response to Information Item 3.d.2

I&M has conservatively assumed a bounding value of 200 lbs of latent debris in each unit for analysis and testing purposes. Within this 200 lbs, 170 lbs (85%) is assumed to be particulate, and 30 lbs (15%) is assumed to be fibrous, which is consistent with Section 3.5.2.3 of the SER. This assumed split between fibrous and particulate is very conservative due to the minimal quantity of fiber sources in containment and the visual observations that were performed during the latent debris sampling.

I&M Response to Information Item 3.d.3

The results of the latent debris sampling are shown below in Table 3d3-1. Although a vertical surface debris quantity was calculated for three of the outages, it was not used to determine the total latent debris value. Instead, a default vertical surface debris inventory of 30 lbs was used in accordance with SER Section 3.5.2.2, Option 1.

Table 3d3-1 Latent Debris Calculated Quantities

Outage	Calculated Horizontal Surface Debris, lbs	Calculated Vertical Surface Debris, lbs	Assumed Vertical Surface Debris, lbs	Total Latent Debris, lbs
U1C20	144.4	NA	30	174.4
U2C16	123.7	8.3	30	153.7
U1C21	149.7	12.0	30	179.7
U2C17	107.9	9.3	30	137.9

From the sampling results, there was very little indication of fibers of any type or paint chips. The material collected primarily consisted of small particulates. The physical data for latent debris was provided in Table 3c2-1, which shows the particulate portion of the latent debris as having a microscopic density of 168 lb/ft³, a characteristic size of 17.3 microns, and an S_v of 5.68E-05 ft. The fibrous portion of the latent debris was shown as having a microscopic density of 175 lb/ft³, a characteristic size of 7.0 microns, and an S_v of 2.3E-05 ft.

Based on the assumed unblocked strainer surface area of 1,850 ft², and given the assumed latent debris fiber quantity of 30 lbs (12.5 ft³), the thickness of the fiber bed that could be formed on the strainers, assuming none of the fibers are able to pass through the strainer, is approximately 1/12 in. This thickness is a factor of 1.5 less than that assumed for a thin bed on the strainer. The strainer area that would support a 1/8 in thin bed is approximately 1200 ft² for the assumed quantity of latent fiber existing in containment.

I&M Response to Information Item 3.d.4

I&M has conservatively assigned 76 ft² of the available surface area of the main strainer (900 ft² total available) and 83 ft² of the available surface area of the remote strainer (1072 ft² total available) for miscellaneous latent debris in containment. These sacrificial

strainer areas were based on the area that was assumed to be blocked for large scale strainer testing (50 ft² for the main, and 72 ft² for the remote) as described in the response to Information Item 3.f.4. Also contained in the response to Information Item 3.f.4 is the discussion of the additional sacrificial strainer area that was actually used during large scale testing as a result of not being able to test with a portion of a pocket. This resulted in an additional sacrificial strainer area of 26 ft² for the main strainer and 11 ft² for the remote strainer. In the response to Information Item 3.b.5, Table 3b5-1 provides the total bounding quantity of debris generated that could potentially block the main and remote strainers. With the debris transport fractions from Tables 3d4-1 and 3d4-2 applied to the debris generated, a bounding quantity of 34.75 ft² of material is available for potential blockage of the main strainer, and 38.96 ft² of material available for potential blockage of the remote strainer. Using the provisions of Section 3.5.2.2.2 of the SER, the assumed bounding effective strainer area blocked for the main strainer is $(0.75)(34.75 \text{ ft}^2) = 26.06 \text{ ft}^2$ and for the remote strainer is $(0.75)(38.96 \text{ ft}^2) = 29.22 \text{ ft}^2$. This provides margin for sacrificial strainer area of 50 ft² for the main strainer and 54 ft² for the remote strainer. Refer to Tables 3d4-1 and 3d4-2 for debris quantities expected to arrive at the main and remote strainers for both DEGB and DGBS.

Tables 3d4-1 and 3d4-2 are composite tables utilizing the worst case debris quantities from Unit 1 and Unit 2.

Table 3d4-1 Bounding Debris at Main Strainer for Sacrificial Strainer Area Consideration for DEGB and DGBS

Debris Type	Debris Generated	Transport Fraction	Debris at Strainer
Electromark Labels (inside ZOI), ft ²	0.7	0.13	0.091
Electromark Labels (outside ZOI), ft ²	39.6	0.03	1.188
Unqualified Labels (all of containment), ft ²	25.94	0.86	22.308
Fire Barrier Tape Small Pieces (< 4 in), ft ²	14.4	0.13	1.872
Fire Barrier Tape Large Pieces (≥ 4 in), ft ²	54.1	0.13	7.033
Flexible Conduit PVC Jacketing, ft ²	1.57	1	1.57
Ice Storage Bag Liner Shards, ft ²	0.87	0.63	0.548
Pieces of Work Platform Rubber, ft ²	0.22	0.63	0.139
Total, ft²	137.4	-	34.75

**Table 3d4-2 Bounding Debris at Remote Strainer for Sacrificial Strainer Area
Consideration for DEGB and DGBS**

Debris Type	Debris Generated	Transport Fraction	Debris at Strainer
Electromark Labels (inside ZOI), ft ²	0.7	0.47	0.329
Electromark Labels (outside ZOI), ft ²	39.6	0.69	27.324
Unqualified Labels (all of containment), ft ²	25.94	0.4	10.38
Fire Barrier Tape Small Pieces (< 4 in), ft ²	14.4	0	0
Fire Barrier Tape Large Pieces (≥ 4 in), ft ²	54.1	0	0
Flexible Conduit PVC Jacketing, ft ²	1.57	0.3	0.471
Ice Storage Bag Liner Shards, ft ²	0.87	0.42	0.365
Pieces of Work Platform Rubber, ft ²	0.22	0.42	0.092
Total, ft²	137.4	-	38.96

Based on data collection completed in Unit 2, Tables 3d4-3 and 3d4-4, below, provide the calculated quantities of debris for Unit 2 for the DEGB and DGBS that are considered for strainer sacrificial area, before applying the provisions of Section 3.5.2.2.2 of the SER. With the debris transport fractions from Tables 3d4-3 and 3d4-4 applied to the Unit 2 calculated quantity of debris, a quantity of 20.68 ft² of material is available for potential blockage of the main strainer, and 32.41 ft² of material available for potential blockage of the remote strainer. Using the provisions of Section 3.5.2.2.2 of the SER, the assumed effective Unit 2 strainer area blocked for the main strainer is $(0.75)(20.68 \text{ ft}^2) = 15.51 \text{ ft}^2$ and for the remote strainer is $(0.75)(32.41 \text{ ft}^2) = 24.31 \text{ ft}^2$.

**Table 3d4-3 Unit 2 Debris at Main Strainer for Sacrificial Strainer Area
Consideration for DEGB and DGBS**

Debris Type	Debris Generated	Transport Fraction	Debris at Strainer
Electromark Labels (inside ZOI), ft ²	0.7	0.13	0.091
Electromark Labels (outside ZOI), ft ²	39.6	0.03	1.188
Unqualified Labels (all of containment), ft ²	9.58	0.86	8.24

Debris Type	Debris Generated	Transport Fraction	Debris at Strainer
Fire Barrier Tape Small Pieces (< 4 in), ft ²	14.4	0.13	1.872
Fire Barrier Tape Large Pieces (≥ 4 in), ft ²	54.1	0.13	7.033
Flexible Conduit PVC Jacketing, ft ²	1.57	1	1.57
Ice Storage Bag Liner Shards, ft ²	0.87	0.63	0.548
Pieces of Work Platform Rubber, ft ²	0.22	0.63	0.139
Total, ft²	121.04	-	20.68

Table 3d4-4 Unit 2 Debris at Remote Strainer for Sacrificial Strainer Area Consideration for DEGB and DGBS

Debris Type	Debris Generated	Transport Fraction	Debris at Strainer
Electromark Labels (inside ZOI), ft ²	0.7	0.47	0.329
Electromark Labels (outside ZOI), ft ²	39.6	0.69	27.324
Unqualified Labels (all of containment), ft ²	9.58	0.4	3.83
Fire Barrier Tape Small Pieces (< 4 in), ft ²	14.4	0	0
Fire Barrier Tape Large Pieces (≥ 4 in), ft ²	54.1	0	0
Flexible Conduit PVC Jacketing, ft ²	1.57	0.3	0.471
Ice Storage Bag Liner Shards, ft ²	0.87	0.42	0.365
Pieces of Work Platform Rubber, ft ²	0.22	0.42	0.092
Total, ft²	121.04	-	32.41

The data collection for unqualified label quantities for Unit 1 will be completed during the Spring 2008 RFO. The values obtained during that outage will be provided in the final response to GL 2004-02 per the schedule provided in the response to Information Item 2.

NRC Information Item 3.e – Debris Transport

The objective of the debris transport evaluation process is to estimate the fraction of debris that would be transported from debris sources within containment to the sump suction strainers.

- 1. Describe the methodology used to analyze debris transport during the blowdown, washdown, pool-fill-up, and recirculation phases of an accident.*
- 2. Provide the technical basis for assumptions and methods used in the analysis that deviate from the approved guidance.*
- 3. Identify any computational fluid dynamics codes used to compute debris transport fractions during recirculation and summarize the methodology, modeling assumptions, and results.*
- 4. Provide a summary of, and supporting basis for, any credit taken for debris interceptors [DIs].*
- 5. State whether fine debris was assumed to settle and provide basis for any settling credited.*
- 6. Provide the calculated debris transport fractions and the total quantities of each type of debris transported to the strainers.*

I&M Response to Information Items 3.e.1 and 3.e.3

I&M performed a conservative and comprehensive debris transport evaluation that evaluated main strainer debris transport during pool fill and recirculation, and remote strainer debris transport during recirculation. Included with these analyses were evaluations of debris transport for both DEGB and DGBS scenarios.

The methodology used to analyze debris transport included each of the following major debris transport modes:

- Blowdown transport – The vertical and horizontal transport of debris by the break jet.
- Washdown transport – The vertical (downward) transport of debris by the containment sprays and break flow.
- Pool fill-up transport – The transport of debris by break and containment spray flows from the RWST to regions that may be active or inactive during recirculation.
- Recirculation transport – The horizontal transport of debris from the active portions of the recirculation pool to the sump strainer by the flow through the ECCS and CTS.

The methodology used in this analysis was based on the GR for refined analyses as modified by the SER, as well as the refined methodologies suggested by the SER in Appendices III, IV, and VI. The specific effect of each mode of transport was analyzed for each type of debris generated, and a logic tree was developed to determine the total transport to the sump strainer. The purpose of this approach was to break a complicated transport problem down into specific, smaller problems that could be more easily analyzed.

The logic tree approach was used for each type of debris. The size distribution and characterization for the specific debris types came from the debris generation calculation (Reference 26). The logic trees used in the debris transport evaluation were somewhat different

than the baseline logic tree provided in the GR. These differences account for certain non-conservative assumptions in the GR as identified by the SER, and account for CNP-specific refinements. The differences involve the transport of large pieces, the erosion of small and large pieces, the potential for washdown debris to enter the pool after inactive areas have been filled, and the direct transport of debris to the sump strainer during pool fill-up. Also, the generic logic tree was expanded to account for a more refined debris size distribution.

The following list provides the assumptions used for the debris transport analysis.

1. General Assumptions

- a. It was assumed that 1/4 in to 4 in pieces of RMI debris can be conservatively treated as 1/2 in pieces. This is a conservative assumption since smaller pieces of RMI tend to be transported more easily.
- b. It was assumed that the Marinite Board debris is equivalent to Cal-Sil debris for transport purposes. This is a conservative assumption since the Marinite debris at CNP is more dense than Cal-Sil and, therefore, would be less likely to be transported in the containment pool.
- c. It was assumed that the RMI would not break down into smaller pieces following the initial generation. This is a reasonable assumption since RMI is a metallic insulation that would not be subject to erosion by the flow of water.
- d. It was assumed that the settling velocity of fine debris (insulation, dirt and dust, and paint particulate) could be calculated using Stokes' Law. This is a reasonable assumption since the particulate debris is generally spherical and would settle slowly (within the applicability of Stokes' Law).
- e. Due to the absence of data, it was conservatively assumed that the transportable miscellaneous debris addressed in the debris generation calculation (ice storage bag debris and rubber) would be transported to the emergency sump during recirculation.
- f. It was assumed that the small and large pieces of fire barrier tape would settle to the floor in regions of lower turbulence similar to other small and large pieces of debris. This is appropriate as the tape falls in the same size range (<4" and >4") as the other small and large debris types (<4" for small RMI, >4" for large RMI, <1"– >3" for Cal-Sil pieces, <2" for small marinite, and >2" for large marinite). The fire barrier tape also has a density that is higher ($98 \text{ lb}_m/\text{ft}^3$) than that of the other large and small debris types ($14.5 \text{ lb}_m/\text{ft}^3$ for Cal-Sil, $34\text{-}46 \text{ lb}_m/\text{ft}^3$ for marinite). As a settling velocity metric for fireproof tape is unknown, the most conservative known settling velocity for small and large debris types (that of small RMI) was used for the fire barrier tape (0.37 ft/s).
- g. It was conservatively assumed that the unqualified labels and flexible conduit PVC jacketing could be treated as readily transportable fines.
- h. It was assumed that the larger overall transport fractions determined from the transport analysis for Loop 2 and Loop 4 breaks could be applied to the breaks in Loops 1 and 3. In general, breaks close to the sump transport a larger fraction of large debris, and breaks farther from the sump transport a larger fraction of fine debris. Therefore, since Loop 2 is closest to the sump, and Loop 4 is farthest from the sump, applying these transport fractions was conservative for the other break locations. It was also assumed

that the alternate break in the PZR surge line would have the same transport fractions as the Loop 4 break and that each of the alternate breaks in the primary loops would have the same transport fractions as the large breaks in those same loops. This is a reasonable assumption given the close proximity of these breaks to each other.

- i. It was assumed that the only insulation debris generated by the reactor cavity break would be RMI. Since the majority of the RMI would not likely be transported out of the reactor cavity and RMI is generally not a problematic insulation type with respect to head loss, the reactor cavity break was not analyzed for debris transport.

2. Logic Trees

- a. It was assumed that the fines generated by a LOCA jet would be distributed to the ice condenser, annulus, and reactor cavity in proportion to the blowdown flow split arrived at in the TMD analysis. This is a reasonable assumption since fine debris generated by the LOCA jet would be easily entrained and carried with the blowdown flow.
- b. It was assumed that none of the small and large piece debris (RMI, Cal-Sil, and Marinite) would be blown to the ice condenser or reactor cavity. This assumption was made to simplify the analysis. This is a conservative assumption since some of this debris could be retained in the ice baskets, and the reactor cavity is an inactive cavity.
- c. It was conservatively assumed that all debris blown into the ice condenser would be trapped by the ice baskets and subsequently washed down with the melting ice flow.
- d. During pool fill-up, it was conservatively assumed that no debris would be washed to inactive cavities such as the reactor cavity and the lower containment and annulus sumps.

3. Debris Distributions

- a. It was assumed that the debris generated inside the ZOI and remaining in the loop compartment at the end of the blowdown phase would be uniformly distributed inside the loop compartment at the beginning of pool fill-up. This is a reasonable assumption since the loop compartment is not subdivided, and for any of the crossover leg breaks, debris would be generated in three of the four SG loops. This debris would easily be blown to the vicinity of the fourth loop.
- b. The ice condenser debris and the debris blown to the ice condenser was assumed to be washed down from the ice condenser immediately following the initiation of ice melt. Since the ice condenser drains discharge all around the loop compartment, this debris was treated as being uniformly distributed in the loop compartment at the beginning of pool fill-up. This is a reasonable assumption since the initial ice melt flow following an LBLOCA is very high.
- c. The unqualified coatings and other miscellaneous debris types outside the ZOI were assumed to fail during recirculation. This is a reasonable assumption since this debris is outside the ZOI and would fail gradually. Based on this assumption, the unqualified debris in upper containment would be distributed in the vicinity of the refueling canal drains (where the majority of the upper containment spray would enter the recirculation pool), the unqualified debris in the annulus was assumed to be uniformly distributed in the annulus, and the unqualified debris in the loop compartment was assumed to be uniformly distributed in the loop compartment.

- d. It was assumed that all of the debris that is not transported to the main strainer or over the flood-up overflow wall DI to the annulus during pool fill-up would be uniformly distributed inside the loop compartment at the beginning of recirculation. This is a conservative assumption since a significant portion of the debris that is not transported over the DI or to the main strainer would be caught at the base of the DI. Assuming this debris is uniformly distributed in the loop compartment at the beginning of recirculation results in a larger fraction of debris being available to transport to the main strainer.

4. CFD Model

- a. The water falling from the break was assumed to do so without encountering any structures before reaching the containment pool. This is a conservative assumption since any impact with structures would dissipate the momentum of the water and decrease the turbulent energy in the pool.
- b. It was assumed that the small fraction of spray water that flows through the fans on the top of the SG enclosures to the annulus is negligible in terms of affecting the pool flow. Therefore, all of the spray water was assumed to be introduced through the refueling canal or CEQ fan room drains.
- c. It was assumed in the pool fill CFD model that the flood-up overflow wall DI would be open to flow until the water level reaches the top of the DI (approximately three feet above the floor). After this point in the pool fill CFD model and in the recirculation pool CFD model, the DI was modeled as fully blocked. This is conservative since it maximizes the amount of flow over the top of the DI, and therefore, would maximize the debris transport over the DI.
- d. It was assumed that the debris transported to the main strainer during the pool fill-up phase would not significantly change the flow through the main strainer. This assumption conservatively maximizes the quantity of debris transported to the main strainer because the main strainer would not be significantly blocked during the pool fill-up phase.
- e. The transport fraction to the remote strainer is dependent on the head loss caused by the debris on the main strainer. Since the debris bed head loss is not determined as a part of the debris transport analysis, it was assumed that, when the predicted debris load reaches the main strainer, it would be 90% blocked or less.
- f. It was assumed that potential upstream blockage points (e.g., drains, fences, grating, etc.) would not inhibit the flow of water through the associated areas.

The basic methodology used for the CNP transport analysis is described below:

1. A three-dimensional model was built using CAD software based on the containment building drawings.
2. A review was made of the drawings and CAD model to determine transport flow paths. Potential upstream blockage points including screens, fences, grating, drains, etc., that could lead to water holdup were identified and evaluated.
3. Debris types and size distributions were gathered from the debris generation calculation for each postulated break location.

4. The fraction of debris blown into the ice condenser, annulus, and reactor cavity was determined based on the flow of steam during the blowdown.
5. The quantity of debris washed down by ice melt and spray flow was conservatively determined.
6. CFD models were developed to simulate the flow patterns that would occur during pool fill-up and recirculation.
 - a. The meshes in the CFD models were nodalized to sufficiently resolve the features of the CAD model, but still keep the cell count low enough for the simulations to run in a reasonable amount of time.
 - b. The boundary conditions for the CFD models were set based on the configuration of the CNP containment building during the recirculation phase.
 - c. The flood-up overflow wall DI was included in the CFD model using two-dimensional baffles.
 - d. The ice melt and containment spray flows were included in the CFD calculation with the appropriate flow rate and kinetic energy to accurately model the effects on the containment pool.
 - e. At the postulated LOCA break location, a mass source was added to the model to introduce the appropriate flow rate and kinetic energies associated with the break flow.
 - f. For the pool fill CFD runs, two-dimensional baffles were used to model the flow resistance through the main and remote sump strainers. For the recirculation CFD model, negative mass sources were added at the sump strainer locations with the appropriate flow split.
 - g. An appropriate turbulence model was selected for the CFD calculations.
 - h. After running the recirculation pool CFD simulations, the mean kinetic energy was checked to verify that the model had been run long enough to reach steady-state conditions.
 - i. Transport metrics were determined based on relevant tests and calculations for each significant debris type present in the CNP containment building.
7. The fraction of debris in the loop compartment that would be transported to the main strainer and to the annulus during pool fill-up was determined based on the pool fill CFD results.
8. The fraction of debris that would be transported to the main strainer and to the remote strainer during recirculation was determined based on the recirculation pool CFD results.

9. The quantity of debris that could experience erosion in the containment pool was determined.
10. The overall transport fraction for each type of debris was determined by combining each of the previous steps in logic trees.

Where necessary, some of the items listed above are described in more detail below.

CAD Model

Attachment 4, Figures A4-2 through A4-10 provide the various CAD model views of containment. The CAD model was developed for Unit 1 only. The model was used for both units because CNP Unit 2 is essentially a mirror image of Unit 1. The obstructions in the annulus from the crane wall openings clockwise to the remote strainer (piping, cable trays, etc.) were conservatively modeled as simple obstacles blocking a large area of flow. This simplification is conservative since a smaller flow area results in higher velocities in this region of the pool.

Upstream Blockage Points

The response to Information Item 3.i, "Upstream Effects," provides a discussion of this topic.

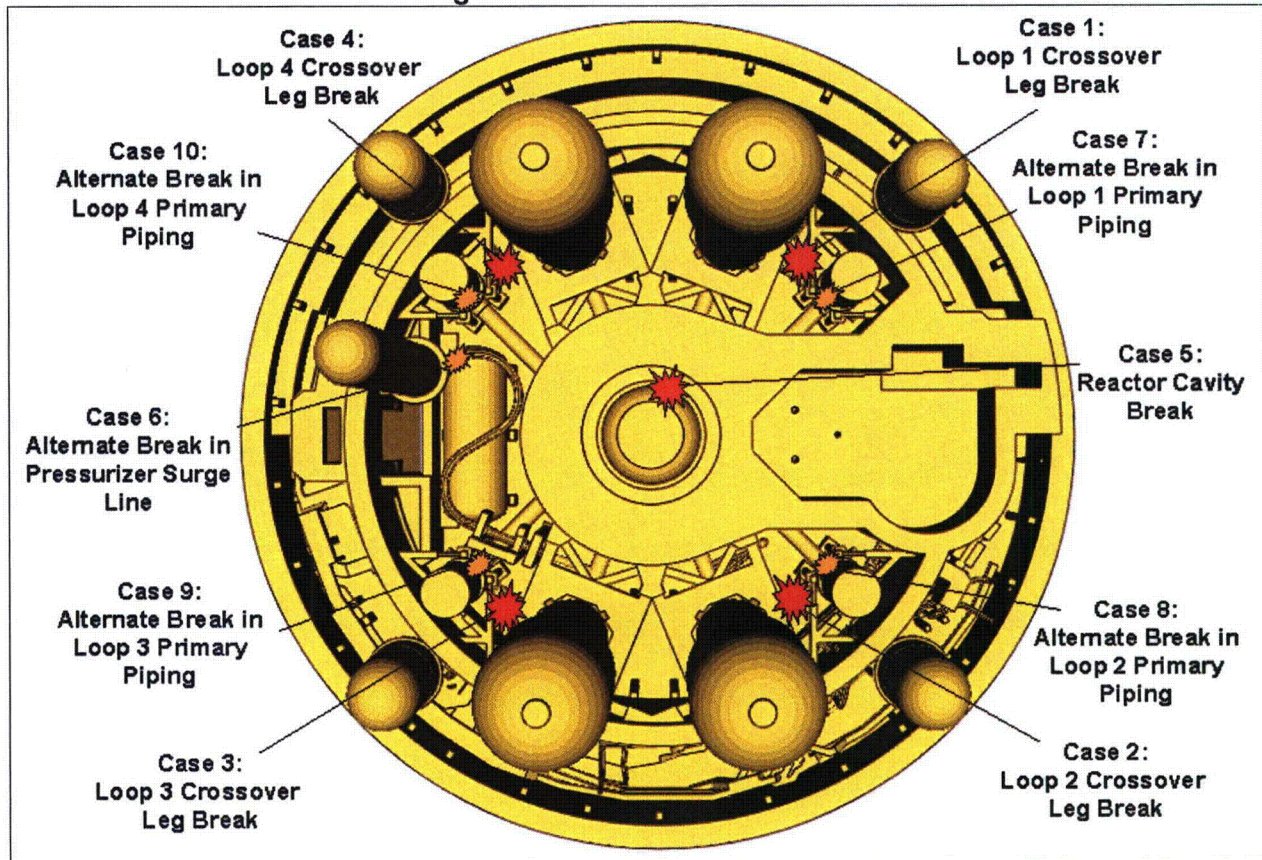
Debris Types and Size Distributions

The debris generation calculation identified ten cases that should be analyzed for transport and head loss. As shown in Figure 3e1-1, below, these cases are for a break in the crossover leg piping on each of the four loops, a reactor nozzle break in the reactor cavity, an alternate break in the PZR surge line, and an alternate break in each of the four primary loops. Based on the types and quantities of debris generated, it was determined in the debris generation analysis that all other large and small break cases are bounded by these ten cases (see the response to Information Item 3.a).

The debris types, sizes, and densities were taken from the debris generation calculation and are shown in Tables 3c1-3 and 3c2-1, in the response to Information Item 3.c, "Debris Characteristics."

The location and quantities of other debris sources outside the ZOI were taken from the debris generation calculation and are shown in Tables 3b1-1 through 3b1-4 in the response to Information Item 3.b, "Debris Generation/Zone of Influence (ZOI) (excluding coatings)." The location and quantities of coatings debris were also taken from the debris generation calculation and are shown in Table 3h2-1 in the response to Information Item 3.h, "Coatings Evaluation."

Figure 3e1-1 Break Locations



Blowdown Transport

The high energy blowdown following a double-ended guillotine pipe rupture would dislocate only the insulation and paint coatings in the vicinity of the break location. Blowdown is considered to be omni-directional within lower containment. Due to the design of CNP's ice condenser containment buildings, steam from the blowdown would relieve out the crane wall to the annulus region as well as through the inlet bay doors into the ice condenser, and through openings to the reactor cavity, carrying debris with it. It is likely that some small debris would adhere to the walls and equipment around the break. However, due to a lack of quantifiable data on this phenomenon, all debris not ejected upward was conservatively assumed to fall to the floor.

Based on the loop compartment TMD analysis performed for CNP (Reference 94), the percentage of the total mass and energy directed to the ice condenser is 70%, the percentage directed to the annulus is 22%, and the percentage directed to the reactor cavity is 8%. Since fine debris would be easily transported with the blowdown flow, it was assumed that the fraction of fines blown into the ice condenser, annulus, and reactor cavity would be proportional to the TMD flow split.

Pieces of RMI, Cal-Sil, Marinite, Electromark labels, and fire barrier tape debris would also be blown toward the ice condenser, annulus, and reactor cavity. However, it was conservatively assumed that none of the small or large pieces of debris would be blown into the ice condenser or to the reactor cavity where they could be retained. Some of the small pieces of debris could be blown over the top of the flood-up overflow wall and through the crane wall openings to the annulus. Based on the flow split to the annulus and the fact that a significant quantity of the debris pieces would be held up on miscellaneous structures or drop out of the flow at sharp turns in the blowdown flow paths, it was conservatively judged that only 5% of the small piece debris would be blown to the annulus.

Since any debris blown into the ice condenser would have to travel past the ice baskets, it was conservatively assumed that all of the debris would be trapped by the baskets and subsequently washed back down as the ice melts, with all of this debris available in the containment pool at the time of initiation of recirculation.

Table 3e1-1 shows the transport fractions for each type/size of debris to the ice condenser due to the blowdown forces for breaks inside the loop compartment. Similarly, Table 3e1-2 shows the transport fractions to the annulus, and Table 3e1-3 shows the transport fractions to the reactor cavity. Note that the majority of the unqualified coatings and miscellaneous latent debris is located outside the ZOI, and therefore, would not be affected by the blowdown flow.

Table 3e1-1 Blowdown Transport Fractions to Ice Condenser

Debris Type	Fines	Small Pieces	Unjacketed Large Pieces	Jacketed Large Pieces
RMI	-	0%	0%	-
Cal-Sil	70%	0%	-	-
Marinite	70%	0%	0%	-
Min-K	70%	-	-	-
Miscellaneous Coatings (Inside ZOI) ¹	70%	-	-	-
Miscellaneous Coatings (Outside ZOI) ²	-	-	-	-
Unqualified Non-OEM Epoxy (Outside ZOI)	-	-	-	-
Latent Debris (Outside ZOI)	-	-	-	-
Electromark Labels (Inside ZOI)	-	0%	-	-
Electromark Labels (Outside ZOI)	-	-	-	-
Unqualified Labels (Outside ZOI)	-	-	-	-
Flexible Conduit PVC Jacketing (Outside ZOI)	-	-	-	-
Fire Barrier Tape (Inside ZOI)	70%	0%	-	-
Transportable Ice Condenser Debris ³	-	-	-	-

(1) Includes qualified and unqualified epoxy and unqualified alkyd coatings.

(2) Includes unqualified OEM epoxy and alkyd coatings, cold galvanizing compound, and non-OEM alkyd coatings.

(3) Includes ice storage bag fibers, ice storage bag liner shards, and pieces of work platform rubber.

Table 3e1-2 Blowdown Transport Fractions to Annulus

Debris Type	Fines	Small Pieces	Unjacketed Large Pieces	Jacketed Large Pieces
RMI	-	5%	0%	-
Cal-Sil	22%	5%	-	-
Marinite	22%	5%	0%	-
Min-K	22%	-	-	-
Miscellaneous Coatings (Inside ZOI) ¹	22%	-	-	-
Miscellaneous Coatings (Outside ZOI) ²	-	-	-	-
Unqualified Non-OEM Epoxy (Outside ZOI)	-	-	-	-
Latent Debris (Outside ZOI)	-	-	-	-
Electromark Labels (Inside ZOI)	-	5%	-	-
Electromark Labels (Outside ZOI)	-	-	-	-
Unqualified Labels (Outside ZOI)	-	-	-	-
Flexible Conduit PVC Jacketing (Outside ZOI)	-	-	-	-
Fire Barrier Tape (Inside ZOI)	22%	5%	-	-
Transportable Ice Condenser Debris ³	-	-	-	-

(1) Includes qualified and unqualified epoxy and unqualified alkyd coatings.

(2) Includes unqualified OEM epoxy and alkyd coatings, cold galvanizing compound, and non-OEM alkyd coatings.

(3) Includes ice storage bag fibers, ice storage bag liner shards, and pieces of work platform rubber.

Table 3e1-3 Blowdown Transport Fractions to Reactor Cavity

Debris Type	Fines	Small Pieces	Unjacketed Large Pieces	Jacketed Large Pieces
RMI	-	0%	0%	-
Cal-Sil	8%	0%	-	-
Marinite	8%	0%	0%	-
Min-K	8%	-	-	-
Miscellaneous Coatings (Inside ZOI) ¹	8%	-	-	-
Miscellaneous Coatings (Outside ZOI) ²	-	-	-	-
Unqualified Non-OEM Epoxy (Outside ZOI)	-	-	-	-
Latent Debris (Outside ZOI)	-	-	-	-
Electromark Labels (Inside ZOI)	-	0%	-	-
Electromark Labels (Outside ZOI)	-	-	-	-
Unqualified Labels (Outside ZOI)	-	-	-	-
Flexible Conduit PVC Jacketing (Outside ZOI)	-	-	-	-
Fire Barrier Tape (Inside ZOI)	8%	0%	-	-
Transportable Ice Condenser Debris ³	-	-	-	-

(1) Includes qualified and unqualified epoxy and unqualified alkyd coatings.

(2) Includes unqualified OEM epoxy and alkyd coatings, cold galvanizing compound, and non-OEM alkyd coatings.

(3) Includes ice storage bag fibers, ice storage bag liner shards, and pieces of work platform rubber.

Washdown Transport

During the washdown phase, debris in upper containment could be washed down by containment sprays, and debris in the ice condenser could be washed down by the melting ice. As discussed in "Blowdown Transport" above, it was conservatively assumed that all of the debris blown into the ice condenser would be trapped and subsequently washed back down through the ice condenser drains. It was also assumed that failed coatings in upper containment would be washed down by the containment sprays.

Table 3e1-4 shows the fraction of debris in the ice condenser and upper containment that would be transported to the pool floor due to washdown, ice melt, and containment spray flows. Washdown fractions for the latent debris and unqualified coatings outside the ZOI were not quantified. Although this debris may be washed down from upper containment, conservative

distributions were developed to simplify the analysis for this debris as described in the "Recirculation Debris Transport" discussion provided in subsequent portions of the response to this information item.

Table 3e1-4 Washdown Transport Fractions of Debris from the Ice Condenser and Upper Containment

Debris Type	Fines	Small Pieces	Unjacketed Large Pieces	Jacketed Large Pieces
RMI	-	-	-	-
Cal-Sil	100%	-	-	-
Marinite	100%	-	-	-
Min-K	100%	-	-	-
Miscellaneous Coatings (Inside ZOI)	100%	-	-	-
Miscellaneous Coatings (Outside ZOI)	100%	-	-	-
Unqualified Non-OEM Epoxy (Outside ZOI)	-	100%	-	-
Latent Debris	-	-	-	-
Electromark Labels (Inside ZOI)	-	-	-	-
Electromark Labels (Outside ZOI)	-	100%	-	-
Unqualified Labels (Outside ZOI)	100%	-	-	-
Flexible Conduit PVC Jacketing (Outside ZOI)	100%	-	-	-
Fire Barrier Tape (Inside ZOI)	100%	-	-	-
Transportable Ice Condenser Debris	100%	-	-	-

Containment Pool CFD Models

The containment pool CFD modeling described in the following sections includes both the pool fill and recirculation modes. The CFD analysis was performed with the Flow-3D[®] Version 9.0 computer code (with the modified subroutine) by ALION.

The pool fill-up debris transport fractions and recirculation pool debris transport fractions were determined through CFD modeling. To accomplish this, the CAD model files were imported into the CFD models, flows into and out of the pool were defined, and the CFD simulations were run until the pool fill-up model showed the pool was full and until steady-state conditions were reached for the recirculation pool model. The result of the CFD analysis was a three-dimensional model showing the turbulence and fluid velocities within the pool. By

comparing the direction of pool flow, the magnitude of the turbulence and velocity, the initial location of debris, and the specific debris transport metrics (i.e., the minimum velocity or turbulence required to transport a particular type/size of debris), the transport of each type/size of debris was determined. The details of the CFD modeling are provided below.

The significant parts of the CFD models are shown below in Figures 3e1-2 and 3e1-3. The sump mass sink, the Loop 2 and Loop 4 break locations, the modeled spray drainage, and the modeled ice melt drainage are indicated.

A total of six CFD simulations were run. For pool fill-up, two cases were run to model breaks in Loops 2 and 4. For recirculation, the same two break locations were modeled and the sump flow split was varied based on clean strainer conditions and 90% blocked main strainer conditions.

Figure 3e1-2 Significant Features Modeled for Pool Fill Simulations

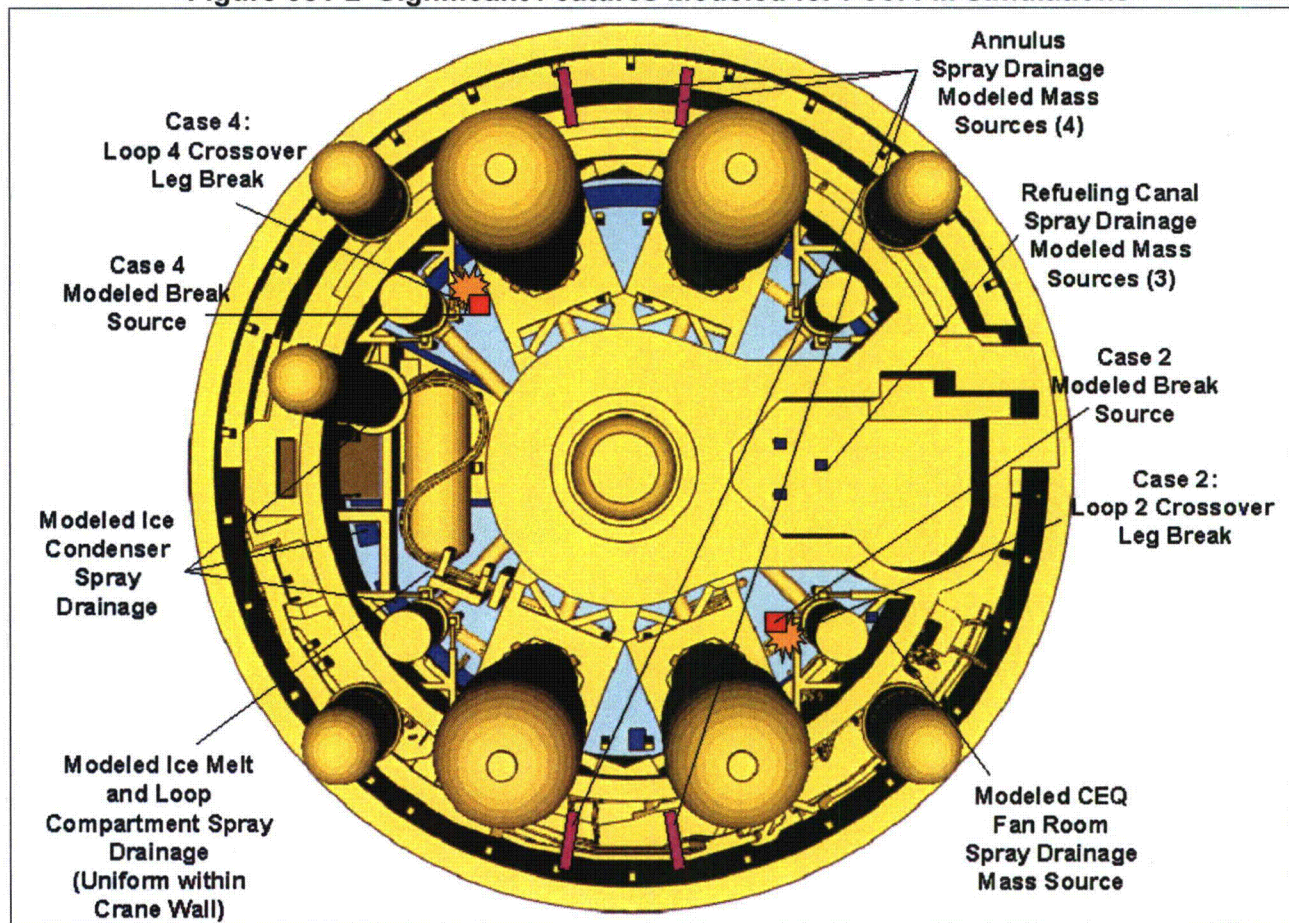
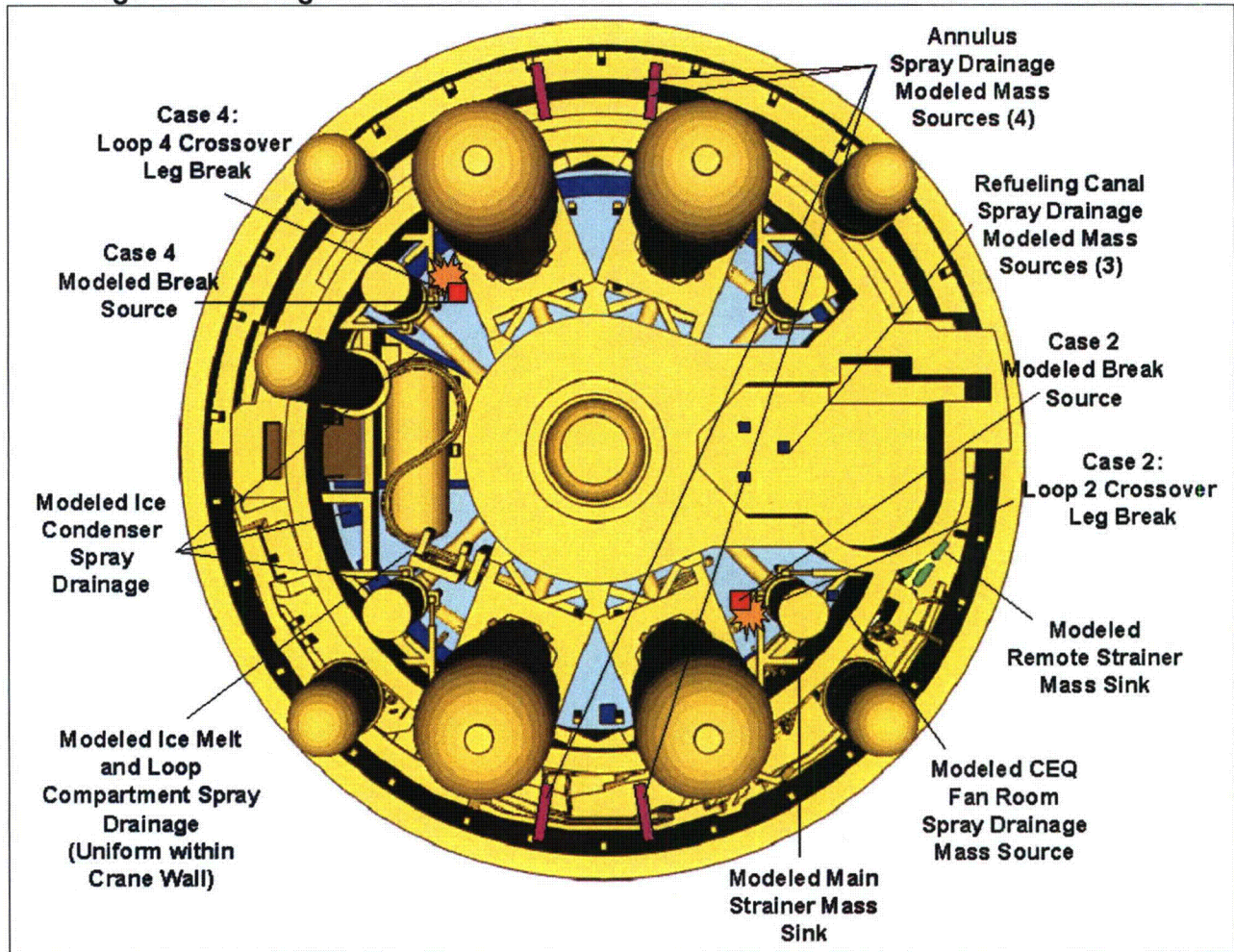


Figure 3e1-3 Significant Features Modeled for Recirculation Pool Simulations



Computational Mesh Used for CFD Simulations

In the CFD models, rectangular meshes were defined that were fine enough to resolve important features, but not so fine that the simulations would take a prohibitively long period to run. A 6 in cell length was chosen as the largest cell size that could reasonably resolve the concrete structures that compose the containment floor.

For the cells right above the containment floor, the meshes were set as 3 in tall to closely resolve the vicinity of settled debris. To accurately define the holes in the flood-up overflow wall, nested meshes with a 3 in x 3 in x 3 in cell size were included in the CFD models. An additional linked mesh with a 6 in x 6 in x 6 in cell size was also included in the pool fill CFD model to incorporate the sump pit volume.

For the pool fill model, the top of the mesh was defined at 8.5 ft above the floor, and for the recirculation model, the top of the mesh was defined at 7 ft above the floor. The total cell count in the pool fill model was 1,367,360, and the total cell count in the recirculation pool model was 1,293,760.

Modeling of the Containment Spray and Ice Condenser Flows

CNP has spray headers in both upper and lower containment. In the lower containment, there are spray headers both in the loop compartment, and in the accumulator rooms in the annulus. The flow split between the upper containment headers, loop compartment headers, and annulus headers was determined using bounding containment spray flow rates. This split was determined to be approximately 67% to the upper containment and 33% to the lower containment. The lower containment split was determined to be approximately 73% to the loop compartment and 27% to the annulus. Given a maximum spray flow of 6,800 gpm, the upper containment spray flow would be 4,556 gpm, the loop compartment spray flow would be 1,638 gpm, and the annulus spray flow would be 606 gpm.

The sprays in the loop compartment would directly impact the pool and were introduced in the model accordingly. The sprays in the annulus discharge to the accumulator rooms, where the flow would collect and drain to the pool in the annulus through hatches in the annulus floor and through the gap between the periphery of the floor at elevation 612 ft and the containment wall. It was assumed that the spray flow would be uniform on both sides of containment, with 303 gpm of flow draining below accumulator rooms 1 and 4, and 303 gpm below accumulator rooms 2 and 3. This is a reasonable assumption since there is one header on each side of the annulus with equivalent piping lengths and numbers of spray nozzles. This flow was conservatively introduced in concentrated locations below an annulus hatch on each side of containment rather than spread out below the hatches and around the periphery.

The sprays in upper containment would drain to three areas: the refueling canal, the CEQ fan room, and through the upper containment fans to the annulus. The flow through the upper containment fans would be small and was assumed to be negligible. The flow through the CEQ fan room was established at 127 gpm. This left 4,429 gpm of spray flow draining through the refueling canal drains. The refueling canal has two 12 in drain pipes and one 10 in drain pipe discharging directly below to the containment pool. It was assumed that the flow split through these pipes would be proportional to the pipe diameters, giving a flow of 1,563 gpm through the two 12 in pipes and 1,303 gpm through the 10 in pipe. Since these three drains are in the same general location, the CFD model is not sensitive to the flow split (i.e., if one of these drains was blocked, the overall pool flow patterns would not change significantly).

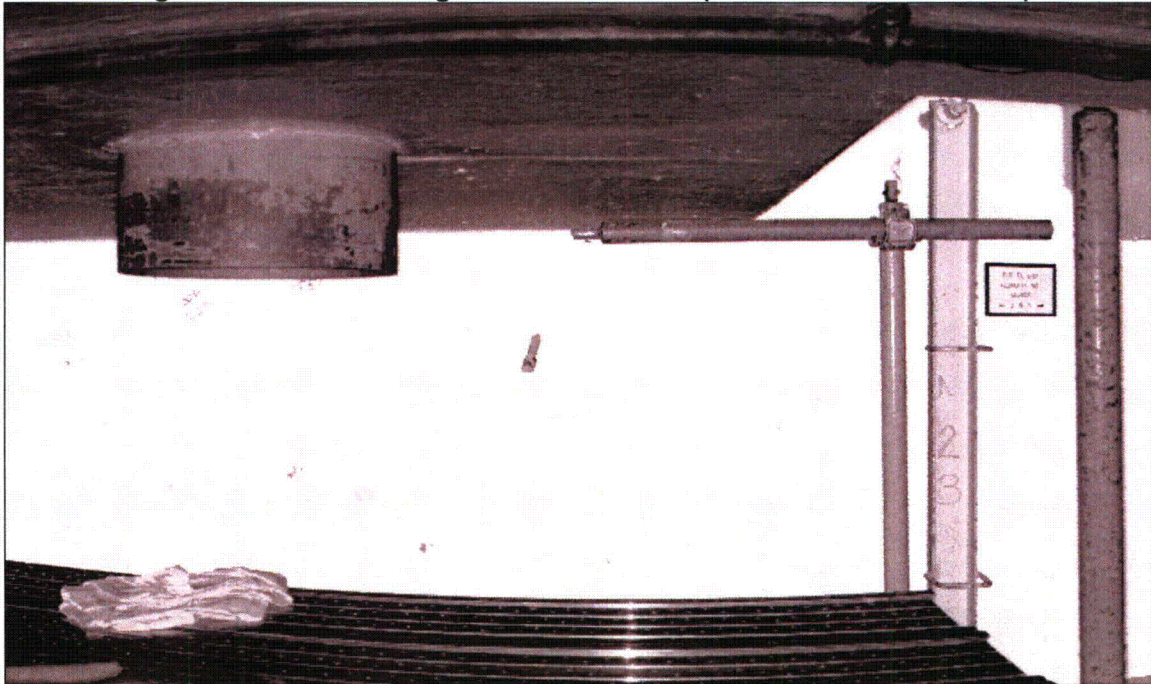
For Unit 1, the CEQ fan room drainage is piped to the annulus sump (next to the remote strainer), and for Unit 2, the drainage is piped to the lower containment sump (next to the main strainer). Since the majority of debris is initially inside the crane wall, the highest transport fractions would result from the Unit 2 configuration where the CEQ fan room spray lands inside the crane wall increasing the total flow (and debris) that would pass through the

crane wall holes to the remote sump. Therefore, the CEQ fan room drainage was modeled as a mass source in the lower containment sump.

When introducing the loop compartment spray and ice condenser flow to the containment pool models, simplifications had to be made due to the unfeasibility of modeling all the individual water droplets/streams that would fall into the pool. Although modeling individual falling droplets is within the capability of Flow-3D[®], the simultaneous modeling of the extremely large number of droplets that would be falling into the containment pool is not within the Flow-3D[®] capability. Accordingly, the introduction of the loop compartment spray and ice condenser drainage to the recirculation pool CFD model was accomplished as follows:

- The kinetic energy of the falling droplets and streams was accounted for through a consideration of the first law of thermodynamics (the conservation of energy).
- The loop compartment spray headers are at an elevation of approximately 649 ft, and are assumed to spray uniformly over the area inside the crane wall. Since the floor is at Elevation 598.78 ft, and the recirculation pool is 5.9 ft deep, this gave a freefall distance of 44.3 ft and a freefall velocity of 53.4 ft/s. However, the terminal velocity of a large water drop is only 29 ft/s. Therefore, the loop compartment sprays were introduced just below the surface of the pool as shown in Figure 3e1-2, using mass source particles with a velocity of 29 ft/s. This is conservative since smaller drops have a lower terminal velocity.
- The refueling canal spray drainage was included in the CFD model by defining a 1 ft² mass source obstacle at the end of each drain pipe. A solid shell was defined around the sides of the three source obstacles to force the spray flow in the same direction as the discharge from the three pipes. Since the bottom of the refueling canal is just above the minimum water level (elevation 604.7 ft), and the drain pipes extend down about 6 in (see Figure 3e1-4), the spray water would enter the pool below the surface. Therefore, it was not necessary to increase the kinetic energy to account for freefall.

Figure 3e1-4 Refueling Canal Drain Line (from laser scan model)



Note: Bottom of drain is shown in upper left section of the picture.

- The annulus spray drainage would drain from the accumulator rooms to the pool through openings in the accumulator room floor at the 612 ft elevation. This drainage was modeled just below the surface of the pool as shown in Figure 3e1-2, using mass source particles. The freefall distance from this floor to the pool is 7.3 ft, giving a freefall velocity of 21.7 ft/s.
- Since the CEQ fan room spray drainage enters the lower containment sump through a drain, it was not necessary to increase the kinetic energy due to freefall. Therefore, this spray water was introduced using a simple mass source.
- The ice melt would flow through 21 drain lines discharging at an elevation of 636.5 ft at various points around the perimeter of the crane wall. Some of the ice melt flowing through the ice condenser drains would reach the pool relatively unobstructed, and some would impact a number of obstacles (grating, equipment, steel beams, etc.), which would break up the individual streams into large droplets and disperse the flow. Therefore, the ice condenser flow was introduced as shown in Figure 3e1-2.
- Since the addition of the ice condenser flow creates a transient condition (raising the water level), a flow equal to the ice melt flow introduced at the floor (5,900 gpm) was drawn out of the model through the exposed area of concrete below 2 ft inside the crane wall. This enabled the CFD calculation to reach steady-state, and had minimal affect on the pool given the large surface area that is used to draw out the water.

For the pool fill CFD model, the spray and ice condenser drainage was introduced in the same locations as for the recirculation pool CFD model. However, since the pool height was changing over time and the model was initiated without any water, the kinetic energy of the

spray and ice condenser flow could not be realistically introduced at the full kinetic energy without causing significant splashing that would prohibitively slow down the calculations. Therefore, for the initial pool fill period up to a level of 3 ft, the spray and ice condenser flows were introduced using mass source particles just above the floor without setting an increased velocity to match the freefall/terminal velocity. After the pool reached a level of approximately 3 ft, the mass source particles were moved to a height of 2.25 ft and the velocity was increased to be consistent with the freefall/terminal velocity of the sprays and ice melt (note that the freefall velocities were calculated from the source height to the floor of the pool, which conservatively neglected the fact that the freefall velocity of the sprays would steadily decrease as the water level increased). Also, for the pool fill CFD model, it was not necessary to artificially remove the ice condenser flow since the purpose of this run was to realistically show the pool fill-up. Due to the decreased ice melt rate that occurs following the initial blowdown period, the pool fill CFD run was restarted after reaching three minutes, to decrease the ice condenser flow rate from 13,637 gpm to 108 gpm.

Modeling of the Break Flow

The water stream falling from the postulated break would introduce momentum into the containment pool that would influence the flow dynamics. This break stream momentum was accounted for by introducing the break flow to the pool at the velocity a freefalling object would have if it fell the vertical distance from the location of the break to the surface of the pool.

For the recirculation pool CFD model, the break stream was introduced in the CFD model by defining a flow region populated with mass source particles and setting the flow rate and velocity similar to the containment spray sources. The break source was situated near the postulated break location, below the surface of the pool. This was done to avoid the splashing (which would drastically increase the calculation run time) that would occur if the source was above the pool surface.

The center of the reactor inlet nozzle (above the postulated break locations) is at an elevation of 614 ft. Since the floor level is at elevation 598.78 ft, and the water level is 5.9 ft, this gives a total freefall distance from the break to the surface of the pool of 9.3 ft, which corresponds to a freefall velocity of 24.5 ft/s.

For the pool fill CFD model, the break flow was introduced similar to the spray flow, with the flow introduced at the floor without increasing the velocity until the water level reached 3 ft. When the run was restarted, the mass source particles were moved up to 2.25 ft and the break flow was introduced at 29 ft/s, which conservatively bounded the freefall velocity from the break height to the 3 ft pool level.

Modeling the Recirculation Sump

The recirculation sump consists of the main sump strainer (inside the crane wall) and a remote sump strainer (in the annulus) that is connected to the main sump by a waterway.

For the recirculation CFD model, the mass sink used to pull flow from the CFD model was defined for the main strainer as shown in Figure 3e1-5, and for the remote strainer as shown

in Figure 3e1-6 (both mass sinks are shown in green). For the two clean strainer CFD runs, a negative flow rate of 13,421 gpm was set for the main strainer mass sink, and a negative flow rate of 979 gpm was set for the remote strainer mass sink. For the two 90% blocked main strainer CFD runs, a negative flow rate of 9,720 gpm was set for the main strainer mass sink and a negative flow rate of 4,680 gpm was set for the remote strainer mass sink. Based on this, the CFD model drew the specified amount of water from the pool over the entire exposed surface area of the mass sink obstacle.

Figure 3e1-5 Main Strainer Sump Mass Sink

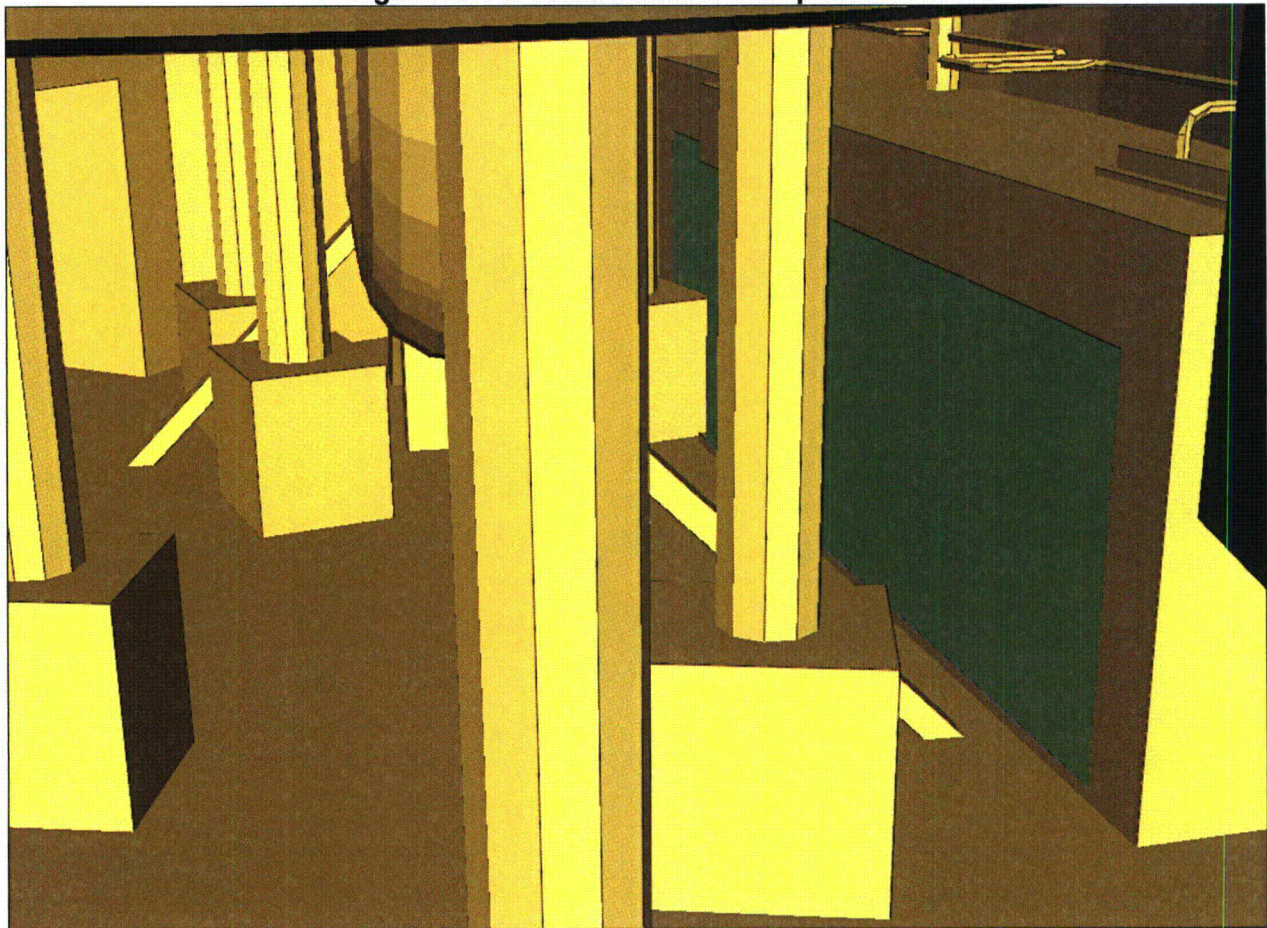
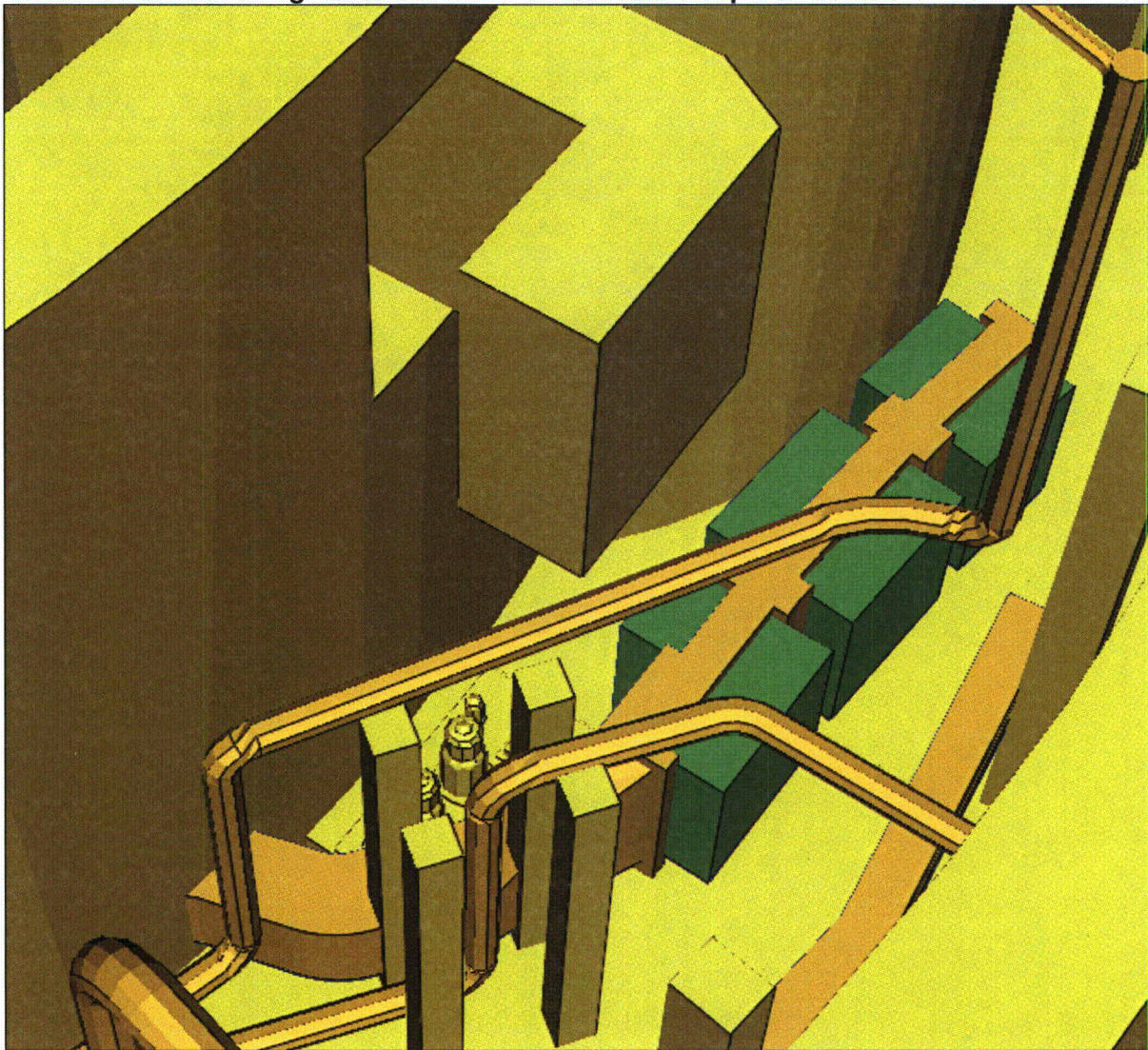


Figure 3e1-6 Remote Strainer Sump Mass Sink

For the pool fill CFD model, a series of two dimensional baffles with a K-factor (resistance factor) of 5.95 were used to model the main strainer. To simplify the analysis of the remote strainer, a baffle with a composite K-factor of 7.80 (accounting for the pressure losses due to the remote strainer and the remote strainer waterway) was placed in the hole in the crane wall where the remote strainer waterway passes through the crane wall to the recirculation sump. The remote strainer and waterway geometry was not included in the pool fill CFD model. The columns shown in Figure 3e1-6 were removed in Unit 2 and will be removed in Unit 1 as a part of the plant modification to install the remote strainer. However, given the size of these columns compared to the overall flow path, this change did not significantly affect the debris transport analysis.

Turbulence Modeling

Several different turbulence modeling approaches can be selected for a Flow-3D[®] calculation. The approaches are (ranging from least to most sophisticated):

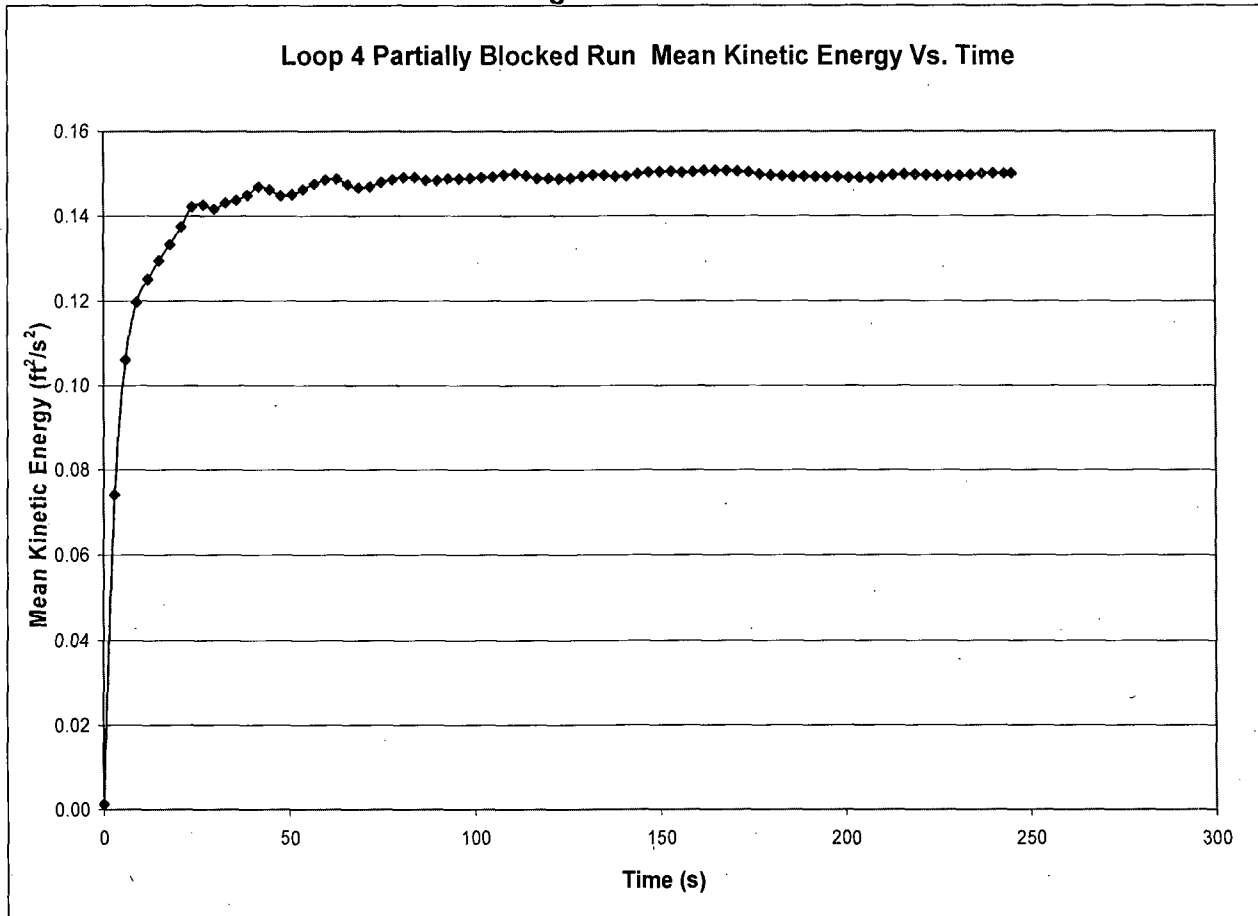
- Prandtl mixing length
- Turbulent energy model
- Two-equation k- ϵ model
- RNG model
- Large eddy simulation model

The RNG turbulence model was judged to be the most appropriate for the CFD analysis due to the large spectrum of length scales that would likely exist in a containment pool during emergency recirculation. The RNG approach applies statistical methods in a derivation of the averaged equations for turbulence quantities (such as turbulent kinetic energy and its dissipation rate). RNG-based turbulence schemes rely less on empirical constants while setting a framework for the derivation of a range of models at different scales. Sensitivity calculations have shown that Flow-3D[®] containment pool calculations utilizing the more sophisticated turbulence models (including the RNG model) give results that differ significantly from calculations utilizing the less sophisticated models. Differences in results between calculations made with the more sophisticated models have been shown to be minimal.

Steady State Calculation

The recirculation pool CFD model was started from a stagnant state at a pool depth of 5.9 ft, and run until steady-state conditions developed. The model was run for a total of five minutes of simulated time for each case, except for the Loop 4 partially blocked case, which was run for a total of approximately four minutes. All of the velocity and TKE results presented in subsequent sections of the response to Information Item 3.e reflect steady-state conditions. The estimated mean kinetic energy as a function of time is shown in Figure 3e1-7 for the Loop 4 partially blocked recirculation pool CFD case. The plot of mean kinetic energy is a good indicator of when steady-state conditions have been reached. Checks were also made of the velocity and turbulent energy patterns in the pool to verify that steady-state conditions were reached.

Figure 3e1-7



Debris Transport Metrics

This section explains and lists the metrics used to evaluate the potential for debris transport in the CNP containment pool. The transport mechanisms involved were:

- Carrying of suspended debris by bulk flow to the sump
- Tumbling/sliding of sunken debris to the sump
- Lifting of sunken debris over a curb

Metrics for predicting debris transport have been adopted or derived from data. The specific metrics are the TKE necessary to keep debris suspended and the flow velocity necessary to tumble sunken debris along a floor or lift it over a curb. The derivation for these metrics is explained below. All of the metrics used are shown in Tables 3e1-5 and 3e1-6.

Minimum TKE Necessary to Suspend Debris

Due to the absence of data, the values of minimum TKE associated with debris suspension were derived from settling velocity and the definition of TKE as follows:

$$TKE = \frac{1}{2} \overline{u_i u_i} \quad \text{Equation 1}$$

$$TKE = \frac{1}{2} \overline{u_i^2} = \frac{1}{2} (\overline{u_1^2 + u_2^2 + u_3^2}) \quad \text{Equation 2}$$

$$TKE = \frac{1}{2} 3 \cdot u_3^2 = \frac{3}{2} V_T^2 \quad \text{Equation 3}$$

In the above equations:

- the over-bar denotes time averaging,
- u_i (a vector) is the fluctuating part of velocity (as opposed to the mean part),
- $u_i u_i$ is a vector inner product,
- u_1 and u_2 are taken to be the horizontal components of the velocity fluctuation,
- u_3 is taken to be the vertical component of the velocity fluctuation, and
- V_T is the terminal (settling) velocity of the debris

The interpretation of this derivation is that the strength of the turbulence needed to reflect fluctuations in the vertical component of velocity are on the order of the settling velocity of the debris if suspension was to be accomplished. The key here is that only vertical velocity fluctuations pertain to settling considerations and there is no reason to suspect that velocity fluctuations in a containment pool are greater in one direction than in another.

Settling Velocity of Fine Material

Fine material is assumed to be spherical in shape and is assumed to settle per Stokes' Law. The relationship is:

$$\underbrace{\frac{4}{3} \pi R^3 (\rho_s g)}_{\text{Weight}} - \underbrace{\frac{4}{3} \pi R^3 (\rho_L g)}_{\text{Buoyant Force}} - \underbrace{6 \pi g \mu V_T R}_{\text{Drag}} = 0 \quad \text{Equation 4}$$

where:

- R = radius of the sphere
- ρ_s = density of the sphere
- ρ_L = density of the liquid
- g = acceleration due to gravity
- μ = viscosity of the liquid

V_T = terminal (settling) velocity of the sphere

Settling of Dirt and Dust

The density and representative diameter of dirt and dust were assumed to be $169 \text{ lb}_m/\text{ft}^3$ and 17.3 microns ($5.675 \times 10^{-5} \text{ ft}$) respectively. Using a temperature of 120°F , and a pressure of 14.7 psia gives a water density and viscosity of $61.7 \text{ lb}_m/\text{ft}^3$ and $1.164 \times 10^{-5} \text{ lb}_f\text{-sec}/\text{ft}^2$ respectively. Inserting these values along with a gravitational acceleration of $32.2 \text{ ft}/\text{s}^2$ gives:

$$V_T = \frac{2R^2 g(\rho_s - \rho_L)}{9g_c \mu}$$

$$= \frac{2(2.84 \times 10^{-5} \text{ ft})^2 (32.2 \text{ ft}/\text{s}^2)(169 \text{ lb}_m/\text{ft}^3 - 61.7 \text{ lb}_m/\text{ft}^3)}{9(32.2 \text{ ft}/\text{s}^2 \cdot \text{lb}_m/\text{lb}_f)(1.164 \times 10^{-5} \text{ lb}_f \cdot \text{s}/\text{ft}^2)} = 1.65 \times 10^{-3} \text{ ft}/\text{s} \quad \text{Equation 5}$$

Using the relationship derived for kinetic energy:

$$TKE = \frac{3}{2} V_T^2 = \frac{3}{2} (1.65 \times 10^{-3} \text{ ft}/\text{s})^2 = 4.08 \times 10^{-6} \text{ ft}^2/\text{s}^2 \quad \text{Equation 6}$$

Therefore, the pool turbulence must be below $4.1 \times 10^{-6} \text{ ft}^2/\text{s}^2$ for dirt and dust to settle. The settling velocity and TKE metrics for other particulate debris types were calculated similarly. Use of a cooler pool temperature (120°F versus 160°F) was conservative since particles would tend to settle more slowly in cooler water.

Settling of Paint Particulate

The density of paint particulate at CNP is $112 \text{ lb}_m/\text{ft}^3$ for the qualified epoxy paint, $94 \text{ lb}_m/\text{ft}^3$ for the unqualified epoxy paint, $98 \text{ lb}_m/\text{ft}^3$ for the unqualified alkyd paint, and $250 \text{ lb}_m/\text{ft}^3$ for the unqualified cold galvanizing compound. The representative size for the coatings debris generated inside the ZOI and the cold galvanizing compound generated outside the ZOI was assumed to be 10 microns , the representative size for the OEM coatings generated outside the ZOI was assumed to be 83 microns , and the representative size for the unqualified non-OEM coatings generated outside the ZOI was assumed to be $4 \text{ mil thick chips}$.

The settling velocity and TKE required to keep the 10 micron paint particulate in suspension was calculated as shown for dirt and dust. For the larger particulate, however, the settling velocity was high enough that it was outside the range of Stokes' Law. Therefore, the settling velocity for this debris was calculated using a stand-alone CFD simulation.

Settling of Min-K Particulate

In the debris generation calculation, Min-K was assumed to fail as 2.5 micron particulate with a density of $162 \text{ lb}_m/\text{ft}^3$.

Settling of Cal-Sil Particulate

In the debris generation calculation, the Cal-Sil destroyed by the postulated breaks was determined to fail in a range from 5 micron particulate to pieces greater than 3 in. The particulate density was assumed to be $144 \text{ lb}_m/\text{ft}^3$.

Settling of Fire Barrier Tape

It was assumed that the small and large pieces of fire barrier tape would settle to the floor in regions of lower turbulence similar to other small and large pieces of debris. This is appropriate as the tape falls in the same size range (<4 in and >4 in) as the other small and large debris types (<4" for small RMI, >4" for large RMI, <1 in – >3 in for cal-sil pieces, <2 in for small marinate, and >2 in for large marinate). The fire barrier tape also has a density that is higher ($98 \text{ lb}_m/\text{ft}^3$) than that of the other large and small debris types ($14.5 \text{ lb}_m/\text{ft}^3$ for Cal-Sil, $34\text{-}46 \text{ lb}_m/\text{ft}^3$ for marinite). As a settling velocity metric for fire barrier tape is unknown, the most conservative known settling velocity for small and large debris types (that of small RMI) was used for the fire barrier tape (0.37 ft/s).

Tumbling and Settling of Paint Chips

The unqualified coatings debris that was assumed to fail as chips at CNP included the unqualified Non-OEM epoxy (4 mils thick, $94 \text{ lb}_m/\text{ft}^3$) and unqualified Non-OEM alkyd (4 mils thick, $98 \text{ lb}_m/\text{ft}^3$) paint. For this analysis, the alkyd chips were conservatively assumed to be transported similarly to unqualified paint particulate. The settling and tumbling velocity metrics for the epoxy chips were taken from NUREG/CR-6916 (Reference 95). The testing described in the NUREG was performed using different sizes of paint chip debris for a variety of coatings systems typically used in nuclear power plants. Since the size distribution and the exact coating system of the unqualified epoxy chips at CNP is not known, the most conservative settling and bulk tumbling velocity metrics from NUREG/CR-6916 were selected from the epoxy chips tested.

The most conservative settling velocity reported (0.13 ft/s) was for the two coat epoxy system with a chip size of 1/64 in to 1/32 in. For larger two coat epoxy chips and the other epoxy chips tested, the settling velocities were as high as 0.46 ft/s.

The most conservative bulk tumbling velocity reported (0.27 ft/s) was also used for the two coat epoxy system, but for curled 1 in to 2 in chips rather than the 1/64 in to 1/32 in chips. The smaller 1/64 in to 1/32 in two coat epoxy chips had a much higher bulk tumbling velocity of 1.01 ft/s. The 0.27 ft/s tumbling velocity is also bounding for the majority of incipient tumbling velocities measured, although a few of the chip types/sizes tested had lower incipient tumbling velocities. The incipient and bulk tumbling velocities for this testing were defined as the velocity at which the first chip begins to move, and the velocity at which 80% of the chips move. The bulk tumbling velocity was judged to

be the most appropriate transport metric for this analysis, since it is most representative of the paint chip debris. Also, the incipient tumbling velocity for a distribution of various sizes of the same two coat epoxy chips was measured to be 0.32 ft/s, which is bounded by the bulk tumbling velocity used for this analysis.

Tumbling of Fine Sunken Material

Given the low turbulence required to keep fine material suspended, if the turbulence is low enough for fines to settle, it is almost certain that the water velocity will not be high enough to slide the fines along the floor. Therefore, the tumbling or sliding of fine sunken (settled) material (e.g., individual fibers, coatings particulate, dirt and dust) along the floor was not considered.

Lifting of Sunken Debris over a Curb

Curbs have the potential to interrupt the movement of sunken debris along a floor. Ramps of debris can, however, build up in front of a curb allowing debris to climb up over the curb more easily. Some data exists for the magnitude of velocity required to lift various types of debris over a curb. However, there is no test data to show what the debris ramp angle, θ , would be. The steeper the angle, the less material will form the debris pile. The commonly reported angle of repose for a pile of loose material is 34° . This would be the upper limit on the steepness of a ramp formed of debris fragments for regions where the pool flow direction is mixed (i.e., due to cross flow or swirling eddies, etc.). Note that if flow approaches a curb at a 90° angle and the velocity is high enough, it is possible to form debris ramps with a steeper angle. The conservative assumption therefore, with respect to the amount of debris captured at curbs where the flow direction is mixed, is that debris ramps formed against curbs or trash racks have an angle of 34° .

Table 3e1-5 and 3e1-6 summarize the metrics used in estimating debris transport in the CNP containment pool.

Table 3e1-5 Debris Settling and Tumbling Transport Metrics

Debris Type	Size	Terminal Settling Velocity, ft/s	Calculated Minimum TKE Required to Suspend, Ft ² /s ²	Flow Velocity Associated with Tumbling, ft/s
RMI	Small Pieces	0.37 ⁽¹⁾	0.21	0.28 ⁽¹⁾
	Large Pieces	0.48 ⁽¹⁾	0.35	0.50
Cal-Sil and Marinite	5 micron particulate (144 lb _m /ft ³)	1.1E-04 ⁽⁵⁾	1.7E-08	NA
	Small Pieces	0.57 ⁽²⁾	0.49	0.33 ⁽²⁾
	Large Pieces	0.64 ⁽²⁾	0.61	0.52 ⁽²⁾
Min-K™	20 micron SiO ₂ agglomerate (137 lb _m /ft ³)	1.5E-03 ⁽⁵⁾	3.6E-06	NA
	2.5 micron TiO ₂ particulate (262 lb _m /ft ³)	6.4E-05 ⁽⁵⁾	6.2E-09	NA
Fiberglass	Individual Fibers	7.4E-03	8.2E-05	NA
Qualified Epoxy	10-micron particulate (112 lb _m /ft ³)	2.6E-04 ⁽⁵⁾	1.0E-07	NA
Unqualified Epoxy (in ZOI)	10-micron particulate (94 lb _m /ft ³)	1.7E-04 ⁽⁵⁾	4.1E-08	NA
Unqualified Alkyd (in ZOI)	10-micron particulate (98 lb _m /ft ³)	1.9E-04 ⁽⁵⁾	5.2E-08	NA
Unqualified OEM Epoxy	83-micron particulate (94 lb _m /ft ³)	1.1E-02 ⁽⁵⁾	1.7E-04	NA
Unqualified OEM Alkyd	83-micron particulate (98 lb _m /ft ³)	1.2E-02 ⁽⁵⁾	2.1E-04	NA
Unqualified non-OEM Epoxy	Epoxy Paint Chips	0.13 ⁽³⁾	2.5E-02	0.27 ⁽⁴⁾
Dirt and Dust	17.3-micron particulate (169 lb _m /ft ³)	1.6E-03 ⁽⁵⁾	4.1E-06	NA

(1) Metrics are for 1/2 in square crumpled foils for small pieces of RMI and 2 in square crumpled foils for large pieces of RMI.

(2) Metrics are for 1 in to 3 in pieces for small pieces of Cal-Sil and >3 in pieces for large pieces of Cal-Sil.

(3) Settling metric is for two coat epoxy 1/64 in to 1/32 in chips.

(4) Tumbling metric is for two coat epoxy 1 in to 2 in curled chips.

(5) Calculated using water properties at 14.7 psia and 120°F.

Table 3e1-6 Flow Velocity Necessary to Lift Sunken Debris Over a Curb

Debris Type	Size	Curb Height, in	Minimum Velocity Needed to Lift Debris Over a Curb, ft/s
RMI ⁽¹⁾	Small Pieces (<4 in)	6	1.0 ⁽²⁾
	Large Pieces (>4 in)	6	1.0 ⁽²⁾

(1) Metrics are for 1/2 in square crumpled foils for small pieces of RMI and 2 in square crumpled foils for large pieces of RMI.

(2) Highest velocity tested (none of the pieces were lifted over the curb).

Pool Fill Debris Transport

The following describes the methodology that was used to determine the quantity of debris that was calculated to be transported to the main strainer and annulus during pool fill.

During pool fill, the flow of water would transport insulation debris from the break location to all areas of the recirculation pool. Some of the debris could be transported to the annulus through the holes in the flood-up overflow wall. Some of the debris could also be transported directly to the main strainer as the sump cavity is filled and as water flows backward through the remote strainer during the pool fill phase. The transport to a given region was calculated assuming that fine debris is uniformly distributed in the pool, and the water entering the pool from the break, sprays, and ice condenser, is clean.

As water pours onto the containment floor, it would initially flow in shallow, high velocity sheets. This sheeting action would cause both small and large pieces of insulation debris (that may not transport easily during recirculation flow) to be scattered around the containment floor. As the water level rises, debris would preferentially be swept to the main strainer and the DI in front of the flood-up overflow wall.

If $x(t)$ denotes the quantity of particulate debris in the pool at time t , then the quantity of particulate in the pool can be described as a function of time as shown in Equation 7:

$$\frac{dx}{dt} = \text{Input Rate} - \text{Output Rate} \quad \text{Equation 7}$$

Since the water entering the pool from the break, spray, and ice condenser flows is assumed to be clean, the input rate of debris is zero. Also, since the flow into the pool is equal to the flow out of the pool (into the cavity), the output rate of debris (from the pool to the cavity) is:

$$\text{Output Rate} = Q \left(\frac{x(t)}{V_{\text{pool}}} \right)$$

Equation 8

where:

Q = the break and spray flow rate
 V_{pool} = the pool volume

Therefore, Equation 7 can be reduced to the following:

$$\frac{dx}{dt} = 0 - Q \left(\frac{x(t)}{V_{\text{pool}}} \right)$$

Equation 9

Assuming the flow rate and pool volume are constant, Equation 9 is linear and separable. Given the initial quantity of debris in the pool, x_i , the quantity of debris in the pool as a function of time can be expressed as:

$$x(t) = x_i e^{-t(Q/V_{\text{pool}})}$$

Equation 10

In the case of pool flow passing through the main strainer and the flood-up overflow wall to the annulus, however, the pool volume inside the crane wall is steadily increasing, and the flow rates through the main strainer and the flood-up overflow wall holes vary over time. If small enough increments are considered, however, the flow rates and pool volume can be considered constant and the fraction of debris transported to the main strainer and the annulus can be calculated using Equation 10 in series as follows:

Table 3e1-7 – Equations for Determining Debris Transport to Main Strainer and Annulus During Pool Fill

Time Step	Fraction of Debris Transported	Equation Number
1	$x_{strainer1} = x_i \cdot (1 - e^{-t_1 \cdot (Q_{strainer1} / V_{pool1})})$	Equation 11
	$x_{annulus1} = x_i \cdot (1 - e^{-t_1 \cdot (Q_{annulus1} / V_{pool1})})$	Equation 12
2	$x_{strainer2} = x_{strainer1} + (x_i - x_{strainer1} - x_{annulus1}) \cdot (1 - e^{-(t_2 - t_1) \cdot (Q_{strainer2} / V_{pool2})})$	Equation 13
	$x_{annulus2} = x_{annulus1} + (x_i - x_{strainer1} - x_{annulus1}) \cdot (1 - e^{-(t_2 - t_1) \cdot (Q_{annulus2} / V_{pool2})})$	Equation 14
3	$x_{strainer3} = x_{strainer2} + (x_i - x_{strainer2} - x_{annulus2}) \cdot (1 - e^{-(t_3 - t_2) \cdot (Q_{strainer3} / V_{pool3})})$	Equation 15
	$x_{annulus3} = x_{annulus2} + (x_i - x_{strainer2} - x_{annulus2}) \cdot (1 - e^{-(t_3 - t_2) \cdot (Q_{annulus3} / V_{pool3})})$	Equation 16
n	$x_{strainern} = x_{strainern-1} + (x_i - x_{strainern-1} - x_{annulusn-1}) \cdot (1 - e^{-(t_n - t_{n-1}) \cdot (Q_{strainern} / V_{pooln})})$	Equation 17
	$x_{annulusn} = x_{annulusn-1} + (x_i - x_{strainern-1} - x_{annulusn-1}) \cdot (1 - e^{-(t_n - t_{n-1}) \cdot (Q_{annulusn} / V_{pooln})})$	Equation 18

where:

n = current time step

$x_{strainern}$ = fraction of debris transported to the main strainer at the current time step

$x_{annulusn}$ = fraction of debris transported to the annulus at the current time step

$x_{strainern-1}$ = fraction of debris transported to the main strainer in the previous time step

$x_{annulusn-1}$ = fraction of debris transported to the annulus in the previous time step

x_i = initial fraction of debris in the pool

t_n = time at the current time step (seconds)

t_{n-1} = time at the previous time step (seconds)

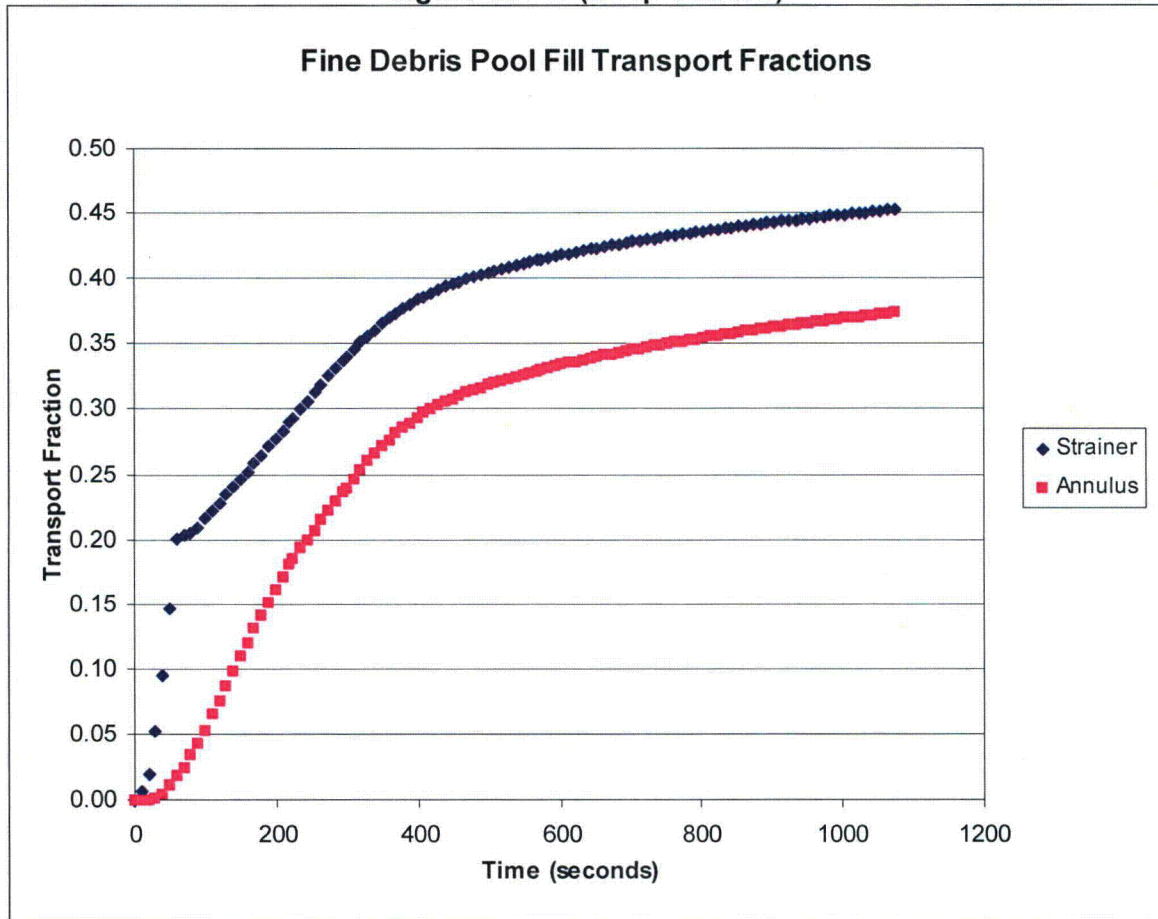
$Q_{strainern}$ = flow through the main strainer flux plane at the current time step (ft³/second)

$Q_{annulusn}$ = flow through the flood-up overflow wall hole flux planes at the current time step (ft³/second)

V_{pooln} = pool volume inside the loop compartment at the current time step (ft³)

The pool fill transport fractions were determined using the flow rates determined through the CFD model and the associated pool volumes. Figure 3e1-8 shows the pool fill transport fractions for fine debris as a function of time. The pool fill transport fraction for fine debris to the main strainer was 45%, and pool fill transport fraction for fine debris to the annulus was 37%.

Figure 3e1-8 (Loop 4 Break)



Since the small and large pieces of debris would not transport as readily during pool fill-up as the fine debris, the transport fractions were determined using the velocities and turbulence in the pool. As discussed in Assumption 3.a, the small-piece debris inside the loop compartment at the beginning of the pool fill phase was assumed to be uniformly distributed. This distribution area is 3,226 ft².

Figures 3e1-17 through 3e1-25 (attached to the end of this section) show velocity contour plots just above the floor (1.5 in) with a TKE iso-surface approximately representative of the TKE required to suspend the various types of debris pieces for various intervals during the pool fill phase.

During the initial portion of the run (before the model was restarted to introduce the break, spray, and ice condenser flows at the full velocity), as the depth of the pool rises, the velocity dropped fairly quickly. However, after the model was restarted (and the run had progressed long enough for the changes to have their full effect), it could be seen that the velocities at the floor of the pool increased significantly. This indicated that the velocity magnitude in the run prior to the restart was slightly underestimated.

For the earlier time steps, the flow direction at the floor in a large portion of the pool was toward the main strainer. Later in the run (after the model was restarted to model the source flows more accurately), however, the results showed that the flow direction for only a small portion of the pool was in the direction of the sump. Therefore, modeling the source flows realistically had an affect on the flow direction as well as the velocity.

Since a comparison of the results during the time steps showed that the overall turbulence and velocities in the pool are highest at approximately 300 seconds, this time step was conservatively used for determining the small and large piece debris pool fill transport fractions.

With the pool velocity magnitudes conservatively established as described above, the evaluation of the remaining debris sources for transport and lift was performed. This involved determining the area where the velocity magnitude was high enough to move or lift the pieces (as provided in Tables 3e1-5 and 3e1-6), each divided by the surface area of the loop compartment. The results of these evaluations are contained in Tables 3e1-8 and 3e1-9, provided below.

Table 3e1-8 Fractions of Debris Available to Transport to the Main Strainer During Pool Fill (Loop 4 Break)

Debris Type	Fines	Small Pieces	Unjacketed Large Pieces	Jacketed Large Pieces
RMI	-	9%	5%	-
Cal-Sil	45%	5%	-	-
Marinite	45%	5%	4%	-
Min-K	45%	-	-	-
Miscellaneous Coatings (Inside ZOI)	45%	-	-	-
Miscellaneous Coatings (Outside ZOI)	-	-	-	-
Unqualified Non-OEM Epoxy (Outside ZOI)	-	-	-	-
Latent Debris	45%	-	-	-
Electromark Labels (Inside ZOI)	-	9%	-	-
Electromark Labels (Outside ZOI)	-	-	-	-
Unqualified Labels (Outside ZOI)	-	-	-	-
Flexible Conduit PVC Jacketing (Outside ZOI)	-	-	-	-
Fire Barrier Tape (Inside ZOI)	45%	9% ⁽¹⁾	-	-
Transportable Ice Condenser Debris	45%	-	-	-

(1) This includes pieces of tape < 4 in and ≥ 4 in.

Table 3e1-9 Fractions of Debris Available to Transport to the Annulus During Pool Fill (Loop 4 Break)

Debris Type	Fines	Small Pieces	Unjacketed Large Pieces	Jacketed Large Pieces
RMI	-	27%	13%	-
Cal-Sil	37%	26%	-	-
Marinite	37%	26%	11%	-
Min-K	37%	-	-	-
Miscellaneous Coatings (Inside ZOI)	37%	-	-	-
Miscellaneous Coatings (Outside ZOI)	-	-	-	-
Unqualified Non-OEM Epoxy (Outside ZOI)	-	-	-	-
Latent Debris	37%	-	-	-
Electromark Labels (Inside ZOI)	-	27%	-	-
Electromark Labels (Outside ZOI)	-	-	-	-
Unqualified Labels (Outside ZOI)	-	-	-	-
Flexible Conduit PVC Jacketing (Outside ZOI)	-	-	-	-
Fire Barrier Tape (Inside ZOI)	37%	27% ⁽¹⁾	-	-
Transportable Ice Condenser Debris	37%	-	-	-

(1) This includes pieces of tape < 4 in and ≥ 4 in.

Recirculation Debris Transport

The following describes the methodology that was used to determine the quantity of debris that was calculated to have been transported to the main strainer and remote strainer during sump recirculation.

Since the various types and sizes of debris will be transported differently during the blowdown, washdown, and pool fill phases, the distribution of this debris at the start of recirculation can vary widely. Insulation debris on the pool floor would be scattered around by the break, spray, and ice condenser flow as the pool fills. Debris in upper containment would be washed down through the refueling canal drains by the spray flow. Debris trapped in the ice baskets would be washed down through each of the ice condenser drains by the melted ice flow. Given the high initial ice melt, it was assumed that all of the latent debris in the ice baskets and the debris blown up into the ice baskets would be washed down very quickly and would be scattered around inside the crane wall before recirculation is initiated.

The following figures graphically show the debris distribution for the various types/sizes of debris. Figure 3e1-9 shows the distribution of fine debris and unqualified coatings, and Figure 3e1-10 shows the distribution for small and large piece debris.

Figure 3e1-9 Distribution of Fine Debris and Unqualified Coatings in the Loop Compartment and Annulus at Start of Recirculation

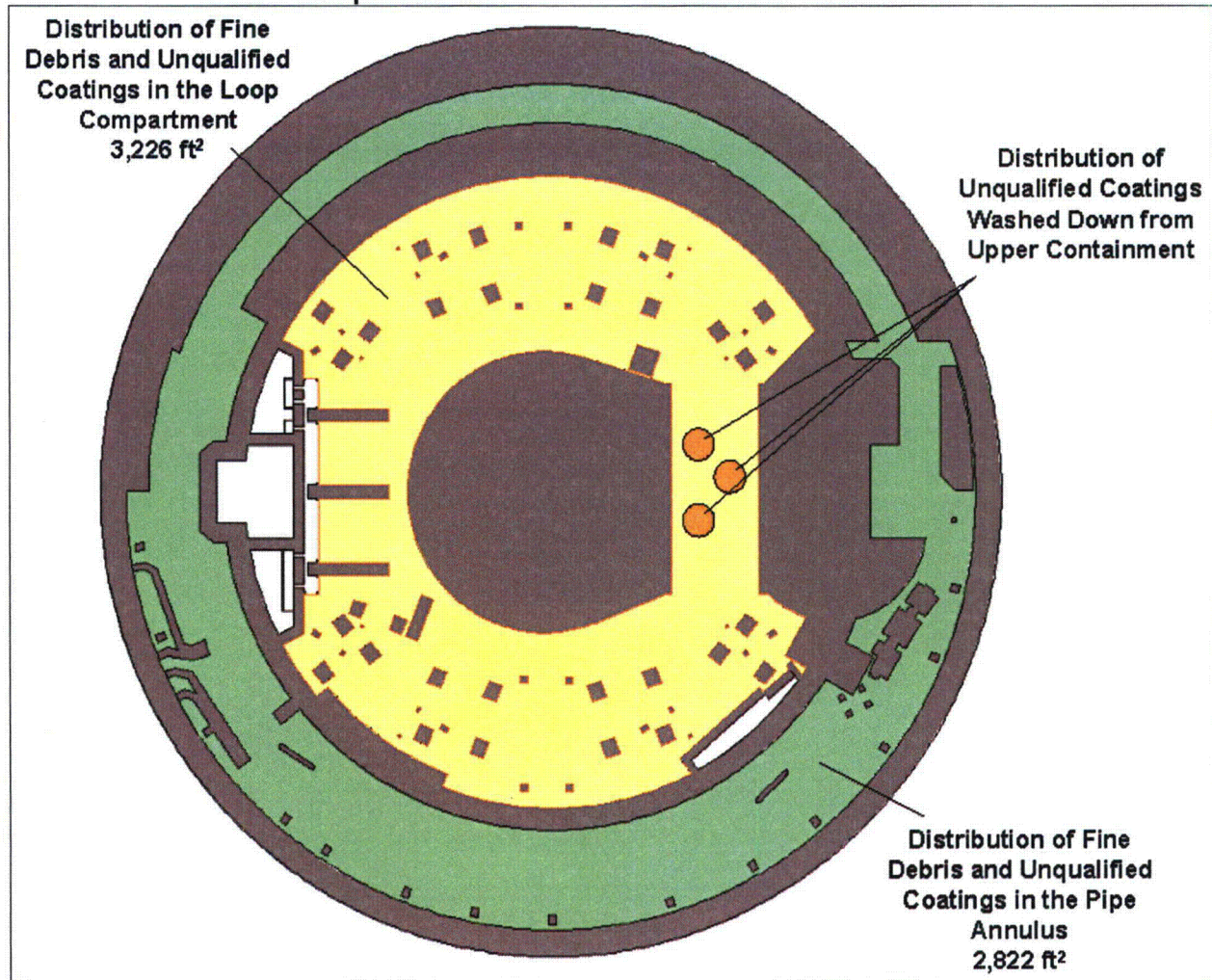
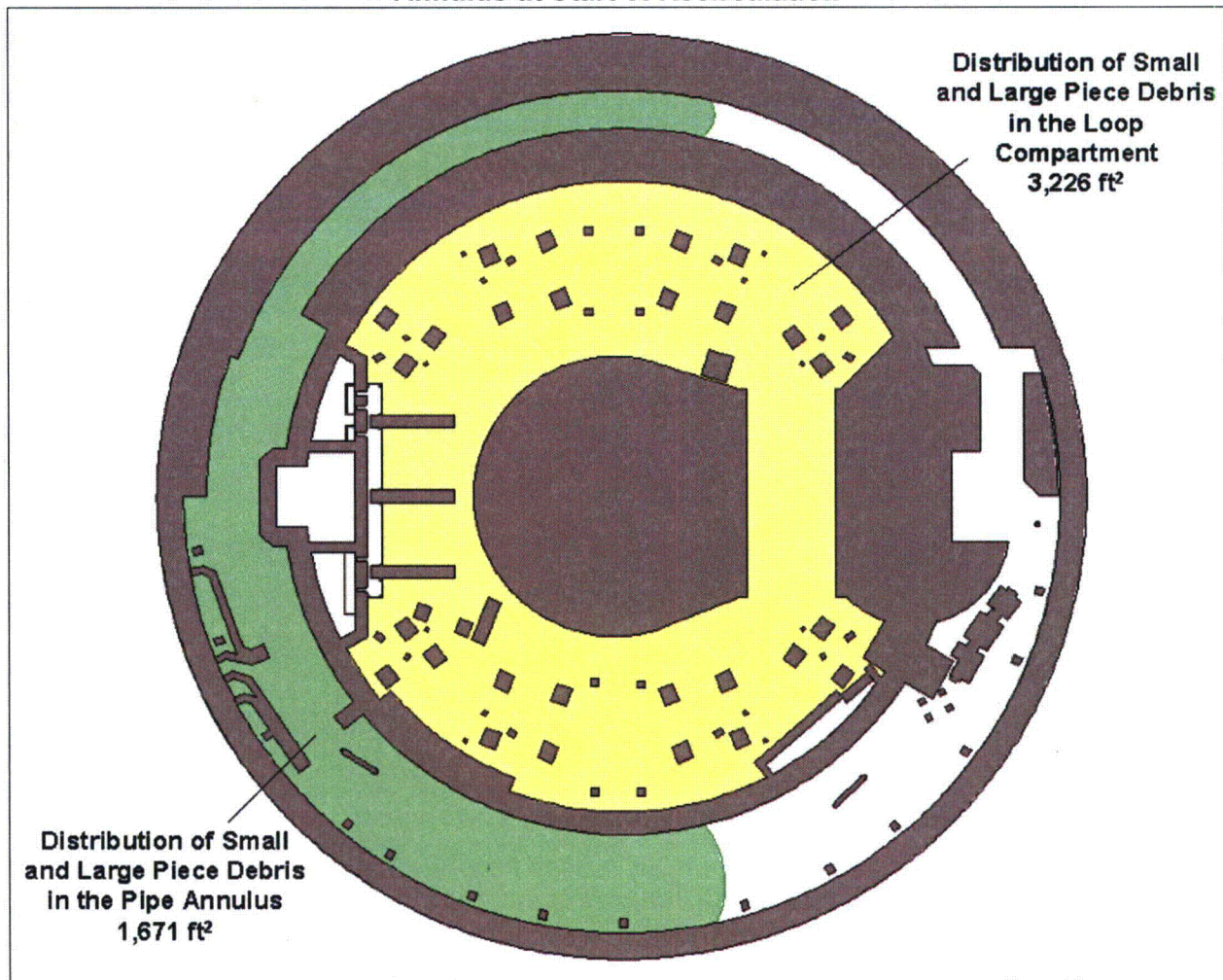


Figure 3e1-10 Distribution of Small and Large Piece Debris in the Loop Compartment and Annulus at Start of Recirculation



The following steps were taken to determine what percentage of a particular type of debris could be expected to transport through the containment pool to the sump strainers.

- Colored velocity and TKE maps indicating regions of the pool through which a particular type of debris could be expected to transport, were generated from the Flow-3D[®] results in the form of bitmap files.
- The bitmap files were overlaid on the initial debris distribution plots and imported into AutoCAD[®] with the appropriate scaling factor to convert the length scale of the color maps to feet.
- Within the debris distribution areas, closed polylines were drawn around the contiguous areas where velocity or TKE was high enough that debris could be carried in suspension or tumbled along the floor to the sump strainers.

- The areas within the closed polylines were determined using an AutoCAD® querying feature.
- The combined area within the polylines was compared to the debris distribution area.
- The percentage of a particular debris type that would transport to each sump strainer was estimated based on the above comparison.

Plots showing the TKE and the velocity magnitude in the pool were generated for each case to determine areas where specific types of debris would be transported. These are shown in Figures 3e1-11 through 3e1-16, below. The limits on the plots were set according to the minimum TKE or velocity metrics necessary to move each type of debris. The overlying yellow areas represent regions where the debris would be suspended, and the red areas represent regions where the debris would be tumbled along the floor. The yellow TKE portion of the plots is a three-dimensional representation of the TKE. The velocity portion of the plots represents the velocity magnitude just above the floor level (1.5 in), where tumbling of sunken debris could occur. Directional flow vectors were included in the plots to determine whether debris in certain areas would be transported to the sump strainer or transported to quieter regions of the pool where it could settle to the floor.

Two recirculation pool CFD simulations were performed for each of the Loop 2 and Loop 4 break locations. The first run used a flow split based on clean strainer conditions, and the second run used a flow split based on the main strainer being 90% blocked by debris. The results of the clean strainer CFD run was used to determine the maximum transport to the main strainer since the flow rate to the main strainer is highest when the strainers are clean. The results of the 90% blocked main strainer CFD run was used to determine the maximum transport to the remote strainer since the flow rate to the remote strainer is highest when the main strainer is blocked by debris. Since the Loop 4 break was determined to be the bounding break for both DEGB and DGBS (refer to the response to Information Item 3.a), all subsequent information presented in this response section will be associated with the Loop 4 break.

For the clean main strainer condition, Figure 3e1-11 shows the direction of pool flow colored by the velocity magnitude. The vectors shown in this plot are unit vectors in the x-y directions, where one vector is displayed for every 16 cells. Figure 3e1-12 shows the relative strength of the TKE on the surface of the pool for the Loop 4 break.

Figure 3e1-11 Vectors Showing Pool Flow Direction for Loop 4 Break with Clean Main Strainer

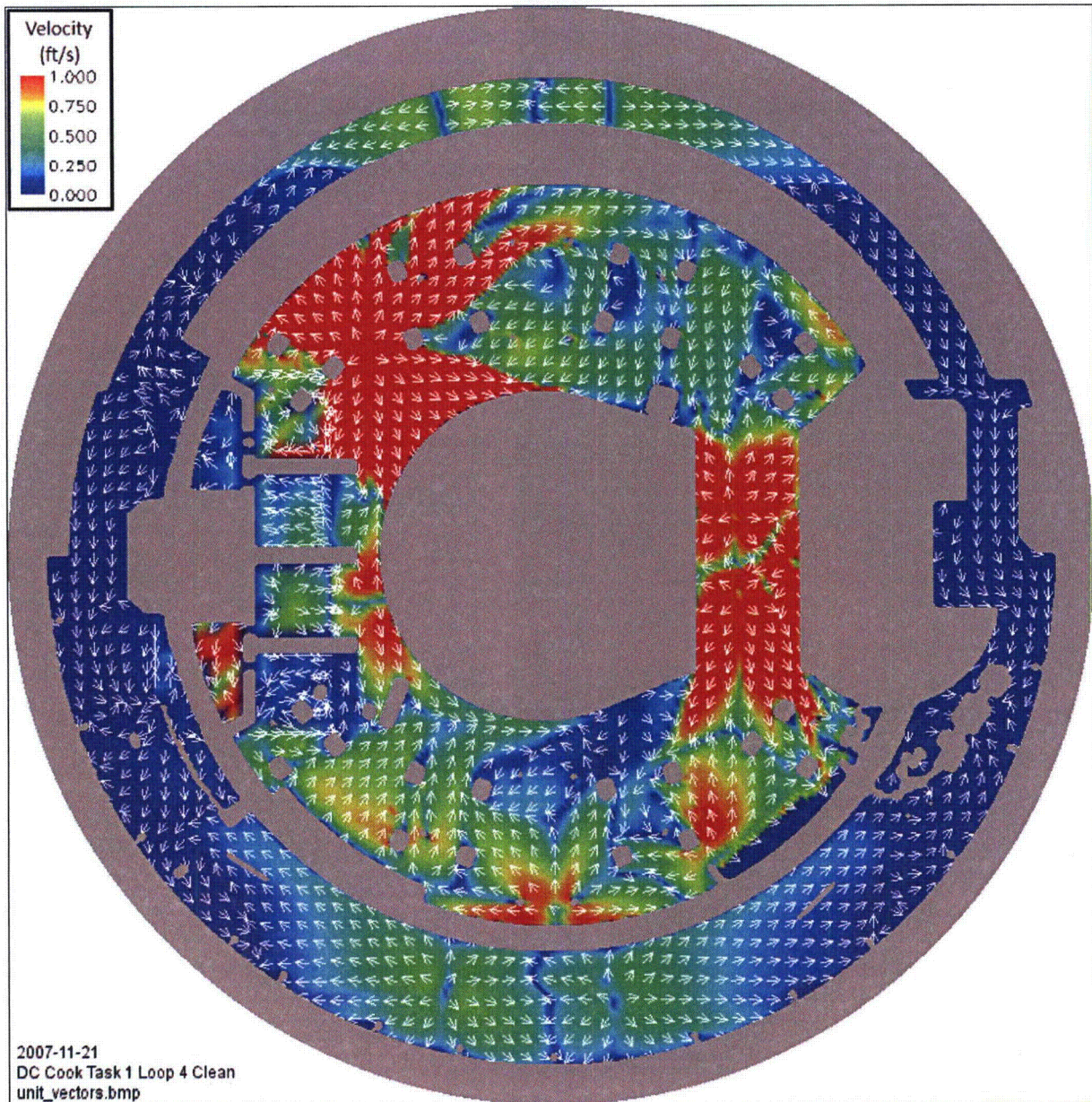


Figure 3e1-12 Relative TKE at Pool Surface Showing General Areas of Turbulence for Loop 4 Break with Clean Main Strainer

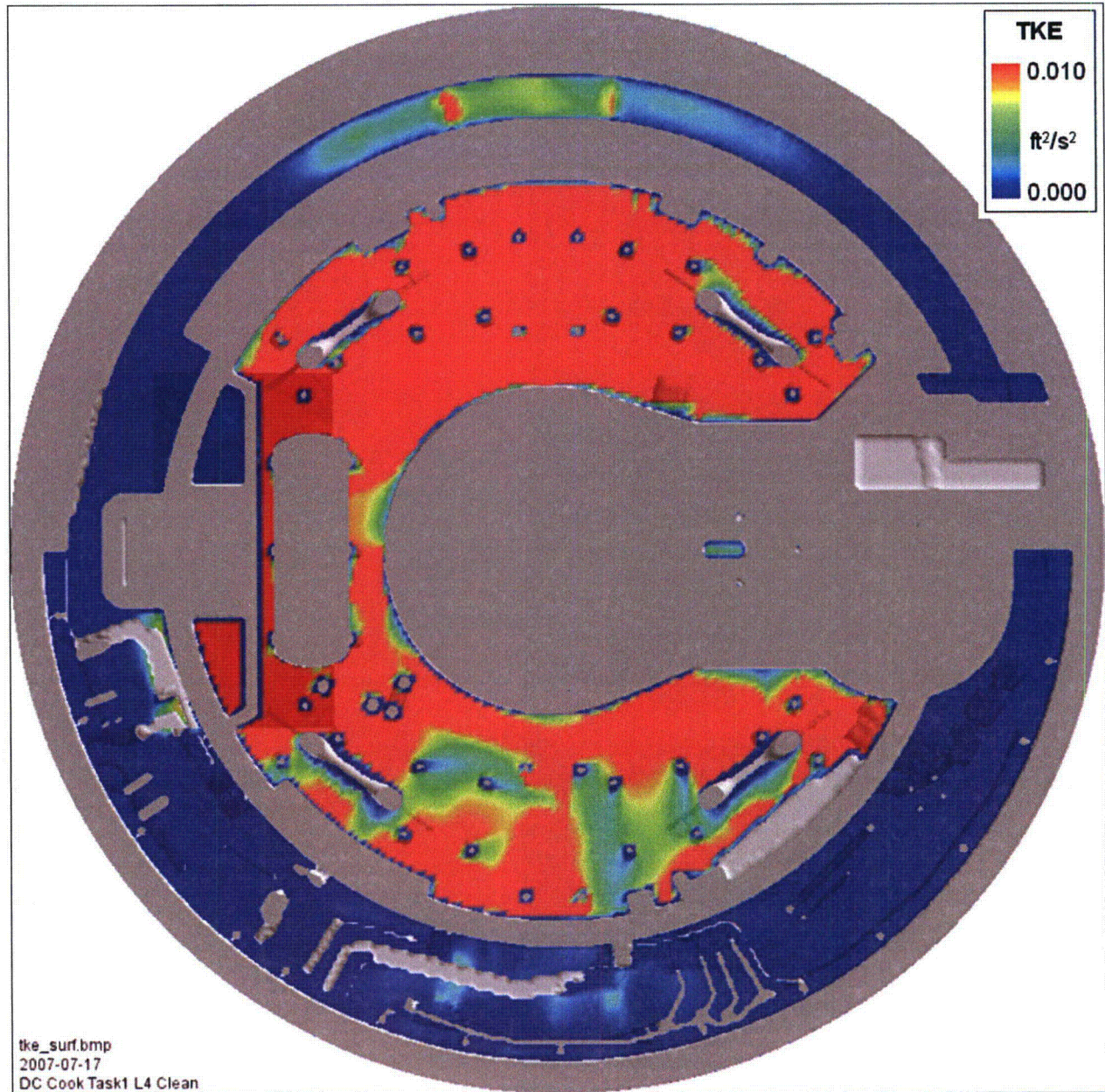
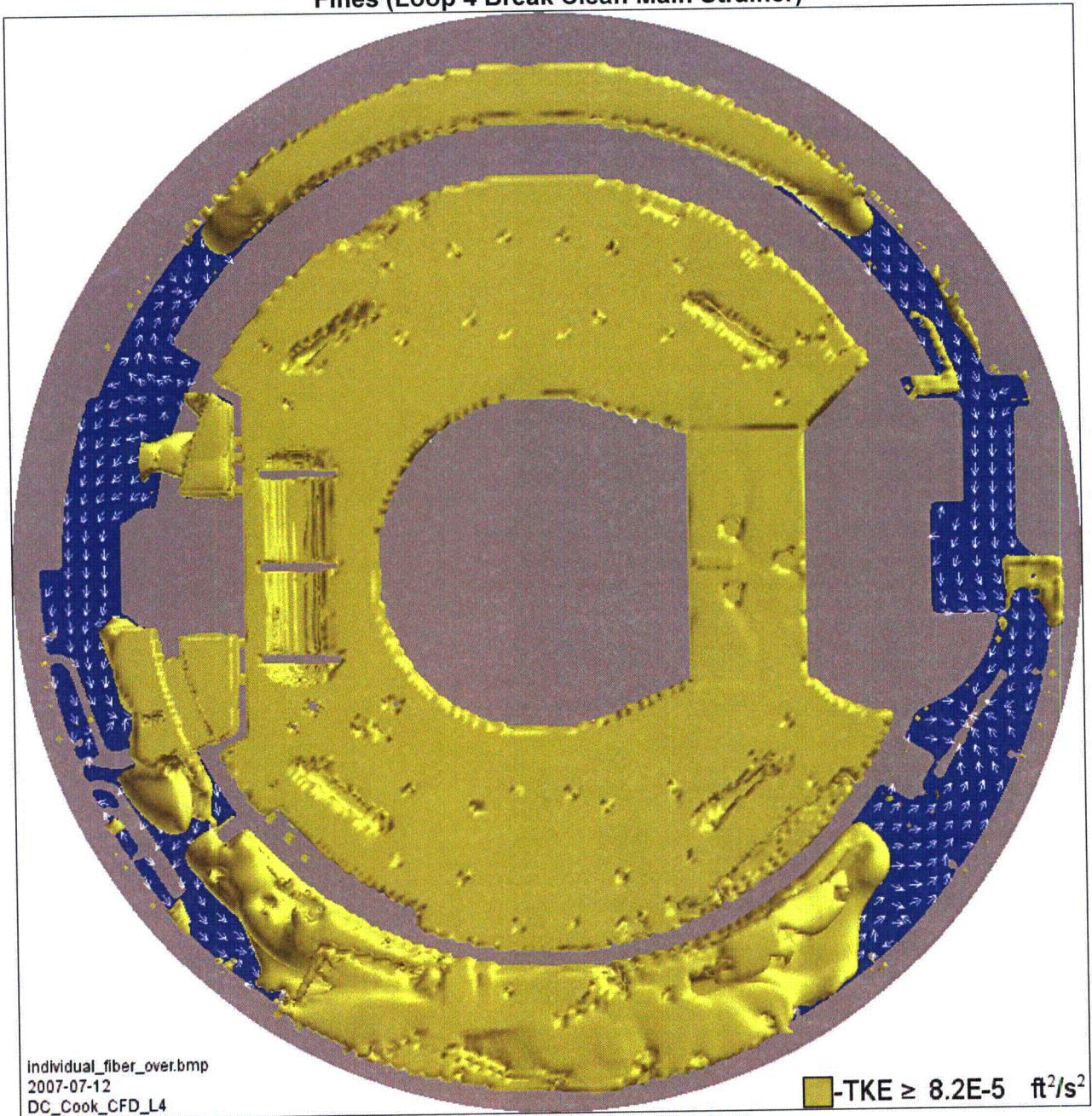


Figure 3e1-13 provides an example of the type of figures that were developed for determination of the areas where transport, tumbling, or suspension of a particular debris source would be expected to occur as described previously in this section.

Figure 3e1-13 TKE with Limit Set at Suspension of Individual Fibers and Particulate Fines (Loop 4 Break Clean Main Strainer)



For the 90% blocked main strainer condition, Figure 3e1-14 shows the direction of pool flow colored by the velocity magnitude. The vectors shown in this plot are unit vectors in the x-y directions, where one vector is displayed for every 16 cells. Figure 3e1-15 shows the relative strength of the TKE on the surface of the pool for the Loop 4 break (for 90% blocked main strainer conditions).

Figure 3e1-14 Vectors Showing Pool Flow Direction for Loop 4 Break with 90% Blocked Main Strainer

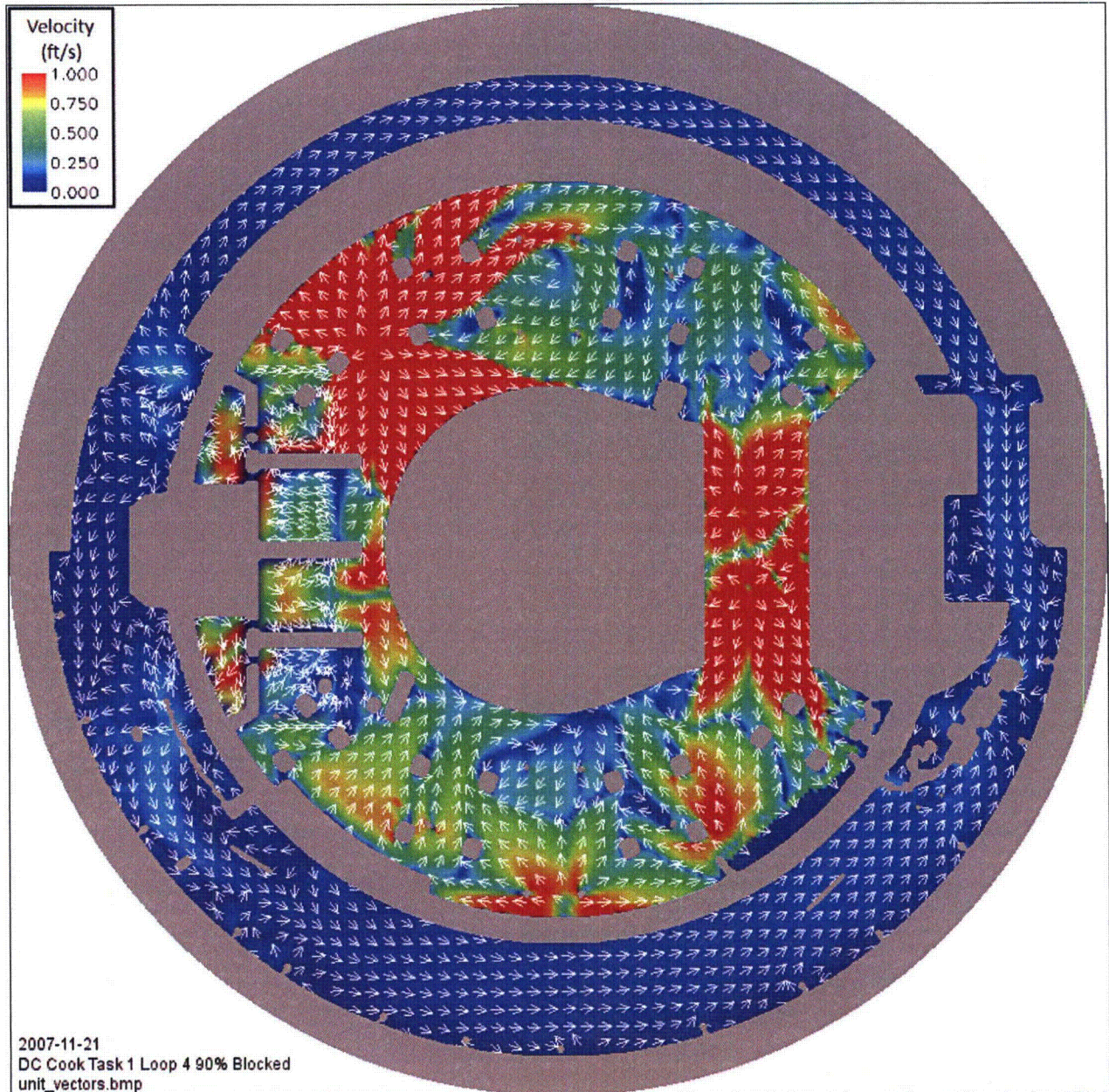


Figure 3e1-15 Relative TKE at Pool Surface Showing General Areas of Turbulence for Loop 4 Break with 90% Blocked Main Strainer

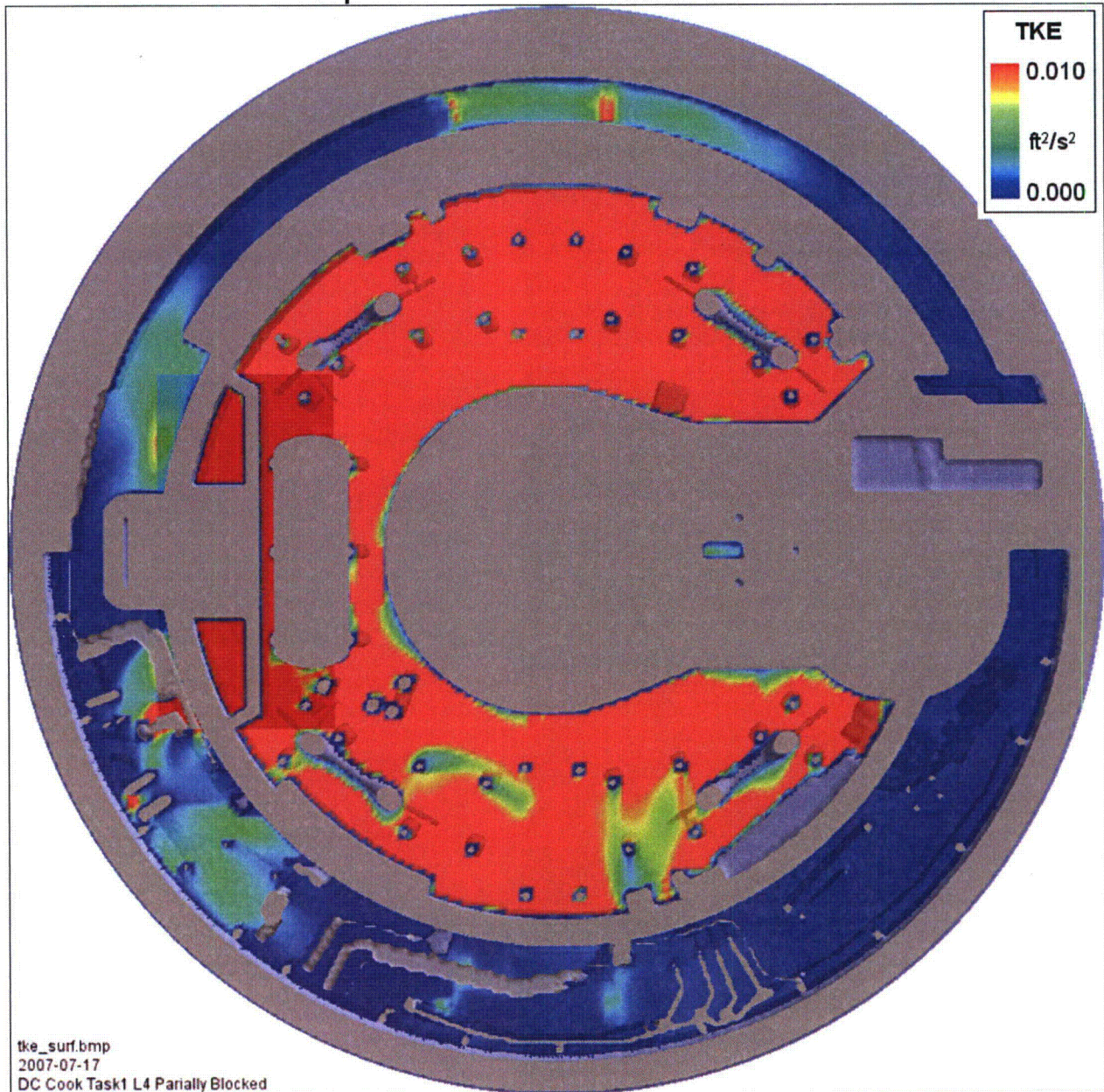
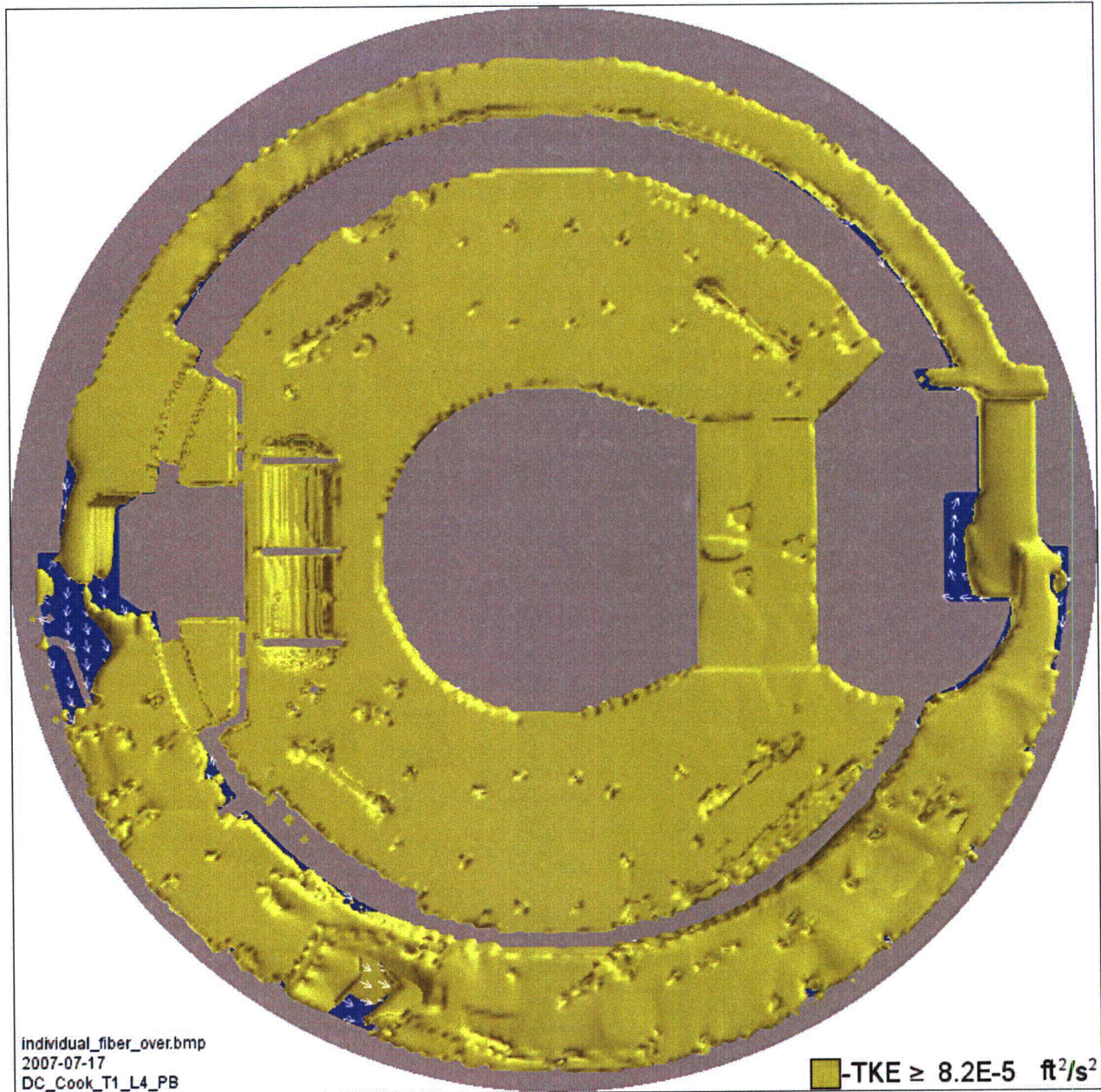


Figure 3e1-16 provides the TKE information associated with latent fibers and particulate fines for the Loop 4 break, 90% blocked main strainer case.

Figure 3e1-16 TKE with Limit Set at Suspension of Individual Fibers and Particulate Fines (Loop 4 Break 90% Blocked Main Strainer)



The overall debris transport results are provided in the response to Information Item 3.e.6.

I&M Response to Information Item 3.e.2

No deviations were taken to the approved guidance for the performance of the debris transport calculation.

I&M Response to Information Item 3.e.4

The DIs installed at CNP in support of the corrective actions to resolve GL 2004-02, as more fully discussed in the response to Information Item 3.j, "Screen Modification Package," were installed to protect flow paths necessary for the recirculation function. These DIs were installed at the drain openings for the CEQ fan rooms and on the loop compartment side of flood-up overflow wall holes. No DIs were installed to specifically limit debris transport to either the main or remote strainer. I&M performed a rigorous development of the flow characteristics associated with the DI installed at the flood-up overflow because it is of significant size and has the potential to significantly impact the pool fill and recirculation debris transport CFD analyses. The results of the analysis were input to the CFD model for both pool fill and recirculation. This modeling effort is described below.

Modeling the Flood-Up Overflow Wall DI

The DI in front of the flood-up overflow wall could not be accurately incorporated into the CFD model by using the CAD geometry unless a very fine mesh resolution was used. Therefore, the DI was modeled directly in Flow-3D[®] using a series of two-dimensional baffles, which define the front, sides, and top of the DI. The DI is made of 1/2 in stainless steel plate that is perforated with 1/2 in diameter holes. The hole spacing gives an overall porosity of approximately 40%.

For the recirculation pool CFD model, the DI was conservatively assumed to be completely blocked by debris. This is conservative since it increases the overall flow over the top of the DI, which increases the potential for small piece debris to transport over the DI, through the annulus, and to the remote strainer.

For the pool fill CFD model, the fraction of fine debris transported to the annulus during the initial pool fill stage would be reduced if the DI was completely blocked. Therefore, the DI was modeled as a porous plate with a defined loss coefficient until the water level reached 3 ft above the floor (a level slightly higher than the top of the DI). At this point, the CFD run was restarted and the DI was modeled as being completely blocked by debris in order to conservatively determine the maximum amount of small piece debris that could be washed over the top of the DI.

To define the DI correctly, it was necessary to determine the pressure loss coefficient. In addition to the porosity, Flow-3D[®] accepts two parameters (KBAF1 and KBAF2) for defining the flow losses across a porous baffle as shown in the following equation:

$$\Delta p = \frac{\rho}{g_c} \cdot (KBAF1 \cdot u + 0.5 \cdot KBAF2 \cdot u|u|)$$

Equation 19

where:

Δp = pressure drop across the baffle (lb_f/ft^2)
 ρ = density of the fluid (lb_m/ft^3)
 u = fluid velocity (ft/s) through the baffle
 $KBAF1$ = linear component of flow loss (ft/s)
 $KBAF2$ = quadratic component of flow loss (unitless)

In Chapter 8-2 of the Handbook of Hydraulic Resistance (Reference 149), values of an overall loss coefficient, ζ , are tabulated for perforated plates with various values of porosity (\bar{f}), Reynolds number (Re), and plate thickness divided by the hydraulic diameter (l/d_h). ζ is defined as follows:

$$\zeta \equiv \frac{\Delta p}{\rho w_1^2 / 2} \quad \text{Equation 20}^1$$

where:

ζ = overall loss coefficient
 Δp = pressure loss across the perforated plate
 ρ = fluid density
 w_1 = velocity in front of the perforated plate

In order for ζ to be unitless, it was necessary to include a factor of g_c in the equation above, which yields:

$$\zeta \equiv \frac{\Delta p \cdot g_c}{\rho w_1^2 / 2} = \frac{\text{lb}_f \cdot \left(\frac{\text{ft}}{\text{s}^2} \cdot \frac{\text{lb}_m}{\text{lb}_f} \right)}{\frac{\text{lb}_m}{\text{ft}^3} \cdot \frac{\text{ft}^2}{\text{s}^2}} = \text{unitless} \quad \text{Equation 21}$$

Rearranging Equation to solve for Δp :

$$\Delta p = 0.5 \cdot \zeta \cdot \frac{\rho}{g_c} \cdot w_1^2 \quad \text{Equation 22}$$

Since w_1 is the velocity of the fluid in front of the baffle, it was necessary to adjust it by the porosity of the baffle, giving the velocity through the baffle, w_0 :

¹ From Page 2 in the Handbook of Hydraulic Resistance: "The values of the local resistance coefficients given in this handbook assume, except for special cases, uniform velocity distribution in the inlet section of the component. Such conditions are usually observed following a smooth inlet nozzle and for steady-state flows. In the case of unsteady-state motion of liquid, the local resistance leads to the loss of flow stability, causing in it the formation of the unsteady-state eddies for the creation of which a certain energy is spent."

$$w_0 = \frac{w_1}{\bar{f}} \quad \text{Equation 23}$$

where \bar{f} is the porosity of the baffle. The velocity w_0 calculated in Equation 23 is analogous to u from Equation 19. Therefore:

$$\Delta p = 0.5 \cdot \zeta \cdot \frac{\rho}{g_c} \cdot (w_0 \cdot \bar{f})^2 \quad \text{Equation 24}$$

$$0.5 \cdot \zeta \cdot \frac{\rho}{g_c} \cdot (w_0 \cdot \bar{f})^2 = \frac{\rho}{g_c} \cdot (KBAF1 \cdot w_0 + 0.5 \cdot KBAF2 \cdot w_0^2) \quad \text{Equation 25}$$

$$\zeta = \frac{2KBAF1 + KBAF2 \cdot w_0}{w_0 \cdot \bar{f}^2} \quad \text{Equation 26}$$

and assuming the KBAF1 term is negligible², Equation reduces to:

$$KBAF2 = \zeta \cdot \bar{f}^2 \quad \text{Equation 27}$$

In the Handbook of Hydraulic Resistance, Diagram 8-1 is applicable for thin perforated plates with sharp edged orifices in the turbulent regime, $l/d_h = 0-0.015$, and $Re = w_0 d_h / \nu \geq 10^5$. Diagram 8-2 is for beveled orifices, so it is not applicable to the CNP DI. Diagram 8-3 is for perforated thick plates in the turbulent regime, $l/d_h > 0.015$, and $Re = w_0 d_h / \nu \geq 10^5$. Diagram 8-4 is for rounded orifices, so it is not applicable to the CNP DI. Diagram 8-5 is for perforated plate with different shapes of orifice edges in the laminar and transitional regimes, $Re = w_0 d_h / \nu < 10^4-10^5$.

The hydraulic diameter of the DI was calculated as follows:

$$l/d_h \equiv \frac{0.5in}{0.5in} = 1.0 \quad \text{Equation 28}$$

Therefore, since l/d_h is greater than 0.015, Diagram 8-1 is not applicable.

For the Reynolds number, it was necessary to calculate the velocity through the baffle, w_0 , and the kinematic viscosity, ν . For a temperature of 160°F, the kinematic viscosity can be calculated as follows:

$$\nu \equiv \frac{\mu}{\rho} \cdot g_c = \frac{8.32 \times 10^{-6} lb_f \cdot s / ft^2}{61.0 lb_m / ft^3} \cdot 32.2 ft / s^2 \cdot lb_m / lb_f = 4.39 \times 10^{-6} ft^2 / s \quad \text{Equation 29}$$

² From Page 3 in the Handbook of Hydraulic Resistance: "At very low Reynolds number ($Re \leq 25$), the second term... can be neglected, while at very large Re [$Re \geq 10^5$] one can neglect the first term." The effect of the two K-factor terms is approximately equal at $Re \approx 10^4$.

The velocity through the DI at CNP was more difficult to calculate since the velocity changes over time. A total of approximately 15,000 gpm of break and spray flow lands inside the crane wall plus a large amount of ice condenser flow, which decreases over time (approximately 13,600 gpm for the first five minutes). The perimeter of the DI is approximately 30 ft, and the porosity is approximately 40%. Therefore, at a water level of 3 in above the floor, assuming that half of the flow goes through the DI and the other half through the main strainer, the velocity through the DI and the Reynolds number were calculated as follows:

$$w_0 \equiv \frac{Q}{A} = \frac{14,300 \text{ gal} / \text{min} \cdot 231 \text{ in}^3 / \text{gal} \cdot 1 \text{ ft}^3 / (12 \text{ in})^3 \cdot 1 \text{ min} / 60 \text{ s}}{30 \text{ ft} \cdot 0.25 \text{ ft} \cdot 0.40} = 11 \text{ ft} / \text{s} \quad \text{Equation 30}$$

$$\text{Re} \equiv \frac{w_0 d_h}{\nu} = \frac{11 \text{ ft} / \text{s} \cdot 0.5 \text{ in} \cdot 1 \text{ ft} / 12 \text{ in}}{4.39 \times 10^{-6} \text{ ft}^2 / \text{s}} = 1 \times 10^5 \quad \text{Equation 31}$$

Since the Reynolds number is approximately 1×10^5 , Diagram 8-3 is the most applicable. This diagram gives a loss coefficient of 5.24. Using Equation 27:

$$KBAF^2 = 5.24 \cdot 0.40^2 = 0.84 \quad \text{Equation 32}$$

If, however, it is considered that the water level has risen to the top of the DI (34 inches) and the ice condenser flow is neglected, then the velocity and Reynolds number are as follows:

$$w_0 \equiv \frac{Q}{A} = \frac{7,500 \text{ gal} / \text{min} \cdot 231 \text{ in}^3 / \text{gal} \cdot 1 \text{ ft}^3 / (12 \text{ in})^3 \cdot 1 \text{ min} / 60 \text{ s}}{30 \text{ ft} \cdot 2.83 \text{ ft} \cdot 0.40} = 0.5 \text{ ft} / \text{s} \quad \text{Equation 33}$$

$$\text{Re} \equiv \frac{w_0 d_h}{\nu} = \frac{0.5 \text{ ft} / \text{s} \cdot 0.5 \text{ in} \cdot 1 \text{ ft} / 12 \text{ in}}{4.39 \times 10^{-6} \text{ ft}^2 / \text{s}} = 5 \times 10^3 \quad \text{Equation 34}$$

This is clearly outside the applicability of Diagram 8-3, so it is necessary to use Diagram 8-5, which gives the following equation:

$$\zeta \equiv \frac{\Delta p}{\rho w_1^2 / 2} = \frac{\zeta_\phi}{f^2} + \bar{\epsilon}_{0\text{Re}} \cdot \zeta_{qu} \quad \text{Equation 35}$$

where:

ζ_ϕ = the laminar loss coefficient taken from Diagram 8-5

$\bar{\epsilon}_{0\text{Re}}$ = a function of the Reynolds number

ζ_{qu} = the turbulent loss coefficient taken from Diagrams 8-1 through 8-4 as applicable

Using Diagram 8-5, $\bar{\epsilon}_{0Re}$ is equal to approximately 0.75 for this case, and ζ_{ϕ} is interpolated to be approximately 0.09.

As shown previously, Diagram 8-3 gave a value of 5.24 for ζ_{qu} . Therefore, the overall loss coefficient is as follows:

$$\zeta = \frac{\zeta_{\phi}}{\bar{f}^2} + \bar{\epsilon}_{0Re} \cdot \zeta_{qu} = \frac{0.09}{0.40^2} + 0.75 \cdot 5.24 = 4.5 \quad \text{Equation 36}$$

Since KBAF1 is not negligible for this case, the KBAF1 term in Equation can be represented as follows:

$$\frac{\zeta_{\phi}}{\bar{f}^2} = \frac{2KBAF1}{w_0 \cdot \bar{f}^2} \quad \text{Equation 37}$$

$$KBAF1 = \frac{1}{2} \cdot \zeta_{\phi} \cdot w_0 = \frac{1}{2} \cdot 0.09 \cdot 0.5 \text{ ft/s} = 0.02 \text{ ft/s} \quad \text{Equation 38}$$

And the KBAF2 term can be represented as follows:

$$\bar{\epsilon}_{0Re} \cdot \zeta_{qu} = \frac{KBAF2}{\bar{f}^2} \quad \text{Equation 39}$$

$$KBAF2 = \bar{\epsilon}_{0Re} \cdot \zeta_{qu} \cdot \bar{f}^2 = 0.75 \cdot 5.24 \cdot 0.40^2 = 0.63 \quad \text{Equation 40}$$

It can be seen that the two K-factors vary somewhat depending on the specific conditions in the containment pool. To simplify the analysis and to account for the unknowns associated with debris blockage and non-steady state flow losses, which are not accounted for in the above calculations, the losses across the DI were defined by setting KBAF1 equal to 0.0 and KBAF2 equal to 1.0. The porosity of the DI baffles was set to 0.40.

Specific evaluations were not performed for the DIs installed at the drain openings in the CEQ fan rooms. The design criteria for these DIs were that they had to provide a greater flow area than the previously installed drain covers, including the consideration that the DIs could become partially blocked by debris that washes into these rooms. I&M had previously performed calculations to determine the flow rate through these drain lines in support of containment sump pool water level determinations.

I&M Response to Information Item 3.e.5

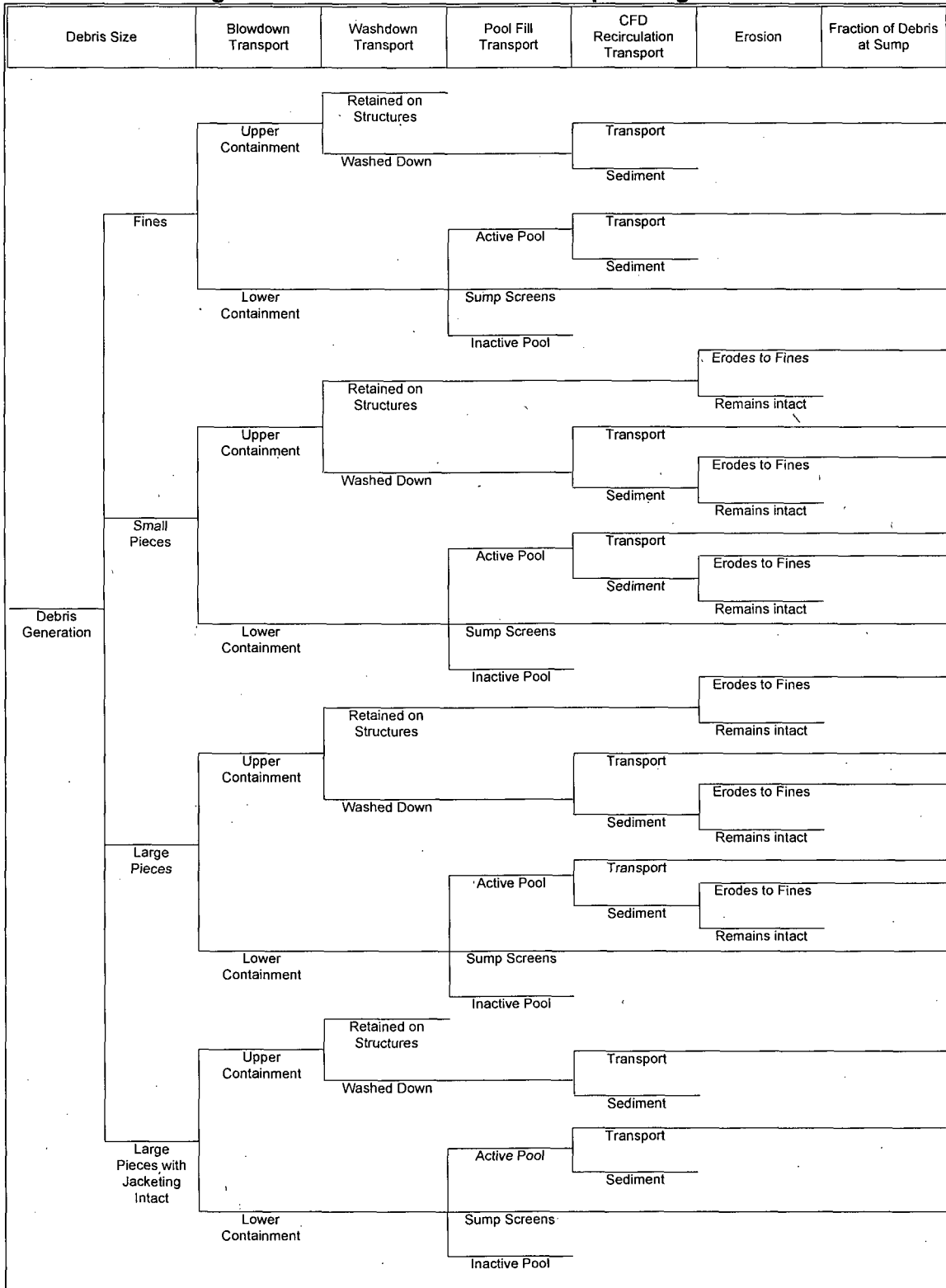
The debris transport calculation does not take any credit for settling of fine debris. See Table 3e6-4 in the response to Information Item 3.e.6.

I&M Response to Information Item 3.e.6

The following approach was used to determine the debris transport fractions and total quantities of each type of debris transported to the strainers.

For each type of debris generated, debris transport logic trees were developed based on the CFD analysis described in the response to Information Item 3.e. These trees were used to determine the total fraction of debris that would reach the main and remote strainers for the postulated cases. Figure 3e6-1 shows the generic debris transport logic tree that was used for this purpose.

Figure 3e6-1 Generic Debris Transport Logic Tree



Tables 3e6-1 through 3e6-10 provide the calculated debris transport fractions and total quantities of each type of debris transported to the main and remote strainers for both pool fill and recirculation for the RCS Loop 4 DEGB and DGBS breaks.

Table 3e6-1 Transport Fraction to Main Strainer at End of Pool Fill for Loop 4 Breaks

Debris Type	Size	Transport Fraction	
RMI	Small Pieces	9%	
	Large Pieces	5%	
Cal-Sil	Fines	32%	
	Small Pieces	Intact	5%
		Eroded to Fines	0%
Marinite	Fines	32%	
	Small Pieces	Intact	5%
		Eroded to Fines	0%
	Large Pieces	Intact	4%
		Eroded to Fines	0%
Min-K	Fines	32%	
Qualified Epoxy	Fines	32%	
Unqualified Epoxy (Inside ZOI)	Fines	32%	
Unqualified Alkyd (Inside ZOI)	Fines	32%	
Unqualified OEM Epoxy (Outside ZOI)	Fines	0%	
Unqualified OEM Alkyd (Outside ZOI)	Fines	0%	
Unqualified Non-OEM Epoxy (Outside ZOI)	Chips	0%	
Unqualified Non-OEM Alkyd (Outside ZOI)	Fines	0%	
Unqualified Cold Galvanizing Compound (Outside ZOI)	Fines	0%	
Latent Fiber (Outside ZOI)	Fines	24%	
Latent Dirt and dust (Outside ZOI)	Fines	24%	
Electromark Labels (Inside ZOI)	Small Pieces	9%	
Electromark Labels (Outside ZOI)	Small Pieces	0%	
Unqualified Labels (Outside ZOI)	Fines	0%	
Flexible Conduit PVC Jacketing (Outside ZOI)	Fines	0%	
Fire Barrier Tape (Inside ZOI)	Fines	32%	
	Small / Large Pieces	9%	
Ice Storage Bag Fibers (Outside ZOI)	Fines	45%	
Ice Storage Bag Liner Shards (Outside ZOI)	Fines	45%	
Pieces of Work Platform Rubber (Outside ZOI)	Fines	45%	

**Table 3e6-2 Overall Transport Fraction to Main Strainer for
Loop 4 Breaks (Pool Fill plus Recirculation)**

Debris Type	Size	Transport Fraction	
RMI	Small Pieces	13%	
	Large Pieces	8%	
Cal-Sil	Fines	44%	
	Small Pieces	Intact	10%
		Eroded to Fines	10%
Marinite	Fines	44%	
	Small Pieces	Intact	10%
		Eroded to Fines	10%
	Large Pieces	Intact	7%
		Eroded to Fines	14%
Min-K	Fines	44%	
Qualified Epoxy	Fines	44%	
Unqualified Epoxy (Inside ZOI)	Fines	44%	
Unqualified Alkyd (Inside ZOI)	Fines	44%	
Unqualified OEM Epoxy (Outside ZOI)	Fines	40%	
Unqualified OEM Alkyd (Outside ZOI)	Fines	14%	
Unqualified Non-OEM Epoxy (Outside ZOI)	Chips	52%	
Unqualified Non-OEM Alkyd (Outside ZOI)	Fines	58%	
Unqualified Cold Galvanizing Compound (Outside ZOI)	Fines	93%	
Latent Fiber (Outside ZOI)	Fines	52%	
Latent Dirt and dust (Outside ZOI)	Fines	52%	
Electromark Labels (Inside ZOI)	Small Pieces	13%	
Electromark Labels (Outside ZOI)	Small Pieces	3%	
Unqualified Labels (Outside ZOI)	Fines	86%	
Flexible Conduit PVC Jacketing (Outside ZOI)	Fines	100%	
Fire Barrier Tape (Inside ZOI)	Fines	44%	
	Small / Large Pieces	13%	
Ice Storage Bag Fibers (Outside ZOI)	Fines	63%	
Ice Storage Bag Liner Shards (Outside ZOI)	Fines	63%	
Pieces of Work Platform Rubber (Outside ZOI)	Fines	63%	

Table 3e6-3 Overall Transport Fraction to Remote Strainer for Loop 4 Breaks

Debris Type	Size	Transport Fraction (90% Blocked Main)	
RMI	Small Pieces	0%	
	Large Pieces	0%	
Cal-Sil	Fines	52%	
	Small Pieces	Intact	0%
		Eroded to Fines	8%
Marinite	Fines	52%	
	Small Pieces	Intact	0%
		Eroded to Fines	8%
	Large Pieces	Intact	0%
		Eroded to Fines	6%
Min-K	Fines	52%	
Qualified Epoxy	Fines	52%	
Unqualified Epoxy (Inside ZOI)	Fines	52%	
Unqualified Alkyd (Inside ZOI)	Fines	52%	
Unqualified OEM Epoxy (Outside ZOI)	Fines	72%	
Unqualified OEM Alkyd (Outside ZOI)	Fines	90%	
Unqualified Non-OEM Epoxy (Outside ZOI)	Chips	0%	
Unqualified Non-OEM Alkyd (Outside ZOI)	Fines	59%	
Unqualified Cold Galvanizing Compound (Outside ZOI)	Fines	35%	
Latent Fiber (Outside ZOI)	Fines	56%	
Latent Dirt and dust (Outside ZOI)	Fines	56%	
Electromark Labels (Inside ZOI)	Small Pieces	47%	
Electromark Labels (Outside ZOI)	Small Pieces	69%	
Unqualified Labels (Outside ZOI)	Fines	40%	
Flexible Conduit PVC Jacketing (Outside ZOI)	Fines	30%	
Fire Barrier Tape (Inside ZOI)	Fines	52%	
	Small / Large Pieces	0%	
Ice Storage Bag Fibers (Outside ZOI)	Fines	42%	
Ice Storage Bag Liner Shards (Outside ZOI)	Fines	42%	
Pieces of Work Platform Rubber (Outside ZOI)	Fines	42%	

Table 3e6-4 on the following page provides a combined total transport fractions for each debris type that is calculated to arrive at the main and remote strainers. Many of these fractions (indicated in bold type) are conservatively greater than 100% of the available debris source.

Table 3e6-4 Combined Transport Fraction to Main and Remote Strainers for Loop 4 Breaks

Debris Type	Size	Transport Fraction (90% Blocked Main)	
RMI	Small Pieces	13%	
	Large Pieces	8%	
Cal-Sil	Fines ⁽¹⁾	96%	
	Small Pieces	Intact	10%
		Eroded to Fines	18%
Marinite	Fines ⁽¹⁾	96%	
	Small Pieces	Intact	10%
		Eroded to Fines	18%
	Large Pieces	Intact	7%
		Eroded to Fines	20%
Min-K	Fines ⁽¹⁾	96%	
Qualified Epoxy	Fines ⁽¹⁾	96%	
Unqualified Epoxy (Inside ZOI)	Fines ⁽¹⁾	96%	
Unqualified Alkyd (Inside ZOI)	Fines ⁽¹⁾	96%	
Unqualified OEM Epoxy (Outside ZOI)	Fines	112%	
Unqualified OEM Alkyd (Outside ZOI)	Fines	104%	
Unqualified Non-OEM Epoxy (Outside ZOI)	Chips	52%	
Unqualified Non-OEM Alkyd (Outside ZOI)	Fines	117%	
Unqualified Cold Galvanizing Compound (Outside ZOI)	Fines	128%	
Latent Fiber (Outside ZOI)	Fines	108%	
Latent Dirt and dust (Outside ZOI)	Fines	108%	
Electromark Labels (Inside ZOI)	Small Pieces	60%	
Electromark Labels (Outside ZOI)	Small Pieces	72%	
Unqualified Labels (Outside ZOI)	Fines	126%	
Flexible Conduit PVC Jacketing (Outside ZOI)	Fines	130%	
Fire Barrier Tape (Inside ZOI)	Fines ⁽¹⁾	96%	
	Small / Large Pieces	13%	
Ice Storage Bag Fibers (Outside ZOI)	Fines	105%	
Ice Storage Bag Liner Shards (Outside ZOI)	Fines	105%	
Pieces of Work Platform Rubber (Outside ZOI)	Fines	105%	

(1) 8% of these fines transport to the reactor cavity (inactive volume) during blowdown transport and are unavailable to transport, thus, less than 100% transport to strainers.

Table 3e6-5 Debris Transported to Main Strainer During Pool Fill for Loop 4 DEGB

Debris Type	Debris Generated	Debris at Strainer
RMI Small Pieces, ft ²	58528	5267.52
RMI Large Pieces, ft ²	19510	975.5
Cal-Sil Fines, lbs	279.9	89.568
Erosion of Cal-Sil Small Pieces to Fines, lbs	232	0
Cal-Sil Small Pieces, lbs	232	11.6
Marinite I Fines, lbs	0.14	0.0448
Erosion of Marinite I Small Pieces to Fines, lbs	0.05	0
Marinite I Small Pieces, lbs	0.05	0.0025
Erosion of Marinite I Large Pieces to Fines, lbs	0.23	0
Marinite I Large Pieces, lbs	0.23	0.0092
Marinite 36 Fines, lbs	1.08	0.3456
Erosion of Marinite 36 Small Pieces to Fines, lbs	0.36	0
Marinite 36 Small Pieces, lbs	0.36	0.018
Erosion of Marinite 36 Large Pieces to Fines, lbs	2.16	0
Marinite 36 Large Pieces, lbs	2.16	0.0864
Min-K, lbs	1.6	0.512
Epoxy Paint (inside ZOI), lbs	216	69.12
Alkyd Paint (inside ZOI), lbs	1.9	0.608
Unqualified OEM Epoxy (outside ZOI), lbs	16.9	0
Unqualified OEM Alkyd (outside ZOI), lbs	74.4	0
Unqualified Non-OEM Epoxy (outside ZOI), lbs	31	0
Unqualified Non-OEM Alkyd (outside ZOI), lbs	3.4	0
Unqualified Cold Galvanizing Compound, lbs	777.5	0
Dirt and dust, lbs	170	40.8
Latent Fiber, ft ³	12.5	3.00
Fire Barrier Tape Fines, ft ²	25.1	8.032
Fire Barrier Tape Small Pieces, ft ²	14.4	1.296
Fire Barrier Tape Large Pieces, ft ²	54.1	4.869
Ice Storage Bag Fibers, ft ³	0.026	0.0117
Ice Storage Bag Liner Shards, ft ³	0.00022	0.000099
Pieces of Work Platform Rubber, ft ³	0.002	0.0009
Electromark Label (inside ZOI), ft ²	0.7	0.063
Electromark Label (outside ZOI), ft ²	39.6	0
Unqualified Labels – Paper, ft ²	0.28	0
Unqualified Labels – Other, ft ²	25.66	0
Flex Conduit PVC Jacketing, ft ²	1.57	0

**Table 3e6-6 Total Debris Transported to Main Strainer During Pool Fill & Recirculation
for Loop 4 DEGB**

Debris Type	Debris Generated	Debris at Strainer
RMI Small Pieces, ft ²	58528	7608.64
RMI Large Pieces, ft ²	19510	1560.8
Cal-Sil Fines, lbs	279.9	123.156
Erosion of Cal-Sil Small Pieces to Fines, lbs	232	23.2
Cal-Sil Small Pieces, lbs	232	23.2
Marinite I Fines, lbs	0.14	0.0616
Erosion of Marinite I Small Pieces to Fines, lbs	0.05	0.005
Marinite I Small Pieces, lbs	0.05	0.005
Erosion of Marinite I Large Pieces to Fines, lbs	0.23	0.0322
Marinite I Large Pieces, lbs	0.23	0.0161
Marinite 36 Fines, lbs	1.08	0.4752
Erosion of Marinite 36 Small Pieces to Fines, lbs	0.36	0.036
Marinite 36 Small Pieces, lbs	0.36	0.036
Erosion of Marinite 36 Large Pieces to Fines, lbs	2.16	0.3024
Marinite 36 Large Pieces, lbs	2.16	0.1512
Min-K, lbs	1.6	0.704
Epoxy Paint (inside ZOI), lbs	216	95.04
Alkyd Paint (inside ZOI), lbs	1.9	0.836
Unqualified OEM Epoxy (outside ZOI), lbs	16.9	6.76
Unqualified OEM Alkyd (outside ZOI), lbs	74.4	10.416
Unqualified Non-OEM Epoxy (outside ZOI), lbs	31	16.12
Unqualified Non-OEM Alkyd (outside ZOI), lbs	3.4	1.972
Unqualified Cold Galvanizing Compound, lbs	777.5	723.075
Dirt and dust, lbs	170	88.4
Latent Fiber, ft ³	12.5	6.5
Fire Barrier Tape Fines, ft ²	25.1	11.044
Fire Barrier Tape Small Pieces, ft ²	14.4	1.872
Fire Barrier Tape Large Pieces, ft ²	54.1	7.033
Ice Storage Bag Fibers, ft ³	0.026	0.01638
Ice Storage Bag Liner Shards, ft ³	0.00022	0.0001386
Pieces of Work Platform Rubber, ft ³	0.002	0.00126
Electromark Label (inside ZOI), ft ²	0.7	0.091
Electromark Label (outside ZOI), ft ²	39.6	1.188
Unqualified Labels – Paper, ft ²	0.28	0.2408
Unqualified Labels – Other, ft ²	25.66	22.0676
Flex Conduit PVC Jacketing, ft ²	1.57	1.57

Table 3e6-7 Total Debris Transported to Remote Strainer for Loop 4 DEGB

Debris Type	Debris Generated	Amount Available to Transport ⁽¹⁾	Actual Debris at Strainer
RMI Small Pieces, ft ²	58528	50919.36	0
RMI Large Pieces, ft ²	19510	17949.2	0
Cal-Sil Fines, lbs	279.9	134.352 ⁽²⁾	133.904
Erosion of Cal-Sil Small Pieces to Fines, lbs	232	208.8	18.56
Cal-Sil Small Pieces, lbs	232	208.8	0
Marinite I Fines, lbs	0.14	0.0784	0.0728
Erosion of Marinite I Small Pieces to Fines, lbs	0.05	0.045	0.004
Marinite I Small Pieces, lbs	0.05	0.045	0
Erosion of Marinite I Large Pieces to Fines, lbs	0.23	0.1978	0.0138
Marinite I Large Pieces, lbs	0.23	0.2139	0
Marinite 36 Fines, lbs	1.08	0.6048	0.5616
Erosion of Marinite 36 Small Pieces to Fines, lbs	0.36	0.324	0.0288
Marinite 36 Small Pieces, lbs	0.36	0.324	0
Erosion of Marinite 36 Large Pieces to Fines, lbs	2.16	1.8576	0.1296
Marinite 36 Large Pieces, lbs	2.16	2.0088	0
Min-K, lbs	1.6	0.896	0.832
Epoxy Paint (inside ZOI), lbs	216	120.96	112.32
Alkyd Paint (inside ZOI), lbs	1.9	1.064	0.988
Unqualified OEM Epoxy (outside ZOI), lbs	16.9	10.14	12.168
Unqualified OEM Alkyd (outside ZOI), lbs	74.4	63.984	66.96
Unqualified Non-OEM Epoxy (outside ZOI), lbs	31	14.88	0
Unqualified Non-OEM Alkyd (outside ZOI), lbs	3.4	1.428	2.006
Unqualified Cold Galvanizing Compound, lbs	777.5	54.425	54.425
Dirt and dust, lbs	170	81.6	81.6
Latent Fiber, ft ³	12.5	6	6
Fire Barrier Tape Fines, ft ²	25.1	14.056	13.052
Fire Barrier Tape Small Pieces, ft ²	14.4	12.528	0
Fire Barrier Tape Large Pieces, ft ²	54.1	47.067	0
Ice Storage Bag Fibers, ft ³	0.026	0.00962	0.00962
Ice Storage Bag Liner Shards, ft ³	0.00022	0.0000814	0.0000814
Pieces of Work Platform Rubber, ft ³	0.002	0.00074	0.00074
Electromark Label (inside ZOI), ft ²	0.7	0.609	0.329
Electromark Label (outside ZOI), ft ²	39.6	38.412	27.324
Unqualified Labels – Paper, ft ²	0.28	0.0392	0.0392
Unqualified Labels – Other, ft ²	25.66	3.5924	3.5924
Flex Conduit PVC Jacketing, ft ²	1.57	0	0

- (1) This column represents the difference between total quantity generated and the quantity delivered to main strainer during pool fill.
- (2) 8% of Cal-Sil fines transport to the reactor cavity (inactive volume) and are subtracted from the debris generated value prior to determining the amount available to transport.

Table 3e6-8 Debris Transported to Main Strainer During Pool Fill for Loop 4 DGBS

Debris Type	Debris Generated	Debris at Strainer
RMI Small Pieces, ft ²	31021	2791.89
RMI Large Pieces, ft ²	10341	517.05
Cal-Sil Fines, lbs	72.5	23.2
Erosion of Cal-Sil Small Pieces to Fines, lbs	46.4	0
Cal-Sil Small Pieces, lbs	46.4	2.32
Marinite I Fines, lbs	0	0
Erosion of Marinite I Small Pieces to Fines, lbs	0	0
Marinite I Small Pieces, lbs	0	0
Erosion of Marinite I Large Pieces to Fines, lbs	0	0
Marinite I Large Pieces, lbs	0	0
Marinite 36 Fines, lbs	0.79	0.2528
Erosion of Marinite 36 Small Pieces to Fines, lbs	0.3	0
Marinite 36 Small Pieces, lbs	0.3	0.015
Erosion of Marinite 36 Large Pieces to Fines, lbs	1.62	0
Marinite 36 Large Pieces, lbs	1.62	0.0648
Min-K, lbs	0	0
Epoxy Paint (inside ZOI), lbs	5.7	1.824
Alkyd Paint (inside ZOI), lbs	1.9	0.608
Unqualified OEM Epoxy (outside ZOI), lbs	16.9	0
Unqualified OEM Alkyd (outside ZOI), lbs	74.4	0
Unqualified Non-OEM Epoxy (outside ZOI), lbs	31	0
Unqualified Non-OEM Alkyd (outside ZOI), lbs	3.4	0
Unqualified Cold Galvanizing Compound, lbs	777.5	0
Dirt and dust, lbs	170	40.8
Latent Fiber, ft ³	12.5	3
Fire Barrier Tape Fines, ft ²	25.1	8.032
Fire Barrier Tape Small Pieces, ft ²	14.4	1.296
Fire Barrier Tape Large Pieces, ft ²	54.1	4.869
Ice Storage Bag Fibers, ft ³	0.026	0.0117
Ice Storage Bag Liner Shards, ft ³	0.00022	0.000099
Pieces of Work Platform Rubber, ft ³	0.002	0.0009
Electromark Label (inside ZOI), ft ²	0.7	0.063
Electromark Label (outside ZOI), ft ²	39.6	0
Unqualified Labels – Paper, ft ²	0.28	0
Unqualified Labels – Other, ft ²	25.66	0
Flex Conduit PVC Jacketing, ft ²	1.57	0

Table 3e6-9 Total Debris Transported to Main Strainer During Pool Fill & Recirculation for Loop 4 DGBS

Debris Type	Debris Generated	Debris at Sump
RMI Small Pieces, ft ²	31021	4032.73
RMI Large Pieces, ft ²	10341	827.28
Cal-Sil Fines, lbs	72.5	31.9
Erosion of Cal-Sil Small Pieces to Fines, lbs	46.4	4.64
Cal-Sil Small Pieces, lbs	46.4	4.64
Marinite I Fines, lbs	0	0
Erosion of Marinite I Small Pieces to Fines, lbs	0	0
Marinite I Small Pieces, lbs	0	0
Erosion of Marinite I Large Pieces to Fines, lbs	0	0
Marinite I Large Pieces, lbs	0	0
Marinite 36 Fines, lbs	0.79	0.3476
Erosion of Marinite 36 Small Pieces to Fines, lbs	0.3	0.03
Marinite 36 Small Pieces, lbs	0.3	0.03
Erosion of Marinite 36 Large Pieces to Fines, lbs	1.62	0.2268
Marinite 36 Large Pieces, lbs	1.62	0.1134
Min-K, lbs	0	0
Epoxy Paint (inside ZOI), lbs	5.7	2.508
Alkyd Paint (inside ZOI), lbs	1.9	0.836
Unqualified OEM Epoxy (outside ZOI), lbs	16.9	6.76
Unqualified OEM Alkyd (outside ZOI), lbs	74.4	10.416
Unqualified Non-OEM Epoxy (outside ZOI), lbs	31	16.12
Unqualified Non-OEM Alkyd (outside ZOI), lbs	3.4	1.972
Unqualified Cold Galvanizing Compound, lbs	777.5	723.075
Dirt and dust, lbs	170	88.4
Latent Fiber, ft ³	12.5	6.5
Fire Barrier Tape Fines, ft ²	25.1	11.044
Fire Barrier Tape Small Pieces, ft ²	14.4	1.872
Fire Barrier Tape Large Pieces, ft ²	54.1	7.033
Ice Storage Bag Fibers, ft ³	0.026	0.01638
Ice Storage Bag Liner Shards, ft ³	0.00022	0.0001386
Pieces of Work Platform Rubber, ft ³	0.002	0.00126
Electromark Label (inside ZOI), ft ²	0.7	0.091
Electromark Label (outside ZOI), ft ²	39.6	1.188
Unqualified Labels – Paper, ft ²	0.28	0.2408
Unqualified Labels – Other, ft ²	25.66	22.0676
Flex Conduit PVC Jacketing, ft ²	1.57	1.57

Table 3e6-10 Total Debris Transported to Remote Strainer for Loop 4 DGBS

Debris Type	Debris Generated	Amount Available to Transport ⁽¹⁾	Actual Debris at Strainer
RMI Small Pieces, ft ²	31021	26988.27	0
RMI Large Pieces, ft ²	10341	9513.72	0
Cal-Sil Fines, lbs	72.5	34.8 ⁽²⁾	34.684
Erosion of Cal-Sil Small Pieces to Fines, lbs	46.4	41.76	3.712
Cal-Sil Small Pieces, lbs	46.4	41.76	0
Marinite I Fines, lbs	0	0	0
Erosion of Marinite I Small Pieces to Fines, lbs	0	0	0
Marinite I Small Pieces, lbs	0	0	0
Erosion of Marinite I Large Pieces to Fines, lbs	0	0	0
Marinite I Large Pieces, lbs	0	0	0
Marinite 36 Fines, lbs	0.79	0.4424	0.4108
Erosion of Marinite 36 Small Pieces to Fines, lbs	0.3	0.27	0.024
Marinite 36 Small Pieces, lbs	0.3	0.27	0
Erosion of Marinite 36 Large Pieces to Fines, lbs	1.62	1.3932	0.0972
Marinite 36 Large Pieces, lbs	1.62	1.5066	0
Min-K, lbs	0	0	0
Epoxy Paint (inside ZOI), lbs	5.7	3.192	2.964
Alkyd Paint (inside ZOI), lbs	1.9	1.064	0.988
Unqualified OEM Epoxy (outside ZOI), lbs	16.9	10.14	12.168
Unqualified OEM Alkyd (outside ZOI), lbs	74.4	63.984	66.96
Unqualified Non-OEM Epoxy (outside ZOI), lbs	31	14.88	0
Unqualified Non-OEM Alkyd (outside ZOI), lbs	3.4	1.428	2.006
Unqualified Cold Galvanizing Compound, lbs	777.5	54.425	54.425
Dirt and dust, lbs	170	81.6	81.6
Latent Fiber, ft ³	12.5	6	6
Fire Barrier Tape Fines, ft ²	25.1	14.056	13.052
Fire Barrier Tape Small Pieces, ft ²	14.4	12.528	0
Fire Barrier Tape Large Pieces, ft ²	54.1	47.067	0
Ice Storage Bag Fibers, ft ³	0.026	0.00962	0.00962
Ice Storage Bag Liner Shards, ft ³	0.00022	0.0000814	0.0000814
Pieces of Work Platform Rubber, ft ³	0.002	0.00074	0.00074
Screw Head, qty	15	15	0
Screw Shanks, qty	5	5	0
Electromark Label (inside ZOI), ft ²	0.7	0.609	0.329
Electromark Label (outside ZOI), ft ²	39.6	38.412	27.324
Unqualified Labels – Paper, ft ²	0.28	0.0392	0.0392
Unqualified Labels – Other, ft ²	25.66	3.5924	3.5924
Flex Conduit PVC Jacketing, ft ²	1.57	0	0

(1) This column represents the difference between total quantity generated and the quantity delivered to main strainer during pool fill.

(2) 8% of Cal-Sil fines transport to the reactor cavity (inactive volume) and are subtracted from the debris generated value prior to determining the amount available to transport.

Additional Figures for Response to Information Item 3.e.1 and 3.e.3.

Figure 3e1-17 TKE and Velocity in the Pool at 220 Seconds - Just Before Restarting to Increase the Break, Spray, and Ice Melt Kinetic Energy (Pool Fill Loop 4 CFD Run)

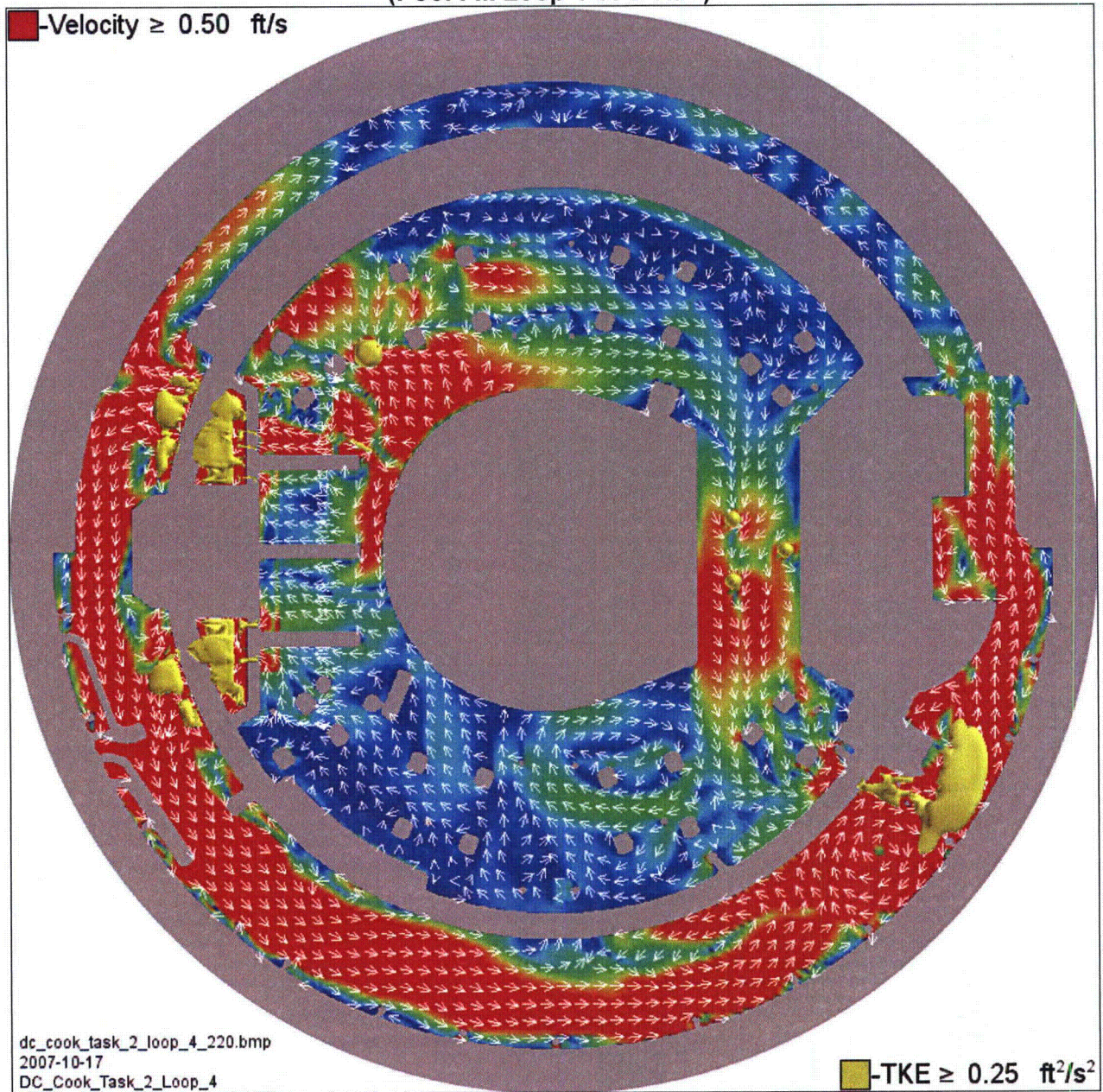


Figure 3e1-18 TKE and Velocity in the Pool at 230 Seconds - Just After Restarting to Increase the Break, Spray, and Ice Melt Kinetic Energy (Pool Fill Loop 4 CFD Run)

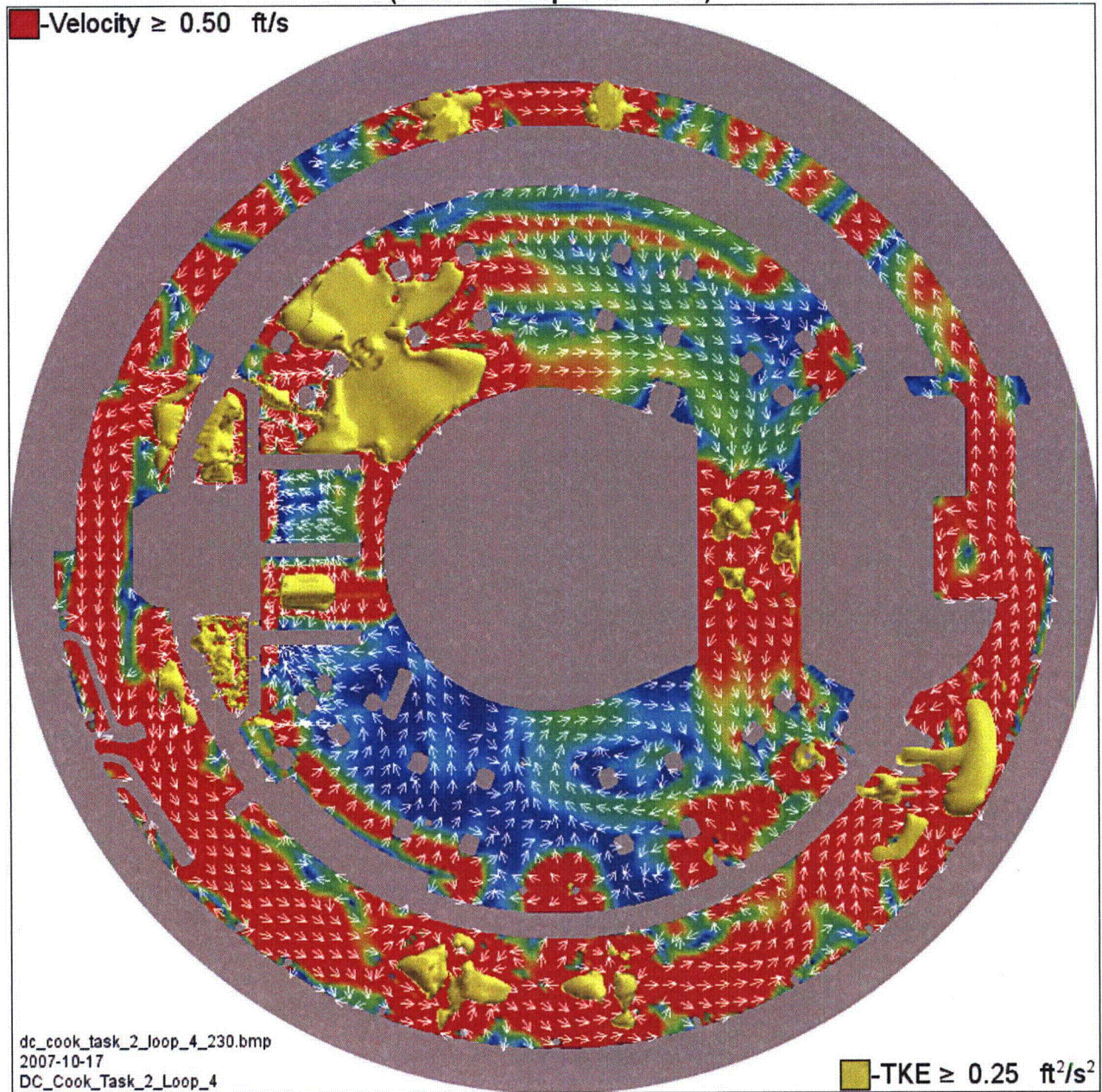


Figure 3e1-19 TKE and Velocity in the Pool at 260 Seconds
(Pool Fill Loop 4 CFD Run)

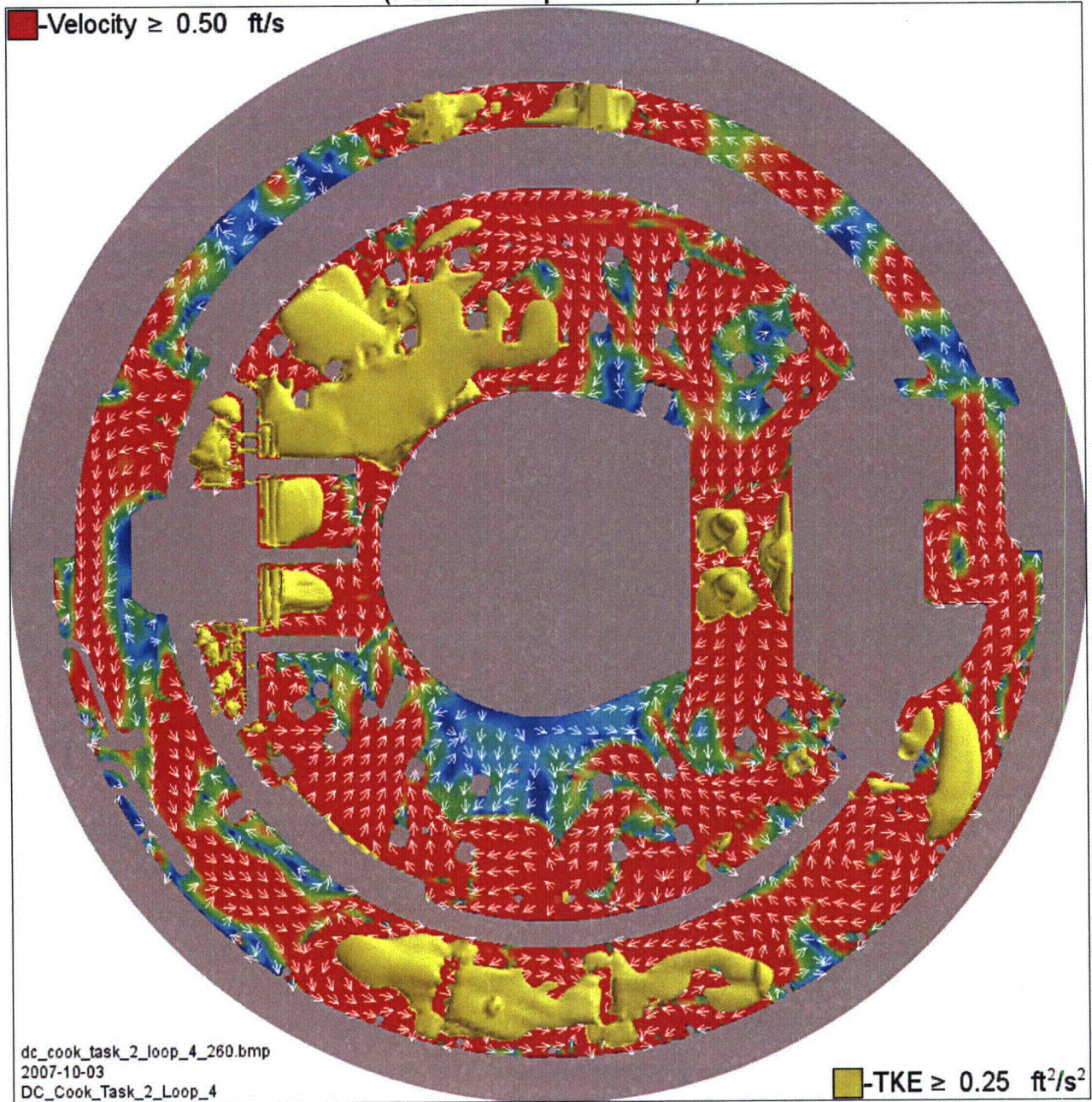


Figure 3e1-20 TKE and Velocity in the Pool at 290 Seconds - Just Before Restarting to Decrease the Ice Melt Flow Rate (Pool Fill Loop 4 CFD Run)

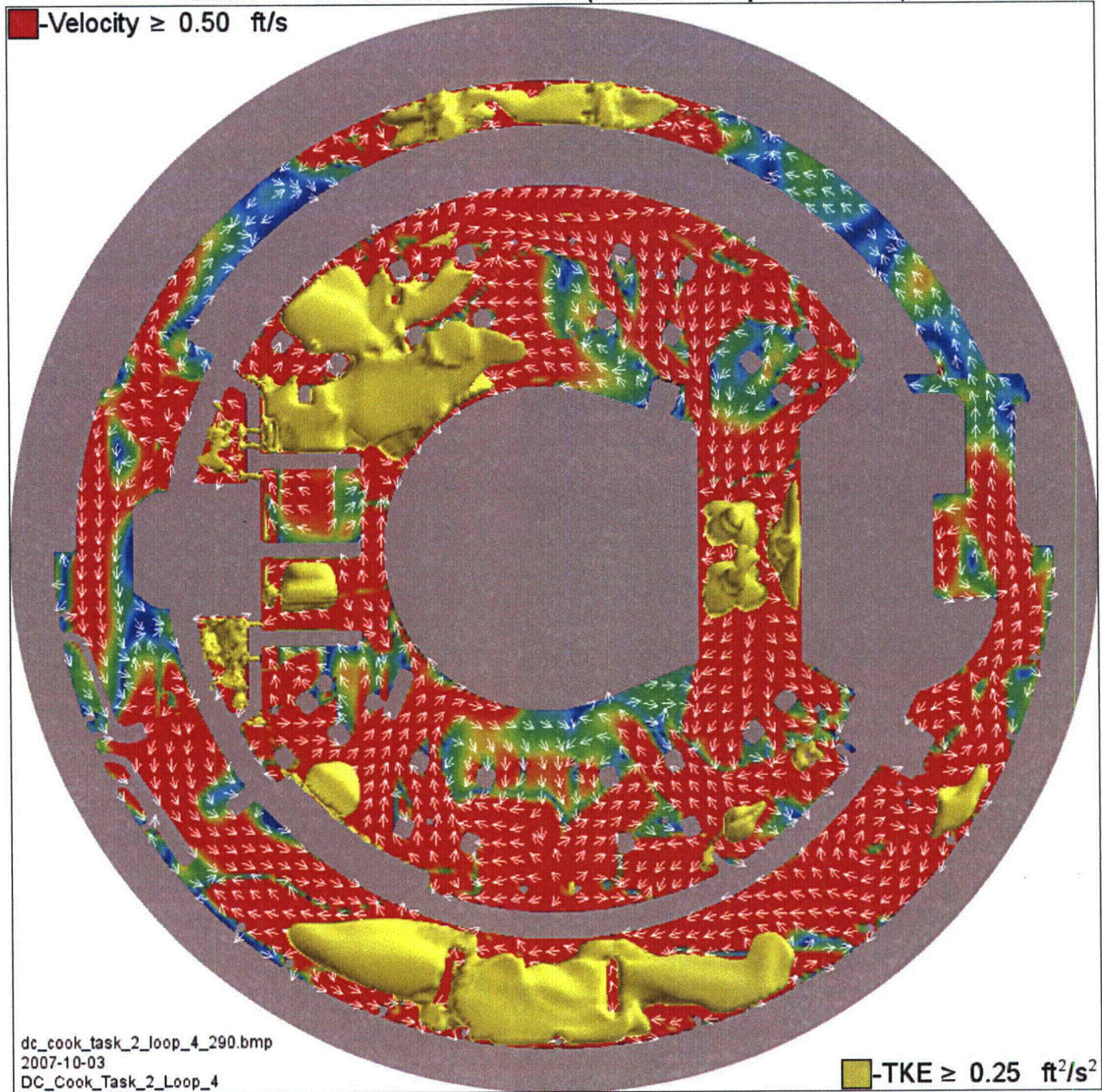


Figure 3e1-21 TKE and Velocity in the Pool at 301 Seconds - Just After Restarting to Decrease the Ice Melt Flow Rate (Pool Fill Loop 4 CFD Run)

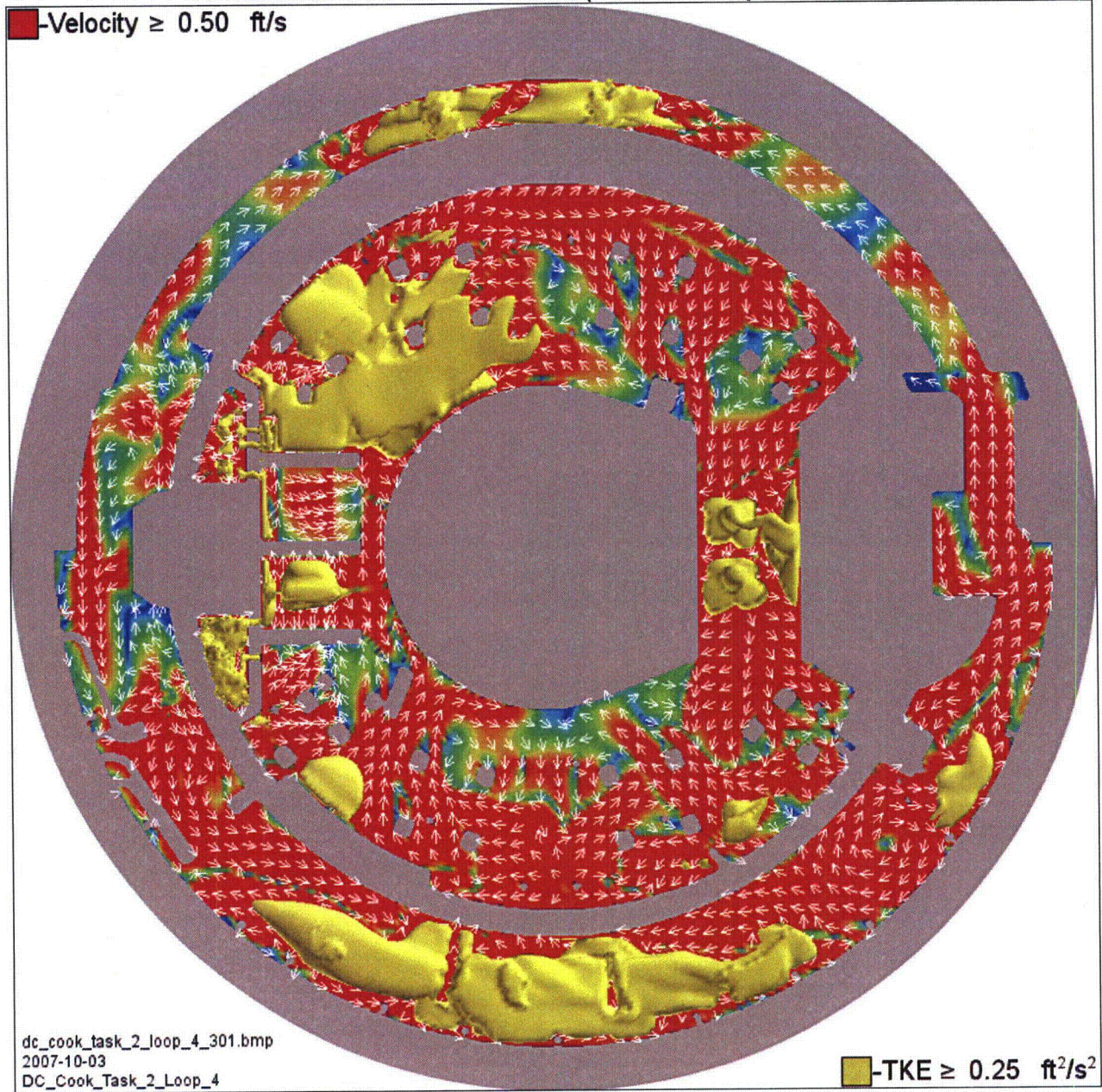


Figure 3e1-22 TKE and Velocity in the Pool at 360 Seconds
(Pool Fill Loop 4 CFD Run)

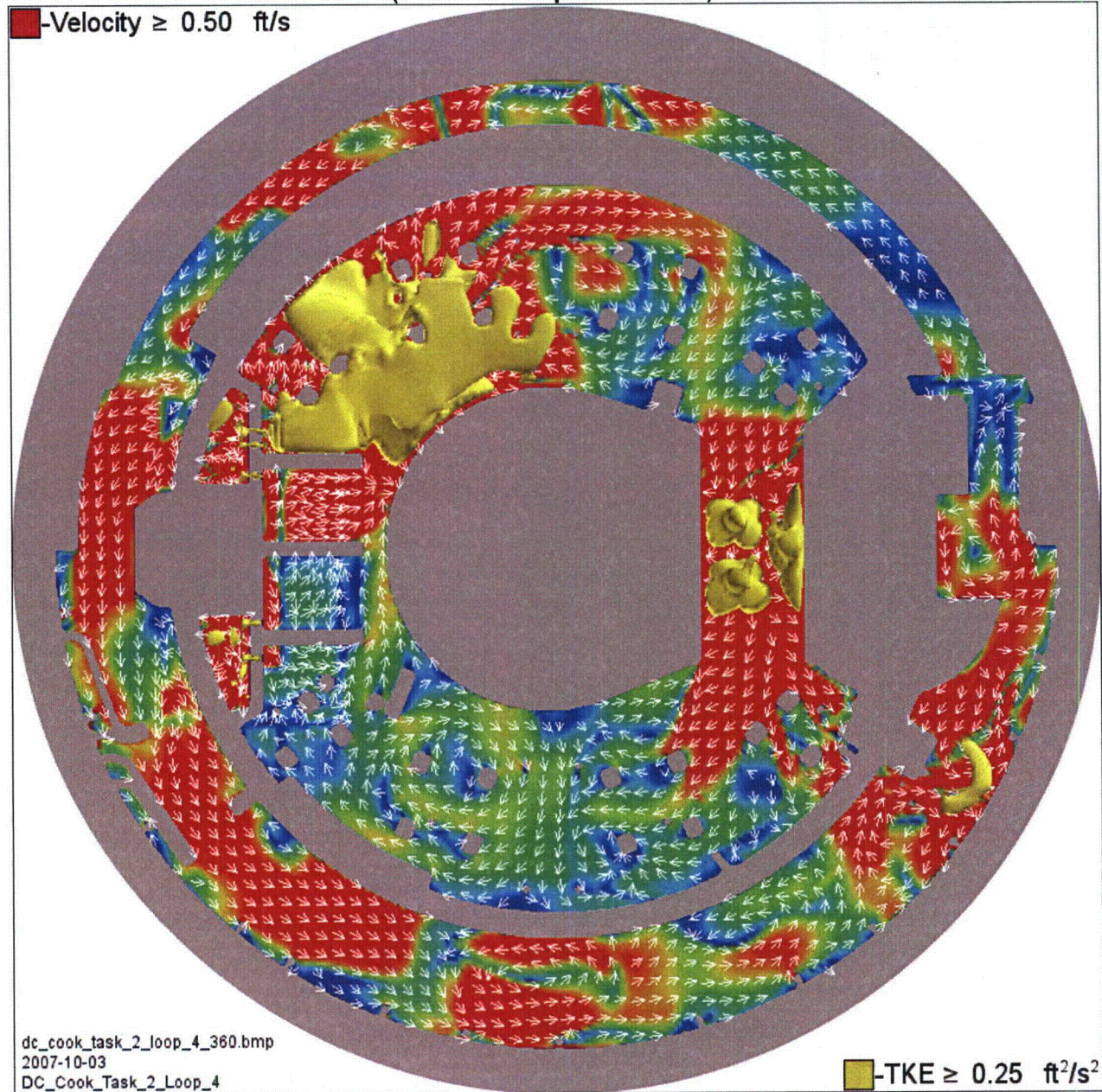


Figure 3e1-23 TKE and Velocity in the Pool at 600 Seconds
(Pool Fill Loop 4 CFD Run)

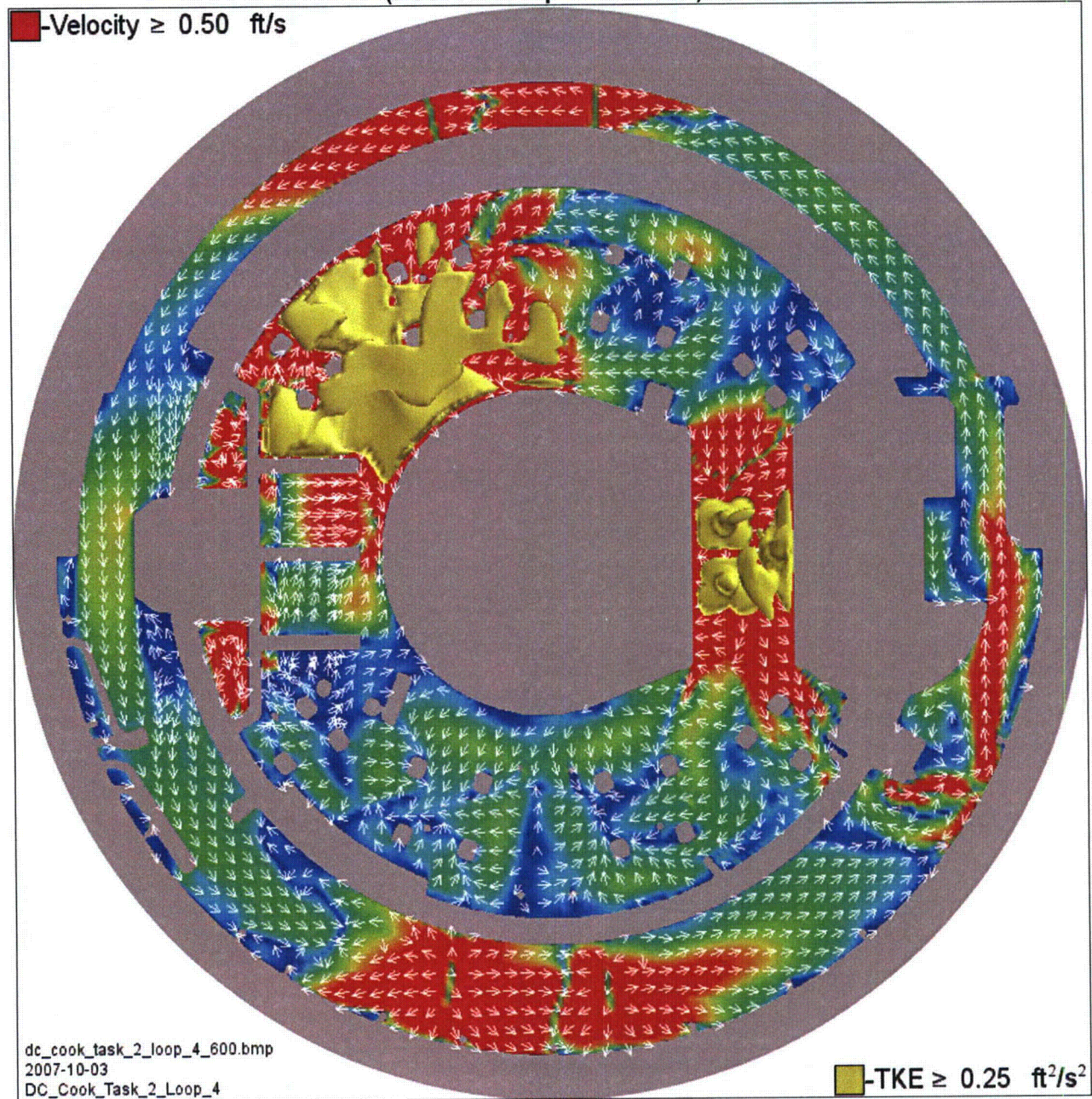


Figure 3e1-24 TKE and Velocity in the Pool at 900 Seconds
(Pool Fill Loop 4 CFD Run)

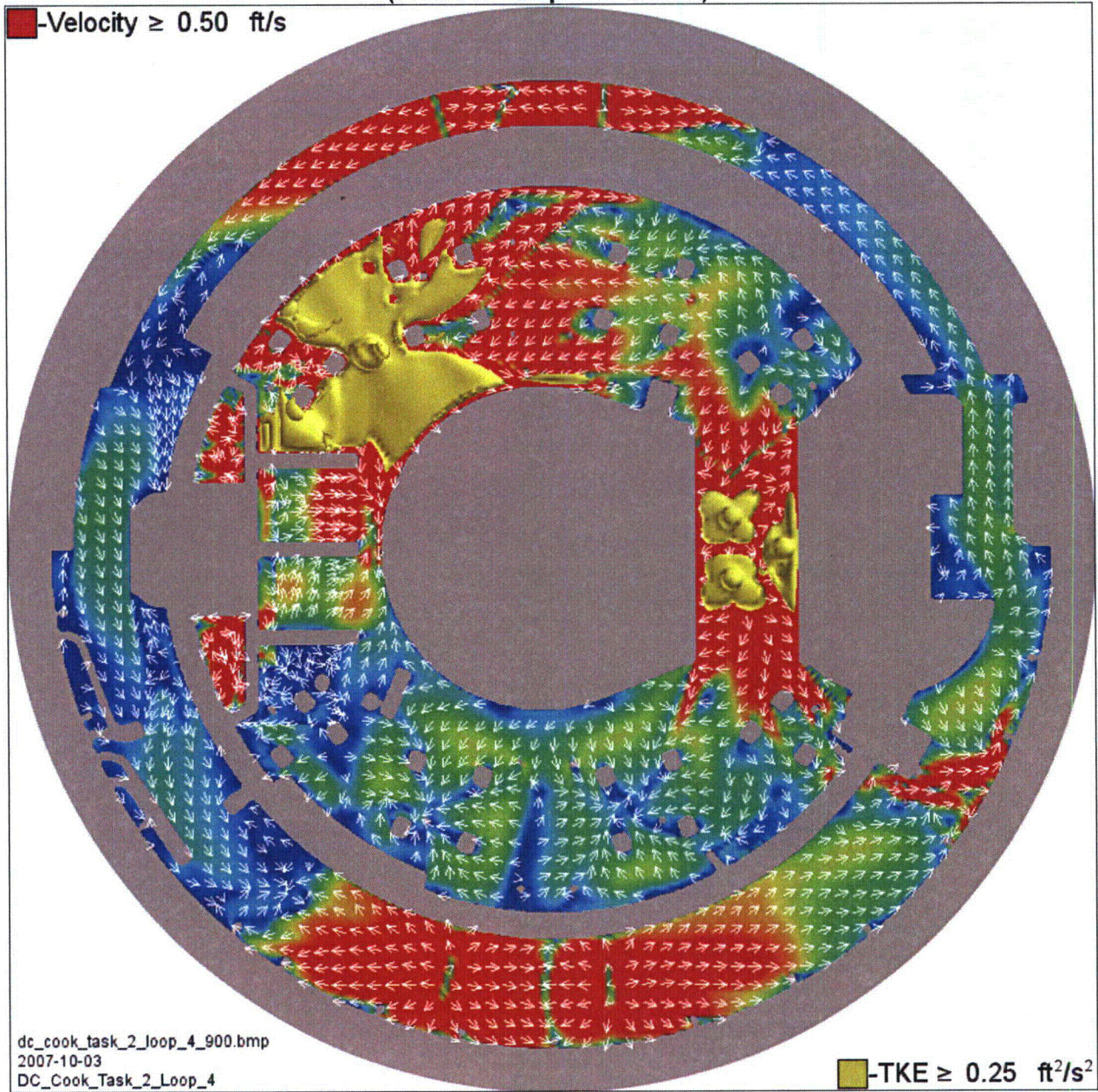
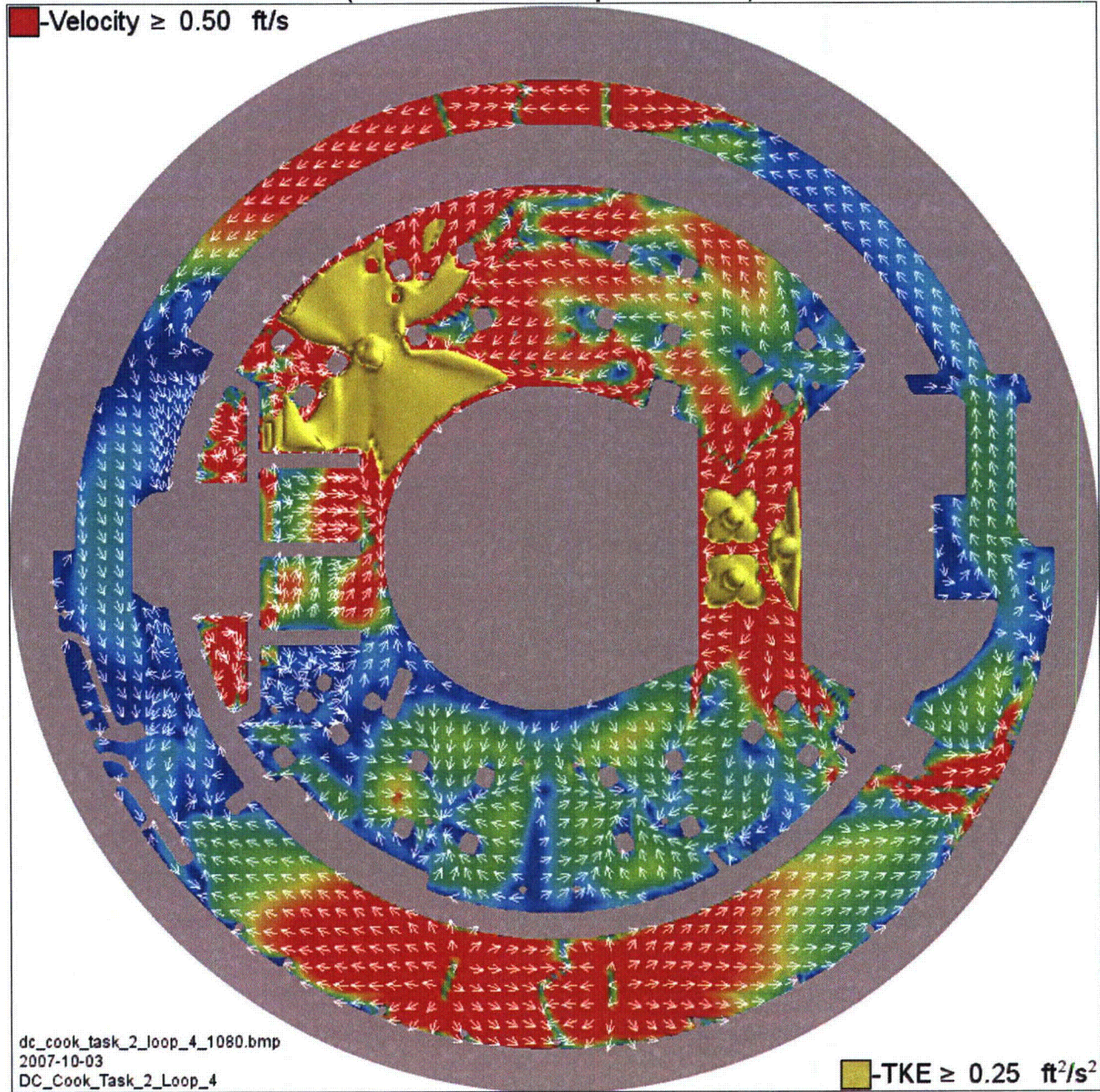


Figure 3e1-25 TKE and Velocity in the Pool at 1,080 Seconds
(End of Pool Fill Loop 4 CFD Run)



NRC Information Item 3.f – Head Loss and Vortexing

The objectives of the head loss and vortexing evaluations are to calculate head loss across the sump strainer and to evaluate the susceptibility of the strainer to vortex formation.

- 1. Provide a schematic diagram of the emergency core cooling system (ECCS) and containment spray systems (CSS).*
- 2. Provide the minimum submergence of the strainer under small-break loss-of-coolant accident (SBLOCA) and large-break loss-of-coolant accident (LBLOCA) conditions.*
- 3. Provide a summary of the methodology, assumptions and results of the vortexing evaluation. Provide bases for key assumptions.*
- 4. Provide a summary of the methodology, assumptions, and results of prototypical head loss testing for the strainer, including chemical effects. Provide bases for key assumptions.*
- 5. Address the ability of the design to accommodate the maximum volume of debris that is predicted to arrive at the screen.*
- 6. Address the ability of the screen to resist the formation of a "thin bed" or to accommodate partial thin bed formation.*
- 7. Provide the basis for the strainer design maximum head loss.*
- 8. Describe significant margins and conservatisms used in the head loss and vortexing calculations.*
- 9. Provide a summary of the methodology, assumptions, bases for the assumptions, and results for the clean strainer head loss calculation.*
- 10. Provide a summary of the methodology, assumptions, bases for the assumptions, and results for the debris head loss analysis.*
- 11. State whether the sump is partially submerged or vented (i.e., lacks a complete water seal over its entire surface) for any accident scenarios and describe what failure criteria in addition to loss of net positive suction head (NPSH) margin were applied to address potential inability to pass the required flow through the strainer.*
- 12. State whether near-field settling was credited for the head-loss testing and, if so, provide a description of the scaling analysis used to justify near-field credit.*
- 13. State whether temperature/viscosity was used to scale the results of the head loss tests to actual plant conditions. If scaling was used, provide the basis for concluding that boreholes or other differential-pressure induced effects did not affect the morphology of the test debris bed.*
- 14. State whether containment accident pressure was credited in evaluating whether flashing would occur across the strainer surface, and if so, summarize the methodology used to determine the available containment pressure.*

I&M Response to Information Item 3.f.1

Schematic diagrams of the Recirculation Sump, ECCS, and CTS are provided in Attachment 4, Figures A4-1, A4-13, A4-14, and A4-15.

I&M Response to Information Item 3.f.2

I&M has two separate strainers with different configurations as discussed in the response to Information Item 3.j.1. Since I&M is using the allowances of Chapter 6 of the GR and SER, there are three break sizes to be considered, the DEGB, the DGBS, and the SBLOCA (i.e., a 2 in diameter or greater break).

As described in the response to Information Item 3, the water level in containment at the initiation of recirculation is greater than the minimum water level during recirculation. Table 3f2-1, below, provides the water level at the initiation of recirculation, the minimum water level during recirculation, the time from event initiation until the minimum water level is reached, and the minimum submergence (height of water over the strainer) for the main and remote strainers for the DEGB, the DGBS, and the SBLOCA. The information provided in the table is from Reference 32.

Table 3f2-1 Strainer Minimum Submergence Determination

Break Size	Containment Water Level at Initiation of Recirculation, ft	Minimum Water Level During Recirculation, ft	Time from Event Initiation until Minimum Water Level, ~ hours	Minimum Submergence Main Strainer, ft	Minimum Submergence Remote Strainer, ft
DEGB	7.7	5.9	9.1	0.9	1.3
DGBS ⁽¹⁾	6.9	5.6	2.5	0.6	1.0
SBLOCA (2 in)	6.8	5.1	9.5	0.1	0.5

(1) This break was analyzed as occurring in the reactor cavity at the reactor vessel nozzle, resulting in 30% of the break flow going to the reactor cavity and 70% going to the loop compartment.

I&M Response to Information Item 3.f.3

CNP Unit 1 and Unit 2 were designed prior to issuance of RG 1.82 (Reference 158). During initial licensing of CNP Unit 2, I&M contracted with Alden to address the adequacy of the CNP recirculation sump design with respect to prevention of significant air entrainment following a LOCA that required recirculation cooling. Alden performed testing of the CNP recirculation sump design using a 1:2.5 scale model of the CNP design. This testing (Reference 31) demonstrated that, if the water level outside the sump is at or above the 602 ft 3 in elevation (the floor elevation is 598 ft 9 3/8 in), with 50% of the strainer area blocked, there would not be any concerns with vortexing or ingestion of air into the ECCS or CTS pumps. The basis for the

602 ft 3 in limit is to ensure there was sufficient height of water to provide the necessary flow over the curb and blocked portions of the strainer. As presented in Table 3f2-1, the calculated minimum water levels outside the sump are significantly above the tested value.

I&M had a vortex analysis performed to provide design input for the level instrument installed inside the recirculation sump, because the Alden original testing did not evaluate a condition in which head loss developed across the strainer. The vortex analysis (Reference 27) was performed by ALION based on the containment water levels determined in Reference 32. In the vortex analysis, it was assumed that the ECCS suction pipes were in the portion of the sump that had a decreasing water level. (See Figure A4-1 in Attachment 4 for the illustration of the CNP recirculation sump and strainer configuration.) The methodology description from Reference 27 is paraphrased below.

When the main strainer is severely blocked by debris, the resulting high head loss is predicted to cause an air cavity to form behind the main strainer inside the sump plenum (front section) which forms a free surface. When the flow condition is hydraulically favorable, a vortex could form between the free surface and the sump suction intake (outlet pipe), potentially resulting in significant air entrainment to the ECCS and CTS pumps. To avoid this condition, an analysis was conducted aimed at examining the potential for vortex formation.

Previous Experimental Vortex Formation Potential Analysis

In the Alden report (Reference 31), experimental, dimensionless, and similarity methods were applied to analyze the potential of vortex formation in the CNP containment recirculation sump. A physical model of the containment sump and a portion of the reactor building forming the approach to the sump were constructed to a geometric scale of approximately 1:2.5. A series of experimental tests were conducted during this study to analyze vortex formation potential in a sump prototype. Froude similarity was used to compare experimental results and construct a simple engineering model based on the prototype data.

The Froude number, Fr , represents the ratio of inertia force to gravitational force:

$$\text{Equation 1}$$
$$Fr = \frac{u}{\sqrt{gS}}$$

where u is the intake velocity, g is gravitational force, and S is the submergence or distance from the intake duct to the free surface. The dimensionless number is appropriate to analyze vortex formation at the free surface since the flow process is dominantly controlled by the inertia and gravitational forces. When the Froude number is equal in the model and prototype, the model and the prototype are dynamically equivalent such that the test results of vortex formation in the scaled model are equivalent to the real sump system. Thus, the experimental results presented in the Alden report of three different configurations were used to support the analysis in the current project:

Alden Case 1: 9,500 gpm sump flow, 18 in diameter suction pipe, 4 ft deep pool (7.33 ft water head above centerline of suction pipe intake)

Alden Case 2: 7,700 gpm sump flow, 18 in diameter suction pipe, 4 ft deep pool (7.33 ft water head above centerline of suction pipe intake)

Alden Case 3: 15,400 gpm sump flow, two 18 in diameter suction pipes, 4 ft deep pool (7.33 ft water head above centerline of suction pipe intakes)

For the three Alden cases, a swirling free surface was observed but no vortex pulling air bubbles into the suction intake nor was any continuous air core was observed.

CFD and Empirical Analysis of Vortex Formation Potential

Based on extensive experimental testing, a critical Froude number was verified to accurately identify when vortex formation occurs. Based on this, the following empirical correlation has been applied to estimate the critical submergence accompanying vortex formation (Chaurette, Jacques P., "Guidelines for Pump System Designers," Fluid Design Inc., May 2003 (see <http://www.fluidedesign.com/help11.html>)):

Equation 2

$$S(in) = D(in) + 0.574 \times Q(gpm) \times \frac{1}{D(in)^{1.5}}$$

To estimate vortex formation potential, the critical submergence $S(in)$ is calculated from Equation 2 using the appropriate intake dimension (D) and the associated flow rate (Q). Note that 0.574 is an empirical constant included in the correlation. If the calculated critical submergence number is larger than the system submergence, vortex formation is likely. Equation 1 indicates that as sump flow (u) increases, the Froude number increases which indicates increased vortex formation potential. Alternatively, as the head above the intake structure (S) increases, the Froude number decreases which indicates less likelihood for vortex formation. Considering Equation 2, as the intake flow (Q) increases the critical submergence increases. For a given system submergence (e.g., height above the center line of the suction intake duct), as the critical submergence increases and approaches the system submergence, vortex formation potential also increases.

Equation 2 was used to estimate the critical submergence for the three Alden cases listed above and for the 100% blocked main strainer case, the 90% blocked main strainer case and the clean main strainer case (that was performed as part of the CFD hydraulic analysis for the installed configuration at CNP). Given the measured pool depth above the suction intake duct (or system submergence), predictions of vortex formation potential for the Alden cases were compared against experimental observation to evaluate the ability of the correlation to accurately predict vortex formation potential. In addition, predicted system submergences for the three CFD cases considered were used to estimate vortex formation potential as well.

For Alden Cases 1 – 3, vortex formation potential was correctly predicted (as confirmed by comparison to experimental observation) when the measured system submergence was

significantly less than the predicted critical submergence. However, the empirical correlation incorrectly predicted vortex formation potential when the measured system submergence was close to the predicted critical submergence. This means the empirical correlation provides a conservative estimate of vortex formation potential and can be used with confidence to estimate potential vortex formation for the CNP sump analysis.

Considering results from all three CFD cases (clean case, 90% blocked case, and 100% blocked case), the empirical correlation predicted a critical submergence of 6.01 ft above the suction elevation (595.5 ft).

The following illustrates how the critical submergence was calculated for the clean case. For this case, there were two 18 in pump suction ducts, so D was taken as 18 in. Each suction duct was assumed to be withdrawing one-half the total sump flow, so Q was taken as 14,400/2 or 7,200 gpm. Inserting these numbers into Equation 2 yielded a critical submergence of 6.01 ft:

$$\begin{aligned} \text{Equation 3} \\ S(\text{in}) &= 18 \text{ in} + 0.574 \times 7,200 \text{ gpm} \times \frac{1}{(18 \text{ in})^{1.5}} = 72.117 \text{ in} \\ S(\text{ft}) &= 72.117 \text{ in} / 12 \text{ in/ft} = 6.01 \text{ ft} \end{aligned}$$

Based on the analysis performed, it was concluded that, as long as the water level in the plenum behind the main strainer remains above elevation 601.5 ft, vortex formation is not expected.

Given this recommendation from the ALION analysis, I&M installed the level switches at an elevation of 601 ft 9 in inside the recirculation sump.

The other concern associated with vortexing is the potential for air to be ingested from the surface of the containment sump pool, through the strainer, and into the sump. This is of particular concern when conditions of minimum submergence exist. To address this, testing was performed at CCI in which the water level was intentionally lowered to approximately 2 in above the strainer pockets at maximum head loss conditions to determine if any vortices would form on the surface of the pool. This testing determined that no vortices formed. To further assure that vortices would not form, the remote strainer at CNP was designed such that it does not have an open top and has a minimum submergence of 6 in. The least submergence calculated for the main strainer would occur during a SBLOCA. The calculated submergence is approximately 1 in. Since the water level analysis documented in Reference 32 is extremely conservative, it is expected that the water level will be substantially higher. Even if some air were to be drawn into the front section of the recirculation sump, the vents in this section would provide for release of the air.

Therefore, the design of the recirculation sump provides substantial protection against excessive air entrainment that could affect the pumps that take suction from the sump.